Triazole-linked reduced amide isosteres: An approach for the fragment-based drug discovery of anti-Alzheimer's BACE1 inhibitors and NH-assisted Fürst-Plattner opening of cyclohexene oxides

Christopher Jon Monceaux

Dissertation submitted to the faculty of the Virginia Polytechnic Institute and State University in partial fulfillment of the requirements for the degree of

Doctor of Philosophy
In
Chemistry

Dr. Paul R. Carlier, Chairman
Dr. Felicia A. Etzkorn
Dr. Harry W. Gibson
Dr. David G. I. Kingston
Dr. Webster L. Santos

December 9, 2010
Blacksburg, VA

Keywords: Fürst-Plattner (*trans* diaxial effect), epoxidation, epoxide opening, click-chemistry, diazotransfer, microtiter plate-based screening, reduced amide BACE1 inhibitors

Triazole-linked reduced amide isosteres: An approach for the fragment-based drug discovery of anti-Alzheimer's BACE1 inhibitors and NH-assisted Fürst-Plattner opening of cyclohexene oxides

Christopher Jon Monceaux

ABSTRACT

In the scope of our BACE1 inhibitor project we used an originally designed microtiter plate-based screening to discover 4 triazole-linked reduced amide isosteres that showed modest (single digit micromolar) BACE1 inhibition. Our ligands were designed based on a very potent (single digit nanomolar) isopththalamide ligand from Merck. We supplanted one of the amide linkages in order to incorporate our triazole and saw a 1000-fold decrease in potency. We then enlisted Molsoft, L.L.C. to compare our ligand to Merck's *in silico* to account for this discrepancy. They found that the triazole linkage gives rise to a significantly different docking pose in the active site of the BACE1 enzyme, therefore diminishing its potency relative to the Merck ligand.

The ability to control the regio- and stereochemical outcome of organic reactions is an ongoing interest and challenge to synthetic chemists. The pre-association of reacting partners through hydrogen bonding (H-bonding) can often to yield products with extremely high stereoselectivity. We were able to show that anilines, due to their enhanced acidity relative to amines, can serve as substrate directing moieties in the opening of cyclohexene oxides. We observed that by judicious choice of conditions we could control the regiochemical outcome of the reaction. These studies demonstrate that an intramolecular anilino-NH hydrogen bond donor

can direct Fürst-Plattner epoxide opening. A unified mechanism for this phenomenon has been proposed in this work which consists of a novel mechanistic route we call "NH-directed Fürst-Plattner." We further studied the opening of cyclohexene oxides by incorporating amide and amide derivative substituents in both the allylic and homoallylic position relative to the epoxide moiety. Our attempts to control regioselectivity in the allylic systems were unsuccessful; however when the directing substituent was in the homoallylic position, we could demonstrate some degree of regioselectivity.

An additional project that the author worked on for approximately one year during his graduate student tenure is not described within this work. In February of 2009 AstraZeneca, Mayo Clinic, and Virginia Tech Intellectual Properties Inc. concomitantly announced that AstraZeneca licensed a portfolio of preclinical Triple Reuptake Inhibitor (TRI) compounds for depression. The lead compound, PRC200, was discovered by a collaborative effort between the Carlier and Richelson (Mayo Clinic Jacksonville) research groups in 1998. The author was tasked to develop backup candidates of PRC200 in order to improve the pharmacokinetics of the lead compound. Due to confidentiality agreements, this work is not reported herein.

Acknowledgements

I would like to begin my acknowledgements by expressing my sincere gratitude to my advisor, Dr. Paul Carlier. The choice of a research advisor is one of the most important decisions one can make in their professional development; I certainly chose wisely. The time he took in order to give advice or talk chemistry whether it was in his office, on Skype, via IM, or even on his iPhone before boarding a flight is something that is truly unique to our research group. I will never forget doing molecular modeling together at a Starbucks in the Charlotte-Douglas International Airport. I am indebted to Dr. Carlier for ensuring that not only was I prepared to succeed as a Ph.D. chemist, but also for his efforts in attempting to secure me any professional position I wanted. I am looking forward to our new relationship and plan to seek his advice and counsel even in my professional career. I must also thank my Advisory Committee, Drs. Etzkorn, Dorn, Gibson, Kingston and Santos. Your advice and input has been indispensable during the course of my graduate career.

Thanks must also be given to fellow graduate students, collaborators, and support staff that made the research described within this dissertation possible. I would like to express gratitude to the members of my research group during my tenure - Dr. Dawn Wong, Dr. Yiqun Zhang, Dr. Danny Hsu, Dr. Jason Harmon, Dr. Larry Williams, Dr. Nipa Deora, Josh Hartsel, Dr. Ming Ma, Yang Sheng Sun, Jenna Templeton, Madeline Nestor, Devin Rivers, Jonathan Meade, Ken Lui, Dr. Qiao-Hong Chen, Stephanie Bryson, Neeraj Patwardhan, Dr. Derek Craft, Astha, Zhenzhen Zhong and Rachel Davis. I would also like to thank Ken Knott from the Santos research group. The kilograms of caffeine we consumed along with the many total syntheses we completed *in expo* were an integral part of my graduate school experience. My collaborators

Chiho Hirate-Fukae and Dr. Yasuji Matsuoka at Georgetown University Hospital also deserve thanks for their contributions to making the BACE1 project a reality. I would also like to thank Anton Sizovs and Qiao-Hong Chen for their help in translating journals from Russian and Chinese respectively.

To conclude, I must give thanks to the people in my life outside the professional circle. I have to thank my Mother and Father who have been along since kindergarten and have now seen me through graduate school. Without your love, guidance, and support this endeavor would not have been possible. I must also thank my Mother and Father In-law, your support was invaluable and very much appreciated. And finally, my wife gets the greatest thanks of all. I am truly blessed to have you in my life – your love, patience, and unwavering encouragement throughout this process was truly precious to me.

Dedication

To Tamara, without you none of this would have been possible. I love you.

Table of Contents

List of Schemes

List of Figures

List of Tables

Chapter 1 Design, Synthesis, and Screening of Triazole Linked BACE1 Inhibitors

1.1 Amyloid Beta Peptide Theory

Alzheimer's disease (AD) is a progressive neurodegenerative disease whose first clinical manifestation is dementia, which eventually leads to death. Data from the 2000 U.S. census indicates that AD currently affects more than 4.5 million Americans.[1] According to the Alzheimer's Association, this affliction is the 6th leading cause of death in the United States.[2] The pathological hallmarks of AD, visible post-autopsy, are the formation of two types of proteinaceous lesions. The first are amyloid plaques, 4 kDa peptide plaques (40 or 42 amino acid residues), referred to as the Aβ peptide.[3] The second is a neurofibrillary tangle composed of intercellular tau proteins.[4] The relationships between these two lesions is not well understood, although a seminal study has shown that accumulation of Aβ in brain regions responsible for cognitive function occurs before dementia and the development of neurofibrillary tangles.[5]

Aβ results from the endoproteolysis of the large precursor protein known as the amyloid precursor protein (APP). APP is expressed ubiquitously throughout the body and Aβ is a normal, albeit a low-level product of APP cleavage.[6] It has been found in human cerebrospinal fluid and plasma.[7] One protease, β-secretase, first cleaves APP between the P1 and P1' methionine and aspartic acid residues respectively. This yields a membrane bound *C*-terminus fragment, C99 and a secreted ectodomain, APPsβ (Figure 1.1). The *C*-terminal fragment, C99 is a substrate for another protease, γ-secretase. This second cleavage event produces an

intercellular domain AICD and the amyloidgenic Aβ peptide. Cleavage via γ-secretase is imprecise and produces Aβ peptides that range in residue lengths of 38 to 43.[8] Most secreted Aβ is of the 38 to 40 residue length. The 42 amino acid residue, Aβ42, is a small component of the γ-secretase cleavage, but unfortunately forms insoluble aggregates much faster than the former and is suspected to be the most amyloidgenic Aβ.[9] Alternatively, APP can be cleaved by another protease, α-secretase to yield a *C*-terminal fragment C83 and a secreted ectodomain APPsα. Just as in the previous case, the C83 is a γ-secretase substrate and is cleaved to yield a non-amyloidgenic peptide p3 and the intracellular domain AICD.[10,11]

Figure 1.1. APP Proteolysis *(Figure adapted from Cole et al.).*[8]

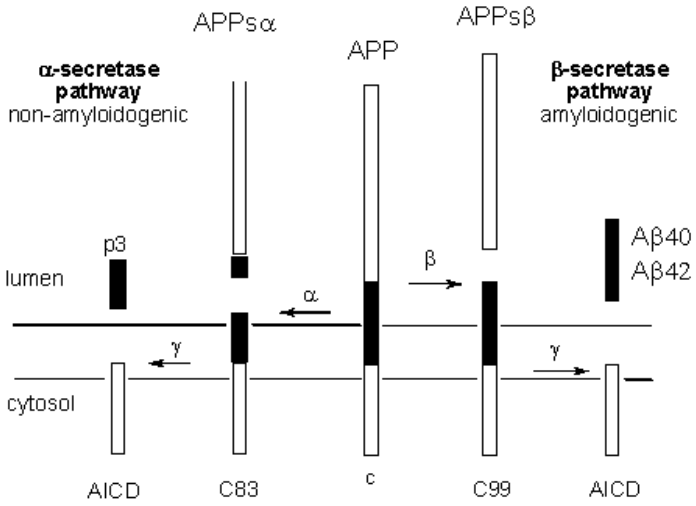

The Schechter and Berger nomenclature is commonly used for the description of protease subsites.[12] By this convention subsites or pockets in the protease are denoted with an S (for subsites) and the substrate amino acid residues are designated P (for peptide). The amino acid residues of the amino-terminal side of the scissile bond are numbered P1, P2, P3, and so on with the number indicating the distance from the scissile amide bond. For example P2 denotes the

second residue from the scissile amide bond on the amino terminal side (Figure 1.2). Likewise, the residues of the carboxy-terminal side are numbered P1', P2', P3', etc.

Figure 1.2. Schechter and Berger Protease Nomenclature.[12]

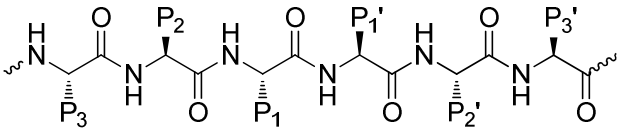

Early onset familial AD, or FAD, is a rare form of AD that develops in humans between the ages of 30 and 60. FAD is caused by mutations in APP at the β-secretase cleavage site. An example is the Swedish mutation (APPswe), a double amino acid mutation from LysMet to AsnLeu at the cleavage site (Figure 1.3, mutations appear in italics).[6] APPswe is a better substrate than the wild type APP (APPwt) for β-secretase cleavage therefore increasing the amount of Aβ produced.[13]

Figure 1.3. APP sequences between P4 and P4'.[6]

Residue	*P4*	*P3*	*P2*	*P1*	*P1'*	*P2'*	*P3'*	*P4'*
APPwt	E	V	K	M	D	A	E	F
APPswe	E	V	*N*	*L*	D	A	E	F

1.2 β-Secretase as a drug target

Prior to 1999, the identities of the APP cleaving enzymes were unknown. Several laboratories independently isolated and characterized β-secretase.[14-18] It was found that β-secretase is a member of the pepsin aspartyl proteases. β-secretase has been given several

designations since its discovery: memapsin 2[15], asp 2[14], and BACE1[17]. The designation BACE1 (beta APP cleaving enzyme 1) has become the most widely adopted and will be referred to as such henceforth.

In order to validate BACE1 as a drug target, studies were conducted on knockout mice to determine if BACE1 had any vital function in vivo. Three seminal studies showed that BACE1 deficient mice (BACE -/-) showed no abnormalities in their development versus wild-type mice.[19-21] Moreover, the BACE1 deficient mice did not produce any Aβ. These results demonstrate that BACE1 is the major contributor to Aβ production and suggest that BACE1 is dispensable.

Rational drug design requires the knowledge of the structural information of the BACE1 enzyme and its interaction with APP. Sauder et al. conducted molecular modeling studies to interrogate interaction of the BACE1 active site with the wild-type APP substrate.[22] Modeling studies suggested that Arg296 of BACE1 formed a salt bridge with the P1' Asp residue of the APP substrate. Additionally, it was postulated that several hydrophobic residues from BACE1 form a pocket (S1 pocket) for a hydrophobic P1 residue. APPswe, the P2-P1 mutation of LysMet to AsnLeu, was found to interact with the Arg296 and the hydrophobic pocket more favorably, substantiating the enhanced cleavage of this substrate. Shortly thereafter, BACE1 was co-crystallized with a transition state isostere and an X-ray crystal structure was determined to 1.9 Å resolution (PDB ID 1FKN).[23] This structure showed that the BACE1 catalytic domain is indeed similar to other aspartic proteases. The catalytic aspartic acid residues, Asp32 and Asp228, formed four hydrogen bonds with the inhibitor. The X-ray crystal structure also revealed the importance of the Arg296 and the hydrophobic pocket (S1) of the active site, corroborating the findings in Sauder's modeling study. These pioneering discoveries suggest

that small molecule inhibitors that target Arg296 and the hydrophobic pocket should provide fertile ground for BACE1 inhibitor discovery.

1.3 Development of BACE1 drug like inhibitors

As mentioned before, BACE1 is a member of the aspartyl protease family. A great deal of research has been dedicated to the development of inhibitors of renin and HIV protease, both members of the aspartyl protease family.[24,25] An X-ray diffraction analysis has shown pepstatin, a known inhibitor of aspartic proteases, complexed with an aspartic protease from the fungus *Rhizopus chinensis* (PDB ID 2APR).[26] This study confirms the hypothesis that the inhibitory capacity of this transition state analogue is attributed to its mimicry of the tetrahedral intermediate of amide bond cleavage (Figure 1.4). This approach, suggested by Linus Pauling in 1946,[27] has allowed chemists to design compounds that mimic the amide cleavage transition state.

Figure 1.4. Mechanism of aspartyl protease amide cleavage *(Figure adapted from Brik et al. and residues labeled for BACE1).*[28]

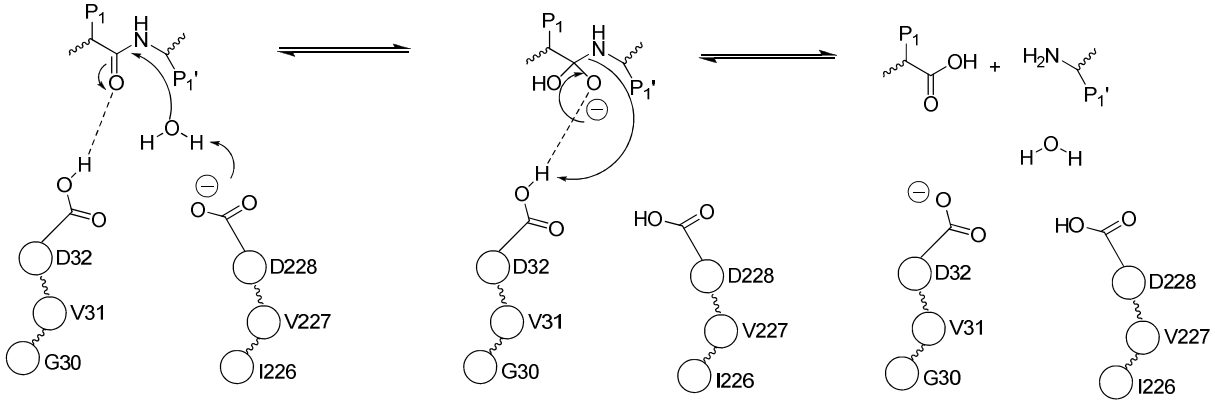

The most common of the BACE1 protease transition state isosteres (TSI) found are the statines, hydroxyethylene (HE), hydroxyethylamine (HEA), and the reduced amide

(Ψ[CH_2NH]), depicted in Figure 1.5. Each scaffold engages the BACE1 active site differently and principal examples of each will be reviewed.

Figure 1.5. Common BACE1 TSI scaffolds.

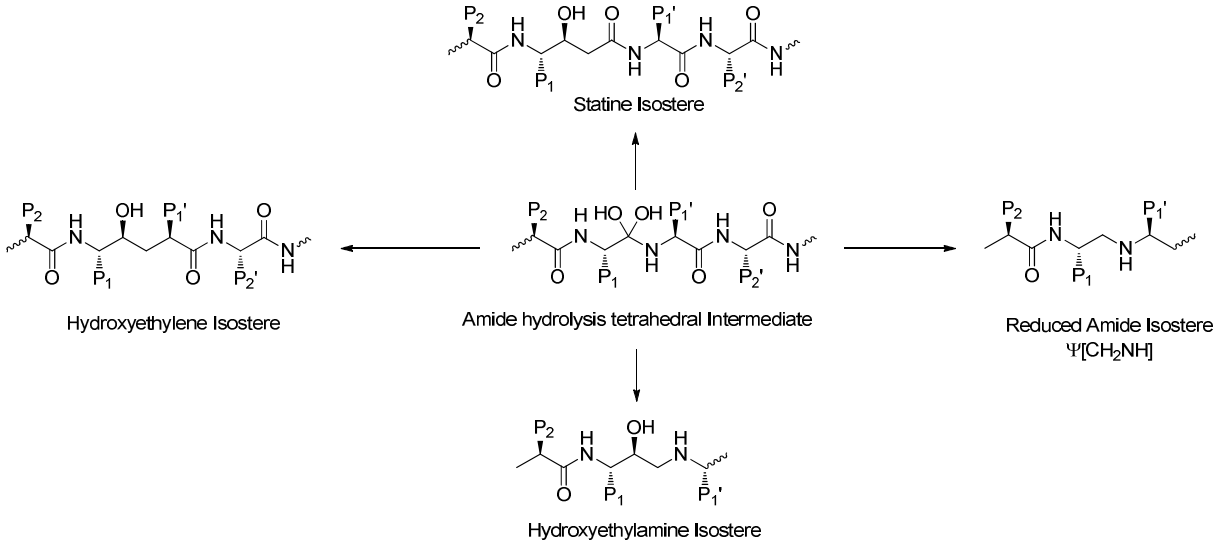

1.3.1 Statine TSI

Statine is a transition state isostere derived from the natural product pepstatin. Pepstatin is a potent inhibitor of several aspartyl proteases, with the exception of BACE1. The statine isostere engages the catalytic Asp32 and Asp228 with the secondary hydroxyl group.[29] The natural APP sequence (wild type) spanning P10 to P4' is as follows: KTEEISEEVKM↓DAEF (note: the downward arrow indicates cleavage occurs between Met (P1) and Asp (P1')). Elan, a pharmaceutical company, along with co-workers at the University of Oklahoma implemented the APPswe mutation (the P2-P1 mutation of LysMet to AsnLeu) as well as a mutation of P1' from Asp to Val to target BACE1.[16] This inhibitor, termed Stat-Val (KTEEISEEVKLStatVAEF), was shown to be a 30 nM inhibitor of BACE1.[30] The 30 nM value is an IC_{50} value which is the concentration necessary to inhibit 50% of the enzyme in an ELISA cell-free assay using a

maltose-binding-protein C-125 Swedish (MBP-C125Swe) as the substrate. Without the Asp to Val mutation the inhibitor was found to be 1000 times less potent (IC_{50} = 40 μM). In order to reduce the molecular weight of this inhibitor truncation studies were explored. Elan showed that deletion of seven residues from the *N*-terminus end (EVNLStatVAEF) preserved the potency of the inhibitor (IC_{50} = 40 nM). However, removal of the *N*-terminus glutamic acid did show a dramatic loss in potency (IC_{50} = 9μM), while acetylation of the *N*-terminus valine of this compound did show a recovery in potency (IC_{50} = 500 nM). Substituting the P2 Asn with Met showed enhanced potency to an IC_{50} of 300 nM. Although this inhibitor showed great promise, the cell permeability needed to be improved. The Elan team conceptually divided the peptidic inhibitor into three regions, an *N*-terminus region, statine core, and *C*-terminus region. Each of these respective regions was independently optimized leading to the first cell-permeable statine BACE1 inhibitors with EC_{50} values as low as 4 μM (***1*-1,** Figure 1.6). The cell-based assay for inhibition of BACE1 was determined by in a human embryonic kidney cell line (HEK-293) transfected with both the substrate and inhibitor.[31]

Figure 1.6. Elan statine inhibitor.[31]

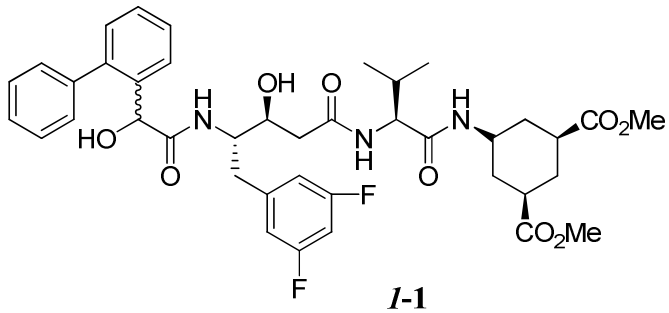

***1*-1**

1.3.2 Hydroxyethylene TSI

In the hydroxyethylene (HE) isostere, the nitrogen of the amide bond from the natural substrate has been replaced by a methylene and the carbonyl has been transformed into a hydroxyl group that is intended to engage the catalytic aspartic acids (D32 and D228). The HE scaffold has extensive application in HIV protease inhibitor design[32], such as the development of a clinical candidate HIV-protease inhibitor, CGP-61755.[33,34] Jordan Tang and Arun Ghosh and co-workers at the Oklahoma Medical Research Foundation (OMRF) reported on the development of a seminal inhibitor, OM99-2 (***1*-2,** Figure 1.7).[35] This 8-mer peptide was found to have K_i values as low as 9.3 nM versus recombinant human BACE1 in a cell-fee assay. Their HE isostere design is based on APPswe substrate (EVNL↓DAEF) as well as the P1' mutation of Asp featured in StatVal (EVNLStatVAEF). Shortly after inhibitor development, the OMRF team published the first account of a ligand (inhibitor ***1*-2**) bound to BACE1.[29]

Figure 1.7. OMRF OM99-2 inhibitor.

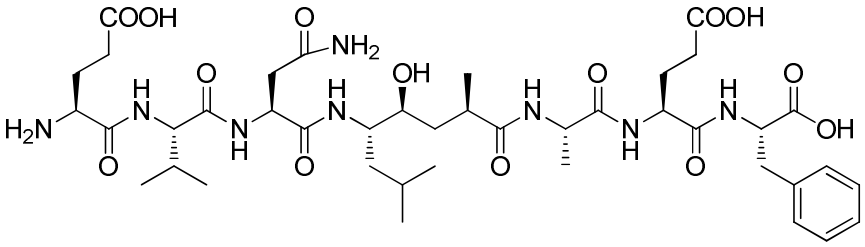

***1*-2**

The OMRF team also explored the preference of BACE1 binding to side chains of their OM99-2 scaffold (E***VN***L↓A***AE***F). [36] The residues in bold italics indicate where variations were made via combinatorial libraries. Of the 130,000 different compounds screened, the researchers found 65 that exhibit strong BACE1 binding. From these, OM00-3 (***1*-3,** ELDL↓AVEF) was found to inhibit BACE1 with a K_i of 0.31 nM, a five-fold increase over OM9902 (OM9902 K_I =

1.6 nM) (Figure 1.8). Kinetic data were determined by measuring formation of cleaved substrate via MALDI-TOF mass spectrometry.[37]

Figure 1.8. OMRF OM00-3 inhibitor with BACE1 hydrogen bond interactions *(Figure adapted from Turner et al. PDB ID 1M4H.[36])*

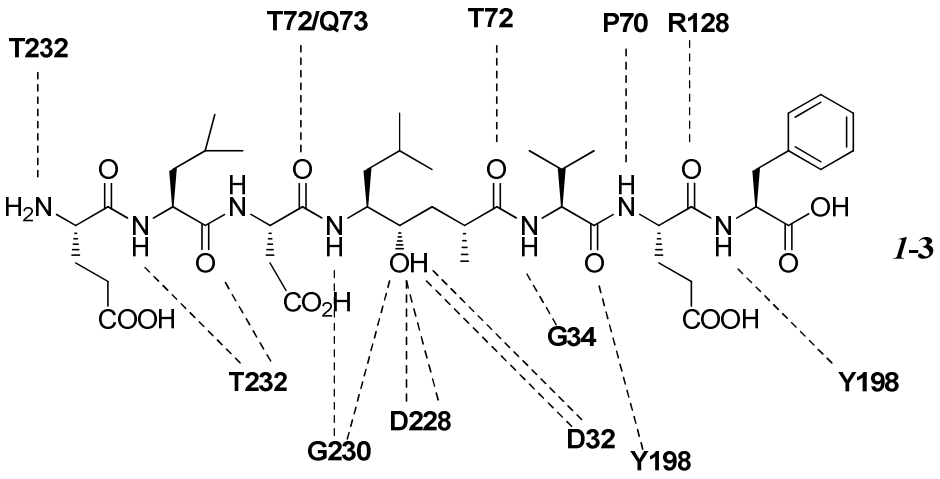

Although these findings were invaluable for the determination of BACE1 binding specificity, the inhibitor's cellular activity had yet to be measured. Lamar and co-workers at Eli Lilly evaluated inhibitors derived from Ghosh's scaffolds and found that they did indeed have excellent enzyme potency, but the inhibitors exhibited poor cellular activity (IC_{50} ~2200 nM).[38] The Eli Lilly team hypothesized that the poor cellular activity was attributed to the limited aqueous solubility of the inhibitors. Variations on the *C*-Terminus of the inhibitors lead to a pyridine moiety with improved aqueous solubility as well as improved cellular activity (IC_{50} ~170 nM). With these results the researchers varied their inhibitor at the P2 and P3 positions (Boc-**VM**F↓AV-$NHCH_2$-4-Pyr; P3 and P2 highlighted in boldface) in order to possibly identify more potent BACE1 inhibitors. Two inhibitors emerged with good enzyme potency (Boc-IAF↓AV-$NHCH_2$-4-Pyr) and (Boc-CH_2CHF_2-AF↓AV-$NHCH_2$-4-Pyr) gave IC_{50} = 42 and 45 nM

respectively. The two inhibitors also showed promising cellular activity IC_{50} = 410 and 400 nM respectively vs. APPswe HEK293.[38]

1.3.3 Lipinski's Rule of Five and the Hydroxyethylamine TSI

Lipinski and co-workers at Pfizer have developed the "rule of five" which is a rule of thumb that relates structural characteristics of a drug candidate to its likely ADME (absorption, distribution, metabolism, and excretion) of a drug candidate.[39] The four postulates state that a drug will have *poor* absorption and permeation if: 1) there are more than 5 H-bond donors, 2) there are more than 10 H-bond acceptors, 3) the molecular weight is greater than 500, and 4) the calculated cLogP is greater than 5. Although there are four postulates, the name is derived from the factor of five contained within each postulate. In order to enhance cellular potency, researchers began designing inhibitors that were cognizant of the "rule of five".

The hydroxyethylamine (HEA) isostere which conforms to the aforementioned "rule of five", is another TSI that has found wide application in HIV protease inhibition.[40-42] Crystallization of an HEA isostere with human BACE1 shows the HEA isostere engages Asp32 with the hydroxyl moiety while the protonated amine moiety donates a hydrogen bond to Asp228 (***1*-4,** Figure 1.9).[43] Tamamura and co-workers at Kyoto University were amongst the first groups to design potent inhibitors of BACE1 containing the HEA isostere. Their "shortest" compound containing P2-P4' residues and a non-peptidic *C*-terminus (DL↓MVLD-NH_2) did not show any inhibitory activity. Addition of a P3 isoleucine (IDL↓MVLD-NH_2) resulted in observable inhibition (IC_{50} = 240 nM, homogenous time resolved fluorescence assay, HTRF). Further addition of a P4 glutamic acid (EIDL↓MVLD-NH_2) resulted in a dramatic enhancement in potency down to 82 nM.[44]

Figure 1.9. Pfizer/Elan HEA isostere complexed with BACE1 *(Figure adapted from Maillard et al. PDB ID 2IQG.).*[43]

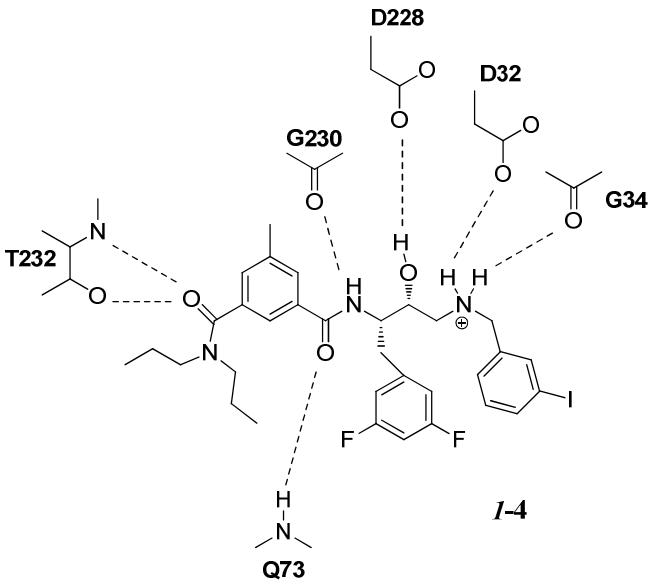

I-4

A joint venture between Elan and Pfizer led to the development of HEA inhibitors whose hydroxyl substituent was in the (*R*) configuration, opposite to all TSI's described heretofore. One of their more potent inhibitors containing the (*R*) configuration was 3000-fold more active than the (*S*) isomer.[43] In addition their findings showed the basic nitrogen in the HEA scaffold enhances cellular potency over a similar HE isostere (Figure 1.10).

Figure 1.10. Pfizer/Elan inhibitors.

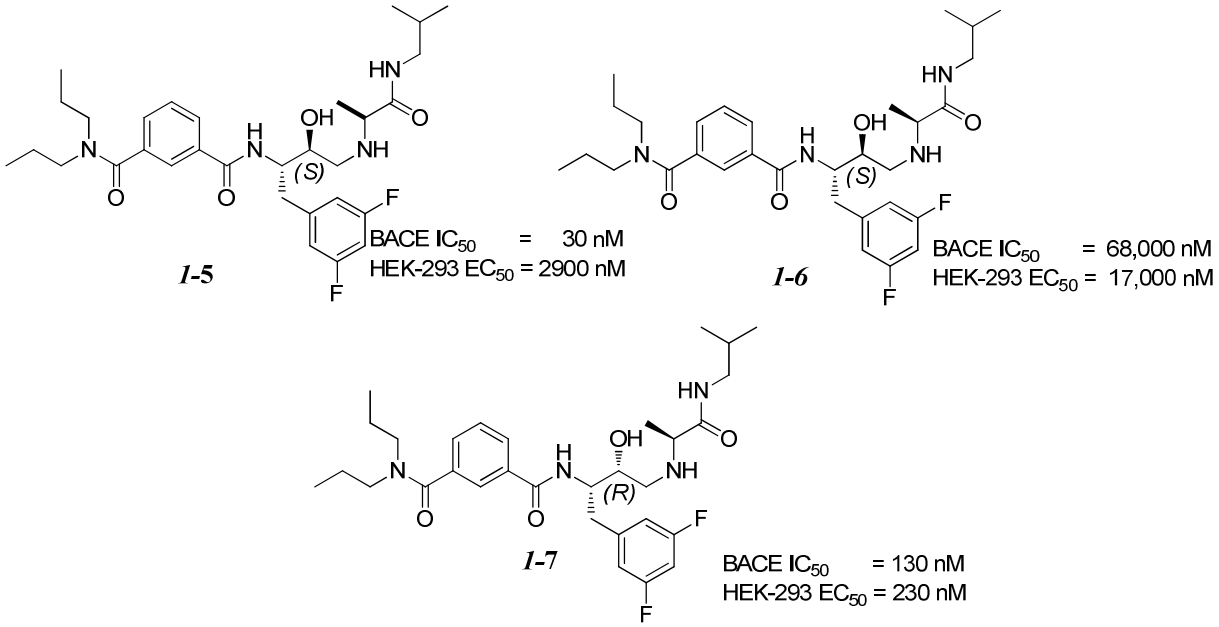

Legend: BACE1 IC_{50} values represent data from cell-free assays; HEK-293 EC_{50} values are derived from cell-based assays.

Replacing the *C*-terminal amide with a benzyl amine showed slight attenuation in potency, but a dramatic increase in cellular activity was observed (Table 1.1). A library search of all available benzyl amines gave two more potent hits. The researchers commented that the P3 *N*,*N*-dipropyl groups are locked into a conformation that allows one of the propyl groups to access the S3 pocket.[43]

Table 1.1 Pfizer/Elan BACE1 inhibitors

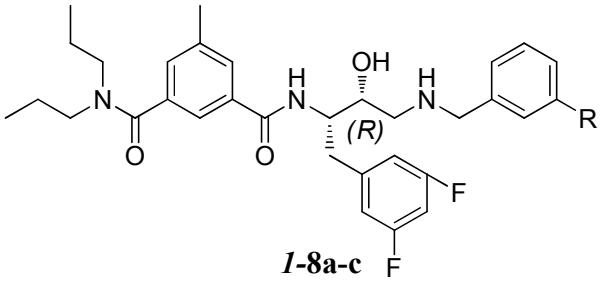

***1*-8a-c**

Drug	*R*	*IC_{50} (nM)*[a]	*EC_{50} (nM)*[b]
***1*-8a**	**H**	130	**40**
***1*-8b**	**I**	5	**3**
***1*-8c**	**OMe**	20	**15**

a - ***BACE1 enzymatic assay was carried out using a MBPC125Swe assay.***[16] **b** - ***Cellular inhibition was determined in HEK-293 cells.***[45]

Stachel and co-workers at Merck added the methyl sulfonamide moiety to the C5 position in a series of isophthalamides (Table 1.2).[46] X-ray crystal structures have shown that the methyl sulfonamide oxygen makes hydrogen bonding interactions with one with Thr232 and Asn233, whereas the other oxygen accepts a hydrogen bond from Arg235. Due to the lowered molecular weight and reduction of amide bonds in the HEA isostere, the inhibitors showed excellent cellular activity versus HEK293 cells transfected with an active mutant APP, APP_NF (wild type APP = KM↓DA, APPswe = NL↓DA, APP_NF = NF↓EV) (Table 2). The data show that their inhibitors are potent against BACE1 and selective against other aspartic proteases such as BACE2 and renin. This is attributed to the more open and less hydrophobic active site of

BACE1 compared to that of other aspartic proteases, namely BACE2. BACE2 is a homologue of BACE1 sharing a 64% AA residue similarity suggesting that BACE2 could possibly cleave APP to yield Aβ.[6] Since BACE2 function *in vivo* has yet to be determined, the Merck team has evaluated the BACE1/BACE2 selectivity of their inhibitors (Table 1.2).

Table 1.2. Merck HEA isostere inhibitors and BACE1 potency (PDB ID 1TQF).[46]

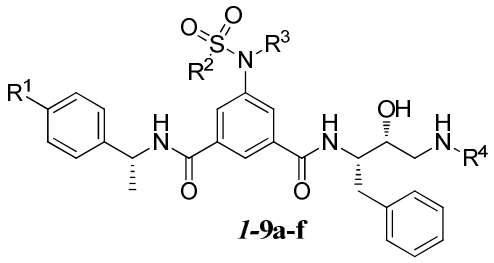

***1*-9a-f**

Drug	R^1	R^2	R^3	R^4	***BACE1 IC_{50} (nM)***[a]	***APP_NF IC_{50} (nM)***[b]	***BACE2 IC_{50} (nM)***[c]	***renin IC_{50} (nM)***[d]
9a	H	Me	Me	cyclopropyl	15	29	230	**>50,000**
9b	F	Me	H	cyclopropyl	636	1180	210	**>50,000**
9c	F	Me	Me	cyclopropyl	10	19	69	**>10,000**
9d	F	Me	Me	H	23	5389	443	**>50,000**
9e	F	Me	Me	ethyl	15	396	260	**>50,000**
9f	H	i-Pr	Me	cyclopropyl	41	25	360	**>50,000**

a - ***BACE1 enzymatic assay was performed using a FRET assay.***[47] **b** - ***Cellular inhibition was determined in HEK-293 cells.***[46]

1.3.4 Reduced amide TSI

The reduced amide ($\Psi[CH_2NH]$) isostere was first utilized in aspartyl protease inhibition to develop potent inhibitors of renin.[48] Crystallization data show that these inhibitors engage the catalytic Asp 228 of BACE1 (Figure 1.11).[49] The Merck team, utilizing their previous success with the methyl sulfonamide HEA isostere,[49,50] modified this scaffold by incorporating a $\Psi[CH_2NH]$ isostere as the key binding element.[49] In the case of their HEA inhibitor, a two pronged engagement of the catalytic aspartates was observed via the hydroxyl and secondary amino group (Figure 1.9). It was found that reduced amide inhibitors, which only engage one of the catalytic aspartates (Figure 1.11), showed potent enzymatic activity while also maintaining cellular activity (Table 1.3). The sulfonamide group was found to occupy the S2 pocket and form two important hydrogen bond interactions from Asn233 and Ser325 to the sulfonamide oxygens (Figure 1.11).

Figure 1.11. Merck inhibitor *1*-11b with BACE1 *(Figure adapted from Coburn et al. PDB code 2QZL.).*[49]

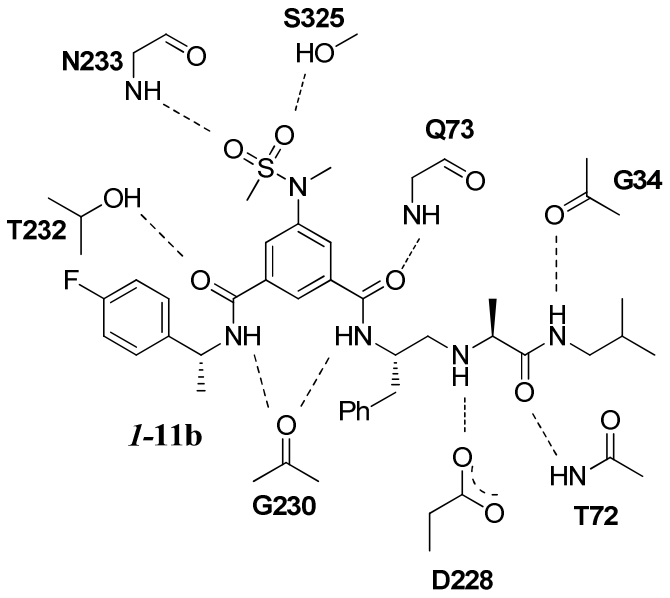

Additionally the researchers comment on the importance of the amide bond immediately C-terminal to the reduced amide.[49] The amide is involved in a key interaction with the residues on the flap, Thr72 and Gly34.[49]

Table 1.3. Merck reduced amide inhibitors showing both enzymatic and cellular activity.[49]

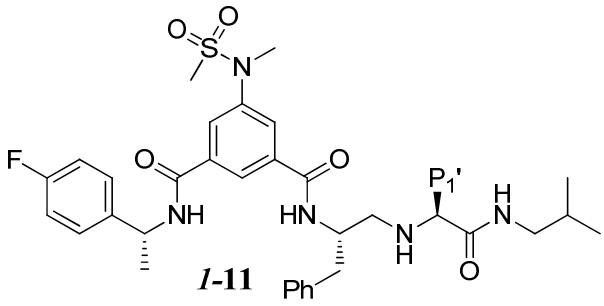

***1*-11**

Drug	*P_1'*	*BACE1 IC_{50} (nM)*	*APP_NF IC_{50} (nM)*
11a	H	117	**3710**
11b	Me	8	**22**
11c	Et	7	**20**
11d	i-Pr	4	**17**
11e	$-CH_2CH_2OH$	13	**751**
11f	$-CH_2CH_2SO_2Me$	13	**17,500**

a - ***BACE1 enzymatic assay was performed using a FRET assay.***[47] **b** - ***Cellular inhibition was determined in HEK-293 cells.***[46]

Although the isophthalamide Merck inhibitors showed both potent enzyme and cellular activity, they cited problems with the pharmacokinetic properties, thus rendering the inhibitors unlikely for further development.[51] Their primary concern was that inhibitors, shown in Table 1.3, were found to be P-glycoprotein (P-gp) transport substrates. Although the inhibitors showed no effect on Aβ levels in a murine model via intravenous (IV) administration, intracranial (IC)

administration in mice did show reductions of Aβ levels by 70%. These finding show the critical importance of an inhibitor being a CNS penetrant.

The Merck team sought out greater CNS penetration by lowering the peptidic character of their isophthalamide inhibitors while preserving their high potency. They comment that macrocyclization has precedence in enhancing inhibitor potency[52-54] and sought to apply this technique to their isophthalamide inhibitors.[51] The researchers note the spatial proximity between P1 and P3 suggests that linking these groups together would yield a potent macrocyclic inhibitor. Their first macrocyclic candidate ***1*-14** did show enhanced potency over its acyclic analogue ***1*-13**, although the potency is quite poor (Figure 1.12). Nevertheless, their argument for macrocyclization was substantiated and further SAR studies were undertaken to yield an inhibitor ***1*-15** with enhanced enzymatic (IC_{50} = 4 nM) and cellular (IC_{50} = 76 nM) potency, that showed an unprecedented Aβ reduction in the murine model via IV administration.

Figure 1.12. Merck reduced amide macrocyclic inhibitors.[51]

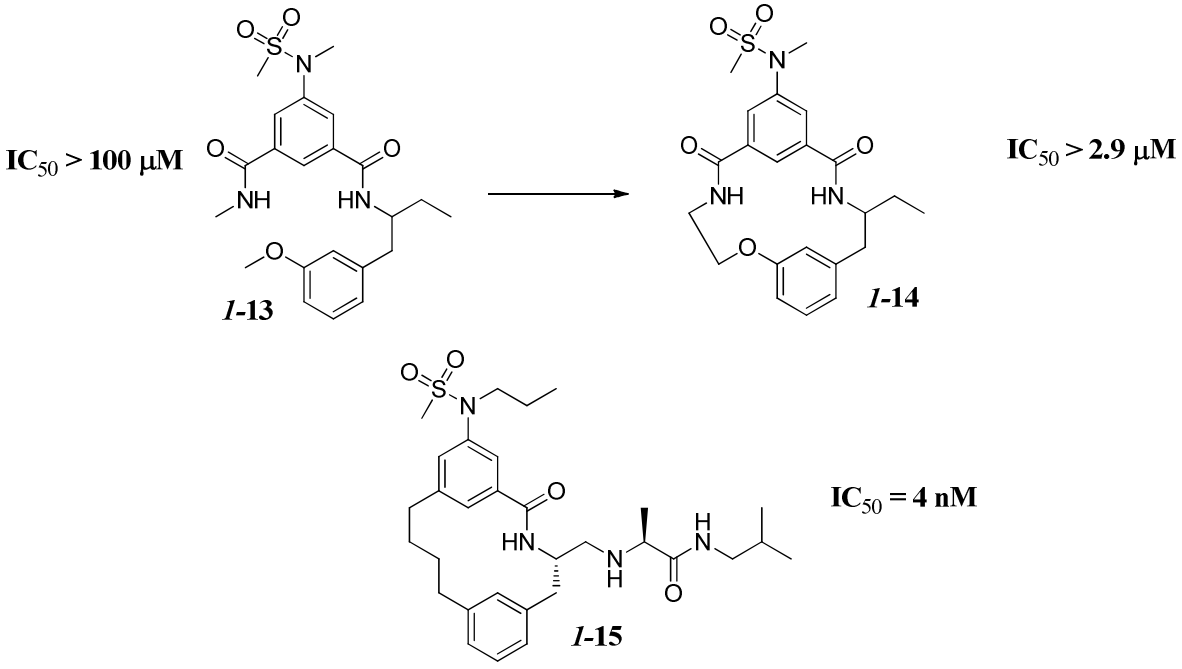

1.3.5 1,2,3-Triazoles as amide surrogates

The previous discussion has summarized published work by other authors that highlights the importance of reducing the peptidic character of the BACE1 inhibitors to achieve cellular and brain penetration. 1,2,3-Triazoles have been shown to be effective amide surrogates in applications such as acetylcholinesterase inhibitors[55] and HIV-1 protease inhibitors.[56] The large dipole in addition to the ability of the sp^2 nitrogen atoms to serve as hydrogen bond acceptors make the 1,2,3-triazole an effective amide mimic.[56] Furthermore, replacement of the P2 amide by an *anti*-triazole confers a strong structural resemblance to a potent Merck oxadiazole inhibitor (***1*-16,** Figure 1.13).[57] An X-ray crystal structure of ***1*-16** bound to BACE1 demonstrated the oxadiazole nitrogens mimic a P2 amide carbonyl in receiving an H-bond from Q73 (PDB ID 2IRZ).[57]

Figure 1.13 Merck oxadiazole inhibitor and our proposed triazole linked inhibitors

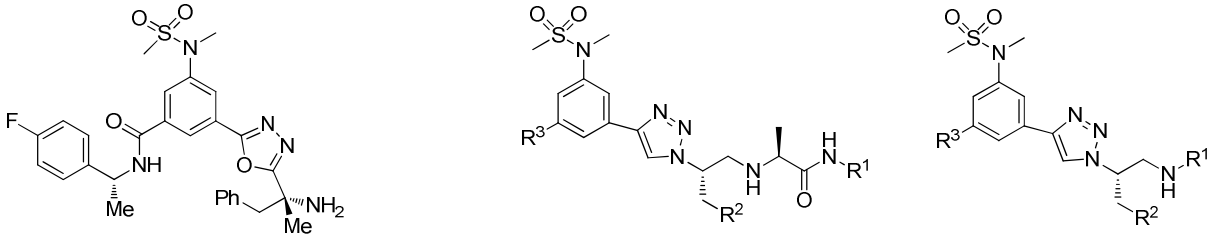

We expect the triazole nitrogens in ***1*-17** or ***1*-18** can serve the same function. Additionally, the incorporation of a 1,2,3-triazole allows exploration via fragment-based drug design (*in-situ* "click" chemistry) and high throughput screening (copper-catalyzed microtiter plate screening) as we will describe below.[56,58-62]

1.4 Synthesis and screening of our 1,2,3-triazole containing inhibitors

1.4.1 Synthesis of acetylenes and azides

The synthesis of our P2 acetylenes is shown in Scheme 1.1. Commercially available 3-bromoaniline ***1*-19** was converted into the methyl sulfonamide over two steps in relatively high yield to give ***1*-20**.[63] The methylsulfonamide was then subjected to Sonogashira cross-coupling conditions to yield the TMS protected acetylene[64] which was subsequently deprotected to give ***1*-21**.[65] We plan to use several different acetylenes and azides in our microtiter plate based screening and will designate each acetylene fragment by **A** and each azide by **Z**. Since ***1*-21** is the first acetylene presented in our synthesis, it is designated **A1**.

***Scheme 1.1. Synthesis of acetylene fragment 1*-21 (A1) lacking a P3 substituent**

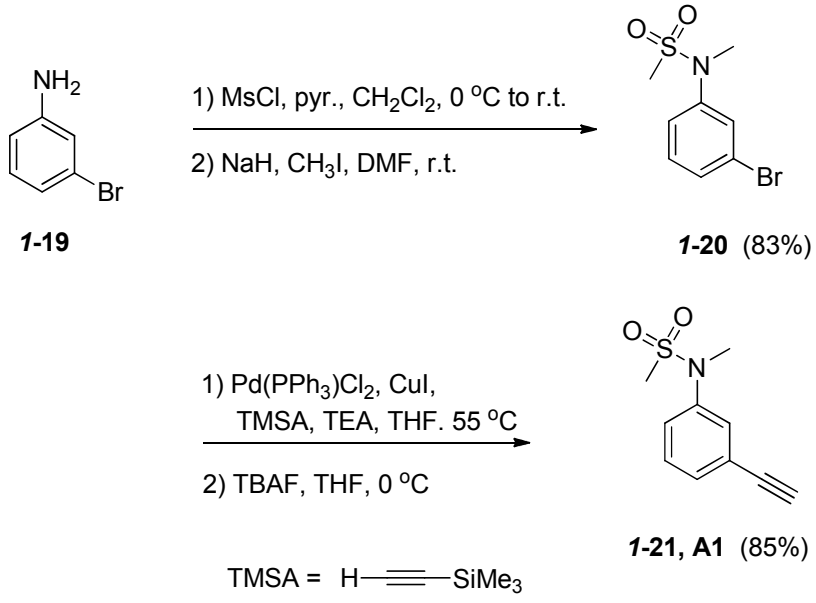

***1*-19** ***1*-20** (83%)

***1*-21, A1** (85%)

As previously discussed, the S3 pocket of the enzyme can be explored by incorporating P3 substituent on our P2 acetylenes. The different amides will help probe the SAR for the S3 pocket. In order to streamline the synthesis, a carboxylic acid precursor was synthesized.

Bromination of 3-nitrobenzoic acid ***1*-22** with NBS and sulfuric acid gave the aryl bromide ***1*-23** in high yield;[66] Esterification and reduction of the nitro group gave ***1*-24**.[67] The aniline was converted to the *N*-methyl sulfonamide over two steps,[63] followed by ester hydrolysis to furnish the carboxylic acid ***1*-25**.

Scheme 1.2. Synthesis of carboxylic acid precursor

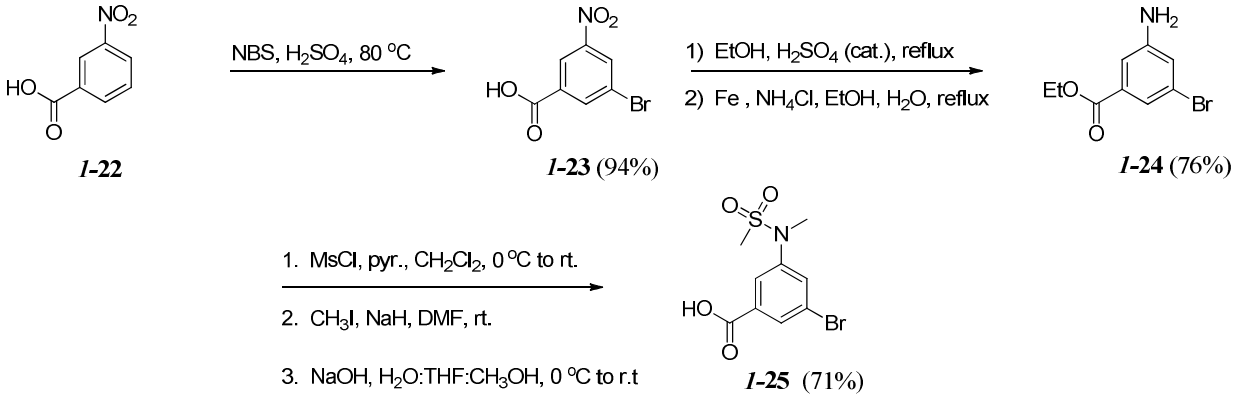

***1*-22** ***1*-23** (94%) ***1*-24** (76%)

***1*-25** (71%)

With ***1*-25** in hand, three steps remained to arrive at the requisite acetylene. Amide condensation gave the requisite P3 amides ***1*-26a-c**. Sonogashira cross-coupling followed by removal of the trimethylsilyl protecting group, gave acetylenes ***1*-27a-c**.[64,65]

Scheme 1.3. Synthesis of acetylenes *1*-27a-c (A2-A4).

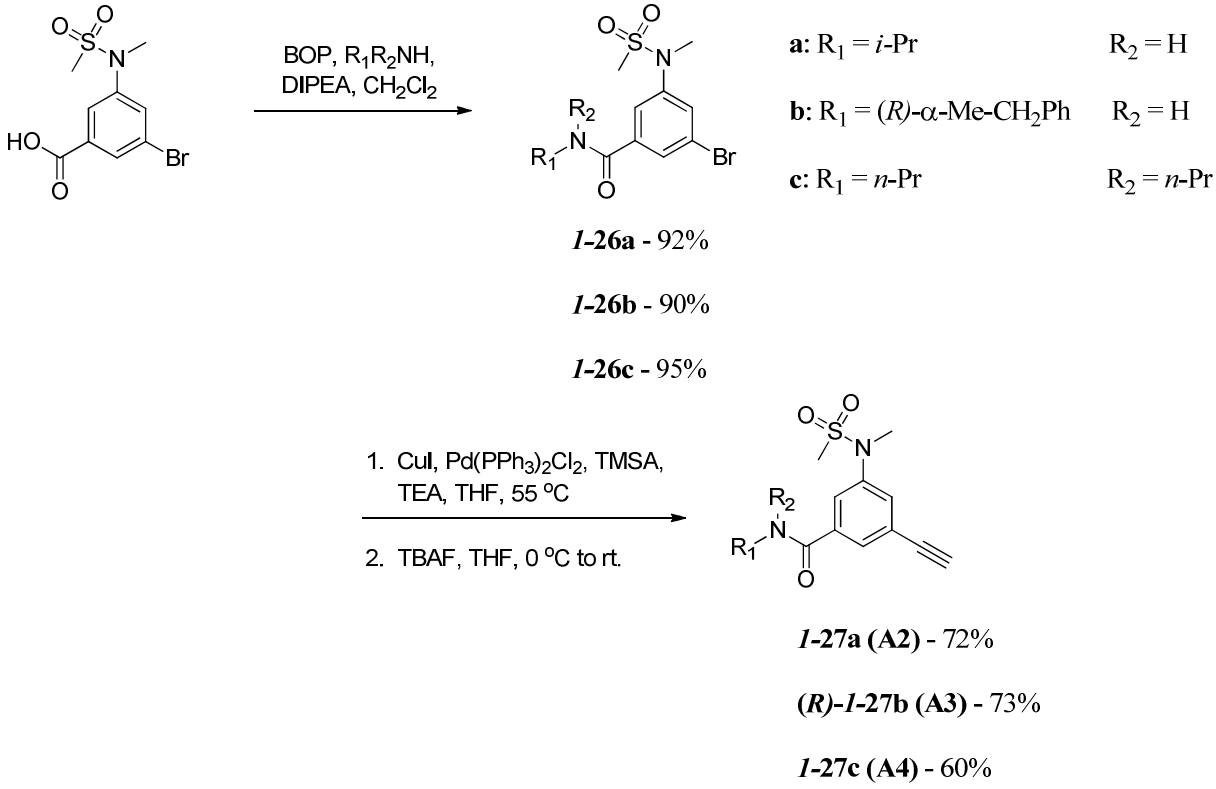

Our attention was then turned to the synthesis of the azide fragments, which are based on (*S*)-alanine. The synthesis of the azides starts with the amide condensation of Z-Ala-OH using the BOP reagent to furnish the amides (*S*)-***1*-29a-d** in high yield (Scheme 1.4).[51]

Scheme 1.4. Amide condensation and hydrogenolysis.

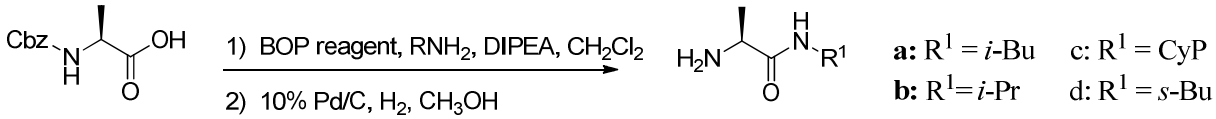

(*S*)-***1*-28**

(*S*)-***1*-29a** (97%)

(*S*)-***1*-29b** (99%)

(*S*)-**1-29c** (91%)

(*S*)-***1*-29d** (83%)

The key step in the construction of a reduced amide isostere is the reductive amination using an aldehyde and amine. The aldehyde was prepared via the Swern oxidation using either the commercially available Z-Phe-ol or Z-Leu-ol (synthesized from (*S*)-Leu-ol and benzylchloroformate).[68] The crude aldehyde was used directly in the reductive amination with the free bases (*S*)-**29a-d**, to give the requisite secondary amines (*S,S*)-***1*-32a-d** and (*S,S*)-***1*-33a-d** (Table 1.4) in moderate yield.

Table 1.4. Results of our reductive amination and diazotransfer

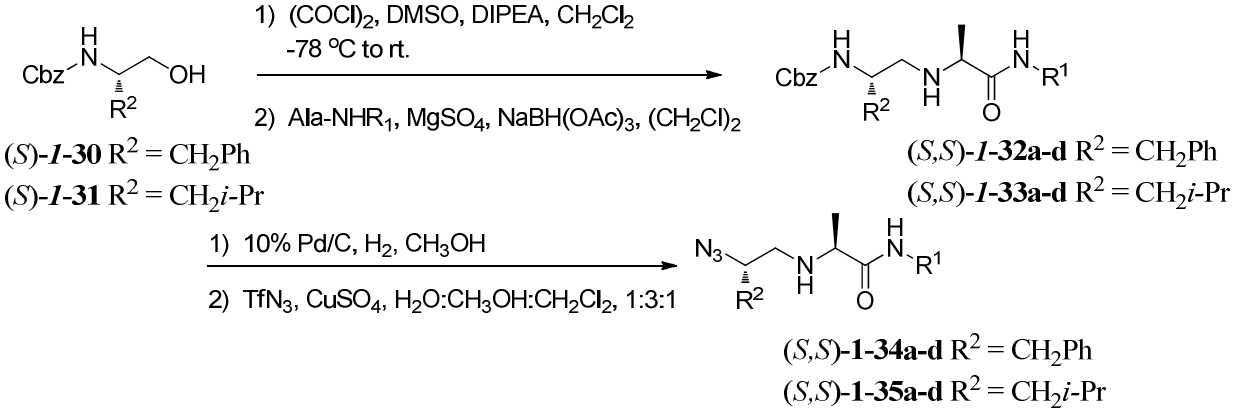

Entry	*R_2*	*R_1*	*Yield for reductive amination*	*Yield for diazotransfer*
1	CH_2Ph	*i*-Bu	***1*-32a** - 64%	***1*-34a** - 60% **Z1**
2	CH_2Ph	*i*-Pr	***1*-32b** - 33%	***1*-34b** - 88% **Z2**
3	CH_2Ph	CyP	***1*-32c** - 66%	***1*-34c** - 67% **Z3**
4	CH_2Ph	*s*-Bu	***1*-32d** - 73%	***1*-34d** - 75% **Z4**
5	CH_2*i*-Pr	*i*-Bu	***1*-33a** - 42%	***1*-35a** - 81% **Z5**
6	CH_2*i*-Pr	*i*-Pr	***1*-33b** - 50%	***1*-35b** - 66% **Z6**
7	CH_2*i*-Pr	CyP	***1*-33c** - 54%	***1*-35c** - 65% **Z7**
8	CH_2*i*-Pr	*s*-Bu	***1*-33d** - 52%	***1*-35d** - 70% **Z8**

Following hydrogenolysis, the substrate contained two amine groups. We discovered that *only* the primary amine reacted in the final diazotransfer reaction to yield the azides ***1*-34a-d** and ***1*-35 a-d** (**Z1-Z8**) in moderate yield. This finding is consistent with the mechanism proposed by Nyffeler et al.,[69] but to our knowledge this is the first example of the diazotransfer reaction performed in the presence of a secondary amine. For azides ***1*-38a-d**, commercially available Boc-Phe-ol (*S*)-***1*-36** was converted via the Swern oxidation[68] to the aldehyde which was immediately used in the reductive (Scheme 1.4) amination with the corresponding benzylic amines to give (*S*)-***1*-37a-d**.

Scheme 1.5. Synthesis of non-peptidomimetic azides

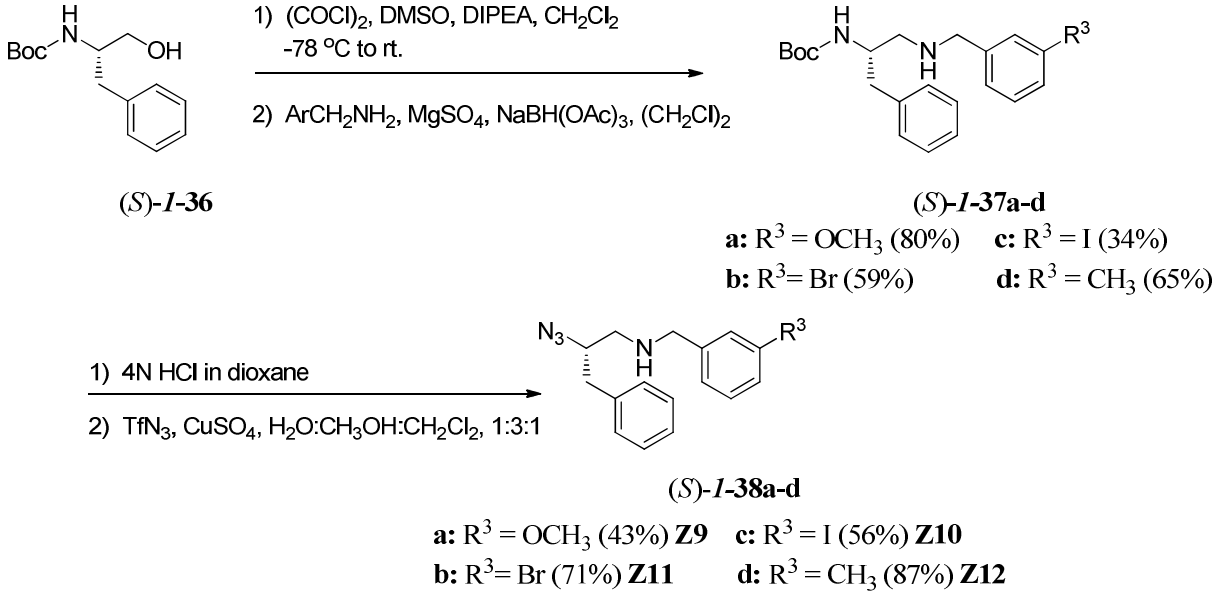

Removal of the Boc group followed by diazotransfer in the presence of an unprotected secondary amine, furnished the non-peptidic azide building blocks (*S*)-***1*-38a-d** (**Z9-Z12**).

1.4.2 CuAAC reaction

With the desired building blocks in hand (**A1-A3**, **Z1-Z12**), a select group of 12 *anti*-triazole-linked BACE1 inhibitor candidates was prepared using the copper(I)-catalyzed azide acetylene cycloadditon (CuAAC), in yields ranging from 40-75%. Compounds were purified by column chromatography and their identity and purity confirmed by ^{1}H and ^{13}C NMR spectroscopy and high resolution mass spectrometry (Figure 1.14). The structures are numbered according to the acetylene and azide to prepare them, and our laboratory's PRC identifiers are also given in Figure 1.14.

Figure 1.14. Triazoles synthesized by preparative CuAAC

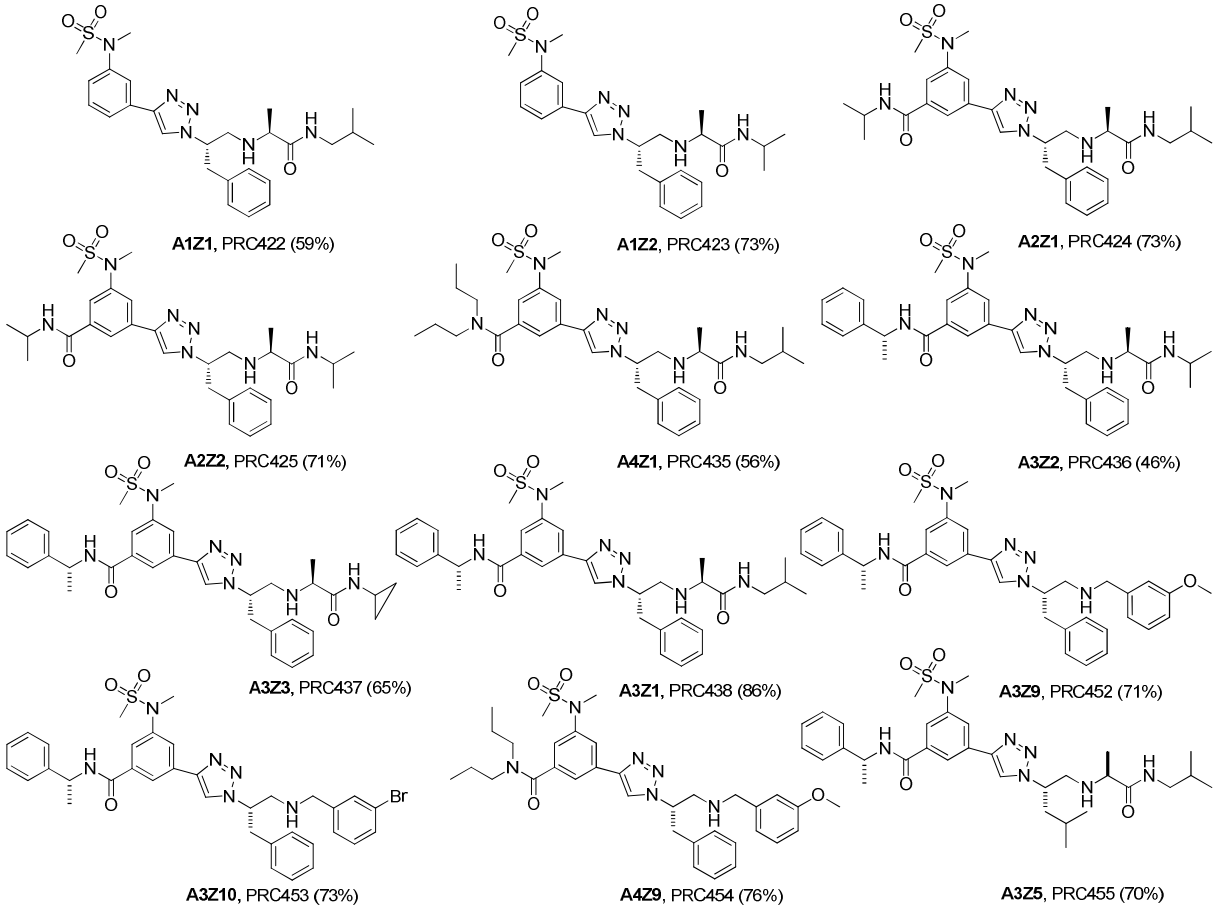

1.4.3 The BACE1 FRET Assay

Compounds were evaluated for BACE1 inhibition in the laboratory of our previous Georgetown University Hospital collaborator Professor Yasuji Matsuoka (in the department of Neurology until June 2008). Assays were performed by his technician, Chiho Hirate-Fukae, and on one occasion the author spent 2 days at Georgetown assisting with the assay. A FRET-based TruPoint^{TM} Beta-Secretase Assay Kit^{384} (Perkin-Elmer) was used to assess BACE1 activity. FRET (fluorescence resonance energy transfer) is a photochemical process where a fluorophore

transfers radiationless electronic energy from a donor (**D**) to another nearby chromophore, the acceptor (**A**).[70] The acceptor can accept the quantum of electronic energy, thereby quenching fluorescence. The efficiency (*E*) of this quenching process is inversely proportional to the sixth power of the distance between **D** and **A** ($E \alpha 1/r^6$).[71] When the distance between **D** and **A** becomes great enough, the quenching is negligible and the quantum yield of the fluorophore is restored. In the BACE1 FRET assay, a BACE1 substrate based upon the Swedish mutation is modified to incorporate a proprietary fluorescent europium chelate at one end (**D**) and a proprietary quencher (**A**, QSY® 7) at the other. Upon BACE1 cleavage the **D-A** distance is greatly increased leading to a lanthanide fluorescence of the D can be detected by a fluorometer (Figure 1.15).[70] Thus at low inhibition (high BACE1 activity), fluorescence will be high, whereas for high inhibition (low BACE1 activity), fluorescence will be low.

Figure 1.15. Concept of the FRET assay *(Figure adapted from CoreHTS® BACE1 Assay Kit protocol).*

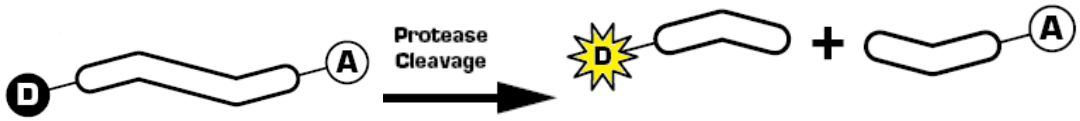

For our assay, compounds were assayed at final concentrations of 6.25 and 0.625 uM, and a known nanomolar potent BACE1 inhibitor, Inhibitor IV (Calbiochem product no. 56578) was used as a positive control at 62.5 and 6.25 nM. The first set of inhibitor candidates sent for assay (**A1Z1, A1Z2, A2Z1,** and **A2Z2**, PRC422-425 respectively) did not exhibit appreciable dose-dependent inhibition under these conditions. However, assay of subsequent inhibitor

candidates (PRC435-438 and PRC452-455) did evidence dose-dependent inhibition (Figure 1.16).

Figure 1.16. Assay of Triazole inhibitors PRC435-438 and PRC452-455.

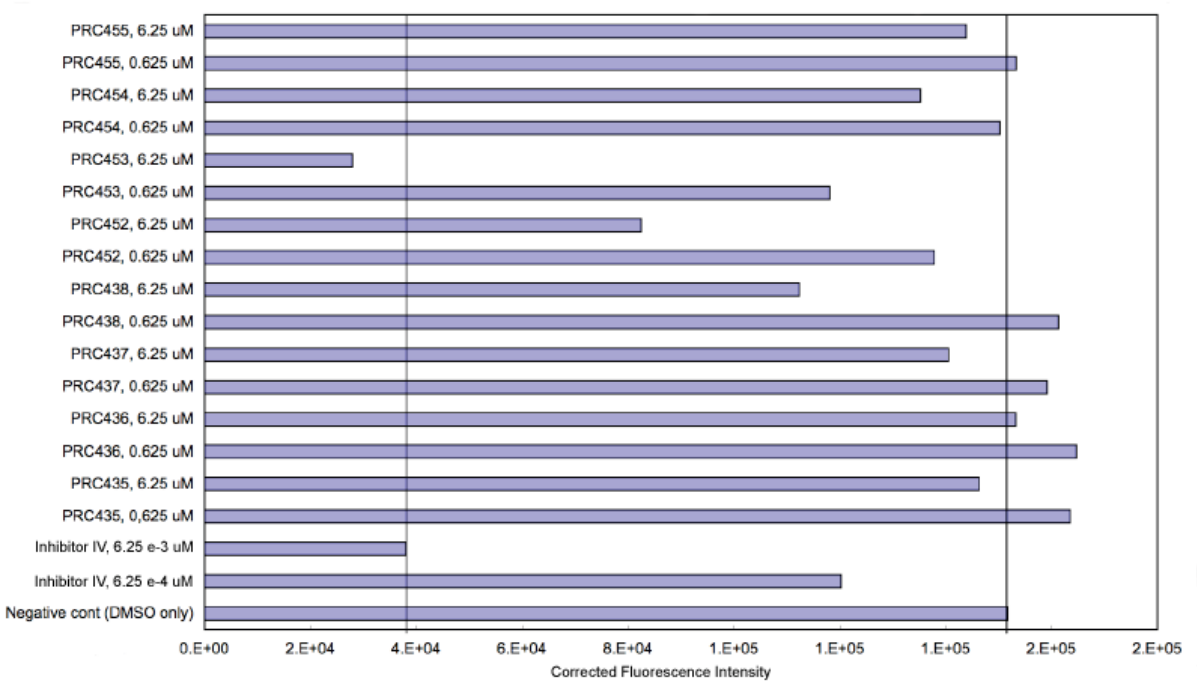

The length of the bars correspond to corrected fluorescence in fluorescence units. Low fluorescence is observed when BACE1 is inhibited.

In particular Figure 1.16 shows that triazoles PRC453 (**A3Z10**) and PRC452 (**A3Z9**) exhibit modest dose-dependent inhibition of BACE1. Calbiochem Inhibitor IV at the bottom of Figure 1.16 provides another example of dose-dependent inhibition, but is obviously much more potent than PRC452 (**A3Z9**) and PRC453 (**A3Z10**). Full dose-response data was then obtained for the positive control Inhibitor IV and PRC452 (**A3Z9**) and PRC453 (**A3Z10**). As shown in Figure 1.17, inhibitor IV has an apparent IC_{50} of 17.5 nM. Figure 1.17 also shows that our inhibitors, **A3Z9** and **A3Z10** have single digit micromolar IC_{50} values. With these results in

hand we were relatively confident we could find a more potent inhibitor if we were to sample a larger chemical space.

Figure 1.17. Dose response of Inhibitors A3Z9 (PRC 452) and A3Z10 (PRC 453) and Calbiochem Inhibitor IV

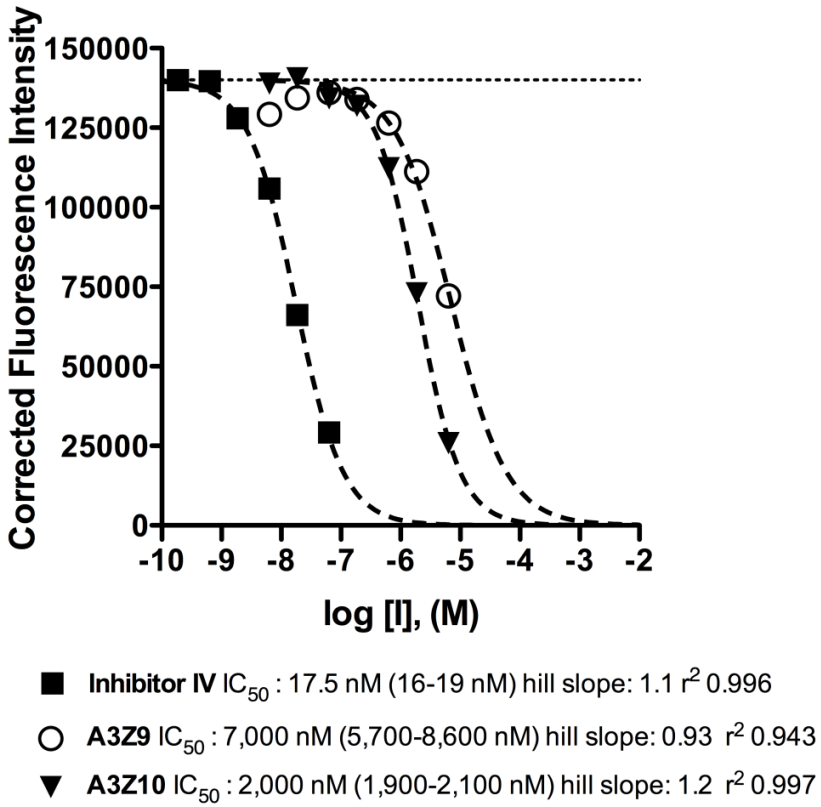

1.4.4 Microtiter Plate Based Screening

High throughput screening (HTS) is a technique used in drug discovery in which a library of potential hits is screened against a target (e.g. enzyme or transporter). Any compound that meets the desired criteria against the target is then modified into a lead compound. Microtiter plate-based screening, a useful HTS strategy developed by Brik et al. was successful in identifying several new HIV protease inhibitors.[72] This method relies upon high-yielding

reactions that are amenable to microscale and can be performed in the presence of water. The high-yielding reaction produces an inhibitor candidate from a set of building blocks, such as an amide from a carboxylic acid and amine. The reactions were run at a high concentration (> 5 mM) and were judged to be complete by either LC-MS or TLC analysis. Upon completion of the reaction, aliquots are taken, diluted to the micromolar range, and screened against the target. Any compounds showing greater than 50% inhibition were further diluted (e.g. nanomolar range). Compounds showing positive results in this screening, i.e. hits, were then synthesized using traditional solution phase techniques and screened as pure compounds.[73] Click chemistry is defined as a set of reactions that must be modular, wide in scope, high-yielding, generate innocuous byproducts, and stereospecific.[74] An example of such a reaction is the copper(I)-catalyzed azide acetylene cycloadditon (CuAAC).[74] This reaction is well suited for application in microtiter plate-based screening in that it is high-yielding and works best in aqueous media.

Lee and researchers were able to use the CuAAC reaction in microtiter screening to find a highly selective inhibitor for human α-1,3-fucosyltransferases (Fuc-T).[75] They modified a known active scaffold to incorporate an acetylene moiety, and then reacted with a library of 85 azides to arrive at the first nanomolar inhibitor of Fuc-T. Brik et al. was able to apply CuAAC microtiter plate-based screening in order to discover novel HIV-1 PR inhibitors.[76] Two different azide cores (***1*-39** and ***1*-40**, Figure 1.18) and 50 different acetylene cores were screened. The azide cores were dissolved in *t*-BuOH (10 mM) and 200 μL of this solution was dispensed into different vials each containing the corresponding acetylene, 200 mL of $CuSO_4$ (300 μM, aqueous), and a small piece of copper turning to give 100 different binary combinations (Figure 1.18) to be screened against HIV-1 Pr. After incubation at 48 h, LC-MS analysis indicated full consumption of the azide core.

Figure 1.18. Microtiter plate-based screening to generate HIV-1 Pr inhibitors.[76]

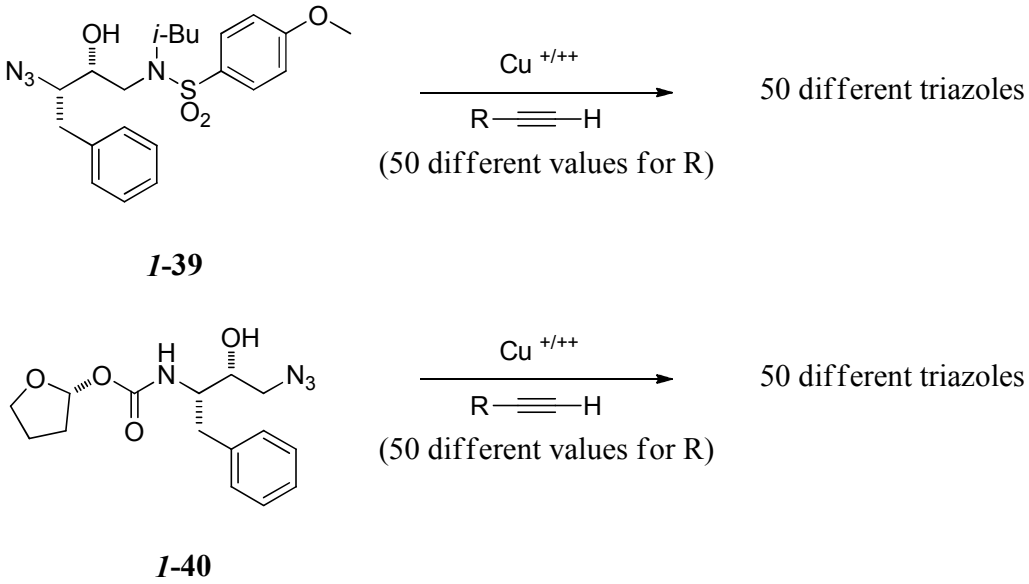

1.4.5 Our Microtiter Plate Based Screening

Based on the findings of Brik et al., we adopted a similar approach in the design of our BACE1 inhibitors. In addition to the acetylenes **A1-A4** which were prepared in our laboratory (cf. Schemes 1.1 and 1.3), acetylenes **A5-A10** donated from the Sharpless lab (Figure 1.19) were added to our screening allow us to sample a larger chemical space. As will be discussed in Chapter 2, the sample of **A10** actually inspired a separate research program in our laboratory. Since 1,4-diethynyl benzene is bifunctional and could make triazole dimers, we gave it two different designations based on the equivalents used for the CuAAC reaction (**A8** 1 equiv.; **A9** 3.6 equiv.).

Figure 1.19. **Additional acetylenes provided by the Sharpless laboratory** *(A5, A6, A8/A9 are commercially available).*

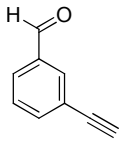

A_5

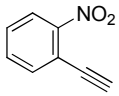

A_6

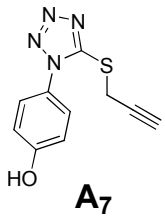

A_7

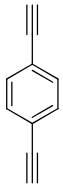

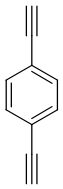

A_8 **A_9 - 3.6 equiv**

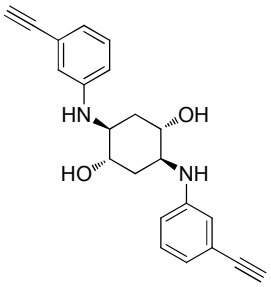

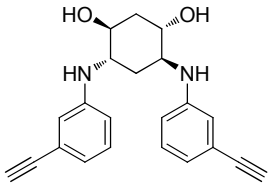

A_{10} - mixture of regioisomers

Azides **Z1-Z12** were prepared in our laboratory as described above (cf. Table 1.4 and Scheme 1.4). To carry out our microtiter plate-based screening we made some modifications to the previously described procedure of Brik et al.[76] In brief, we omitted the copper turning and used sodium ascorbate to generate the required Cu(I) species. We also added acetonitrile as a co-solvent with *t*-BuOH. In detail, a 20 mM solution of an azide in tert-butanol (100 uL) was combined with a 24 mM solution of an acetylene in acetonitrile (100 uL) and 200 uL of water containing copper sulfate (0.5 mM) and sodium ascorbate (5 mM) in a 1 dram scintillation vial. The vials were purged with argon, capped and sealed with parafilm, and shaken to achieve homogeneity. After 5 days at room temperature, LC/MS analysis of the **A2Z1** reaction indicated greater than 95% consumption of the azide and formation of the expected triazole. We thus applied this protocol to prepare all possible combinations of **A1-A10** with **Z1-Z12**. After 5 days,

these reactions were diluted 31.25-fold with water to achieve a nominal inhibitor concentration of 160 uM, assuming quantitative conversion of the azide to the triazole. These nominally 160 uM solutions were then used directly in the BACE1 assay (Perkin Elmer TruPoint™ Beta-Secretase Assay Kit), which affords a nominal 10 uM final concentration in the assay. Note that the final concentration of $Cu(^{+}/^{++})$ and ascorbate in the assay were 4 μM and 40 μM respectively. Of the 120 compounds screened, 3 binary combinations of azide and acetylene appeared to show significant inhibition at 10 uM (Figure 1.20).

Figure 1.20. Results of the microtiter screening.

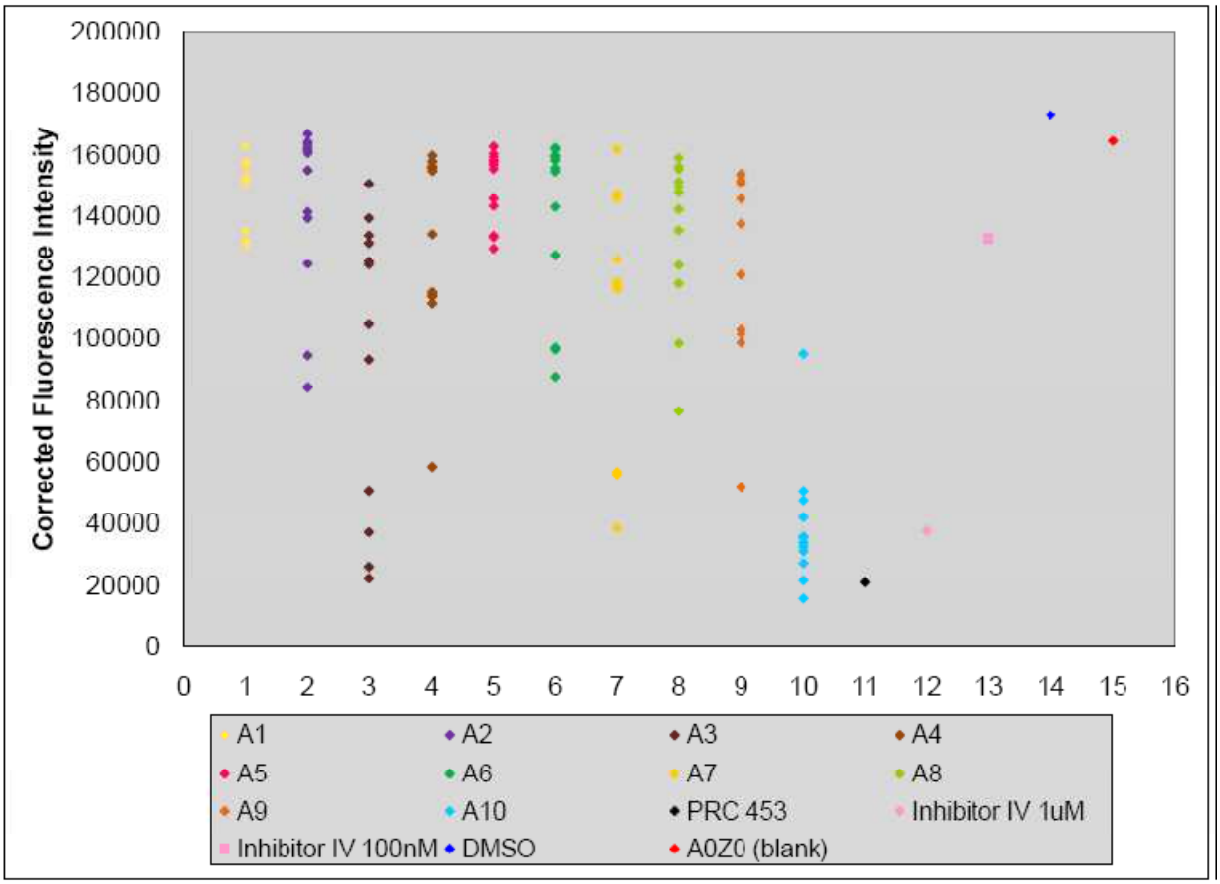

Each column represents an acetylene (**A1-A10** cf. Scheme 1.1, Scheme 1.3, andFigure 1.19) denoted by a color which is paired with 12 azides (Z1-Z12 Table 1.4) to form an *anti*-triazole. Lower fluorescence indicates greater inhibition by the triazole.

Each column in Figure 1.20 contains an acetylene (**A1-A10**) and each dot represents an *anti*-triazole formed from the 12 azides used. The **DMSO** column (column 11) represents a single point analysis that contained only DMSO, water, and fluorogenic substrate. The **A0Z0** column (column 12) contains the components of the DMSO column plus the $CuSO_4$ and ascorbate catalysts affording us with a blank. These negative controls were incorporated into the assay to ensure the CuAAC components and solvents did not quench fluorescence. Additionally, controls were incorporated in which no copper was added to ensure that the acetylenes or azides alone were not responsible for any quenching (this data is not shown in Figure 1.20). Gratifyingly **A3Z9** and **A3Z10** (Figure 1.20 the two lowest data points in the **A3** column) appeared to show modest inhibition in the microtiter-plate based assay, just as these two triazoles had in the FRET based assay discussed previously. However, we were quite surprised to see a new binary combination **A10Z10** emerge**.** The regioisomers of **A10** were separated (**A10a** – C_i symmetric diol and **A10b** – C_2 symmetric diol). These compounds were then synthesized via the copper-catalyzed azide acetylene cycloaddition (CuAAC) to give authentic samples to be assayed. Unfortunately, the compounds only showed modest inhibition of BACE1 (Figure 1.21). Several negative controls were incorporated into the assay to ensure the CuAAC components such as solvents, $Cu^{2+,}$ and ascorbate did not quench fluorescence.

Figure 1.21. Dose response of Inhibitors A10aZ10 and A10bZ10 and Calbiochem Inhibitor IV.

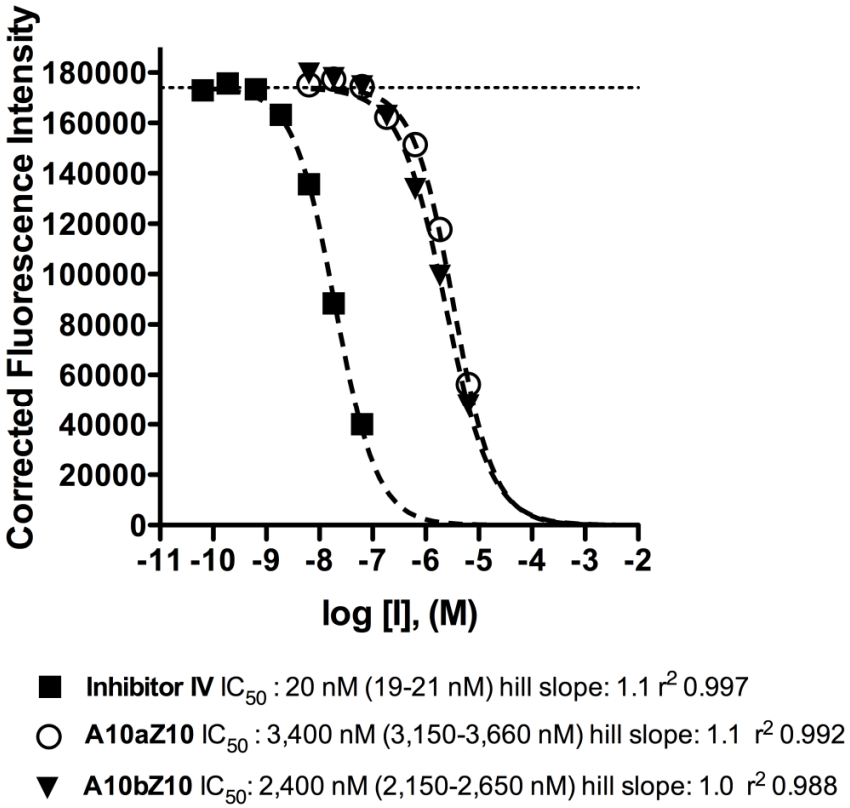

1.5 *In silico* docking of our triazole linked BACE1 inhibitors

To assess why our replacement of the oxadiazole heterocycle in ligand **16** (Figure 1.13) with a similar 1,2,3-triazole **A3Z10** caused a significant loss in BACE1 enzymatic potency our collaborators at Molsoft L.L.C were able to virtually (i.e. *in silico*) dock our inhibitors within the active site of the BACE1 enzyme. From the work of Rajapakse[77] they extracted the ligand ***1*-16** (Figure 1.22, PDB ID 2IRZ) co-crystallized within the BACE1 active site. The PDB object was then converted into an ICM (internal coordinate mechanics) object and the best docking pose within the active site was found through *in silico* docking. Here we can see that an ideally

placed ammonium moiety in ligand ***1*-16** forms a salt bridge with the Asp228 residue (Figure 1.22).

Figure 1.22. Ligand *1*-16 virtually docked by Molsoft from PDB 2IRZ.

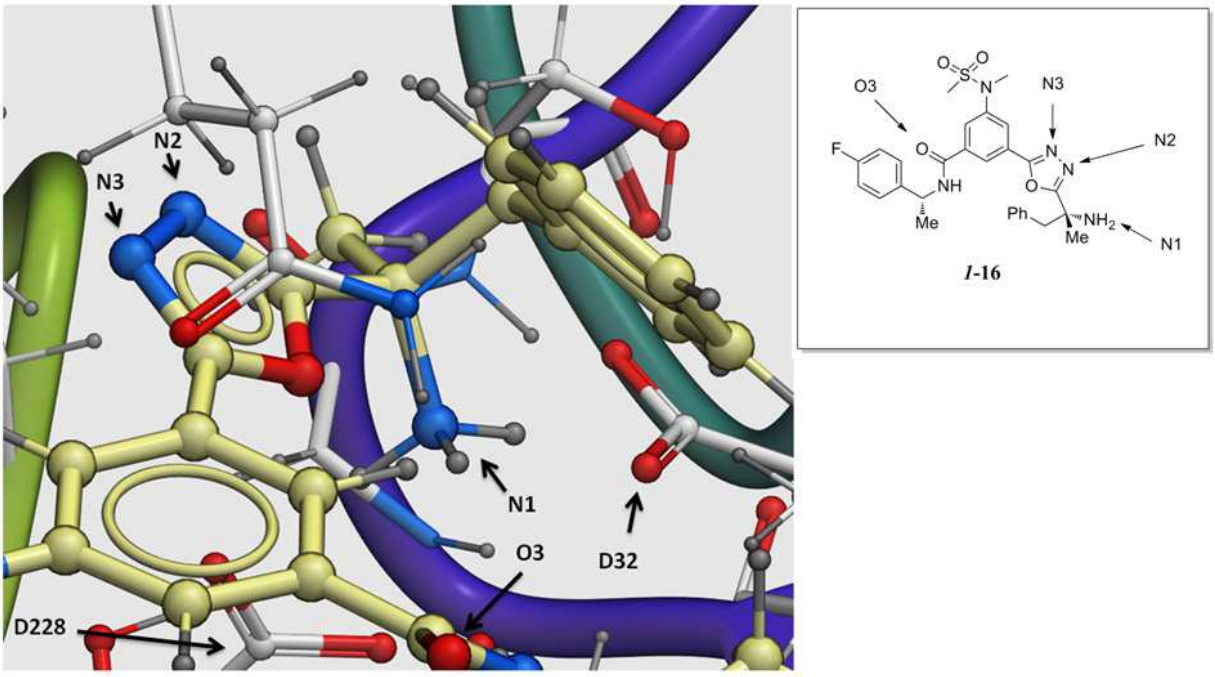

Figure 1.23 shows both ***1*-16** and our most potent 1,2,3-triazole heterocycle **A3Z10** overlaid in the active site of the enzyme. From Figure 1.23 it is apparent that the left hand portion both ligands (P3-P2) adopt a very similar docking pose.

Figure 1.23. Ligand *1*-16 and A3Z10 virtually docked and overlaid by Molsoft from PDB 2IRZ.

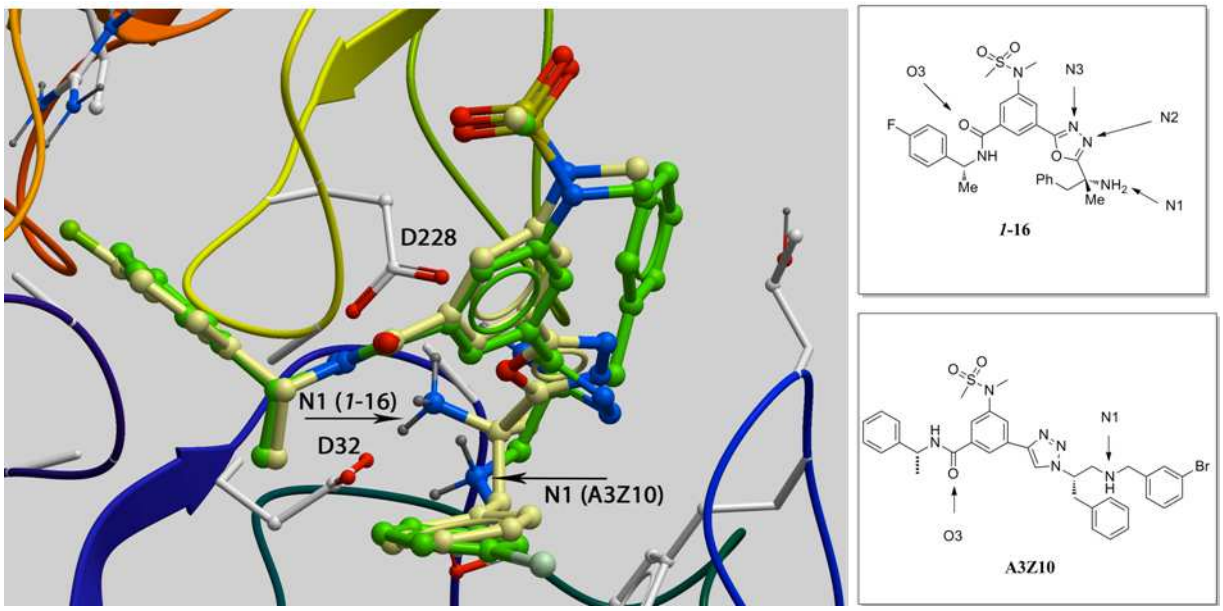

The carbon atoms in ***1*-16** are off-white and the carbon atoms in **A3Z10** are green.

However, we can clearly see that the ammonium (N1) is no longer in an optimal position in which to form a salt bridge to Asp228 residue (Figure 1.23) which is a feature of reduced amide BACE1 inhibitors (cf. Figure 1.11). Figure 1.24 shows only the A3Z10 ligand which we can directly compare to Figure 1.22.

Figure 1.24. Ligand A3Z10 docked by Molsoft from PDB 2IRZ.

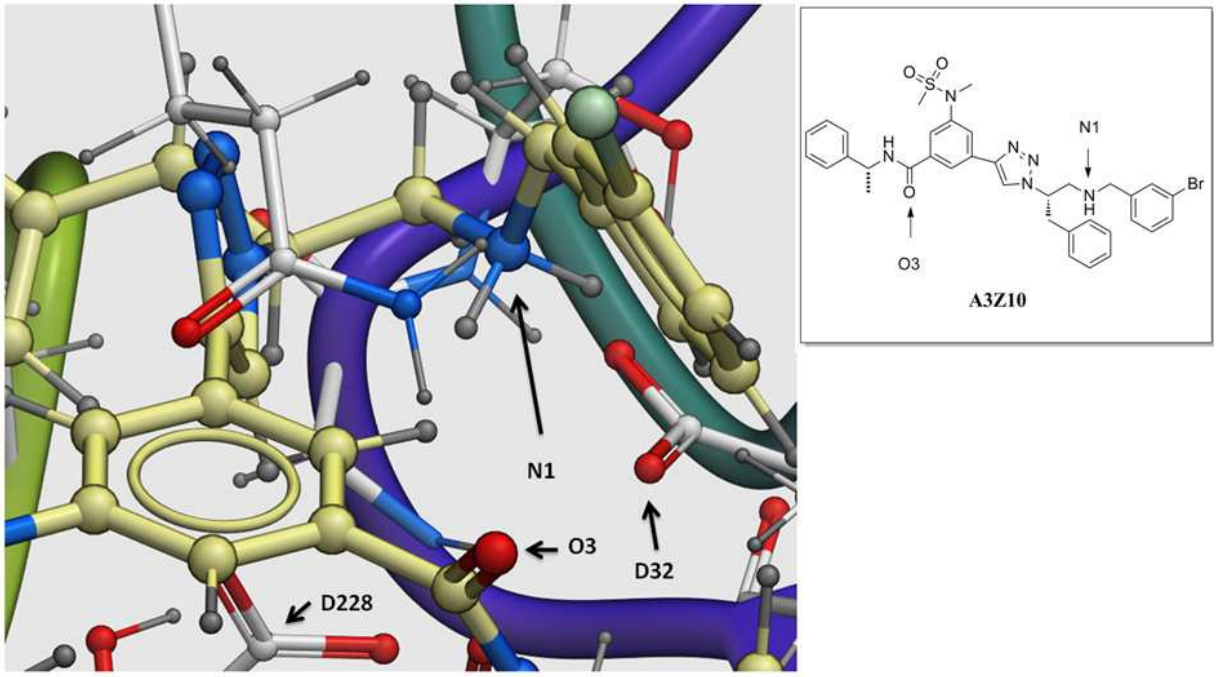

Based on these findings, significant modifications (such as the repositioning of the basic amine nitrogen in order to engage Asp228) of our lead compound **A3Z10** will be required in order to improve the potency of our ligands.

1.6 Conclusions from the Triazole linked BACE1 Inhibitor Project

In the course of this work, 120 reduced amide TSI compounds were screened using an original modification of the established Cu-catalyzed microtiter screening technique. Additionally, we have shown that the copper mediated diazotransfer reaction can be performed in the presence of unprotected secondary amines. Realization of this technology can expedite the construction of azides for application in “click” chemistry based drug discovery.

Chapter 2 Regioselective synthesis of aniline-derived 1,3- and C_i-symmetric 1,4-diols from 1,4-*trans*-cyclohexadiene-dioxide and the synthesis of aniline-derived 1,3- and 1,2-Diols from 1,3-*trans*-cyclohexadiene-dioxide

2.1 *Trans*-diaxial effect or the Fürst-Plattner rule

2.1.1 Applications of epoxides and arene oxides

Epoxides are quite reactive towards nucleophilic substitution due to the inherent ring strain in three membered rings. This high free energy is lowered considerably upon opening by the nucleophile (Scheme 2.1). Because of this reactivity towards nucleophilic opening, epoxides are useful synthetic intermediates in the formation of alcohols.[78]

Scheme 2.1. Nucleophilic opening of ethylene oxide (*2*-1) to give azidoalcohol (*2*-2).

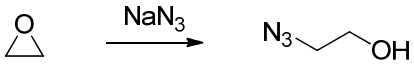

***2*-1** ***2*-2**

Epoxides also find application as biological intermediates. Aromatic hydrocarbons that enter the body can be enzymatically converted into arene oxides by the enzyme cytochrome P_{450} (CYP, Scheme 2.2). The arene oxide (***2*-4**) then has 2 different fates, a rearrangement pathway to give the phenol (***2*-5**) or nucleophilic attack to form the addition product (***2*-6**), both more water soluble than the hydrocarbon (***2*-3**) thus facilitating clearance.

Scheme 2.2. Oxidation of hydrocarbons by CYP to produce arene oxides.

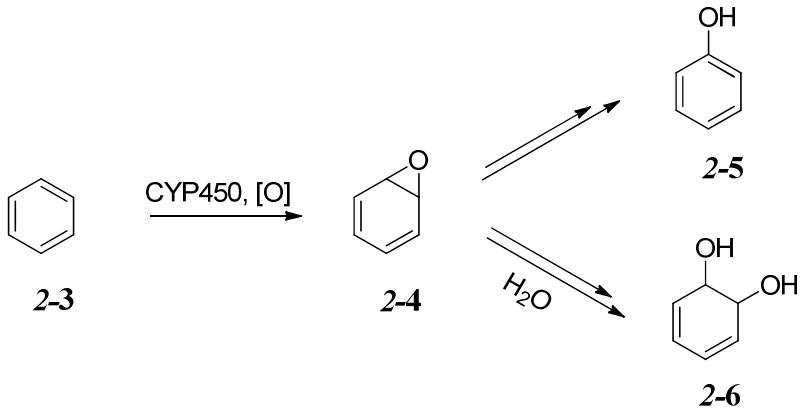

However, arene oxides can be carcinogenic if DNA components (such as nucleosides) open the arene oxide thus interfering with DNA transcription, which can lead to genetic mutations.[78]

2.1.2 Nucleophilic openings of epoxides

As a consequence of the stereoelectronic requirements of the S_N2 reaction, under basic or neutral conditions, the opening of a symmetrical epoxide (***2*-7**, Scheme 3) proceeds via backside attack of one of the oxygen bearing carbons giving ***2*-8** (result of attack at C1) or its enantiomer *ent*-***2*-8** (attack at C2).[79]

Scheme 2.3. Nucleophilic opening of a symmetrical epoxide.

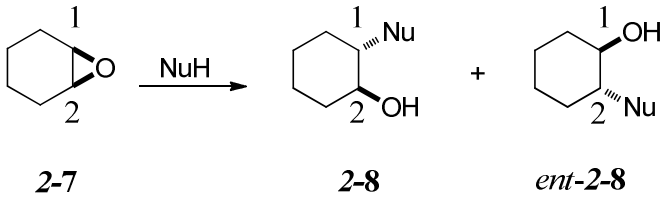

In the case of an unsymmetrical epoxide (Scheme 2.4, ***2*-9)**, two different regioisomers could be formed (Scheme 2.4). One possibility would yield product (***2*-10**) which is the consequence of nucleophilic attack at C2.

Scheme 2.4. Opening of a asymmetric epoxide.[79]

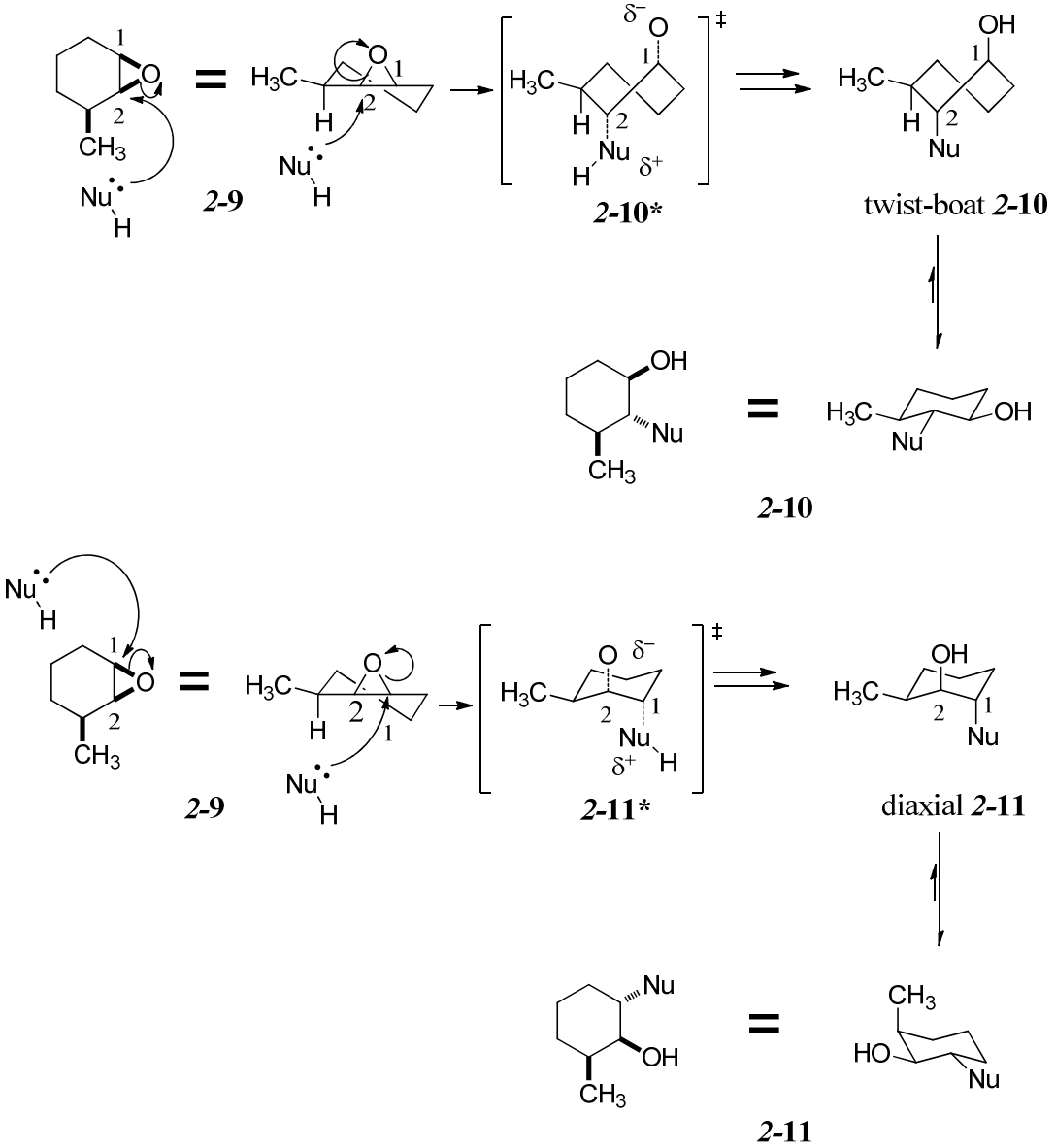

Although the product accommodates all heavy atoms in a favorable equatorial relationship, the stereoelectronic requirements of the S_N2 reaction require that the opening at C2 go through a high energy twist boat TS (***2*-10***) thus being the less favorable pathway. The favored pathway involves nucleophilic attack at C1 which would give a lower energy diaxial chair TS (***2*-11***), the initially formed diaxial conformer would then ring flip to accommodate as many equatorial heavy atoms (***2*-11**) as possible.[80] This regiocontrol phenomenon is known as the *trans*-diaxial effect, or the Fürst-Plattner (FP) rule.[81,82]

2.2 Notable literature examples of the trans-diaxial effect and cyclohexane epoxides

2.2.1 Fürst-Plattner (FP) control

An example of the FP rule in a similar system was shown in the synthesis of (±)-deoxynojirimycin by Bagal et al.[83] In the course of their synthesis, a single diastereomer of a piperidine (*rac*-***2*-12**, relative configuration determined by X-ray crystallography) was reacted with trichloroacetic acid (Scheme 2.5). After protonation of the substrate, the conjugate base of trichloroacetic acid attacks the epoxide at C5 as per the Fürst-Plattner rule to give the *trans*-diaxial ring opening via a chair intermediate (*rac*-***2*-13**, relative stereochemistry determined by X-ray crystallography) in >99:1 dr.

Scheme 2.5. Ring opening reaction of a piperidine epoxide.[83]

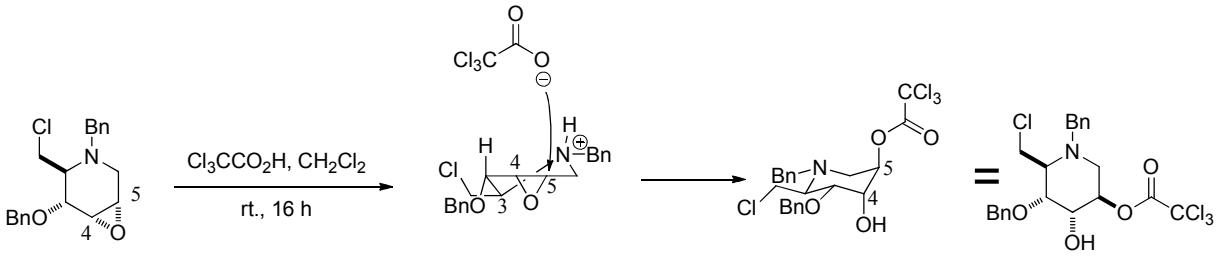

rac-***2*-12**

diaxial *rac*-***2*-13** (94%)

The Fürst-Plattner (FP) rule proved useful in the synthesis of β-amino alcohol chiral auxiliaries by Chrisman et al.[84] Here the researchers epoxidize enantiomerically pure (*R*)-(+)-limonene ((*R*)-(+)-***2*-14**) to give an inseparable 1:1 diastereomeric mixture of *cis*-limonene (***2*-15**) oxide and *trans*-limonene oxide (***2*-16**, Scheme 2.6).[85]

Scheme 2.6. Epoxidation of (*R*)-(+)-limonene.[85]

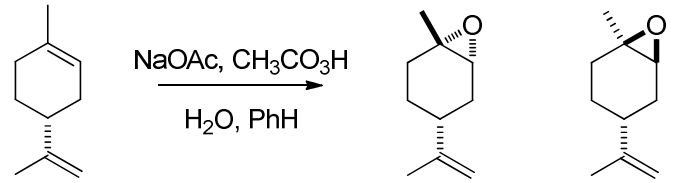

(*R*)-(+)-***2*-14** ***2*-15** ***2*-16**

1:1 Mixture

Nevertheless, when the diastereomeric mixture was treated with morpholine and a catalytic amount of water the researchers found that the *cis*-limonene oxide (***2*-15**) underwent ring opening with aqueous morpholine much faster than the *trans*-limonene oxide (Scheme 2.7, **16**).[84] Here the *cis*-limonene oxide undergoes regioselective FP opening at C2 to give (-)-(***2*-17**). For this substrate FP control matches the S_N2 preference for attack at the secondary carbon (C2)

over the tertiary C1. In the case of the *trans*-limonene oxide (***2*-16**), the FP controlled opening at C1 is much slower due to the fact S_N2 like reactions are highly disfavored at a tertiary center.

Scheme 2.7. Opening of limonene oxides with morpholine.[84]

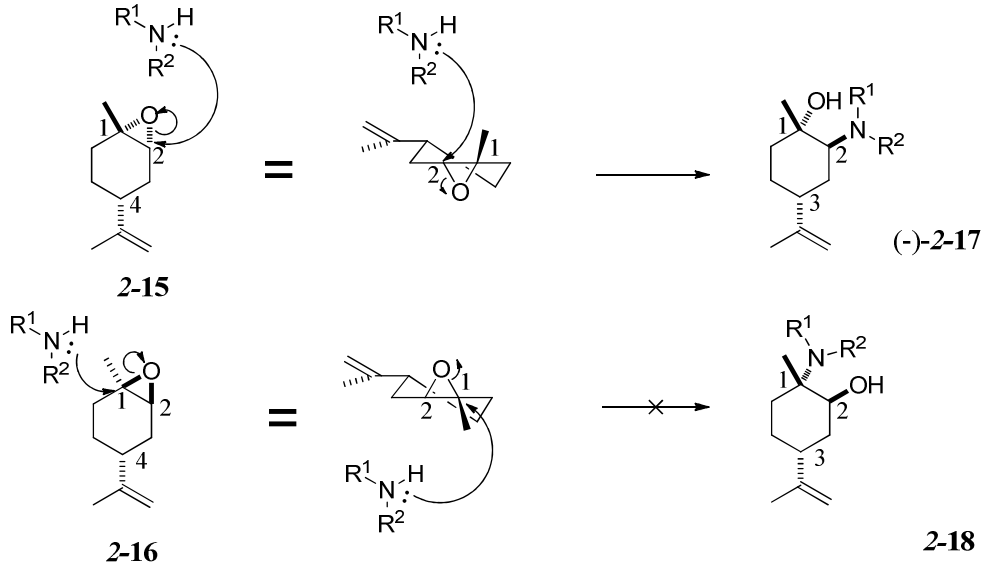

The researchers found that 12 hours was sufficient time to completely convert ***2*-15** to (-)-***2*-17** while leaving ***2*-16** unreacted. It is interesting to note that *neither* diastereomer underwent ring opening under solvent free conditions (T = 100 ^{o}C, 7 days) which emphasizes the effectiveness of water as a catalyst/medium in epoxide opening reactions.

2.2.2 Chelation controlled FP

(-)-Vesamicol is a potent inhibitor of the vesicular acetylcholine transporter (VAChT) which is used to probe presynaptic cholinergic mechanisms in order to better understand neurodegenerative diseases such as Alzheimer's Disease.[86] The Scheunemann group provided an example of FP controlled epoxide opening to arrive at novel derivatives of vesamicol which effectively inhibit VAChT.[87] The researchers start by partial elimination of 1,4-cyclohexane diol

(Scheme 2.8, ***2*-19**) followed by stereoselective epoxidation of the resulting homoallylic alcohol to give a diastereomerically pure epoxide (*rac*-***2*-20**). Finally *O*-benzylation furnishes their desired epoxide core (*rac*-***2*-21**).

Scheme 2.8. Synthesis of vesamicol analogues.[87]

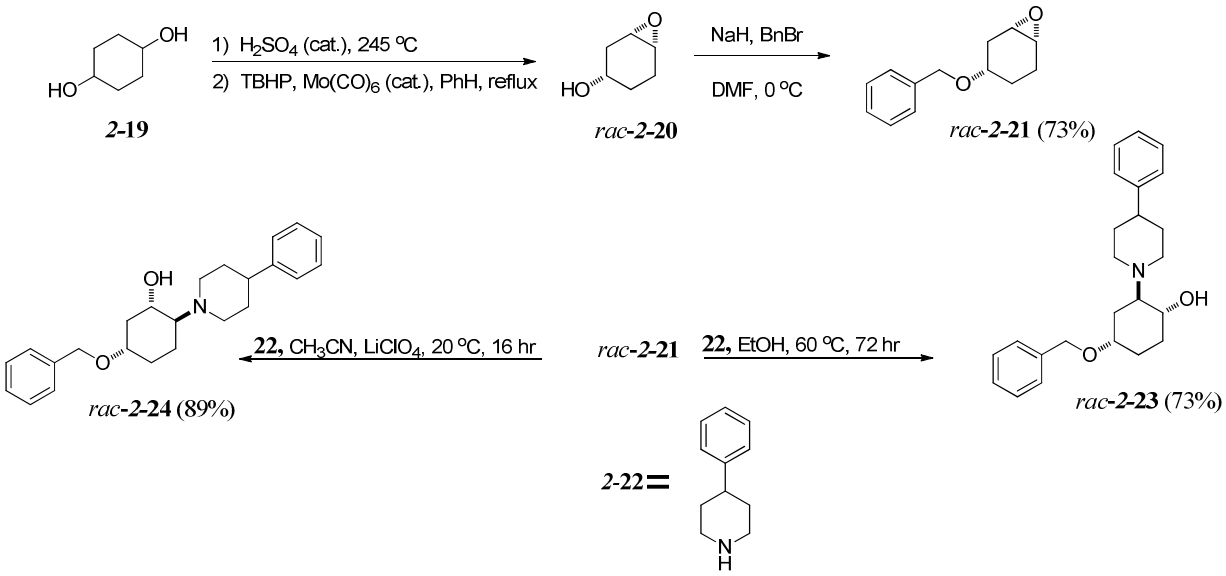

FP controlled epoxide opening of *rac*-***2*-21** with 4-phenylpiperidine (*rac*-***2*-22**) in ethanol gives *rac*-***2*-23** as a single regioisomer. However using lithium perchlorate in aprotic solvent, the researchers were able to synthesize the otherwise inaccessible regioisomer *rac*-***2*-24**. The phenomenon leading to *rac*-***2*-24** is known as chelation controlled FP epoxide opening.[88] In the case of the opening in ethanol solvent, the benzyloxy ether adopts an equatorial confirmation (Scheme 2.9, eq-*rac*-***2*-21**) and the epoxide accepts a hydrogen bond from the ethanol solvent to catalyze the opening. This would result in the expected FP controlled product *rac*-***2*-23**. When an aprotic solvent such as acetonitrile is used, the lithium cation chelates to the pendant benzyl ether oxygen atom *and* the epoxy oxygen atom. In order to achieve this intramolecular

chelation, the benzyl ether must adopt an axial conformation (ax-*rac*-***2*-21**).[89] The lithium cation then serves as a Lewis acid catalyst for the FP controlled ring opening to give the chelation controlled regioisomer *rac*-***2*-24.**

Scheme 2.9. Chelation controlled FP epoxide opening.[88-90]

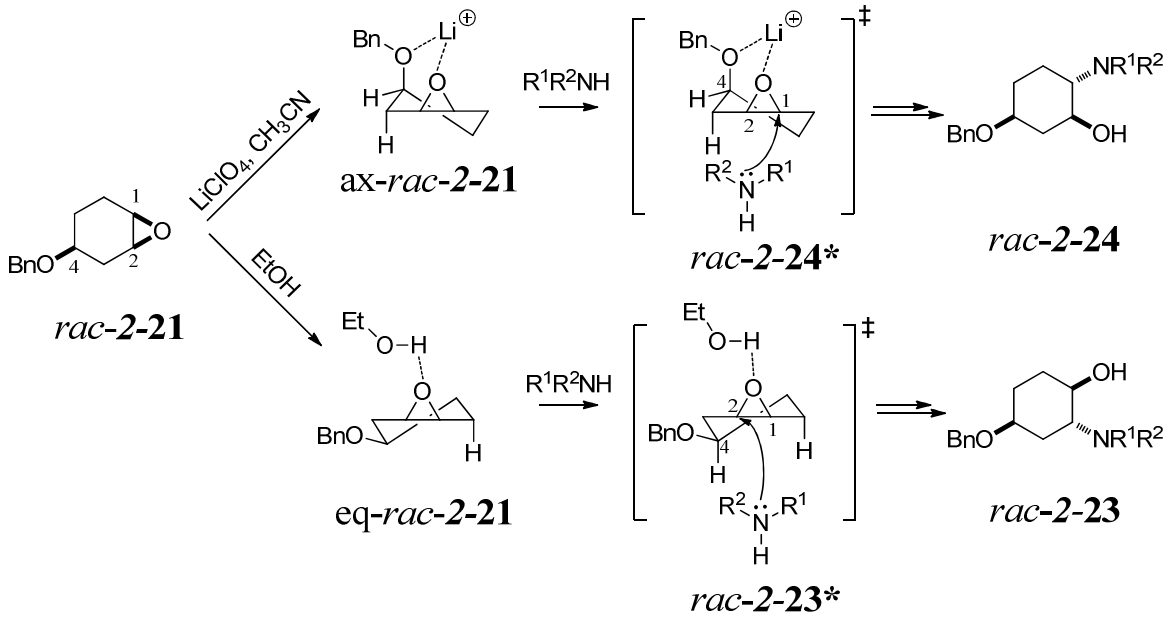

2.2.3 Intramolecular H-bond FP control

Another example of how judicious choice of reaction conditions can favor one FP pathway over another was provided by the Sharpless group. Here the researchers show that the regioselectivity can be controlled by solvent choice. Their example employs *cis*-cyclohexadiene diepoxide (***2*-25**) and its opening with benzyl amine. Under solvent free (neat) conditions, the first epoxide is opened by the benzyl amine presumably through neat autocatalysis[74,91] to give the epoxy amino alcohol (*rac*-***2*-26**, Scheme 2.10).

Scheme 2.10. Ring opening of *cis*-1,2:4,5-cyclohexadiene diepoxide with $BnNH_2$.[74]

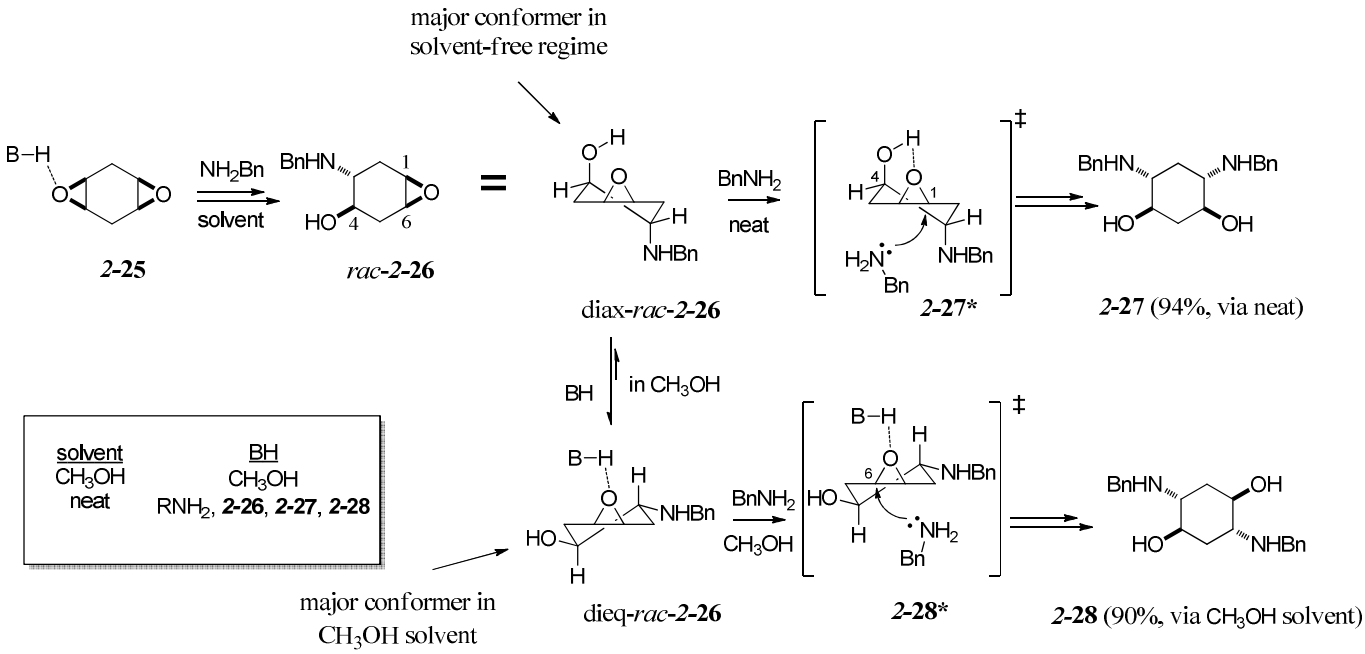

In methanol, the protic solvent assists in the first epoxide opening by H-bond activation to give the same epoxy amino alcohol (*rac*-***2***-**26**). At this point, two pathways emerge, based on the nature of the solvent. For the second epoxide opening in the neat pathway, the epoxide is best activated by an *intramolecular* H-bond from the pendant hydroxyl group (Scheme 2.10, ***2***-**27***) which can only occur when the hydroxyl is in a pseudoaxial position. Subsequent FP controlled epoxide opening occurs transition state ***2***-**27*** to yield ***2***-**27** as a single regioisomer.[74] In the case of the reaction in methanol, the methanol serves as an *intermolecular* H-bond catalyst for the second epoxide opening. Additionally, methanol as a *solvent* would overwhelm any intramolecular H-bonding rendering the diax-*rac*-***2***-**26** conformer energetically unfavorable. Thus ring opening preferentially occurs via transition structure ***2***-**28***, giving ***2***-**28** as a single regioisomer. We term the branched mechanism in Scheme 2.10 a 'regio-bifurcation.' As we will

show in several other examples in this chapter, solvent can play a major role in determining which regio-bifurcation pathway channel dominates.

Sharpless also demonstrates well controlled regioselectivity for the opening of *trans*-1,4,-cyclohexadiene dioxide ***2*-29** with ammonia in water. Opening of the first epoxide gives the epoxy amino alcohol (***2*-30**, Scheme 2.11). Here the diaxial conformer (diax-*rac*-***2*-30**, Scheme 2.11) does not profit from energy lowering via intramolecular H-bonding due to the poor acidity (pK_a ca. 35) and therefore weak H-bonding capability of the pendant secondary amine. Since the diaxial conformer is not the favorable intermediate, ring flip to the diequatorial conformer (dieq-*rac*-***2*-30**, Scheme 2.11) with intermolecular activation by water primes the system for attack at C6 to furnish the 1,3-diol (***2*-32**) exclusively (i.e. 1,3 regioselectivity).

Scheme 2.11. Ring opening of *trans*-1,2;4,5-cyclohexadiene diepoxide with ammonia.[74]

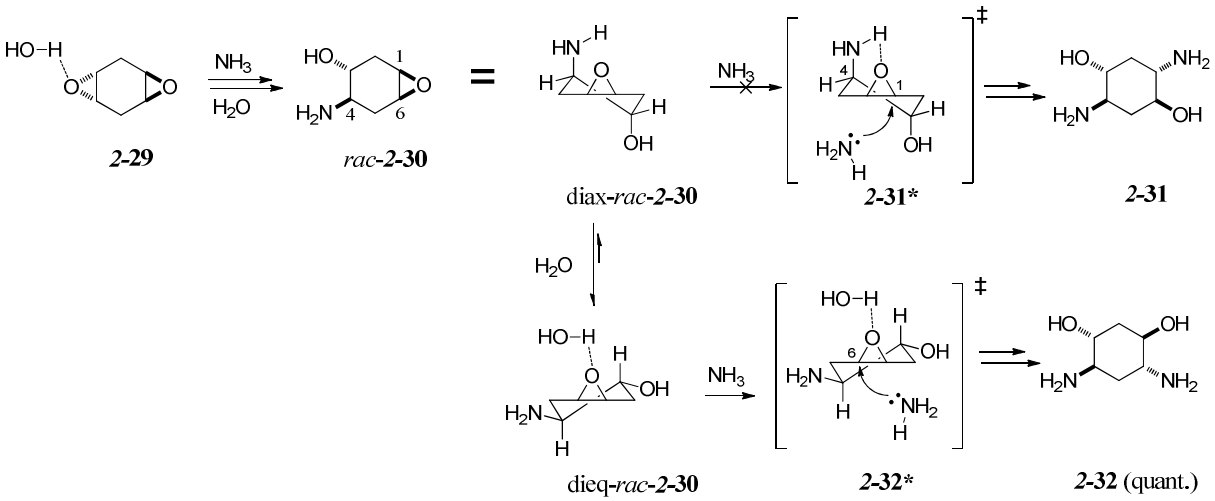

Several other examples for the ring opening of *trans*-1,2:4,5-diepoxycyclohexane (***2*-29**) show this exclusive 1,3 selectivity. Examples include the use of aliphatic primary and secondary amines,[92,93] pyrazole,[94] and azide ion (cf. Table 2.1).[95,96]

Table 2.1. Ring opening of *trans*-diepoxide *2*-29 with nitrogen nucleophiles.

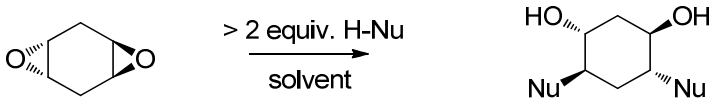

***2*-29** 1,3-diol

Entry	*Nucleophile*	*Solvent*	*Temperature*	*% Yield*	*Reference*
1	NH_2Et	H_2O	55	98	16
2	$NH(Me)_2$	neat	109	69	16
3	HN_3	DMSO/ H_2O	75	NR[a]	20
4	NaN_3	EtOH	75	70	18
5	NH_3	H_2O	100	quant.	14
6		neat	120	67	17

[a] The yield is not reported in the communication.

2.2.4 Nucleophilic delivery FP control

Interestingly, there are accounts of nucleophilic delivery controlled FP which yield the 1,4-diol. Craig et al.[92] demonstrate this phenomenon by treating an ethereal solution of ***2*-29** with $LiAlH_4$ to furnish the 1,4-diol exclusively (Scheme 2.12). Here the researchers propose the first epoxide opening with the $LiAlH_4$ gives the epoxy alkoxide (*rac*-***2*-33**, Scheme 2.10), which then activates the alane to give the *ate* complex (***2*-34***). The *ate* complex then transfers the hydride in an intramolecular guidance manner, which upon alkaline aqueous work-up gives the

1,4-diol (***2*-34**) exclusively. Without such guidance the 1,3-diol would be expected to predominate.

Scheme 2.12. Ring opening of *trans*-1,2:4,5-cyclohexadiene diepoxide with $LiAlH_4$.[92]

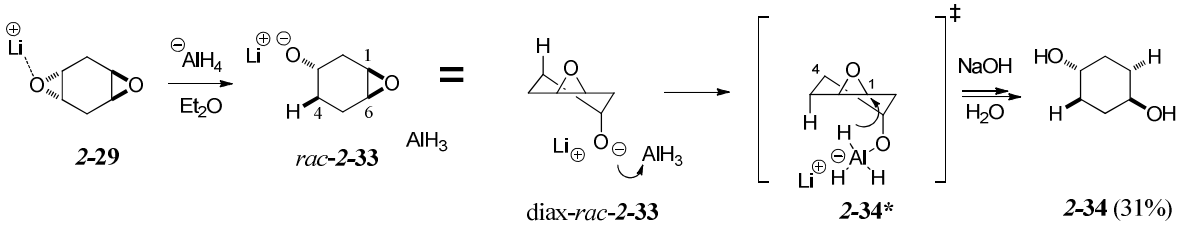

The Jacobsen group is credited with the discovery of metal salen-catalyzed asymmetric ring-opening (ARO) of epoxides. This process furnishes an enantioenriched azido alcohol (37) from meso epoxide (2-35) in high enantiomeric excess through the use of the chiral (salen)CrN_3 complex (Scheme 2.13, 2-36b).[87] Although a mechanism has been established, it is still debated whether the (salen)Cr catalyst serves to activate the epoxide or is involved in the nucleophilic delivery of the azide.[97]

Scheme 2.13. ARO of *meso* epoxides via chiral (salen)CrN_3 complex *(Scheme adapted from Hansen et al.).*[97]

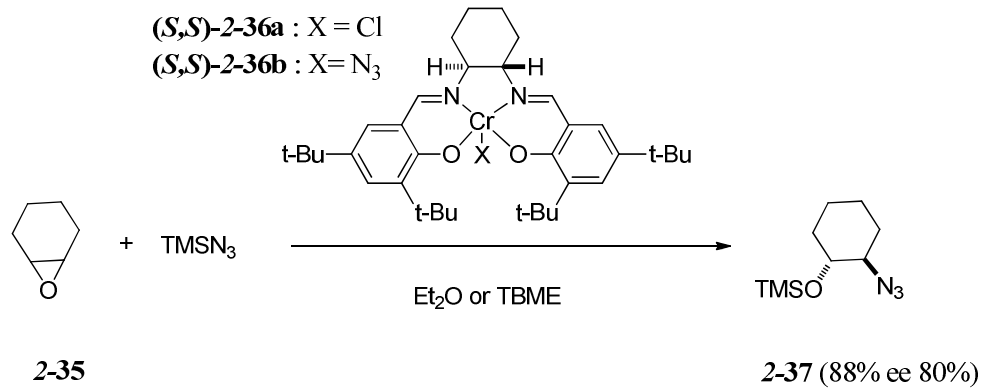

The Nelson group applied ARO to arrive at an enantioenriched diazido diol (Scheme 2.14, 2-38) from the diepoxide (2-29). Here they treated the diepoxide with $TMSN_3$ and 4 mol % (R,R)-2-36a. Interestingly the researchers found that in addition to their expected product (2-38) that was formed in moderate enantiomeric excess (70%), the centrosymmetric 1,4-diazido diol (2-39) was formed as a significant byproduct (72:21; 1,3-:1,4-diazido diol).[98] Interestingly 2-38 is only formed at lower reaction concentrations (0.5 M in 2-29) and not at higher concentrations (3.0 M in 2-29). It is also relevant to note that the achiral byproduct 2-39 is formed only when the salen catalyst is used. The researchers presume the salen catalyst is liable to provide this bifurcation pathway; however, they do not provide any mechanistic details as to how this may occur.

Scheme 2.14. Asymmetric ring opening of bis-epoxide.

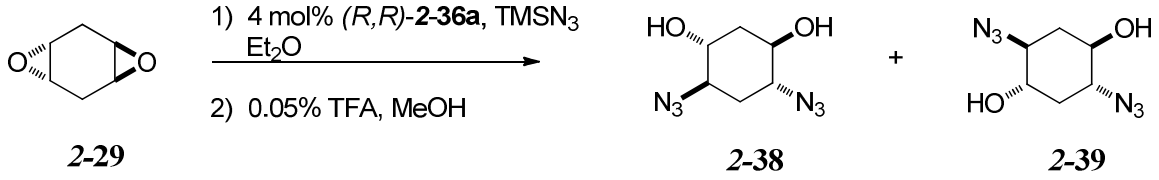

2-29 *2*-38 *2*-39

[*2*-29]	2-38:*2*-39
3.0 M	100:1
0.5 M	72:21

2.3 Regioselective synthesis of aniline-derived 1,3- and symmetric 1,4-diols from 1,2:4,5-*trans*-cyclohexadiene-dioxide

2.3.1 Synthesis of the 1,2;4,5-*trans*-bis-epoxide (*2*-29).

The previous sections of this chapter describe work by other authors. We began our investigations of FP-controlled epoxide opening with 1,2:3,4-*trans*-bis-epoxide ***2*-29**. Although there are several methods to prepare ***2*-29** in the literature, this synthesis posed an immediate challenge. The Hermann group found that methyltrioxorhenium (***2*-40**, MTO) is an effective catalyst for olefin oxidation when using H_2O_2 as the oxidant (Scheme 2.15).[99] Unfortunately the use of anhydrous H_2O_2 (in *t*-BuOH solvent) was necessary due to the instability of the catalyst in the presence of water. The researchers point to the formation of perrhenic acid, which then catalyzes the destruction of the epoxide via opening.

Scheme 2.15. Catalytic cycle for the olefin oxidation using MTO and H_2O_2.

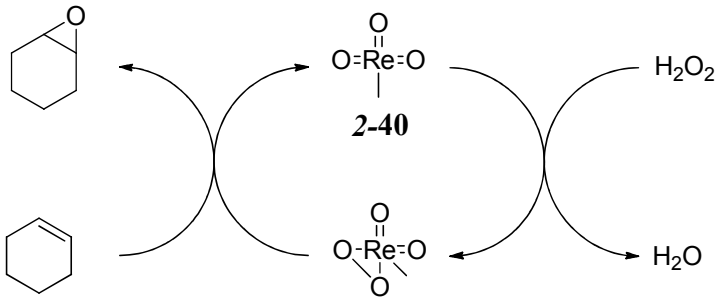

The Sharpless group later found that the addition of pyridine and pyridine derivatives to the system had three valuable effects: 1) prevention of catalyst decomposition, 2) remarkable epoxidation rate acceleration via speeding up of catalyst turnover, and 3) prevention of the acid

catalyzed ring opening.[100] A case in point is our synthesis utilizing Sharpless' protocol (Sharpless MTO oxidation henceforth) on 1-phenylcyclohexene (***2*-41**, Scheme 2.14) to form *rac*-**2-42** in high yield.

Scheme 2.16. Sharpless MTO oxidation of 1-phenylcyclohexene *2*-41.*[100]*

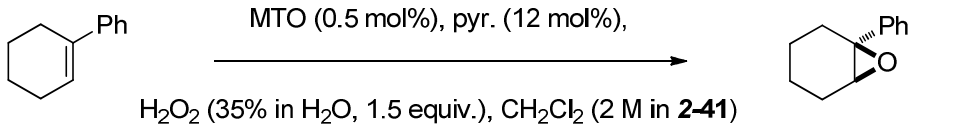

***2*-41** ***rac-2*-42** (91%)

Another interesting application of the Sharpless MTO oxidation is the highly diastereoselective epoxidation of cyclic dienes (Table 2.2, note these are reported by Sharpless et al., not the author). Surprisingly, yields are not reported in this communication but the desired *trans*-bis-epoxide (***2*-29**) is shown in entry 2. Following the Sharpless MTO procedure described in Rudolph et al. we could only achieve a maximum yield of 10%. During our optimization of this reaction, we found two major issues. First was the volatility of the diepoxide (***2*-29**); while our compound was found to have a melting point of 106 ^{o}C (107 ^{o}C lit.[100]), sublimation was an issue. Several hundred milligrams of our product could be found in the vacuum pump trap after attempting to dry *in vacuo*! Second was ineffective conversion of the monoepoxide to the diepoxide. GC-MS studies of our crude mixture throughout the course of a 48 hour reaction period (after 48 hours, the characteristic yellow color of the activated MTO complex had disappeared) showed that the major product of the reaction was the cyclohexadiene monoepoxide (a volatile liquid at atmospheric pressure, bp = 152 ^{o}C)[85] and unreacted 1,4-cyclohexadiene.

Table 2.2. Sharpless MTO oxidation of dienes *(Table adapted from Rudolph et al.).*[100]

Entry	*Substrate*	*Product*	*Time (h)*	*ratio mono:di*	*dr for diepoxide (anti:syn)*
1[b]		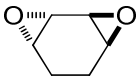	3	1.2:1	99:1
2[b]		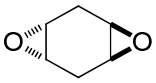	6	1:100	96:4
3	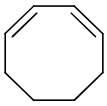	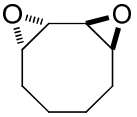	7	1:1.3	99:1
4	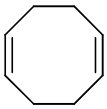	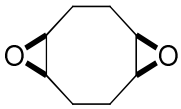	5	1:100	1:99

[a] Reaction conditions: $c_{substrate}$ = 2M; 0.5 mol% MTO, 12 mol% pyridine, 2.5equiv 50% H_2O_2, CH_2Cl_2, rt. Selectivities and rates determined by ^{1}HNMR [b] Reaction performed at 10 °C. [c] Chemoselectivity with respect to epoxidation.

Initially we attributed the poor conversion to low purity of our pyridine or MTO. However, a model reaction using 1-phenylcyclohexene (***2*-41**) and commercially available 50% H_2O_2 gave the desired epoxide ***2*-42** in 95% (cf. 91% lit.[100]). Assured the MTO and pyridine were of sufficient quality, the concentration of the commercially available 50% H_2O_2 could still be questioned since ***2*-42** can be prepared using just 30% H_2O_2 (% w/w).[100] A $KMnO_4/H_2SO_4$ titration[101] was performed verifying the peroxide had a concentration of 51.6%. With all of the starting materials found to be of sufficient quality, modifications of the published procedure were carried out. It was found that if the equivalencies of the peroxide, MTO, and pyridine as per Rudolph et al.[100] were doubled while holding the substrate concentration the same, we could

improve the yield to 66% (a slight modification of the work-up was also necessary - see Chapter 4 for details). The Nelson group reports an isolated yield of 75%, using the Sharpless MTO procedure without providing synthetic details.[102] Given that we could achieve a 66% yield on a gram scale, it was judged unnecessary to optimize our reaction any further.

2.3.2 Bimolecular reactions "on water".

The Breslow[88] and Sharpless[91] groups are credited with showing that the rates of several unimolecular and bimolecular organic reactions are greatly accelerated when they are performed as vigorously stirred heterogeneous suspensions "on water".[103] One of the first examples of this acceleration is in the Diels-Alder reaction.[104] The Breslow group found that in the cycloaddition reaction of cyclopentadiene (***2*-43**) and methyl vinyl ketone (***2*-44**) a change in solvent from isooctane to methanol resulted in a 12-fold rate increase. However, when the solvent was changed from isooctane to water, a remarkable 730-fold increase in rate was observed. In the transition state (***2*-45***) the two hydrocarbon surfaces must come together in order to form the alkene product ***2*-45**. In the "on water" reactions, the hydrophobic dienes are forced to aggregate in order to decrease the hydrocarbon-water interfacial area. This forced aggregation is known as the hydrophobic effect and is likely responsible for the dramatic rate increase.

Scheme 2.17. Diels-Alder cycloadditon of cyclopentadiene (*2*-43) and butanone (*2*-44).

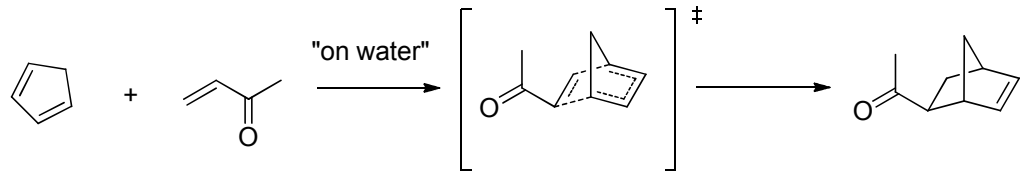

2*-43** ***2*-44** ***2*-45 ***2*-45**

The Sharpless group has shown many examples involving cycloadditions, ene reactions, Claisen rearrangements, and nucleophilic opening of epoxides.[91] In the case of the epoxide openings "on water", the Sharpless group studied the opening of cyclohexadiene monoepoxide (***2*-46**) with *N*-(3-chlorophenyl)piperazine (***2*-47**) in different solvent media (Table 2.3). The "on water" reaction (Entry 4) was complete at 50 ^{o}C in 12 hours whereas in other media such as solvent free or in ethanol (Entries 2 and 3), the reactions took approximately three days to reach completion. Interestingly, the reaction was extremely slow in toluene solvent (Entry 1).

Table 2.3. Nucleophilic epoxide opening of cyclohexadiene monoepoxide *(2*-46) with *N*-(3-chlorophenyl)piperazine (*2*-47) in different solvent media.

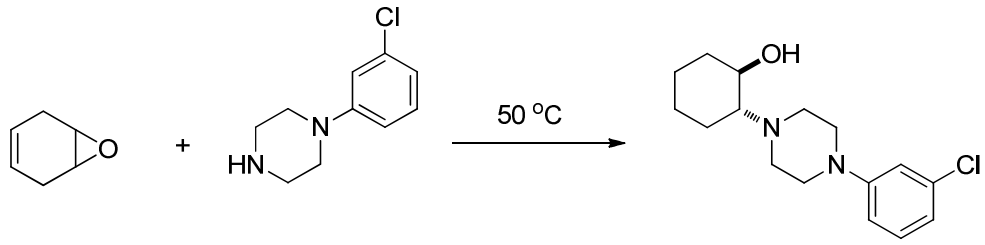

***2*-46** ***2*-47** ***2*-48**

Entry	*Solvent*	*Concentration (M)*	*Time (hr)*	*% Yield*
1	PhMe	1	120	<10[b]
2	neat	3.88[a]	72	76
3	EtOH	1	60	89
4	"on water"	3.88[a]	12	88

[a] concentrations calculated from a measured density of a 1:1 mixture of **46** and **47**. [b] Determined by ^{1}H-NMR analysis of crude reaction mixture.

Upon completion of the reaction in entry 4, the product is of high purity and can be collected either by filtration or extraction with organic solvent. A theory put forward by Jung and Marcus explains this rate acceleration when reactions such as an epoxide opening are accelerated so greatly. The researchers propose that "dangling OH" hydrogen bond donors at the interface are especially effective for lowering activation barriers of selected reactions (Figure 2.1).[105] They report calculations that indicate rate accelerations similar to these observed. Note

that, if the reaction is run in water (homogenous) the water molecules surround the hydrophobic organic reactant, forming a peripheral hydrogen bond network. This network must break in order for the water to serve as an H-bond donation catalyst.

Figure 2.1. "On water" catalysis vs. aqueous homogenous epoxide opening reaction *(Figure adapted from Jung et al.).*[105]

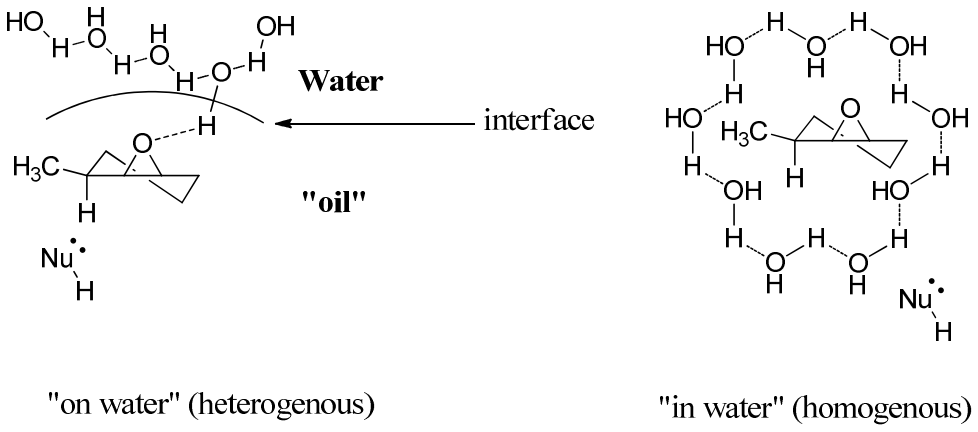

2.3.3 "On water" nucleophilic epoxide opening of *trans*-diepoxide (*2*-29) with 3-ethynyl aniline.

In the context of our BACE1 inhibitor screening, a sample of the acetylene **A10** was received as a donation from the Sharpless laboratory. Although the vial label purported the contents to be a 1,3-dianilino diol, the ^{1}H- and ^{13}C-NMR showed the **A10** sample to be a mixture of compounds. A simple retro-synthetic analysis led us to believe the compound was synthesized from *trans*-diepoxide (Scheme 2.18, ***2*-29**) and 3-ethynylaniline (***2*-49a**).

Scheme 2.18. Likely synthesis of A10 from *trans*-diepoxide (*2*-29).

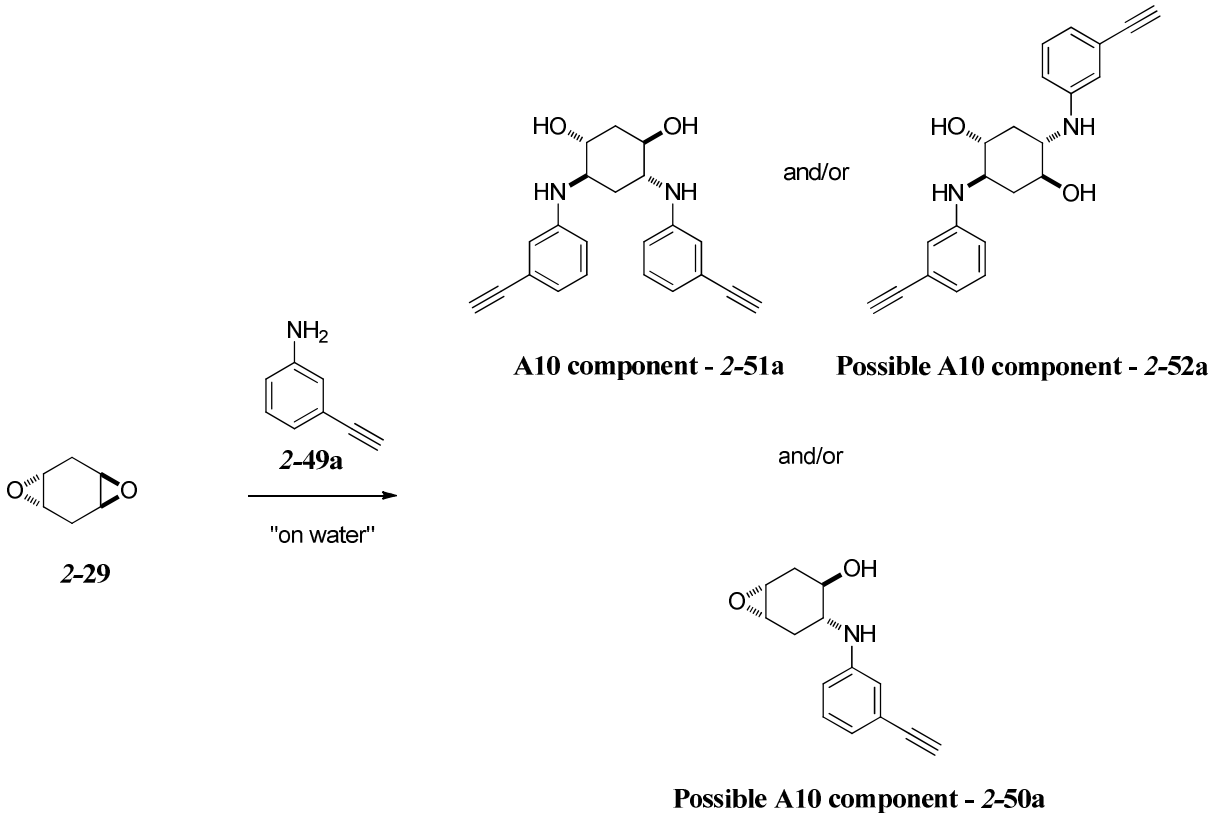

Cognizant that the 1,3-diol is the favored product from the nucleophilic opening of ***2*-22**, we were fairly certain that ***2*-51a** was a component of our **A10** mixture. TLC analysis (35% EtOAc in hexanes) showed that the mixture had two components which were easily separated by flash chromatography. Once the components were separated ^{1}H- and ^{13}C-NMR spectra were obtained. The more polar of the two components (the later eluting compound) showed four distinct resonances in the aliphatic region of ^{13}C-NMR spectrum (note: the signals further downfield ca. 77.3 and 85.6 ppm correspond the sp carbons in the acetylene moiety), which is consistent with a time averaged C_2-symmetric cyclohexene 1,3-dianilino diol (***2*-51a** Figure 2.2).

Figure 2.2. ^{13}C-NMR of the aliphatic region of the 1,3-diol *2*-51a.

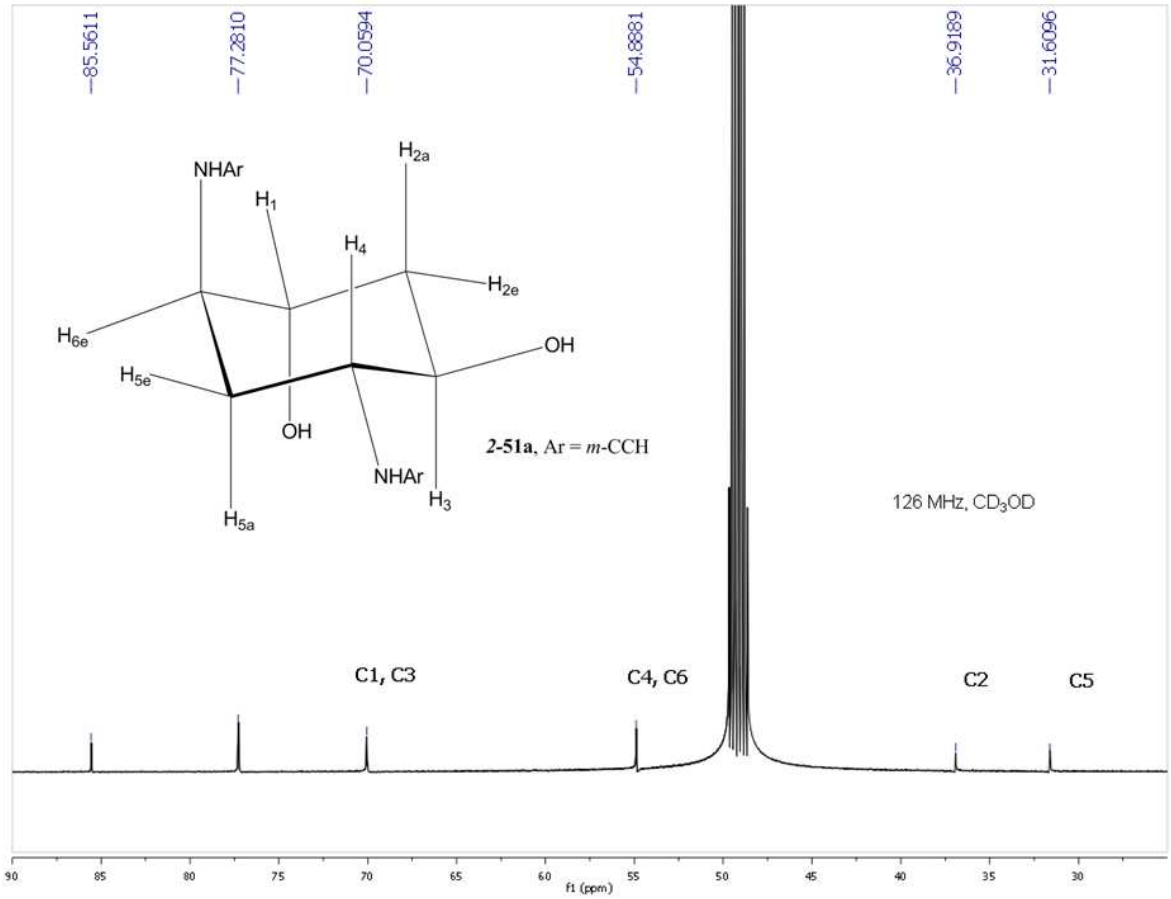

The less polar of the components showed only three resonances in the aliphatic region of the ^{13}C-NMR spectrum, and is consistent with an instantaneous C_i-symmetric cyclohexene 1,4-dianilino diol (***2*-52a**, Figure 2.3). We could now rule out ***2*-50a** due to its C_1-symmetry which would give 6 distinct resonances in ^{13}C-NMR.

Figure 2.3. ^{13}C-NMR of the aliphatic region of the 1,4-diol *2*-52a.

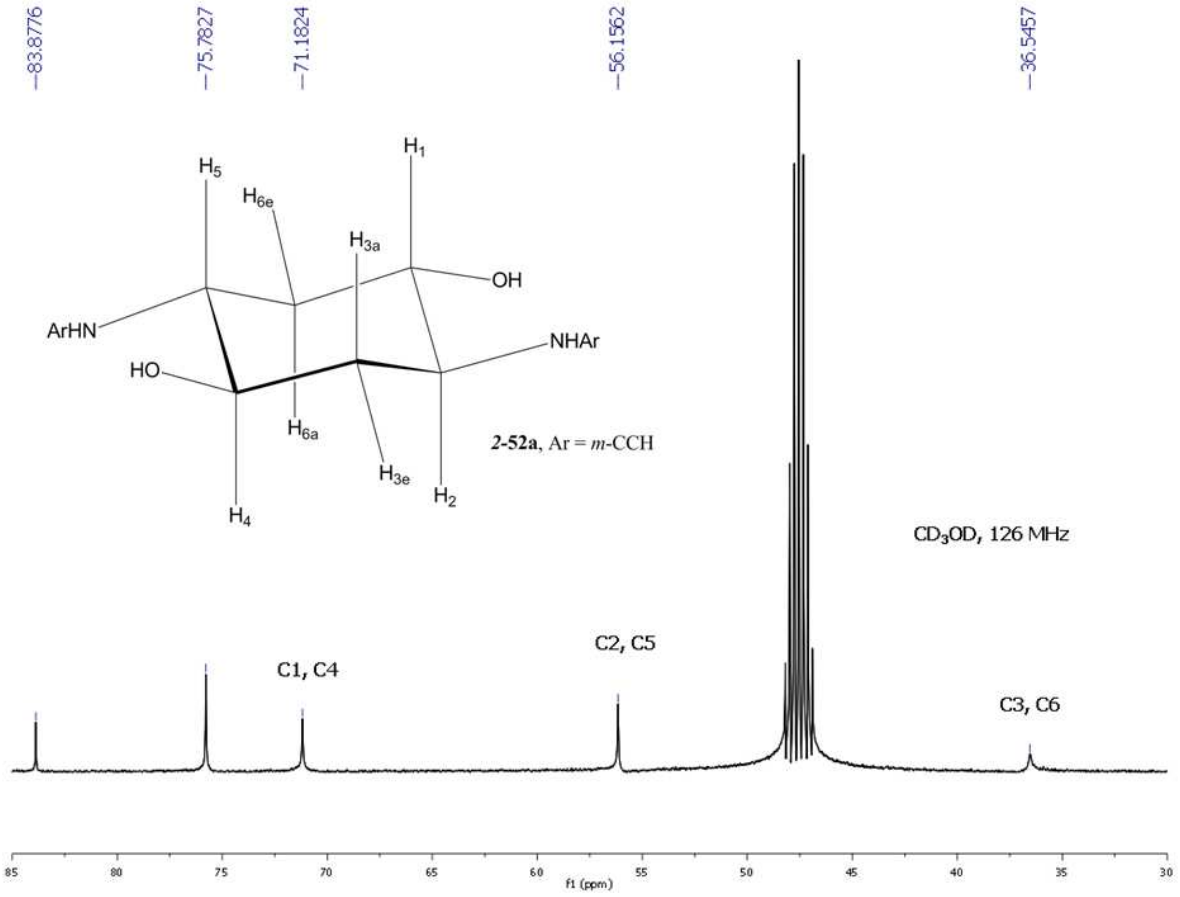

Now with an understanding of the reaction mixture we attempted to synthesize ***2*-51a** and ***2*-52a** from ***2*-29** in our laboratory. Surprisingly, we formed a 1:1 mixture of the desired C_2-symmetric 1,3-dianilino diol ***2*-51a** and the rarely seen C_i-symmetric 1,4-dianilino diol ***2*-52a**.

In order to assign the stereochemistry, analysis of proton coupling constants was necessary. By drawing the cyclohexane chair model of the 1,3-diol (Figure 2.4, ***2*-51a**), one finds there are two equal energy conformers ***2*-51a** and ***2*-51a'**, both of which are C_1-symmetric,

Figure 2.4. ^{1}H-NMR analysis of *2*-51a to confirm stereochemistry.

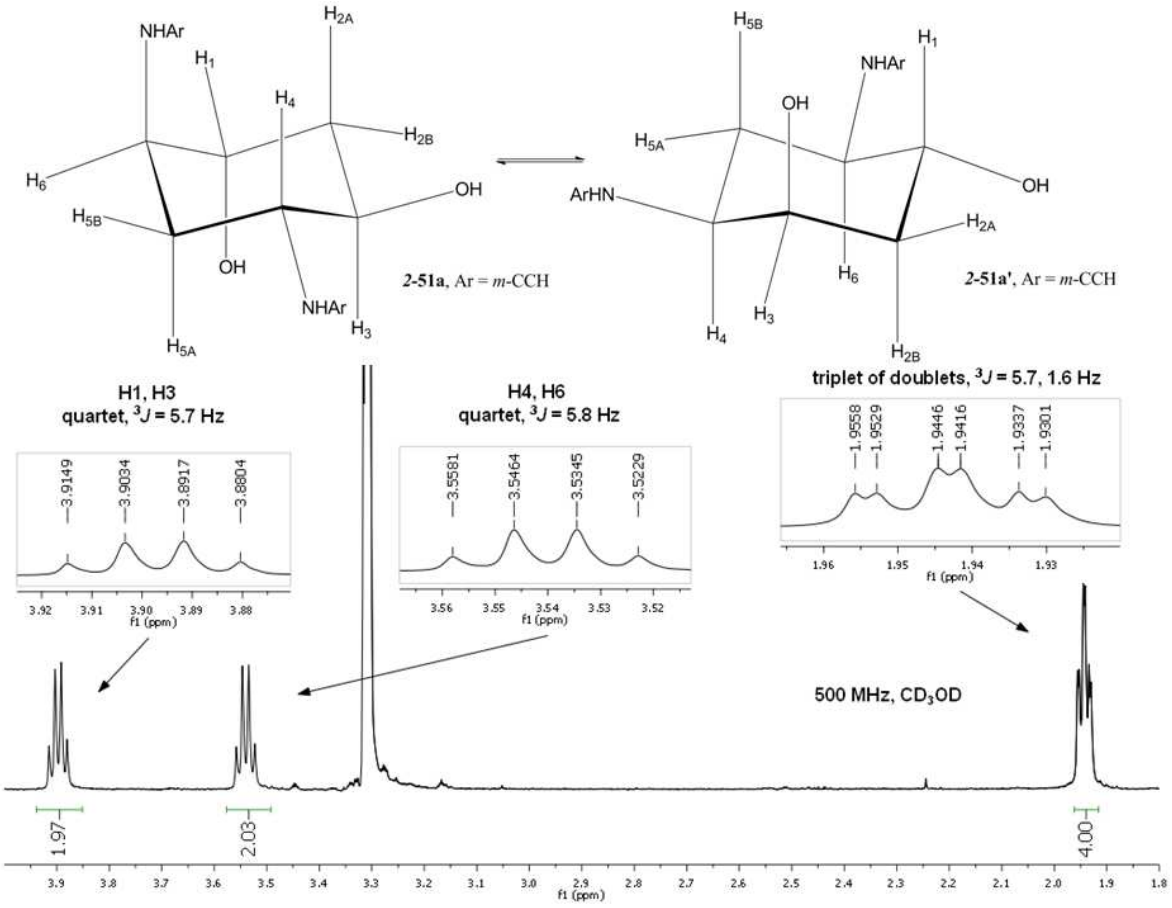

wherein each ring carbon (C1-C6) and proton (H1-H6) are distinct. However, rapid chair-chair interconversion at room temperature exchanges pairs of inequivalent nuclei to give apparent time average C_2 symmetry. The behavior has important consequences for the ^{1}H-^{1}H coupling constants. For example H1 in the rightmost chair conformer ***2*-51a'** has an antiperiplanar (axial-axial or aa) relationship to H6, which is expected to give a coupling constant of 9-12 Hz. But in the conformer ***2*-51a**, H1 now has a gauche (equatorial-equatorial or ee) relationship to H6 leading to a much smaller coupling constant (ca. 4-6 Hz). On the NMR time scale at room temperature, we would expect to see an averaging of the coupling constants. In the analysis of ***2*-**

51a a value of 5.7 Hz was observed for $^{3}J_{H1H6}$. The remaining protons and coupling constants are summarized along with an expansion the aliphatic region of the ^{1}H NMR spectrum of ***2*-51a** (CD_3OD, 500 MHz) in Figure 2.4.

In the case of the 1,4-diol, drawing the cyclohexane chair model one finds there is only one low energy, all-equatorial conformer (Figure 2.5). This C_i-symmetric structure will therefore not exhibit any evidence of dynamic behavior, and only 3 ring carbon and 4 ring proton

Figure 2.5. ^{1}H-NMR analysis of *2*-52a to confirm stereochemistry.

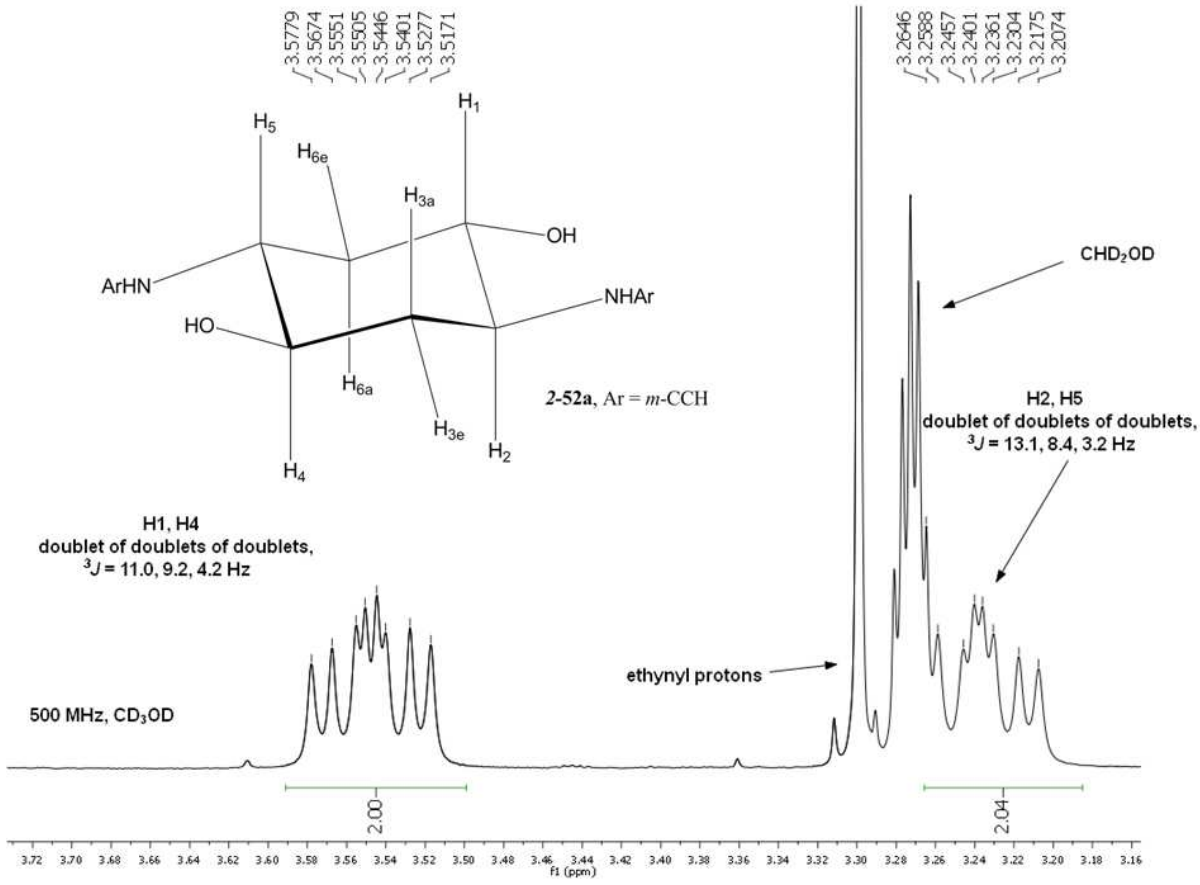

resonances are expected (Figure 2.5). Because of the locked all-equatorial conformation, H1 will always maintain an antiperiplanar (axial-axial or aa) relationship to H6a and H2. In this case one

would predict a large coupling constant (10-12 Hz) which was indeed the case, $^{3}J_{H1H6a}$ = 11.0 Hz. However, in the analysis of ***2*-52a** a value of 9.2 Hz was observed for $^{3}J_{H1H2}$. This diminished value is most likely due to the noted phenomenon that if one of the two coupled protons is geminal to an electronegative moiety (in this case H1 and H2 are both geminal to an electronegative moiety) that the coupling constant can be attenuated by 1-2 Hz.[106,107] The remaining coupling constants are summarized along with an expansion of the aliphatic region of the ^{1}H NMR spectrum (CD_3OD, 500 MHz) in Figure 2.5.

2.3.4 N-H directed FP opening of *trans*-diepoxide *2*-29 with aniline nucleophiles.

Centrosymmetric 1,4-diols derived from ***2*-29** and nitrogen nucleophiles have been characterized previously in only one case, as a byproduct in chiral Lewis acid-catalyzed reactions with $TMSN_3$ (cf. **2.2.4**).[98,102] Aside from the interesting C_i-symmetry of ***2*-52a**, we viewed that the complete lack of 1,3-diol regioselectivity seen in reaction with ***2*-49a** merited further investigation. The analogous reaction of ***2*-29** with benzyl amine (***2*-49b**) gave only the 1,3-diamino diol ***2*-51b** in high yield (Scheme 2.19).

Scheme 2.19. Opening of *trans*-diepoxide (*2*-29) with 3-ethynylaniline (*2*-49a) and $BnNH_2$ (*2*-49b).

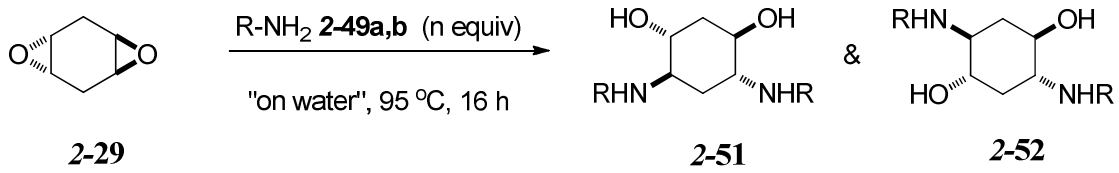

2-29 *2*-51 *2*-52

	R	n	Yield (*2*-51 & *2*-52)	*2*-51:*2*-52 ratio
a	3-HCC-C_6H_4	4	88%	50:50
b	$PhCH_2$	2	95%	100:0

The obvious difference between the reactions is the nucleophile used in the opening. Although the nucleophiles are both amines, the 3-ethynylaniline (***2*-49a**) has a remarkable lack of regioselectivity. To determine whether electronic effects play a significant role in the ring opening regioselectivity, reactions of ***2*-29** with five other anilines ***2*-49c-g** under the same conditions (Table 2.4) were performed. Anilines bearing electron-donating substituents (e.g. ***2*-49c**,**d**) gave the 1,3-diols ***2*-51c** and ***2*-51d** in 100% regioselectivity (entries 1 and 2). Unsubstituted aniline **49e** gave a 84:16 mixture of regioisomers (entry 3), and anilines bearing electron withdrawing substituents (e.g. ***2*-49f**, ***2*-49a**, ***2*-49g**, entries 4-6) evidenced increasing amounts of the 1,4-diol.

Table 2.4. Reactions of *2*-29 with anilines *2*-49a,c-g "on water".

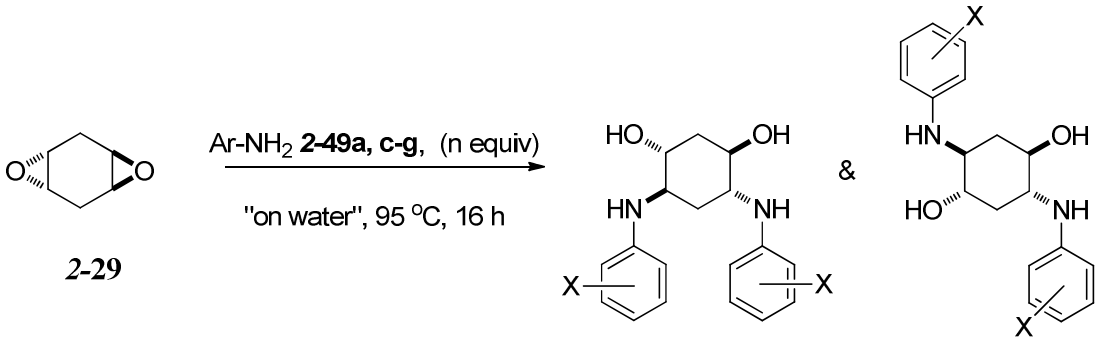

2-29 *rac-2*-51a, c-g *2*-52a, c-g

Entry	*Aniline*	*n*	*X*	*sigma value*[108]	*1,3:1,4*[a]	*% yield of major isomer*[b]
1	***2*-49d**	2	*p*-OCH_3	-0.27	100:0	96
2	***2*-49c**	2	*p*-CH_3	-0.14	100:0	90
3	***2*-49e**	2	H	0.0	84:16	60(71)
4	***2*-49f**	4	*p*-F	0.15	76:24	62(81)
5	***2*-49a**	4	*m*-CCH	0.21	50:50	44(88)
6	***2*-49g**	8	*m*-Cl	0.37	22:78	56(72)

[a] Crude product ratios measured by ^{1}HNMR before purification. [b] Chromatographed yield of major regioisomers (for entry 5 - recovery for **51a** is given). The value in parenthesis indicates the % recovery of this isomer from the crude product mixture.

As Table 2.4 illustrates, selectivity for the 1,4-diol increases with the sigma value of the substituent; *m*-chloroaniline ***2*-49g** gives a 22:78 ratio of the 1,3- and 1,4-diols. Finally, whereas reaction with electron-rich anilines ***2*-49c**,**d** was complete within 4 hours at 95 °C, the electron

deficient anilines required high equivalency and prolonged reaction times (16 h) to give complete conversion.

Based on these results we reasoned that interplay of the relatively weak nucleophilicity and enhanced hydrogen bond donating ability of anilines (i.e., increased acidity) relative to aliphatic amines (cf. Table 2.5) was responsible for the formation of the 1,4-diols ***2*-52** in reactions with ***2*-49a** and ***2*-49e-g**.

Table 2.5. Comparison of the pKa values of aliphatic amines to anilines in DMSO solvent.[84,109]

Entry	***Amine***	***pKa***
1	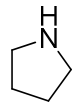	44[109]
2		41[109]
3	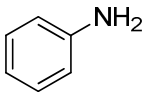	30.6[84]
4	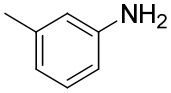	31.0[84]
5	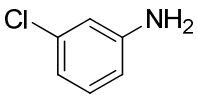	28.5[84]

A unified mechanism for formation of both regioisomers is given in Scheme 2.20. Opening of ***2*-29** with one equivalent of amine gives the epoxy amino alcohol *rac*-***2*-50**. According to the accepted stereoelectronic requirements for epoxide opening, ***2*-50** should be formed in the diaxial-conformation (diax-*rac*-***2*-50**).

Scheme 2.20. Regio-bifurcation pathway for the opening of *2*-29 with anilines "on water".

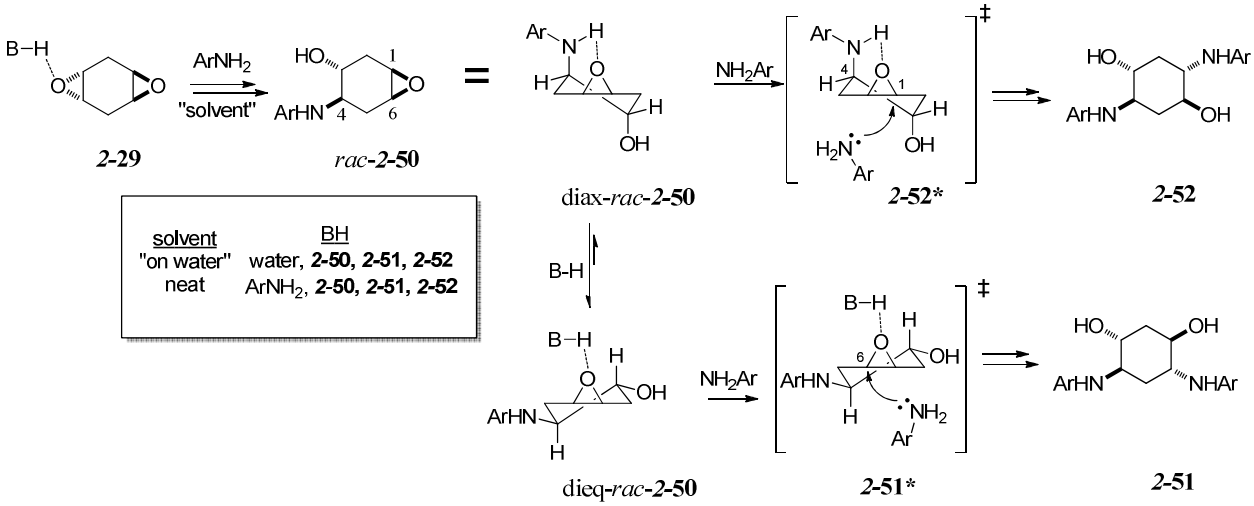

In this conformation it is possible for the newly installed amino substituent at C4 to donate a hydrogen bond to the epoxide oxygen, thereby activating it for attack. If the second epoxide opening proceeds directly via transition structure ***2*-52***, the Fürst-Plattner effect will favor amine opening at C1, giving 1,4-diol ***2*-52**. We describe this route to ***2*-52** as "NH-directed Fürst-Plattner." As we noted in Scheme 2.10, a similar directing effect of a pendant *cis*-hydroxyl group has been invoked in ring-opening of cyclohexene oxides (cf. Scheme 2.10).[74] However, if ***2*-50** relaxes from its diaxial conformation to the more stable diequatorial conformation (dieq-*rac*-***2*-50**) prior to the second attack, the Fürst-Plattner effect would favor opening at C6 via

transition structure ***2*-51***, giving 1,3-diol ***2*-51**. In this case, hydrogen bond assistance of the second epoxide opening is likely provided by water.

Since aliphatic amines like ***2*-49b** (or electron rich anilines ***2*-49c** and ***2*-49d**) are poor hydrogen bond donors relative to water, the second ring opening is expected to proceed via the diequatorial transition state ***2*-51***, giving 1,3-diol opening products in high selectivity (Scheme 2.20). As mentioned earlier, this standard Fürst-Plattner mechanism also accounts for the high 1,3-diol selectivity seen in reaction of ***2*-29** with azide ion[74,110] and pyrazoles.[94] However, the substantially increased acidity of anilines relative to amines (Table 2.5) should make them competent hydrogen bond donors, rendering the 1,4-diol pathway transition structure ***2*-52*** similar in energy to transition structure ***2*-51***. Furthermore, one would expect that the 1,4-pathway would become increasingly viable with electron deficient anilines, just as Table 2.4 demonstrates.

In addition, as depicted in Scheme 2.20, partitioning between the 1,3- and 1,4-diol pathways also depends on the concentration and competence of intermolecular hydrogen bond donors BH. In "on water" conditions, interfacial water likely plays a dominant role in epoxide activation.[91] A logical approach to further improve 1,4-selectivity would thus be to perform reactions under conditions where the concentration of such intermolecular hydrogen bond donors is minimized.

Our first attempts to achieve this goal involved running the reactions in aprotic solvents at elevated temperatures (Table 2.6) with a relatively nucleophilic aniline (***2*-49d**). Interestingly no reaction was observed in any of these cases (Entries 1-3) after 16 h, illustrating the importance of hydrogen-bond assistance for the first ring-opening to give *rac*-***2*-50** (Scheme

2.20). However, success was realized under neat (solvent free) conditions at 150 °C (16 h, Table 2.6). Under these conditions we envision that high reactant concentrations and hydrogen-bonding assistance from a second aniline molecule initially facilitates the first ring-opening to give the epoxy amino alcohol *rac*-***2*-50**.

Table 2.6. Attempts to open trans-diepoxide *2*-29 with aprotic solvents.

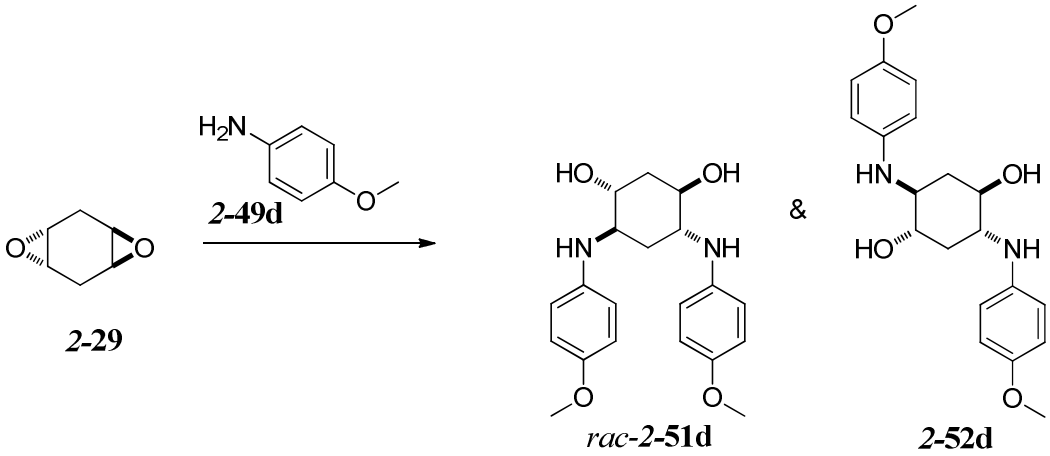

Entry	*Solvent*	*[2-42d]*	*Temperature (^oC)*	*Time (hr)*	*% Conversion*
1	CH_3CN	1 M	80	16	0
2	DMF	1 M	95	16	0
3	Mesitylene	1 M	150	16	0
4	neat	6.6 M[a]	150	16	100

[a] all reactants assumed to have density = 1 g/mL. **[*2*-29]** = 1.65 M for entry 4.

In Entry 4 the aniline concentration is 6.6-fold higher than those employed in the acetonitrile, DMF, and mesitylene reactions (Entries 1-3). As hoped, under neat conditions, all the anilines

showed a predominance of 1,4-diol ***2*-52** (Table 2.7). Note that the 1,4-selectivity is greatest for the electron-deficient anilines ***2*-49a**, **f-g** and unsubstituted aniline ***2*-49e** (cf. Table 2.7, entries 3-7).

Table 2.7. Reactions of *2*-29 with anilines *2*-49a,c-g solvent free.

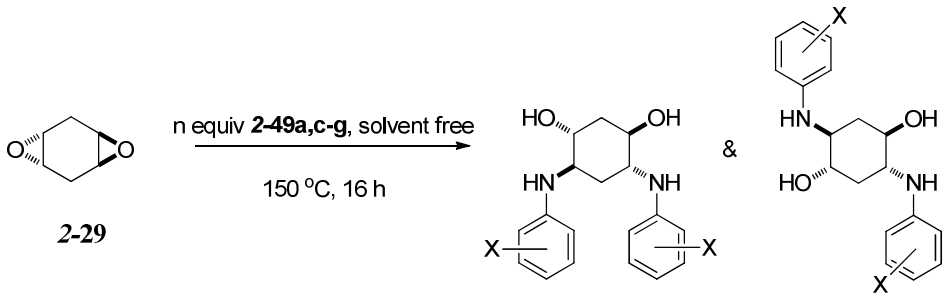

2-29 *rac-2*-51a,c-g *2*-52a,c-g

Entry	*Aniline*	*n*	*X*	*sigma value*[108]	*1,3:1,4*[a]	*% yield of major isomer*[b]
1	***2*-49d**	4	*p*-OCH_3	-0.27	40:60	42(70)
2	***2*-49c**	4	*p*-CH_3	-0.12	40:60	51(87)
3	***2*-49e**	4	H	0.0	20:80	45(55)
4	***2*-49f**	4	*p*-F	0.15	3:97	74(76)
5	***2*-49a**	8	*m*-CCH	0.21	8:92	28(30)
6	***2*-49g**	6	*m*-Cl	0.37	10:90	84(93)

[a] Crude product ratios measured by ^{1}HNMR before purification. [b] Chromatographed yield of major regioisomers. The value in parenthesis indicates the % recovery of this isomer from the crude product mixture.

This observation is consistent with the expected enhanced acidity and hydrogen-bonding ability of these anilines. The low yield seen in solvent-free reaction of ***2*-49a** reflects competing side reactions, perhaps due to the reactivity of the acetylene unit at 150 °C; nevertheless high 1,4-selectivity is seen (8:92, Table 2.7, entry 5). The fact that selectivity for the 1,4-diol is not absolute under solvent-free conditions points to the participation of a second epoxy amino alcohol ***2*-50** and diols ***2*-51**, ***2*-52** as intermolecular hydrogen bond donors (BH) in the 1,3-diol pathway (Scheme 2.20).[74,91] This competing pathway would be most problematic in reaction with electron-rich anilines ***2*-52c-d**, since the corresponding pendant anilino groups in ***2*-52c-d** are poor H-bond donors relative to the alcohol groups present in ***2*-50**, ***2*-51**, and ***2*-52.** This reasoning also accounts for the observation that neat reaction of ***2*-29** with benzyl amine ***2*-49b** (4 equiv) affords 1,3-diol ***2*-51b** as the sole product (94% yield).

To provide a further test of the key role of intramolecular H-bonding from the pendant aniline in 1,3- vs. 1,4-diol selectivity, reactions were performed using *N*-methyl aniline ***2*-49h**. In this case, the epoxy amino alcohol intermediate ***2*-50h** would lack an amino hydrogen, and thus the 1,4-diol pathway should not be viable. As hoped, these experiments confirmed our mechanistic hypothesis: both under neat and "on water" conditions, opening of ***2*-29** with *N*-methyl aniline ***2*-49h** exclusively provided the 1,3-diol ***2*-51h** (Table 2.8).

Table 2.8. Reactions of *2*-29 with aniline *2*-49h.

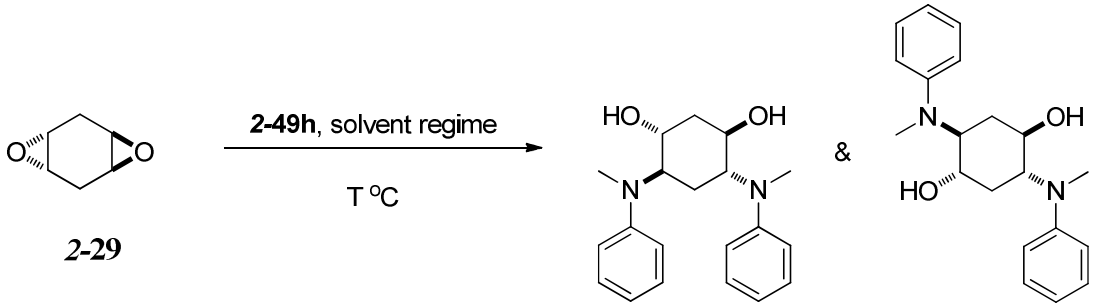

2-29 *rac-2*-51h *2*-52h

Entry	*Aniline*	*regime*	*T °C*	*1,3:1,4*[a]	*% yield of major isomer*[b]
1	***2*-49h**	"on water"	95	100:0	97
2	***2*-49h**	neat	150	100:0	91

[a] Crude product ratios measured by ^{1}HNMR before purification. [b] Chromatographed yield of major regioisomers.

Auxiliary confirmation of the role of the pendant amino NH of ***2*-50** on the regioselectivity of the second epoxide opening was achieved by experiments to arrive at unsymmetrical 1,3- and 1,4-diols. Scheunemann has previously reported synthesis of unsymmetrical 1,3-diols from ***2*-29** via the intermediacy of epoxy amino alcohols (e.g. *rac-2*-50i, Scheme 2.21).[93]

Scheme 2.21. Formation of an unsymmetrical 1,3-diol from trans-diepoxide *2*-29.[93]

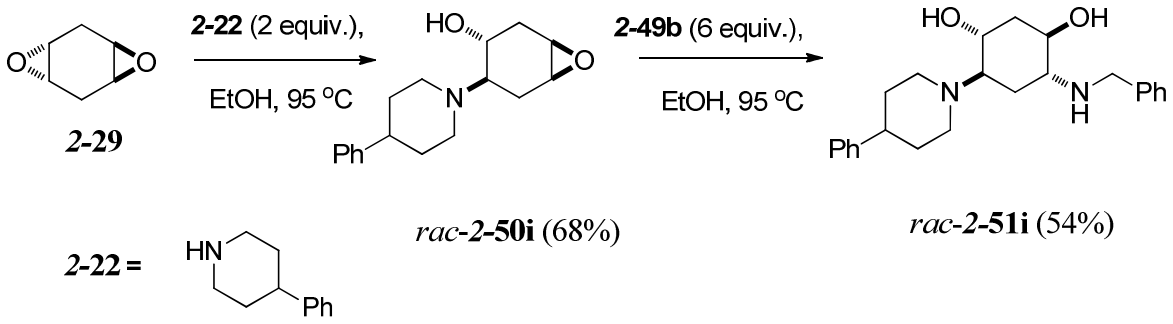

However, prior to our work preparation of the corresponding unsymmetrical 1,4-diols has not been possible. Thus we treated ***2*-29** with 0.25 equiv of anilines ***2*-49f** and ***2*-49h** in refluxing isopropanol to give epoxy amino alcohols *rac*-***2*-50f** and ***2*-50h** in 68 and 42% yield, respectively (Scheme 2.22).

Scheme 2.22. Regiocontrolled route to unsymmetrical 1,3- or 1,4-diols.

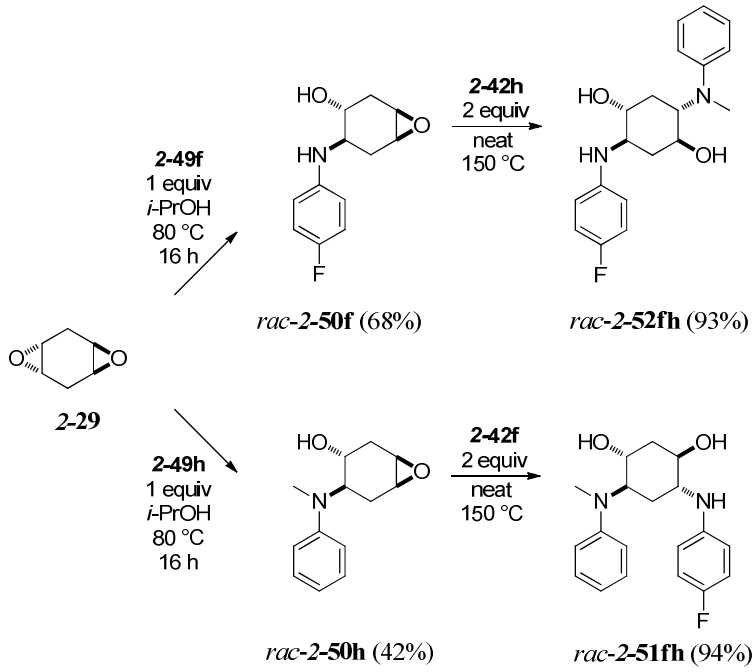

By virtue of its pendant *p*-fluoroanilino group, ***2*-50f** is poised to react with an incoming aniline under solvent-free conditions to give the 1,4-diol product. Thus *rac*-***2*-50f** was treated with *N*-methyl aniline ***2*-49h**, and the unsymmetrical 1,4-diol *rac*-***2*-52fh** was obtained in 93% yield. Conversely, epoxy amino alcohol *rac*-***2*-50h** cannot react in the 1,4-manifold, since it lacks an intramolecular hydrogen bond donor. Thus treatment of *rac*-***2*-50h** with *p*-fluoroaniline ***2*-49f** under *solvent-free* conditions exclusively affords the 1,3-diol *rac*-***2*-51fh** in 94% yield.

2.3.5 Aberrant aniline openings of *trans*-diepoxide *2*-29.

Tables 4 and 7 list anilines that were successful for the opening of ***2*-29** and conformed to a particular trend which we could rationalize by the electron withdrawing capability of the aniline used. However two particular anilines that we screened gave an unexpected result when run "on water". 3-Acetylaniline (***2*-49j**) and 3-cyanoaniline (***2*-49k**), which have sigma values similar to and much greater than ***2*-49g** respectively (Table 2.9), did show high 1,4- selectivity as expected when reactions were performed neat. Interestingly, when the reactions were performed "on water" the electron deficient anilines ***2*-49j** and ***2*-49k** showed 1,3- selectivity!

Table 2.9. Opening of trans-diepoxide *2*-29 with electron deficient anilines.

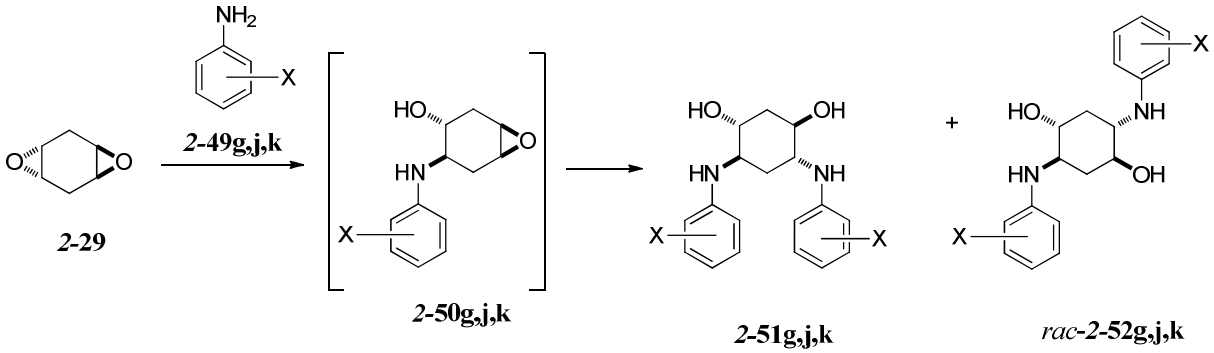

Entry	*Aniline*	*X*	*Sigma value*	*"on water" 1,3:1,4*[a]	*"neat" 1,3:1,4*[a]	*ClogP of 50*[b]
1	***2*-49j**	*m*-CH_3CO	0.36	75:25	8:92	0.075
2	***2*-49g**	*m*-Cl	0.37	22:78	10:90	1.101
3	***2*-49k**	*m*-CN	0.62	78:22	0:100	0.220

[a] ratios determined by crude 1H-NMR of reaction mixture. [b] ClogP calculated by ChemDraw 11

We rationalized that perhaps the polar functional groups were improving water solubility of the epoxy alcohol intermediates ***2*-50j** and ***2*-50k**. A ClogP calculation did indeed show that the polar functional groups are expected to significantly increase the solubility of ***2*-50j** and ***2*-50k** in water relative to that of ***2*-50g**. Thus it seemed possible that the ring opening of ***2*-50j** and **50k** might be occurring *in water* where the intermediate epoxy alcohol ***2*-50** would be activated by intermolecular H-bonding by the surrounding water *solvent* (1,3-pathway), thus overwhelming any intramolecular H-bonding from the pendant aniline (1,4-pathway).

Another interesting result was observed when the solvent for the dual opening of ***2*-29** was changed from "on water" to isopropanol. Initially we thought that the 1,3-selectivity would be nearly perfect, due to the intermolecular H-bonding by the isopropanol solvent in a homogenous reaction. However, the 1,4-selectivity increased (Table 2.10).

Table 2.10. Opening of trans-diepoxide *2*-29 with isopropanol solvent.

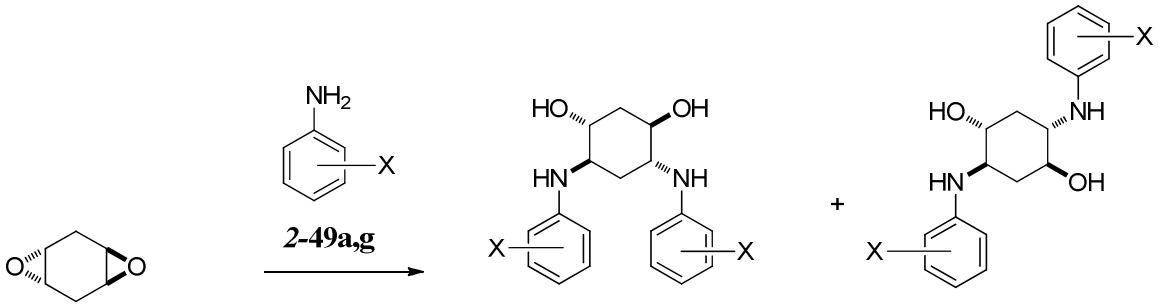

***2*-29** ***rac-2*-51a,g** ***2*-52a,g**

Entry	*Aniline*	*X*	*1,3:1,4 "on water"*	*1,3:1,4 i-PrOH*[a,b]	*1,3:1,4 "neat"*
1	***2*-49a**	m-CCH	50:50	19:81	8:92
2	***2*-49g**	m-Cl	22:78	13:87	10:90

[a] ratios determined by crude 1H-NMR of reaction mixture. [b] Reaction ran at 90 °C

We hypothesized that while the *i*-PrOH reaction medium is indeed homogenous, the isopropanol may be a poor intermolecular H-bond donor relative to interfacial water in the "on water" experiment. Thus in *i*-PrOH, intramolecular H-bonding from the pendant aniline (1,4-pathway) is better able to compete. A possible follow-up experiment would be to try the

openings in hexafluoroisopropanol, which is a better intermolecular H-bond donor than isopropanol. If our hypothesis is correct, we would expect to see an decrease in 1,4-selectivity.

2.4 Synthesis of aniline-derived 1,3- and symmetric 1,4-diols from 1,2:3,4-*trans*-diepoxide (*2*-54).

2.4.1. Synthesis of 1,2:3,4-*trans*-diepoxide *2*-54.

Having success with the opening of the 1,2:4,5-*trans*-diepoxide ***2*-29**, we decided to extend the scope of our study to other systems that could exhibit N-H directed FP. Sharpless MTO oxidation of 1,3-cyclohexadiene (***2*-53**) was an obvious choice for the synthesis of the chiral 1,2:3,4-*trans*-diepoxide (***2*-54**, Table 2.2 entry 1).[100] The experimental procedure again proved difficult to reproduce. The researchers comment that the reaction is performed at 10 ^{o}C and apparently gives poor conversion of the monoepoxide to the diepoxide (cf. Table 2.2). In our hands we found it difficult to maintain a reaction temperature of 10 ^{o}C on a large scale due to the exotherm involved upon drop-wise addition of the 50% H_2O_2. Furthermore, we could never achieve a recovery greater than 10%. Further literature research indicated that the conventional *m*-CPBA olefin oxidation formed the *trans*-diepoxide (Scheme 2.23, ***2*-47**) in 100% de, which we obtained in 52% yield after chromatography on a gram scale as a colorless oil (cf. 78% lit.[111]).

Scheme 2.23. Our synthesis of 1,2:3,4-trans-bis-epoxide (*2*-54).

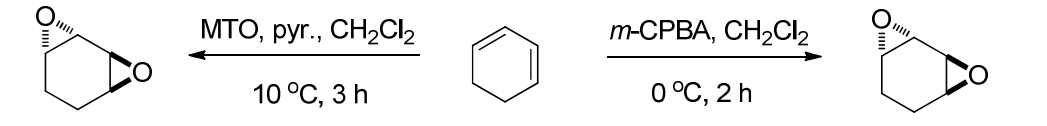

rac-***2*-54** (14%) ***2*-53** *rac*-***2*-54** (52%)

2.4.2. Previously reported nucleophilic openings of *trans*-diepoxide *2*-54.

Kozlov reported that the opening of ***2*-54** could be achieved in aqueous dimethyl amine (***2*-49l**) in methanol at 50 °C to furnish the 1,3-diol exclusively ***2*-58l**, Scheme 2.24).[112] However, it was not possible to determine whether the first nucleophilic opening occurred at C1/C4 (the exterior epoxy carbons) or at C2/C3 (the interior epoxy carbons) since both pathways give the same regioisomer and enantiomer under FP control.

Scheme 2.24. Kozlov's opening of *trans*-diepoxide *2*-54 with dimethyl amine *2*-49l.

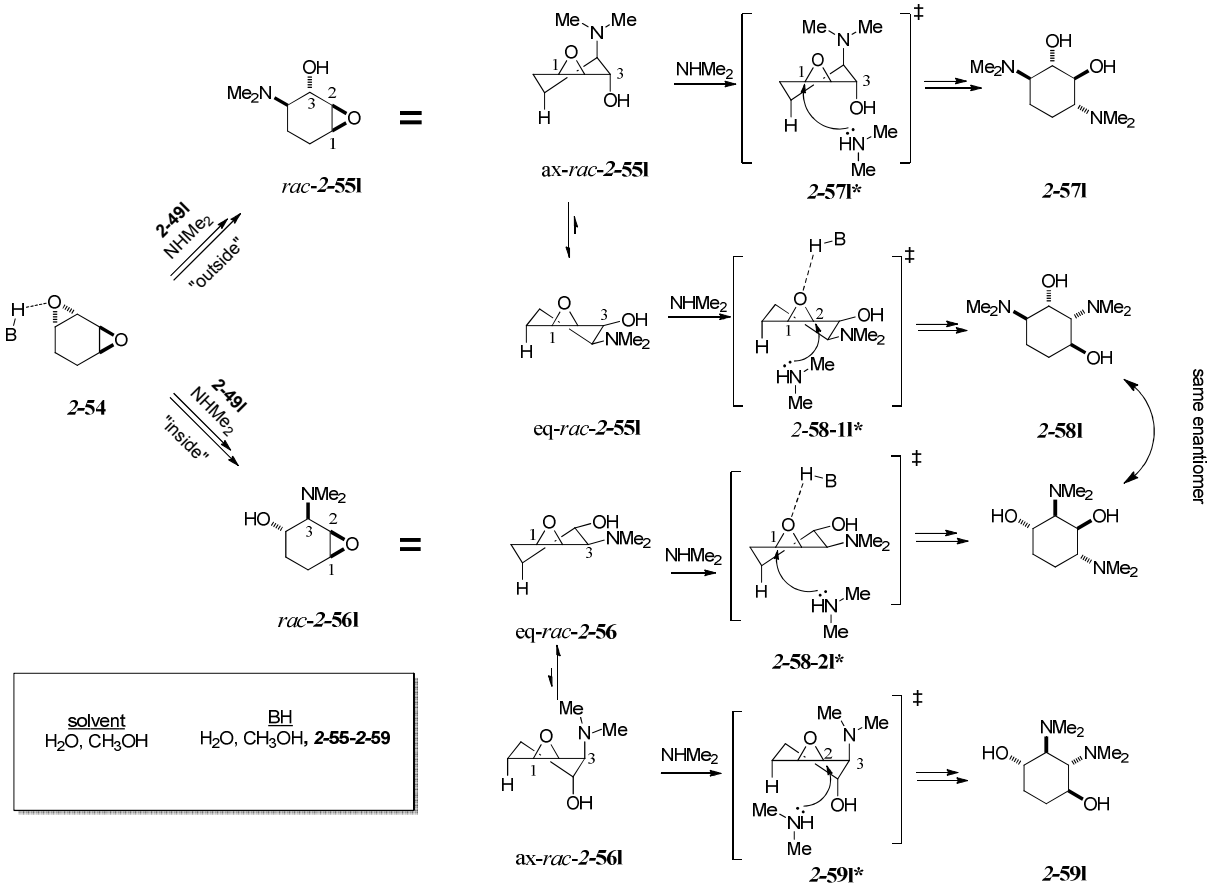

Earlier work by Kozlov showed that when biasing the reaction to mono opening (10:1 ***2*-54**:***2*-49l**) the epoxy aminoalcohol (Scheme 2.24, ***2*-56**) which is derived from "inside" opening was the only product detected.[113] This can be rationalized by FP controlled epoxide opening. Attack at C1/C4 would be disfavored by a 1,2-diaxial interaction between the incoming nucleophile and the pseudoaxial hydrogen atom on C6/C5 (See Figure 2.6). However, if the incoming nucleophile attacks at C2/C3 it will encounter a more favorable 1,3-diaxial interaction.[112]

Figure 2.6. Mercury representations of the B3LYP/6-31G* optimized geometry of 1,2:3,4-trans-diepoxide (*2*-54).

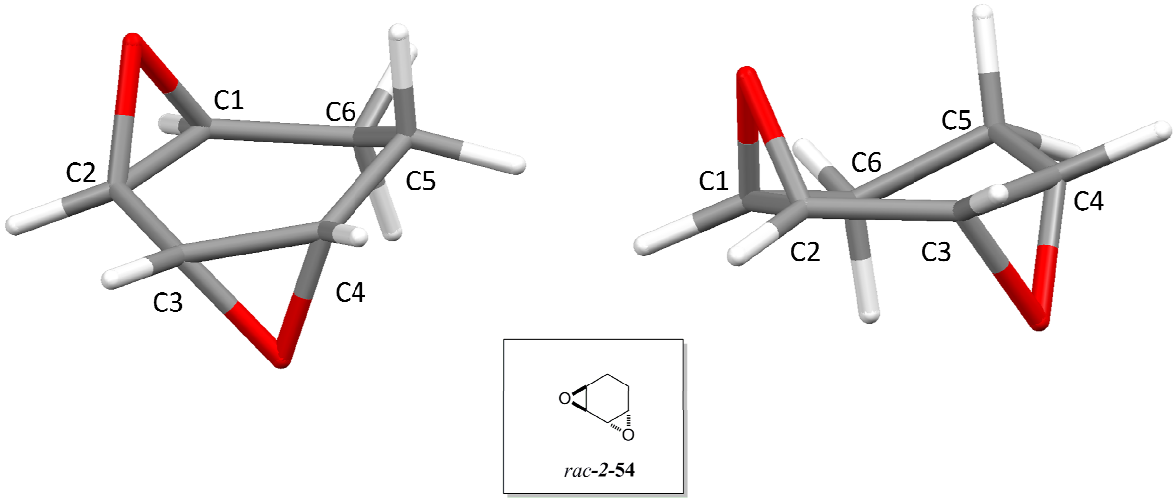

Gruber-Khadjawi showed that opening of ***2*-54** with azide anion produced only the 1,3-diazido diol (***2*-62**, Scheme 2.25).[95] Unaware of the work by Kozlov, Gruber-Khadjawi proposed that initial opening can occur at either C3 or C4. If opening occurs at C4 ("outside" attack) the epoxy azido alcohol (**60**) is formed and likely adopts an all equatorial conformation (dieq-*rac*-***2*-60**). FP dictates that the second opening must occur at C2 which gives the 1,3-diazido diol (***2*-62**). Alternatively, if the azide attacks first at C3 ("inside" attack) a regioisomeric epoxy azido alcohol (***2*-61**) is formed. However, due to the FP control the second opening must occur at C1, thus giving the diazido diol (***2*-62**) from a different intermediate.

Scheme 2.25. Gruber-Khadjawi's ring opening of *2*-54 with azide nucleophile.

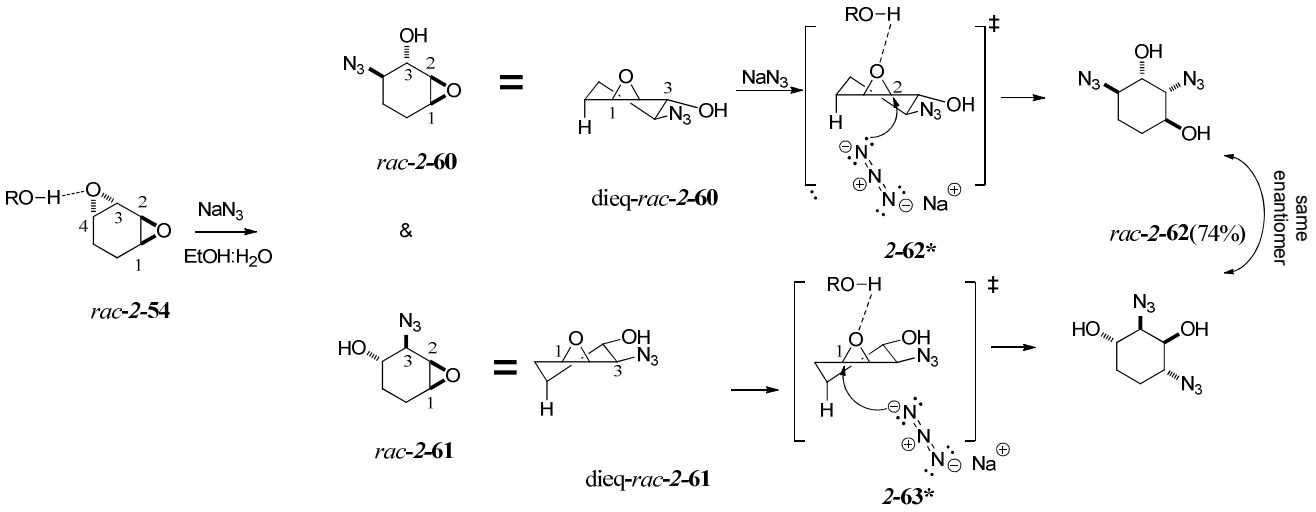

Another reported study of the nucleophilic opening of ***2*-54** was performed by the Rickborn group.[114] The researchers explored the reduction of ***2*-54** with $LiAlH_4$ and found that in ether solvent, they were able to isolate three different *trans*-diols (***2*-66**-***2*-68**, Scheme 2.26). Their results can be explained using FP and nucleophilic delivery controlled FP. The researchers stipulate that ***2*-54** can be opened either from the "outside" or "inside", and one of the products (***2*-66**) can only be accounted for by "outside" opening. The viability of the "outside" pathway contrasts with the observations by Kozlov with amine nucleophiles.[112,113,115] If "outside" attack occurs, intermediate ***2*-64** can react via the initially formed axial conformation, accepting a second hydride at C1 via a nucleophilic delivery FP mechanism (cf. Scheme 2.2) to give the 1,2-*trans*-diol as a minor product (***2*-66**). A 1,3-*trans*-diol (***2*-67**) can be derived from two pathways. Either it can be formed through the equatorial conformation (eq-*rac*-***2*-64**) in the "outside" attack mechanism, *or* **54** can undergo "inside" opening furnishing the equatorial conformer (eq-*rac*-***2*-65**) which yields ***2*-67**. Finally the achiral 1,4-trans-diol (***2*-68**) is formed from the nucleophilic delivery FP mechanism via the axial conformer (ax-*rac*-***2*-65**).

Scheme 2.26. Rickborn's reductive opening of trans-diepoxide *2*-54 with $LiAlH_4$.[114]

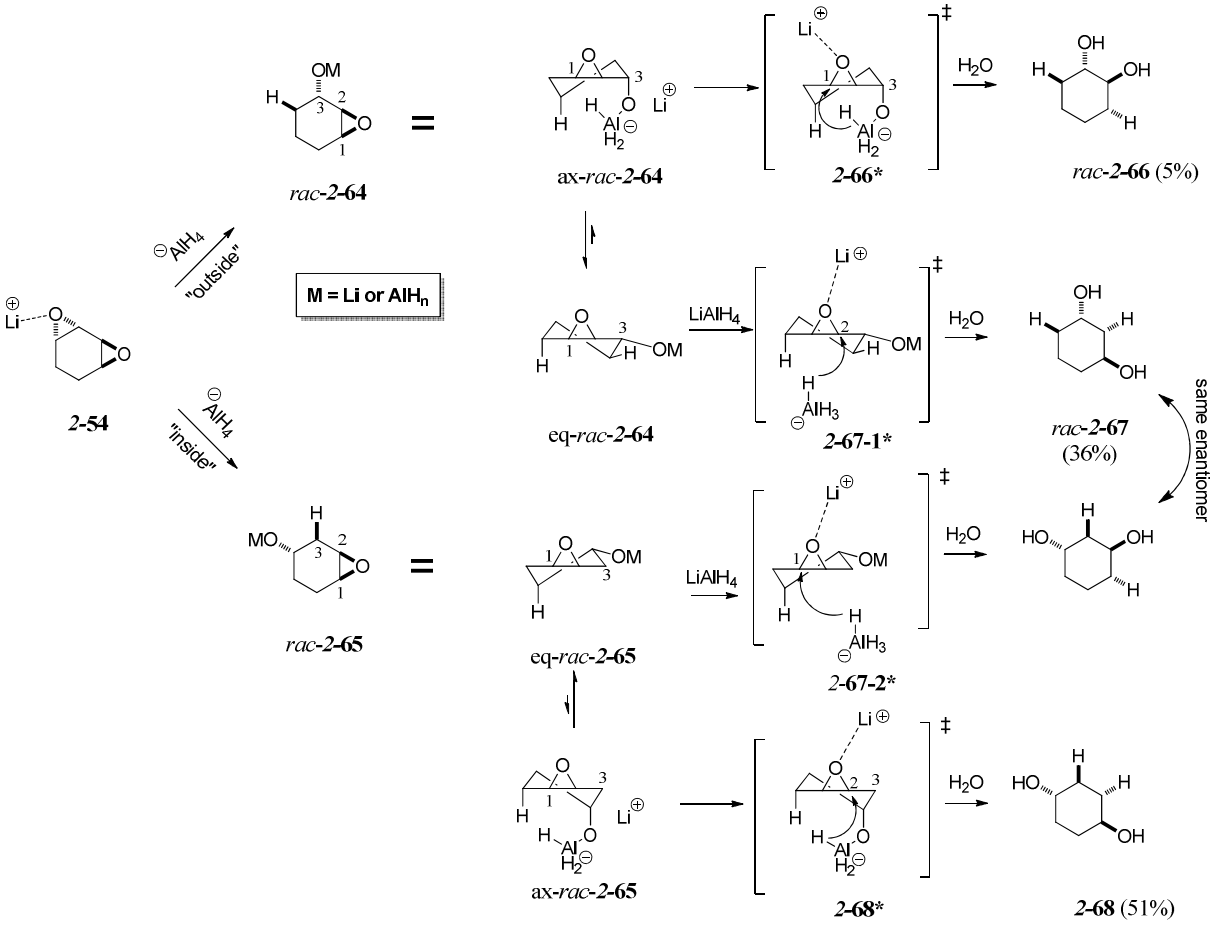

2.4.3. Nucleophilic openings of *2*-54 with anilines.

We have a private communication from the Sharpless group that ***2*-54** reacts with aliphatic amines to give 1,3-diol products exclusively, which is also seen in the work of Kozlov.[112,113,115] We confirmed this result by opening ***2*-54** with benzyl amine (***2*-49b**) to give the corresponding 1,3-diol (***2*-58b**, Scheme 2.27).

Scheme 2.27. Opening of trans-diepoxide *2*-54 with amine nucleophiles.

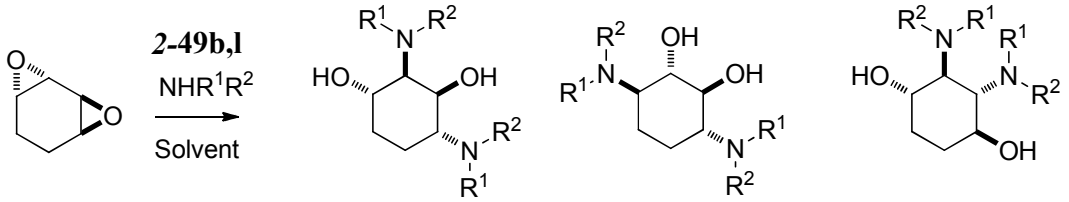

rac-2-**54** *rac-2*-**58a,f,l** *rac-2*-**57a,f,l** *rac-2*-**59a,f,l**

	R^1	R^2	Yield (***2*-58**)	Yield (***2*-57 or *2*-59**)
b*	$PhCH_2$	H	86%	0%
f*	p-F C_6H_4	H	50%	20%
l**	CH_3	CH_3	80%	0%

* - experiments performed in our laboratory

** - experiment performed by Kozlov et al.[40]

From our success with N-H assisted FP with aniline nucleophiles we first attempted accessing the 1,2-diol or 1,4-diol (both accessible only through N-H assisted FP, Scheme 2.28) by opening ***2*-54** with *p*-fluoroaniline (***2*-49f**) "on water" and under solvent free conditions. In the "on water" system, the opening gave two new products as judged by TLC. We postulate that the products are two of the possible three *trans*-diols (cf. Schemes 2.24 and 2.27, ***2*-57f**, ***2*-58f**, and/or ***2*-59f**).

Scheme 2.28. Our opening of trans-diepoxide *2*-38 with aniline nucleophiles "on water".

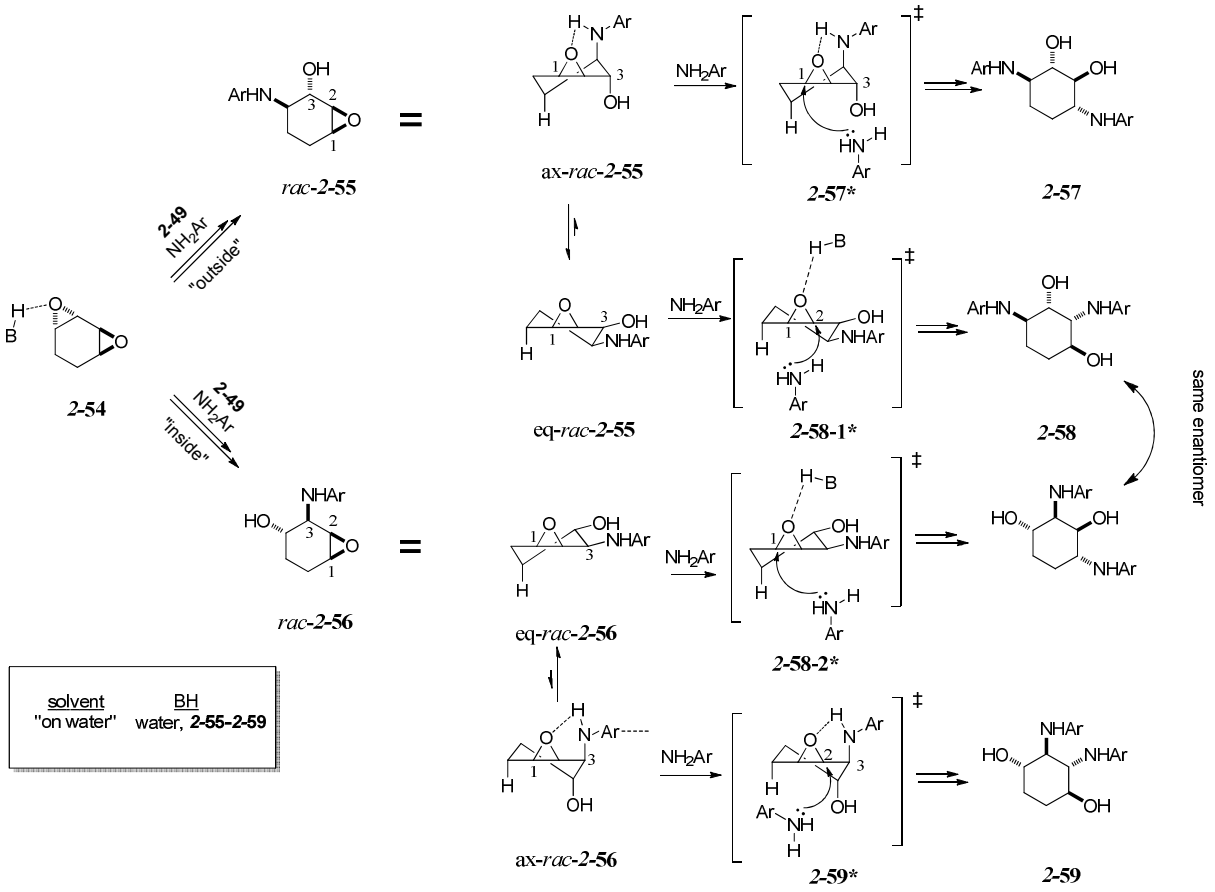

2.4.4. Structural determination of C_2-symmetric diol by NMR.

After isolation of the two products their structures were determined by correlation NMR spectroscopy. The major product (63:37) was the *trans*-1,3-diol ***2*-58** which is derived from either "inside" or "outside" opening followed by unassisted FP (Scheme 2.28). Since the 1,3-diol ***2*-58** is C_1-symmetric, the compound was easily identifiable by ^{13}C-NMR which showed 6 distinct resonances in the aliphatic region. Our minor product was clearly a C_2-symmetric compound showing only 3 distinct resonances in the aliphatic region (Figure 2.7), indicating we had formed either ***2*-57f** or ***2*-59f**.

Figure 2.7. ^{13}C-NMR of either *2*-57f or *2*-59f.

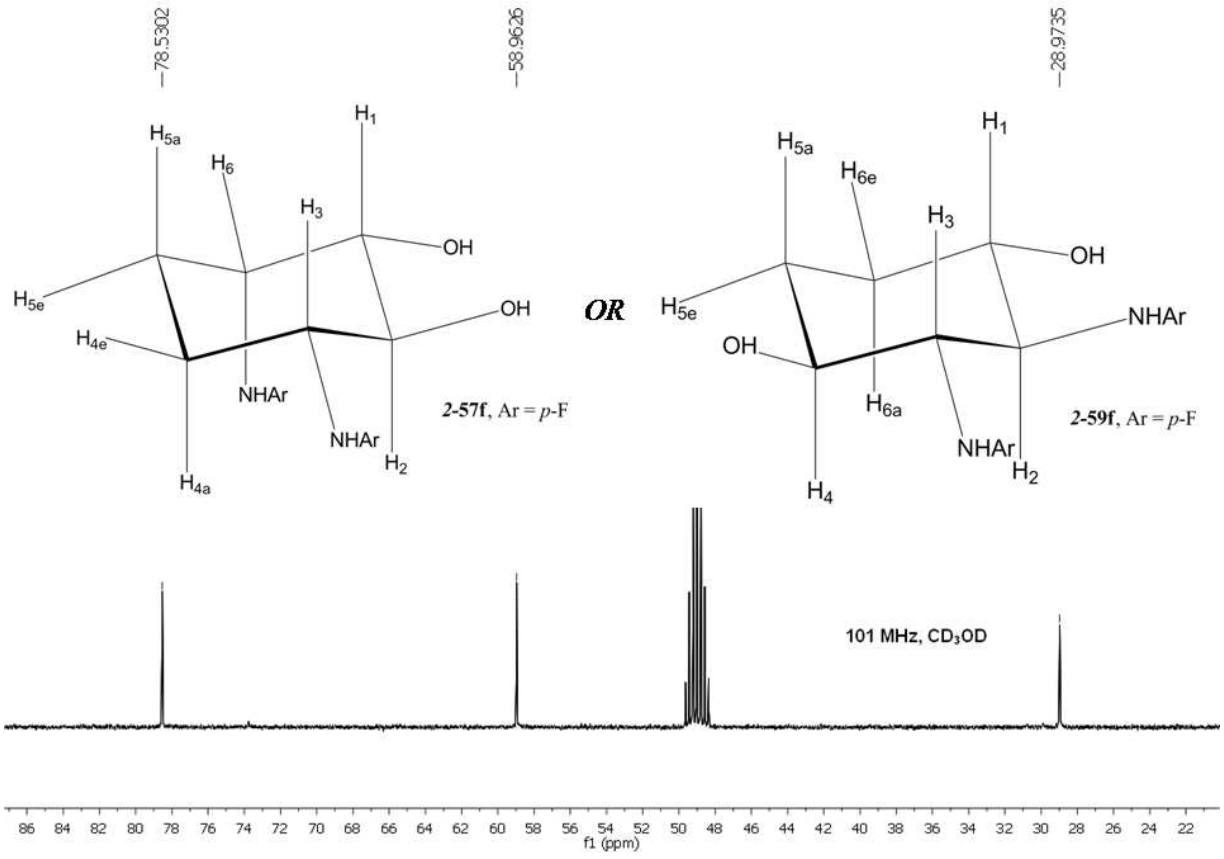

However, ^{1}H-^{13}C HSQC combined with ^{1}H-^{1}H COSY spectroscopy allowed us to determine which C_2-symmetric diol was formed. First, the HSQC allowed us to determine the value of the chemical shift for the α-anilino protons (Figure 2.8).

Figure 2.8. ^{1}H-^{13}C HSQC correlation spectra of *2*-57f or *2*-59f determining the chemical shifts of the α-anilino protons.

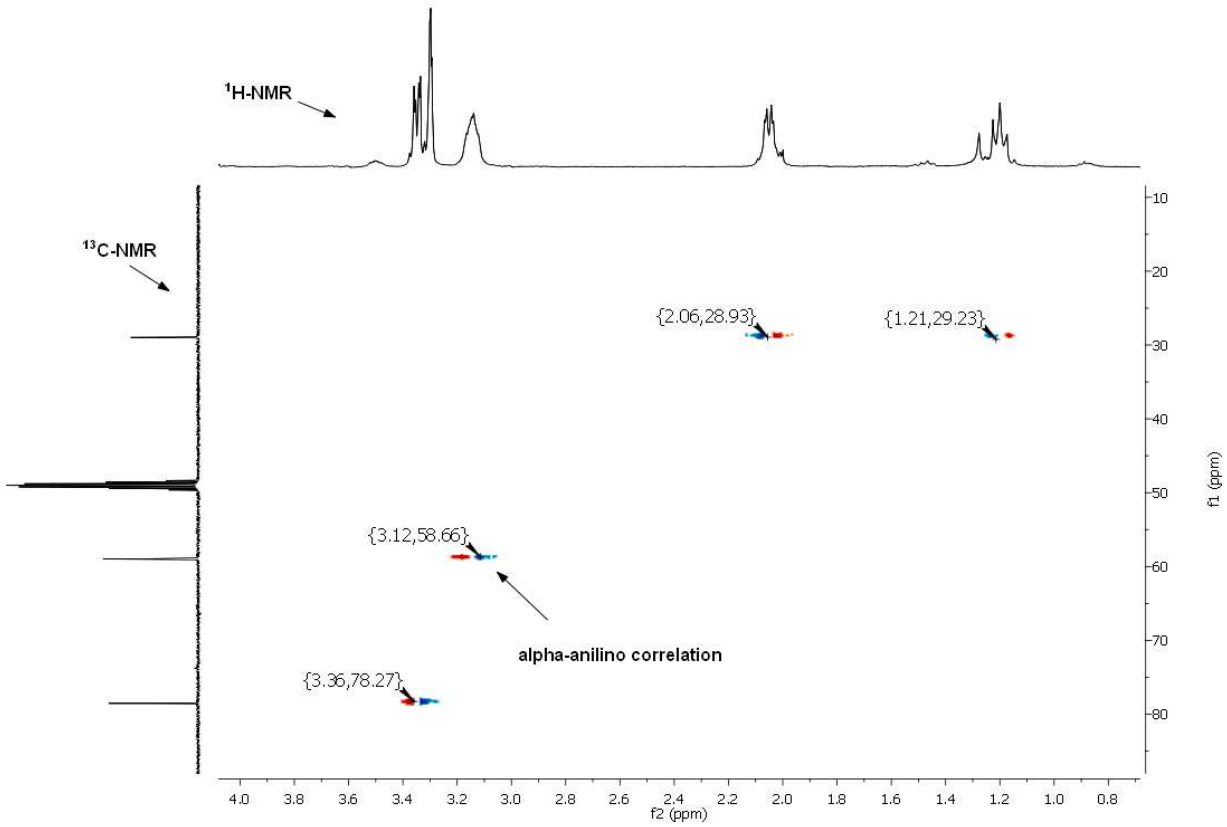

Postulating that the α-anilino carbons would be further up-field than the more electron deficient α-hydroxy carbons, we assigned the ^{13}C-shift of the α-anilino carbons to the signal at 58.7 ppm. With HSQC we could assign the α-anilino protons to the signal at 3.1 ppm. Upon knowing the shift of the α-anilino protons, we used ^{1}H-^{1}H COSY (Figure 9) to find whether the α-anilino protons coupled to only the α-hydroxy protons (which would give ***2*-59f**) or the methylene protons (which would give ***2*-57f**) and the α-hydroxy protons. ^{1}H-^{1}H COSY verified the 1,2-diol ***2*-57f** was our C_2-symmetric product by showing the α-anilino - methylene ^{3}J coupling (e.g. $^{3}J_{H3H4}$).

Figure 2.9. ^{1}H-^{1}H COSY spectrum demonstrating the α-anilino methylene proton coupling corresponding to *2*-57f.

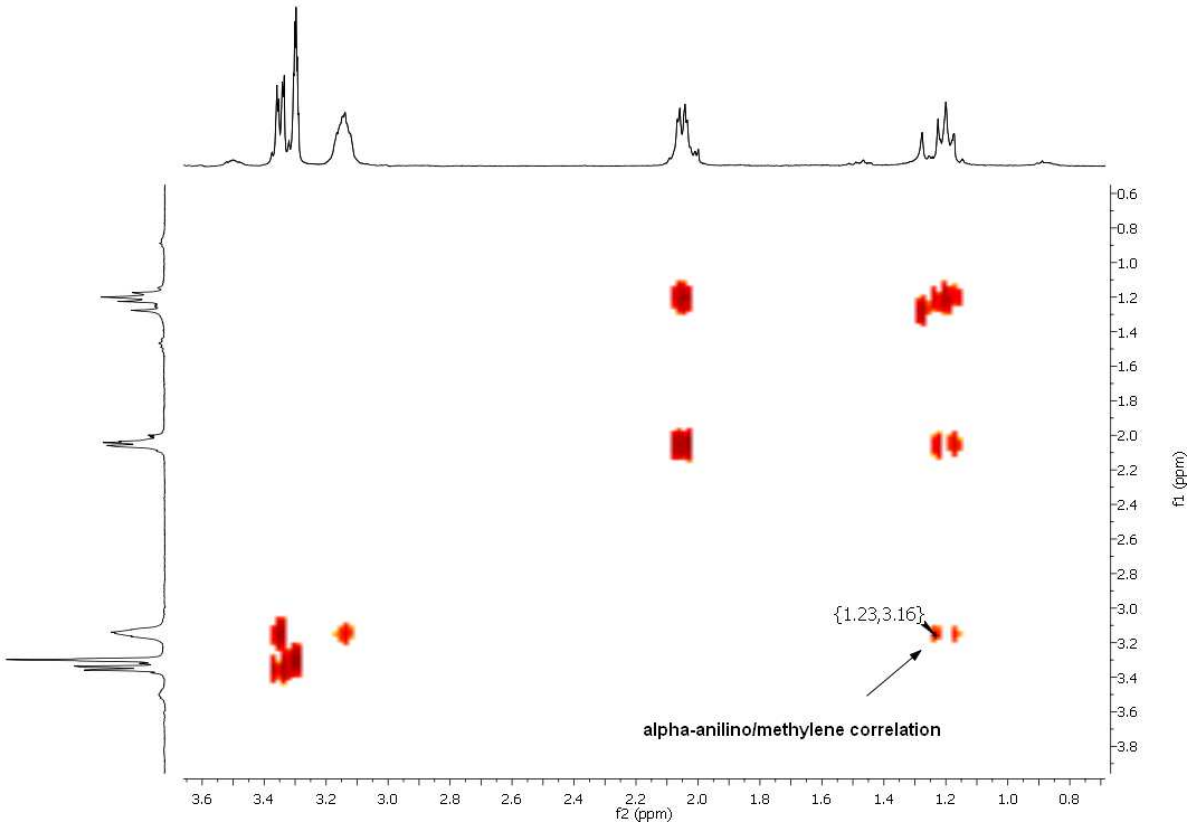

Recall that the *trans*-1,2-diol ***2*-57f** can only be formed by "outside" opening followed by N-H assisted FP. Interestingly there was no evidence for the formation of the *trans*-1,4-diol, which would be formed from the Kozlov like "inside" opening followed by N-H assisted FP.

We were quite excited by these results with *p*-fluoroaniline; N-H assisted FP was operating "on water" with higher efficacy relative to our openings of *trans*-1,2:4,5 diepoxide ***2*-29** (Table 2.4, Entry 4). However, when other anilines were used in the opening of ***2*-54**, no convincing trend was seen between regioselectivity and the Hammet sigma value (Table 2.11). Unlike the case of *trans*-1,2:4,5 diepoxide ***2*-29**, the 1,3:1,2-selectivity is insensitive to the nature of the aniline substituent.

Table 2.11. Our results of differing aniline nucleophile on product distribution.

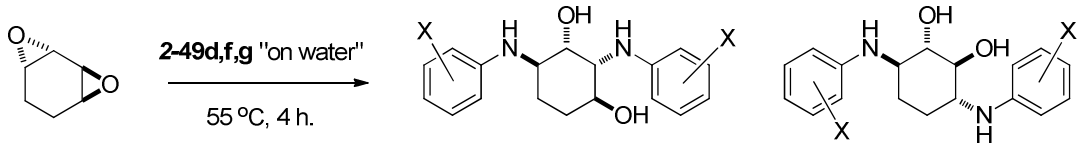

*rac-**2*-54** *rac-**2*-58** *rac-**2*-59**

Entry	***Aniline***	***n***	***X***	***sigma value*[108]**	***1,3:1,2*[a]**	***% recovery***
1	***2*-49d**	2	*p*-OCH_3	-0.12	66:34	84%[b]
2	***2*-49f**	2	*p*-F	0.15	63:37	50%[c]
3	***2*-49g**	2	*m*-Cl	0.37	62:38	89%[b]

[a] Crude product ratios measured by ^{1}H-NMR before purification. [b] Crude recovery of a mixture of regioisomers.. [c] Chromatographed yield of major regioisomer

We sought to improve 1,2-diol selectivity by reducing intermolecular H-bonding by running the reactions under solvent free or in aprotic conditions. Unfortunately the solvent free and aprotic solvents (DMF and NMP) failed to give any reaction at 95 ^{o}C and showed significant decomposition at temperatures in excess of 120 ^{o}C for openings with ***2*-49d,f,g**. Thus the thermal lability of ***2*-54** at temperatures required for solvent-free reaction prevents us from testing the hypothesis that N-H directed FP could be effective in this system.

2.4 Conclusions

In conclusion, we have shown that previously inaccessible C_i-symmetric 1,4-diols can be prepared from *trans*-1,2:4,5-diepoxycyclohexane ***2*-29** and anilines. The 1,3-:1,4-diol product ratio in reactions of ***2*-29** with anilines was found to be sensitive to both electronic effects in the aniline, and to the nature of the reaction conditions. Highest selectivities for the 1,4-diol products ***2*-52** are obtained with electron-poor anilines under neat conditions (Table 2.7). Highest selectivities for the 1,3-diol products ***2*-51** are obtained with electron-rich anilines using "on water" conditions (Table 2.4). The superior hydrogen-bonding ability of a pendant anilino group (relative to an aliphatic amino) in the epoxy amino alcohol intermediate ***2*-50** is proposed to allow access to the 1,4-diol regioisomer via intramolecular H-bond stabilized transition structure ***2*-52*** (Scheme 2.20). To the best of our knowledge, the potential of an appropriately acidic intramolecular NH hydrogen bond donor to direct ring-opening of cyclohexene oxides has not previously been recognized in the literature. Additionally, by judicious choice of reactant order and reaction conditions, it is possible to synthesize unsymmetrical 1,3- and 1,4-diols from ***2*-29** and anilines in high selectivity and yield (Scheme 2.22). However, our studies with 1,2:3,4-*trans*-diepoxide (***2*-54**) were less successful. Although the opening of ***2*-54** with benzyl amine

(***2*-49b**) gave the 1,3-diol as expected, the neat reactions with three different anilines (***2*-49d,f,g**) or benzyl amine (***2*-49b**) did not work. Furthermore, regardless of the aniline used in the "on water" openings, we could only achieve roughly a 2:1 selectivity for 1,3-diol over the 1,2-diol. Though disappointing, this result is noteworthy on two counts. Firstly, the 1,2-diol ***2*-57** requires outside opening of ***2*-54** with anilines. Such outside opening of ***2*-54** has not been observed previously in reactions with other amines ***2*-49b** and **49l**. Secondly, formation of ***2*-57** requires N-H assisted opening of the intermediate ***2*-55**. Neither of these phenomena has been reported previously in the literature.

Chapter 3 Stereoselective epoxidation of allylic and homoallyic amides and their subsequent openings with anilines.

3.1 Directed epoxidation reactions for 2-substituted cyclohexenes

3.1.1 Directed peracid epoxidation reactions of allylic alcohols.

One of the first examples of the pre-association of reaction partners through H-bonding resulting in a product with high stereoselectivity was shown by Henbest[116] in the peracid oxidation of 2-cyclohexenol (Scheme 1).[117]

Scheme 3.1. Henbest peracid oxidation of 2-cyclohexenol *3*-1.

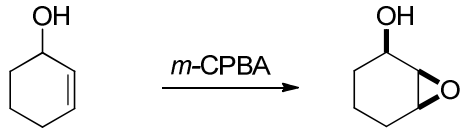

rac-3-1 *syn-3-2* (dr 10:1)

This result can be rationalized by Bartlett's butterfly mechanism[118] involving the nucleophilic alkene and the electrophilic peracid (Scheme 3.2). The H-bond formation between the hydroxyl hydrogen from either the pseudoaxial or pseudoequatorial conformer (Scheme 3.2, **eq-*3*-2*** and **ax-*3*-2***) enables delivery of the oxygen via guidance to the olefin, thus installing the oxygen *syn* to the directing hydroxyl group.

Scheme 3.2. Mechanism of Henbest peracid oxidation.[117]

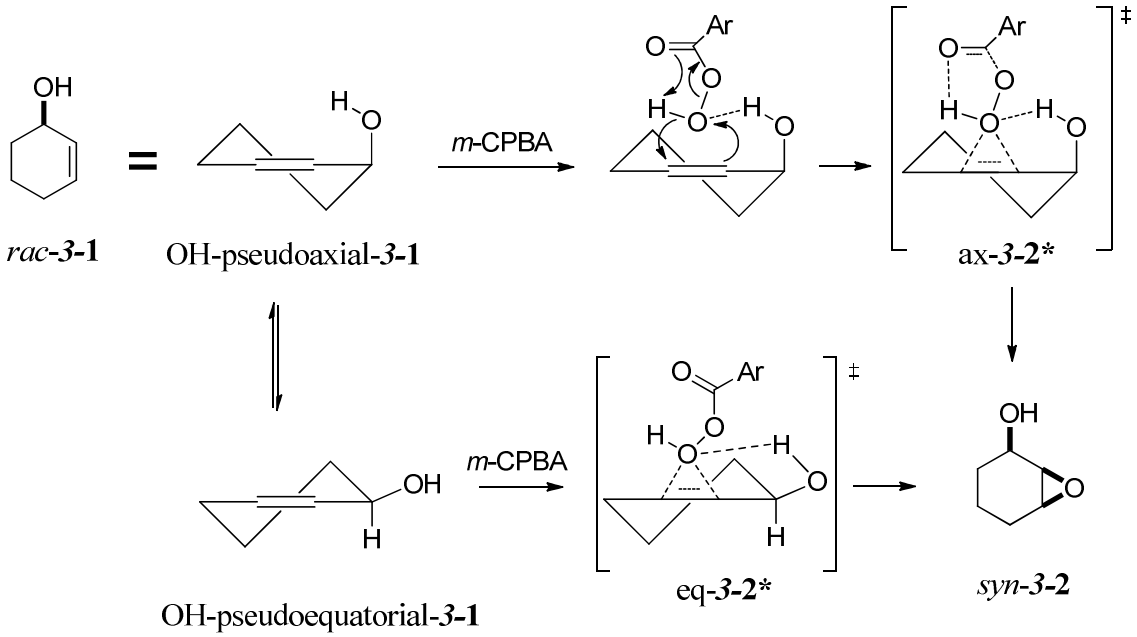

The Whitham group explored the reaction mechanism by performing the peracid oxidation on both *cis*-5-*tert*-butylcyclohexen-2-enol (Scheme 3.3, ***3*-3**) and *trans*-5-*tert*-butylcyclohexen-2-enol (***3*-4**).[119] Scheme 3.3 shows that both isomers are conformationally locked in order to accommodate the sterically demanding *tert*-butyl group in an equatorial position. By having the directing hydroxyl group locked in either a pseudoaxial (*rac*-***3*-4**) or psuedoequatorial (*rac*-***3*-3**) conformation, the researchers were able to measure the selectivities and rates of epoxidation to determine which hydroxyl conformation directs epoxidation with greater efficacy.

Scheme 3.3. Epoxidation mechanism for conformationally locked directing groups.[119]

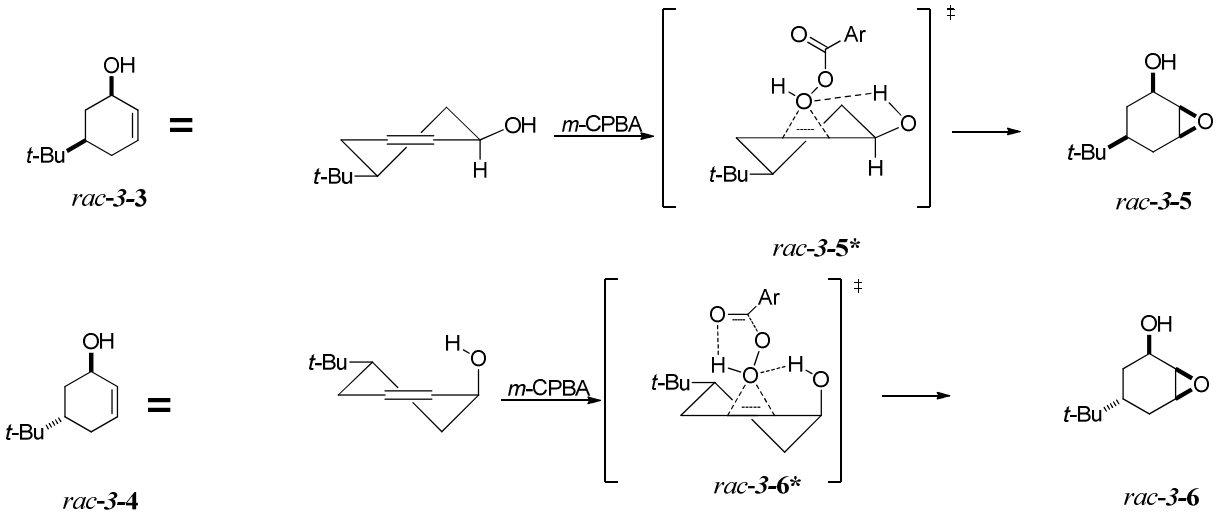

Table 3.1 summarizes the results of their experiments and indicates that the hydroxyl group better directs from the pseudoequatorial (***3*-5***) than the pseudoaxial position (***3*-6***). Moreover, the epoxidation of the conformationally locked allylic alcohol (***3*-3**) is considerably more selective than the same reaction for the conformationally flexible 2-cyclohexenol (***3*-1**).

Table 3.1. Selectivities and rate constants for perbenzoic acid epoxidation of allylic alcohols.[119]

Entry	*Substrate*	$k \times 10^3$ ($M^{-1}*sec^{-1}$)	*syn:anti selectivity*
1	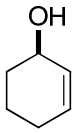 *rac*-***3***-**1**	3.45	10:1
2	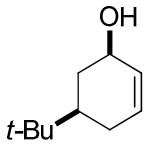 *rac*-***3***-**3**	4.8	24:1
3	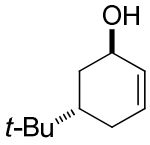 *rac*-***3***-**4**	0.67	5:1

3.1.2 Directed peracid epoxidation reactions of allylic amides.

In addition to epoxidation direction by hydroxyl groups, it was discovered that amide groups can also effectively control stereoselective oxidation. Goodman was one of the first to show this Henbest effect for allylic amides by the stereoselective oxidation of *N*-(cyclohex-2-en-1-yl)benzamide (***3***-**7**) with *m*-CPBA to furnish the *syn*-epoxide (***3***-**8**) in perfect stereoselectivity

(Scheme 3.4).[86] The researchers did not comment on nor investigate whether the amide is a more effective director in either the pseudoequatorial or pseudoaxial position.

Scheme 3.4. Directed epoxidation by an allylic amide (*3*-7).

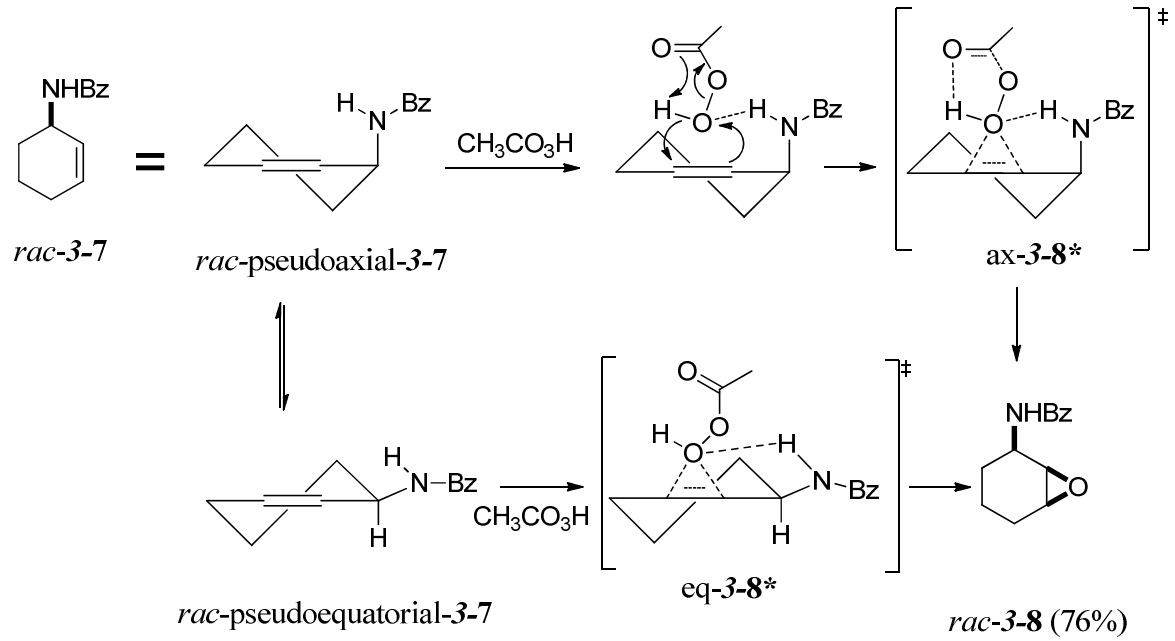

This perfect selectivity for epoxidation was also demonstrated for allylic amides in the androstane research of Lukacs and Fukushima.[120] Here treatment of either allylic amide (Scheme 3.5, ***3*-9** and ***3*-10**) furnishes the corresponding *cis*-epoxide (***3*-10** and ***3*-12**) in high yield and perfect stereoselectivity.

Scheme 3.5. Stereoselective epoxidation of androstane containing allylic amides.[120]

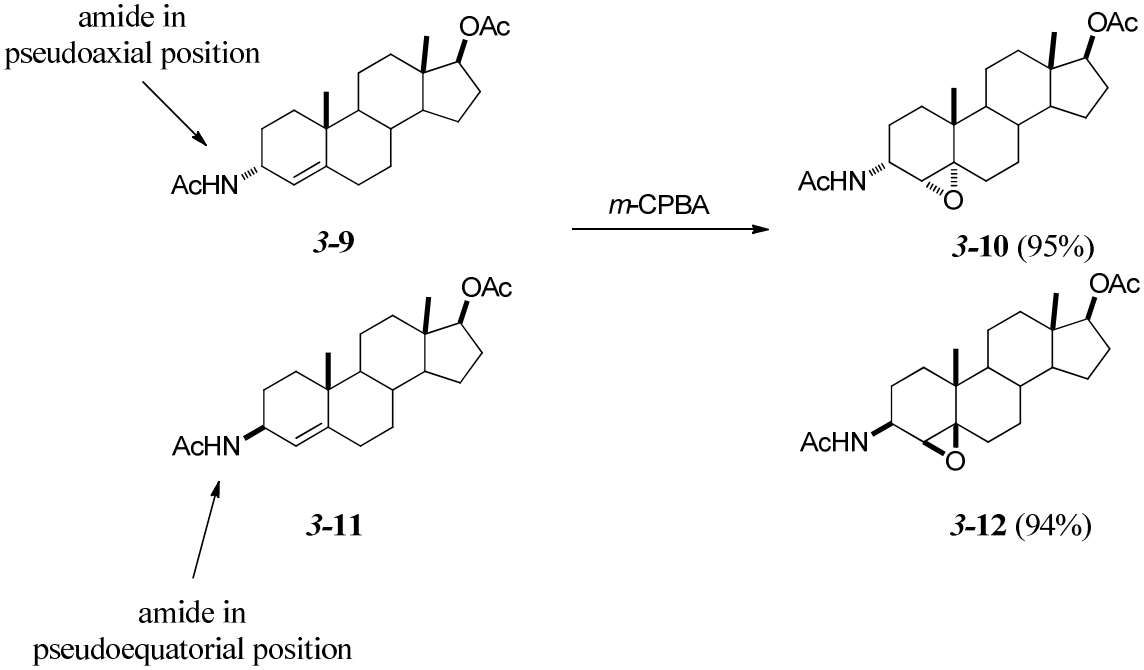

Other groups bearing a relatively weak N-H (or acidic) bond have been shown to exhibit *syn*-directive effects for allylic substrates with high stereoselectivity. Bäckvall showed that an allylic tosylamide can direct with high stereoselectivity (Table 3.2, Entry 1).[121] Several carbamates are also capable of this directive effect with high stereoselectivity as shown in a recent publication by the O'Brien group (Entries 2 - 11).[122] All of the epoxidations carried out gave essentially quantitative yields and high *cis* selectivity; however it is interesting to note that the amides (Entries 9-11) gave the greatest stereoselectivity.

Table 3.2. Stereoselective epoxidation of *N*-protected allylic amines.[121,122]

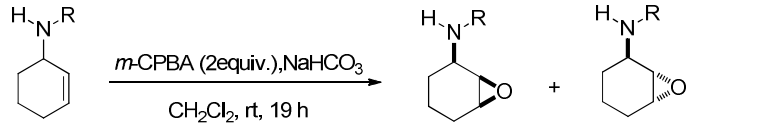

rac-3-13a-j *rac-cis-3*-14a-j *rac-trans-3*-14a-j

Entry	*R*	*alkene*	*epoxide*	*(±)cis:trans*[a]
1	Ts	***3*-13a**	***3*-14a**	96:4[b]
2	Ts	***3*-13a**	***3*-14a**	90:10
3	Ms	***3*-13b**	***3*-14b**	90:10
4	*o*-Ns	***3*-13c**	***3*-14c**	90:10
5	*p*-Ns	***3*-13d**	***3*-14d**	95:5
6	CO_2Me	***3*-13f**	***3*-14e**	90:10
7	CO_2Bn	***3*-13f**	***3*-14f**	90:10
8	$CO_2{}^t$-Bu	***3*-13g**	***3*-14g**	85:15
9	$Cl_3CC(O)$	***3*-13h**	***3*-14h**	95:5
10	PhC(O)	***3*-13i**	***3*-14i**	98:2
11	^{t}-BuC(O)	***3*-13j**	***3*-14j**	98:2

[a] Stereoselectivity measured by ^{1}H-NMR analysis of crude product mixture. [b] Reaction performed by Backvall et. al.[121]

3.1.3 Synthesis of allylic amides.

In order to explore the possibility of an N-H assisted FP pathway for the opening of 2-amido substituted *syn*-cyclohexene oxides (***3*-14**) we needed to synthesize a series of allylic amides. In the aforementioned work by O'Brien (Table 3.2), the researchers were able to synthesize several allylic amides and derivatives utilizing the Isobe[123] modification of the Overman rearrangement.[124] The Overman rearrangement is a 1,3-transposition of an oxygen to a nitrogen function (specifically a trichloroacetamide ***3*-13h**, Scheme 3.6) that proceeds through a [3,3]-sigmatropic rearrangement.

Scheme 3.6. The Overman rearrangement.[124]

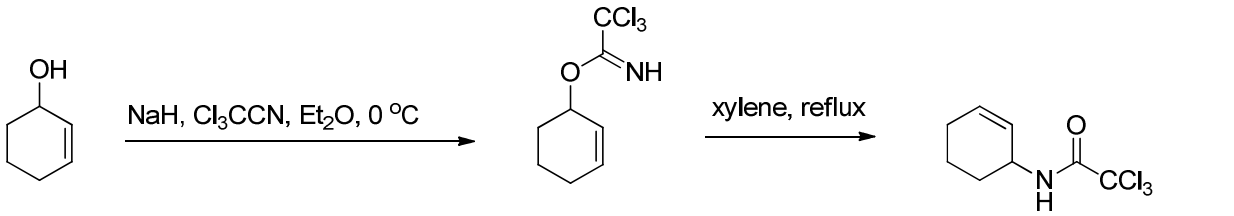

***3*-1** ***3*-15** ***3*-13h** (61% over two steps)

The Isobe modification of the Overman rearrangement consists in adding inorganic base (K_2CO_3 or $NaHCO_3$) in the second step in order to trap any acids present during the thermal rearrangement. The Isobe group demonstrated the advantage of the addition of inorganic base in their attempts to synthesize a key intermediate in their tetrodotoxin synthesis (***3*-18**, Scheme 7). In the absence of K_2CO_3 in the second step, the Overman rearrangement of ***3*-16** gave the desired product ***3*-18** as well as an aromatized by-product ***3*-19**.

Scheme 3.7. Addition of K_2CO_3 and the outcome of the Overman rearrangement.[123]

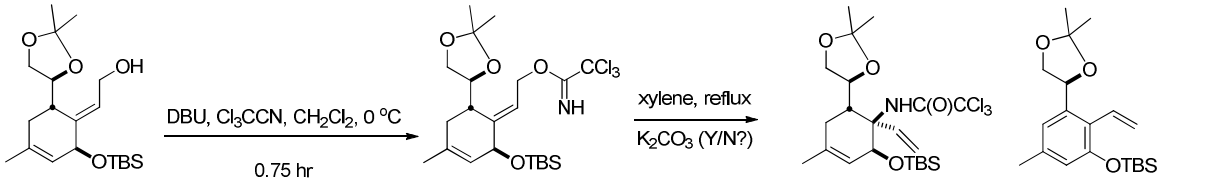

***3*-16** ***3*-17** ***3*-18** (Y - 62%, N - 37%) ***3*-19** (Y - 0%, N - 32%)

Although the researchers did not give any mechanistic details for the formation of the by-product ***3*-18**, they state it is most likely a result of acid catalyzed elimination of the newly installed trichloroacetamide followed by air-oxidation. However, when K_2CO_3 was employed in the thermal rearrangement, ***3*-18** was the only product detected. The researchers then applied their modification to several other allylic alcohols and concluded that the addition of K_2CO_3 to the thermal rearrangement step of the Overman rearrangement limited the formation of by-products and increased recoveries of the desired trichloroacetamide.

In the O'Brien study, the modification of the Overman rearrangement was not applied to the allylic alcohol ***3*-1** to give ***3*-13h**. O'Brien gives a brief synthetic route to ***3*-13h** in 81% overall yield (Scheme 3.8).[122]

Scheme 3.8. O'Brien synthesis of trichloroacetamide *3*-13h.[122]

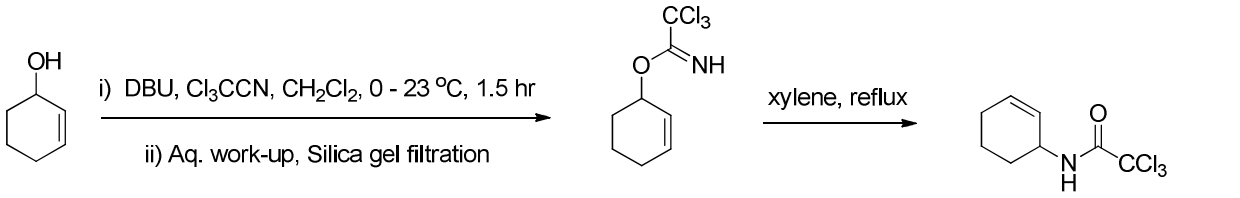

***3*-1** ***3*-15** ***3*-13h** (81% over two steps)

However, in our hands using the O'Brien procedure we were unable to form ***3*-13h**. Upon closer review of the report of Isobe, we learned it was important to form the trichloroimidate from cyclic allylic alcohols such as ***3*-1** at -20 ^{o}C and quench the reaction at -20 ^{o}C with saturated aqueous NH_4Cl. Performing the first step at -20 ^{o}C is necessary due to the instability of the trichloroimidates derived from cyclic allylic secondary alcohols (e.g. ***3*-1**) which are known to eliminate trichloroacetamide.[123-125] Additionally, Isobe claims the trichloroimidates such as ***3*-15** are acid labile and should not filtered through silica gel but rather filtered through anhydrous K_2CO_3. Incorporating these two modifications into the O'Brien procedure, we were able to obtain ***3*-13h** in 92% yield (Scheme 3.9).

Scheme 3.9. Our synthesis of trichloroacetamide *3*-13h utilizing a modification of the Overman rearrangement.

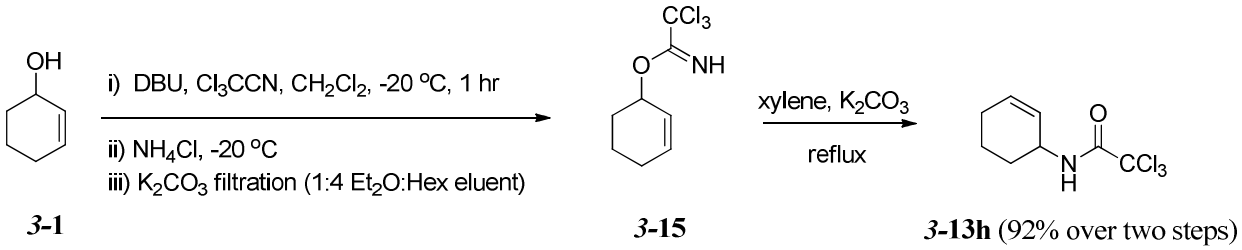

***3*-1** ***3*-15** ***3*-13h** (92% over two steps)

The O'Brien group hydrolyzed the trichloroacetamide ***3*-13h** to furnish the allylic amine ***3*-20** which was isolated as the hydrochloride salt. The amine hydrochloride ***3*-20** was then used in conjuction with a variety of acyl chlorides to furnish the amide and amide derivatives (***3*-13a-f,j-i, *3*-13g** from Boc_2O**,** Table 3.2) in high yield. However, in our hands we could never isolate the hydrochloride salt ***3*-20** (Scheme 3.10) in appreciable yield, likely due to poor recovery of the amine from the aqueous solvent upon hydrolysis. Rather than optimize our extraction

technique, we decided to explore other synthetic routes that would lead us to the allylic amine ***3*-20**.

Scheme 3.10. Our attempts at hydrolysis of trichloroacetamide to give the allylic amine *3*-20.

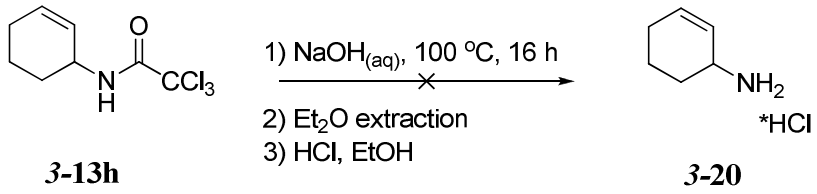

***3*-13h** ***3*-20**

The amination of allylic halides is one of the simplest and most direct ways to synthesize our desired allylic amine ***3*-20**.[126] We developed a three step procedure based on the work by Brouillette[127] to arrive at ***3*-20** starting from the commercially available 3-bromocyclohexene ***3*-21** (Scheme 3.11). The nucleophilic substitution of the allylic halide ***3*-21** by azide was performed in a warmed THF/water solution to furnish the allylic azide ***3*-22**. After extraction into ether followed by scrupulous removal of water by anhydrous magnesium sulfate, $LiAlH_4$ was carefully added and the suspension was stirred at reflux for 48 hours to ensure complete reduction of the azide. A Fieser work-up was performed and the crude allylic amine ***3*-20** was trapped with either nosyl chloride or benzyl chloroformate to furnish the amide derivatives ***3*-13d** and ***3*-13f** respectively.

Scheme 3.11. Our synthetic route to give allylic amide derivatives *3*-13d and *3*-13f.

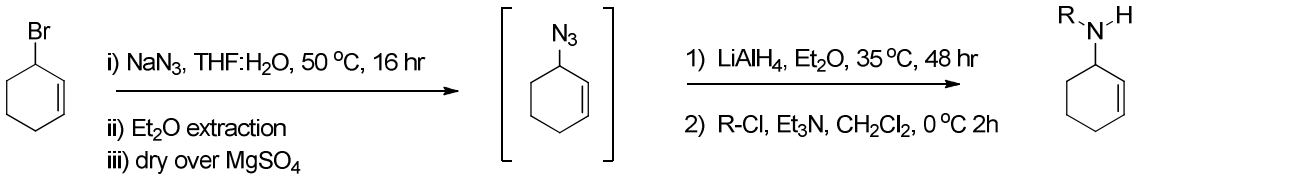

***3*-21** ***3*-22**

***3*-13d** R = Ns (56%, over 3 steps)

***3*-13f** R = Cbz (57%, over 3 steps)

With the allylic amide ***3*-13h** and two derivatives ***3*-13d** and ***3*-13f** we were poised to attempt the N-H directed epoxidation reactions as described by O'Brien.[122] Fortunately, we were able to achieve the same stereoselectivity and near quantitative yield as reported by O'Brien to furnish the *cis*-epoxides ***3*-14h,d,f** (Scheme 3.12).

Scheme 3.12. Our results for the epoxidation of allylic amide *3*-13h and derivatives *3*-13d,f.

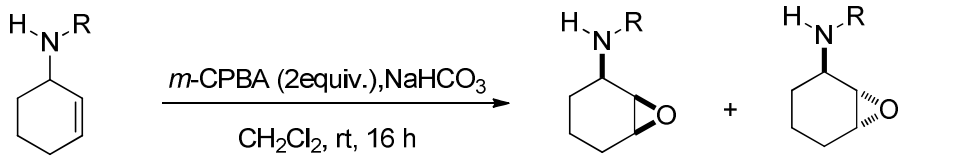

***cis-3*-14h,d,f** ***trans-3*-14h,d,f**

***3*-13h** R = $C(O)CCl_3$ ***3*-14h** (>99%, 95:5 *cis:trans*)

***3*-13d** R = Ns ***3*-14d** (95% 98:2 *cis:trans*)

***3*-13f** R = Cbz ***3*-14f** (>99%, 90:10 *cis:trans*)

3.2 Directed and undirected FP controlled openings of 2-substituted cyclohexene oxides.

3.2.1 N-H ammonium directed epoxidations.

As discussed in **3.1** the directed epoxidation of allylic alcohols and amides with high levels of stereoselectivity has been well documented. However, the epoxidation of allylic amines is at present much less studied. This can be attributed to the *N*-oxidation of amines by a variety of oxidizing agents namely peracids. A report by Quick et al. demonstrates how to avoid the *N*-oxidation problem by pre-treating the allylic amine (Scheme 3.13, ***3*-22**) with trifluoroacetic acid.[128] The trifluoroacetate salts (***3*-22**-H^+, a mixture of diastereomers) is then treated with trifluoroperacetic acid which directs epoxidation to furnish the epoxides with high stereoselectivity.

Scheme 3.13. Chemoselective epoxidation of an allylic amine with CF_3CO_3H.[128]

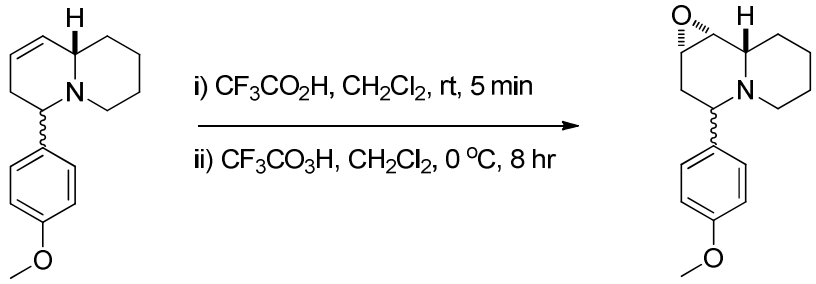

***3*-22** ***3*-23** (76%)

The high stereoselectivity is most likely due to direction from the ammonium hydrogen on N1 in protonated ***3*-22** which is *trans* relative to the hydrogen at C3 (Figure 3.1).

Figure 3.1. Mercury representation of the B3LYP/6-31G* optimized geometry of the protonated quinolizine *3*-22-H$^+$.

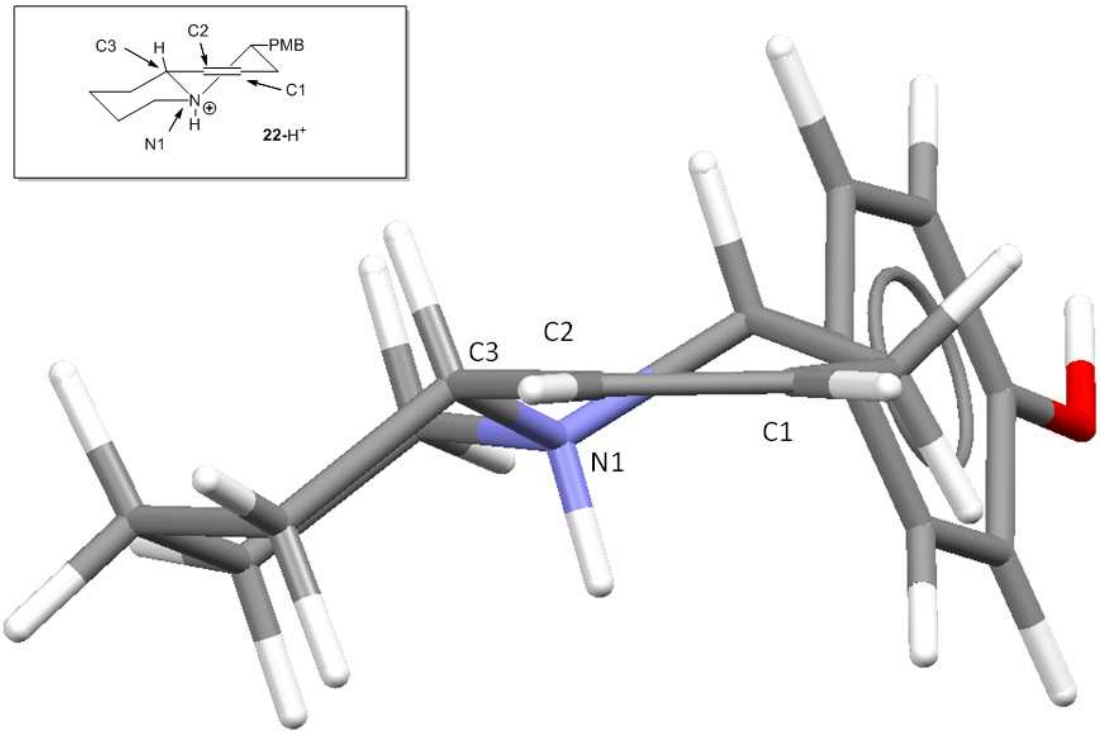

Asensio et al. has shown that the tosylate salt of ***3*-20** undergoes *syn*-selective oxidation with *m*-CPBA as the oxidant to give ***3*-24** (Scheme 3.14).[129] The researchers attribute this high *syn*-selectivity to N-H direction of the peracid elecrophile, analogous to the amide examples (cf. Schemes 3.4, 3.5 and Table 3.1).

Scheme 3.14. Asensio's N-H ammonium directed epoxidation of allylic amine *3*-20.[129]

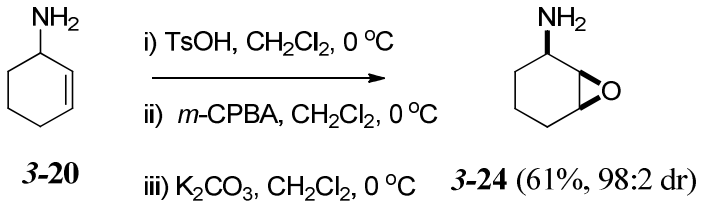

***3*-20** ***3*-24** (61%, 98:2 dr)

Another example of this *syn*-selective ammonium directed epoxidation is in a report by Edwards et al.; the researchers show that the trifluoroacetate salt (Scheme 3.15, ***3*-25**) undergoes epoxidation with *m*-CPBA stereoselectively to give ***3*-26**.[130] It is interesting to note that the endocyclic (relative to the ammonium salt) olefin does not undergo oxidation, providing further evidence that directed reactions are also accelerated reactions (cf. Table 3.1, Entries 2 and 3).

Scheme 3.15. Edward's N-H ammonium directed epoxidation of spirocycle *3*-25.[130]

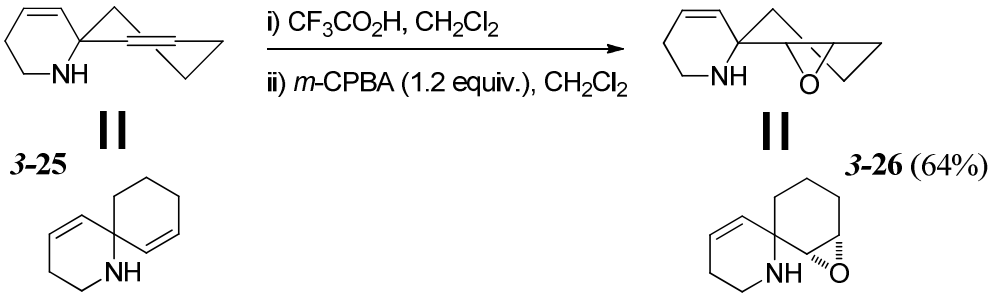

***3*-25** ***3*-26** (64%)

3.2.2 Opening of *syn*-2-substituted cyclohexene oxides.

The Davies group has shown that when an allylic amine such as ***3*-27** is treated with a large excess of trichloroacetic acid followed by treatment with *m*-CPBA gives a trichloroacetate ***3*-29** product in high stereoselectivity and regioselectivity.[131] The trichloroacetate ***3*-29** is a result of FP controlled opening of the *syn*-2-substituted cyclohexene oxide intermediate ***3*-28** by the excess trichloroacetic acid (Scheme 3.16). Subsequent hydrolysis of the labile trichloroacetate furnished the *anti*-1,2-diol ***3*-30**.

Scheme 3.16. Davies' ammonium directed dihydroxylation of allylic amine *3*-27.[131]

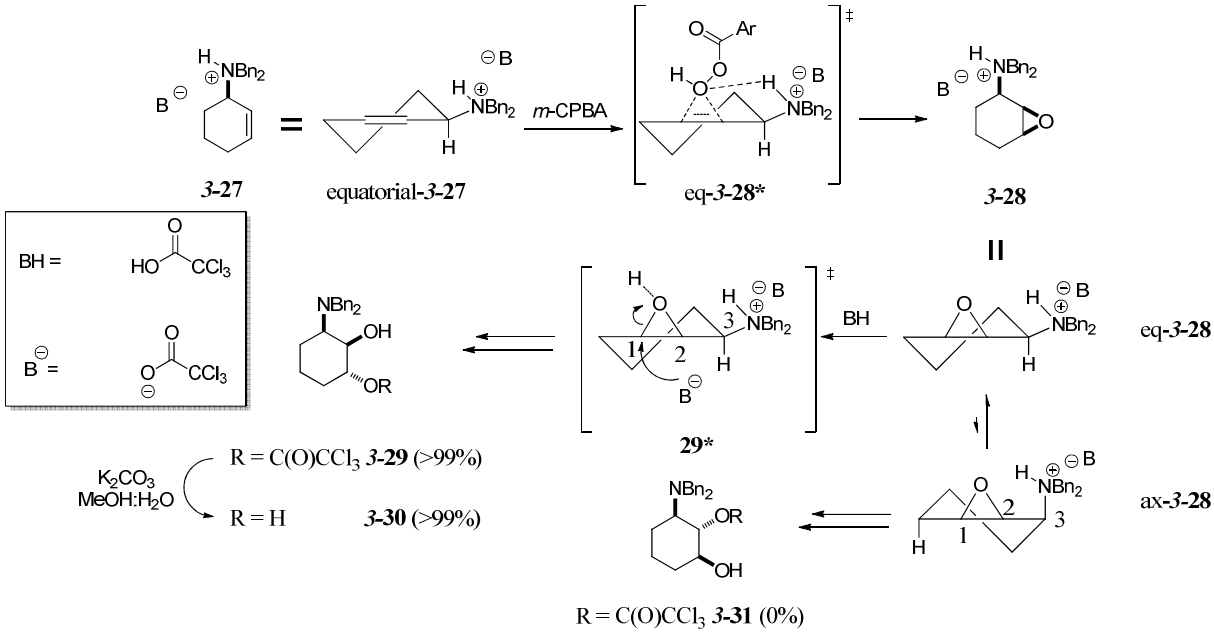

The Davies group attributes their highly stereoselective epoxidation to a "Henbest like" transition state (eq-***3*-28***) which directs the epoxidation to the *syn*-face (relative to the directing ammonium group) of the olefin. The researchers ascribe the perfect regioselectivity to the interplay of two stereoelectronic effects. In eq-***3*-28** nucleophilic attack is governed by the FP stereoelectronic effect, therefore attack must occur at C1 to furnish ***3*-29**. The second electronic effect arises from acid-catalyzed ring opening of epoxides proceeding through a late transition state.[132] The authors state "The oxirane carbon atom undergoing nucleophilic attack possesses considerable carbocationic character, which presumably favours nucleophilic attack at C1 where the effects of the electron-withdrawing *N,N*-dibenzylammonium moiety are minimized."[131] Interestingly the researchers do not observe the trichloroacetate (***3*-31**) resulting from the conformer in which the ammonium group is axial (ax-***3*-28**), suggesting that N-H directed FP is not viable due to the inductive effect of the proximal *N,N*-dibenzylammonium substituent.[131]

With three different *syn*-2-substituted cyclohexene oxides (Scheme 3.12, ***3*-14h,f,d**) in hand we set out to investigate whether any N-H directed FP opening of the epoxides was possible. Having prior success in N-H directed FP opening of 1,2:4,5-trans-diepoxide (***2*-29**) with aniline nucleophiles we attempted our first experiments with *p*-fluoroaniline (***2*-49f**), *p*-anisidine (***2*-49d**), and *m*-chloroaniline (***2*-49g**) all "on water". The reactions were judged to be complete after 3 hours and TLC indicated the formation of one product for the opening of ***3*-14h,f,d** (Table 3.3). ^{1}H-NMR indicated that we had formed the expected FP product ***3*-32** exclusively as expected based on the results of intermolecular epoxide activation. In Scheme 3.16 the FP product (***3*-29**) results from intermolecular activation of the epoxide by the trichloroacetic acid. To mitigate the intermolecular activation and allow the reaction to proceed through intramolecular catalysis (Scheme 3.16, ax-***3*-28**), reactions were run solvent free. Attempts to run the reactions in neat or in aprotic solvents again proved unsuccessful due to the thermal lability of the substrates analogous to the results seen in the opening of the 1,2:3,4-*trans*-diepoxide ***2*-54.** In the "on water" systems, the ***3*-32** was never formed (Table 3.3), suggesting that the inductive effect of the electron-withdrawing amide group disfavors opening at C2 therefore favoring opening distal to the amide group at C3, which is analogous to finding of the Davies group (Scheme 3.16).

Table 3.3. Our results for the opening of *syn*-2-substituted epoxides *3*-14 with aniline nucleophiles.

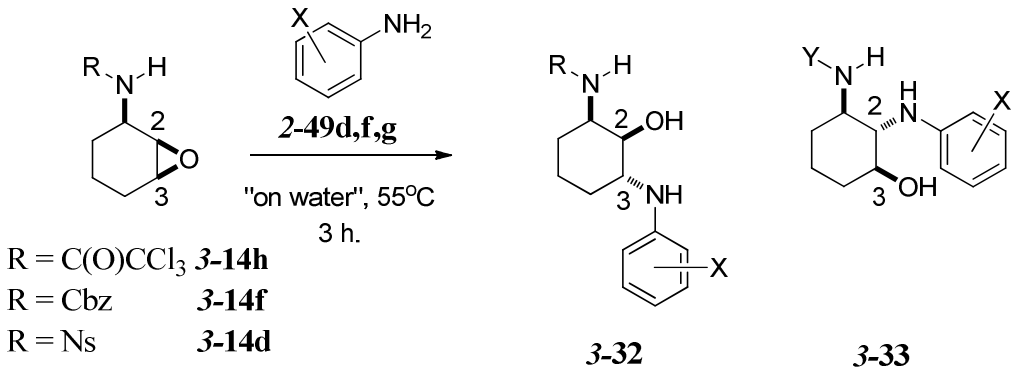

Entry	*Epoxide*	*Aniline*	*Major Product*	*32:33*[a]	*% Recovery*[b]
1	**14h**	**2-49f**	**32a**	100:0	89
2	**14f**	**2-49f**	**32b**	100:0	87
3	**14d**	**2-49f**	**32c**	100:0	55[c]
4	**14h**	**2-49d**	**32d**	100:0	82
5	**14h**	**2-49g**	**32e**	100:0	90

[a] Ratios determined by ^{1}H-NMR analysis of crude product mixture. [b] Measured recovery of crude product. [c] Measured recovery of pure chromatographed product.

During our crude ^{1}H-NMR analysis we were quite surprised to find that the α-amido proton (Figure 3.2, H1) gave a doublet of triplets. This result indicates the product conformation

is one where both the aniline and hydroxyl substituent are in the axial position while the amide (or in the case of ***3*-32c**, the amide derivative nosylamide) lies in an equatorial position. This

Figure 3.2. ^{1}H-NMR analysis for FP opening of syn-epoxide *3*-13 to give *3*-32c.

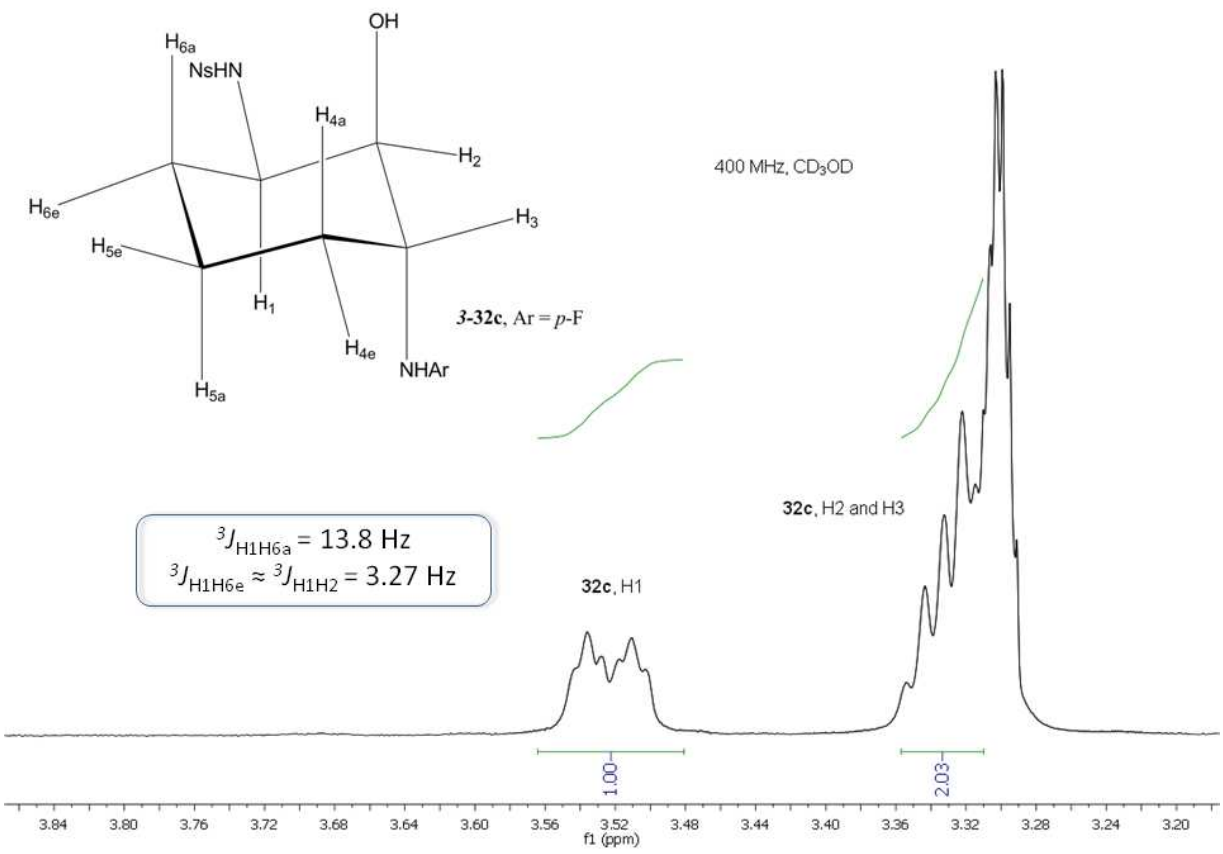

product conformation is also consistent with analogous compound ***3*-29** made in the Davies lab which was unambiguously determined by X-ray analysis.[131] We also submitted a purified sample of ***3*-32df** for X-ray analysis and were gratified to see that our results indeed agreed with our ^{1}H-NMR analysis and the work in the Davies lab (Figure 3.3). We are not sure why this diaxial conformation is favored.

Figure 3.3. Mercury representation of the X-ray crystal structure of *3*-32c.

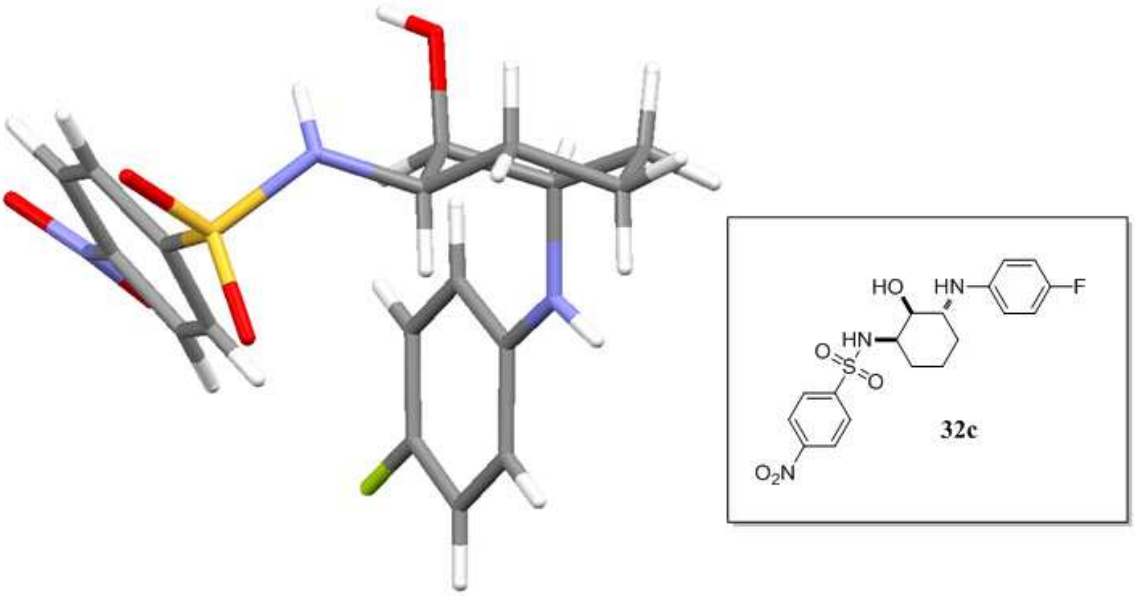

3.3 Directed epoxidation reactions for 3-substituted cyclohexenes

3.3.1 Directed peracid epoxidation reactions of homoallylic alcohols.

When compared to the peracid oxidation of the allylic cyclohexenol (***3*-1**), the analogous peracid oxidation of the *homoallylic* cyclohexenol (***3*-35**) occurs with far less diastereoselectivity (Table 3.4). However, much higher diastereoselectivities and rates of reaction have been achieved using metal-catalyzed epoxidation reactions pioneered by Sharpless and co-workers.[133,134]

Table 3.4. Relative rates and stereoselectivities for epoxidation of cyclohexene derivatives.[134]

Entry	*Substrate*	*Peracid krel.*	*$Mo(CO)_6$ krel.*	*$VO(acac)_2$ krel.*
1	 ***3*-34**	1	1	1
2	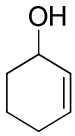 ***3*-1**	0.55 (92:8)[a]	4.5 (98:2)	>200 (98:2)
3	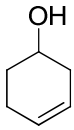 ***3*-35**	0.42 (60:40)	11.0 (98:2)	10.0 (98:2)

[a] Values in parenthesis indicates diastereoselectivity (*syn:anti*)

Another contrast in the peracid oxidation of homoallylic cyclohexanol ***3*-35** to the allylic analogue ***3*-1,** is that when the hydroxyl is biased in an axial position (Scheme 3.17, ***3*-38**), it effectively directs the incoming oxygen *syn* whereas from a biased equatorial position (***3*-36**) the outcome is stereorandom (cf. Scheme 3.17).[135] 1

Scheme 3.17. Selectivities for oxidation by equatorial (*3*-36) or axial (*3*-38) hydroxyl direction.[135]

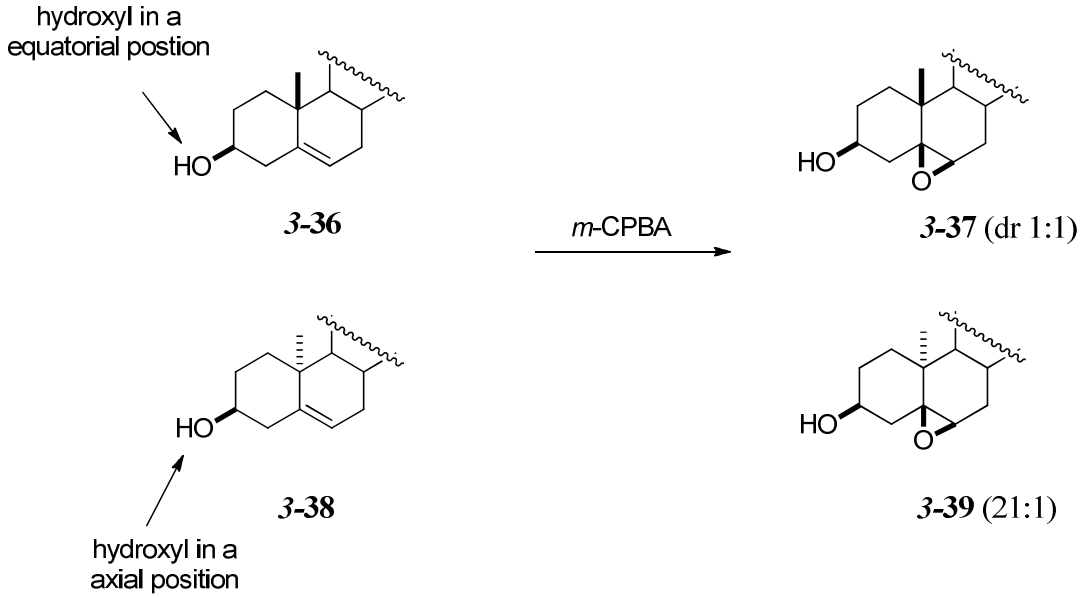

Hoveyda et al.[116] have proposed a transition structure (Figure 3.4) based upon the principles described for the allylic system (cf. Scheme 3.2), while incorporating the requirement that the directing hydroxyl group must adopt a pseudoaxial position in order to effect stereoselectivity.

Figure 3.4. Proposed transition structure for the epoxidation of homoallylic alcohols.[116]

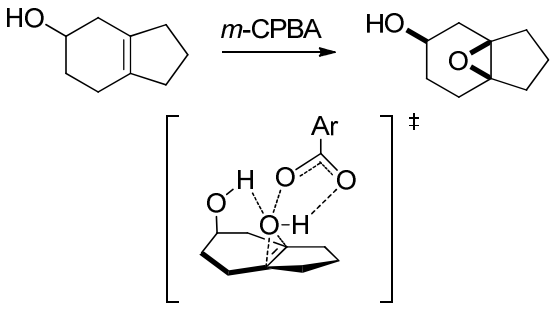

3.3.2 Directed peracid epoxidation reactions of homoallylic amides and amide derivatives.

The Fülöp group has shown *cis*-selective epoxidations of carbamate protected β-aminoesters using *m*-CPBA (Table 3.5, Entries 1-3).[136,137] Regardless of the carbamate substituent, the reactions resulted in perfect diastereoselectivity with moderate yields. Additionally, a study by Rotella supports these results with several related examples (Table 3.5 Entries 4-7).[138,139]

Table 3.5. Fülöp's epoxidation of *cis*-β-N-protected amino esters.[136-139]

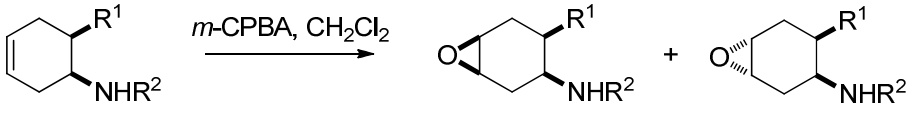

***3*-40a-f,g** ***3*-41a-f,g** ***3*-42a-f,g**

Entry	R^1	R^2	*Alkene*	*Epoxide formed*	*% Yield*
1	CO_2Et	CO_2Bn	***3*-40a**	***3*-41a**	59
2	CO_2Bn	CO_2Bn	***3*-40b**	***3*-41b**	65
3	CO_2Et	$CO_2{}^tBu$	***3*-40c**	***3*-41c**	58
4	$NHCO_2Bn$	CO_2Bn	***3*-40d**	***3*-41d**	86
5	CH_2OH	CO_2Bn	***3*-40e**	***3*-41e**	83
6	CH_2OAc	CO_2Bn	***3*-40f**	***3*-41f**	72
7	$CH_2OTBDMS$	CO_2Bn	***3*-40g**	***3*-42g**	54

Rotella attributes the high diastereoselectivity to an H-bonding interaction between the acidic carbamate N-H bond and the peracid in the transition state analogous to the example in Figure 3.4.[138] The *syn*-relationship of the substituents in ***3*-40a-f** forces at least one the substituents into an axial position. The likely transition state for the epoxidation of **40a** is shown in Scheme 3.18 (***3*-41a***). The Fülöp group claims through ^{1}H-NMR analysis that the cyclic olefin (***3*-40**) adopts a half-chair conformation (**NHZ-ax-*3*-40a**) in which the *ester group is in an equatorial position* while the *carbamate adopts an axial position*. In this axial position the carbamate is available to direct epoxidation via *syn*-delivery of the oxidant to furnish the *syn*-epoxide in perfect diastereoselectivity.[137] However, in the case of ***3*-40g** (Table 5, entry 7) the *trans*-epoxide is formed as the major product. Rotella proved through ^{1}H-NMR analysis of ***3*-40g** that the carbamate group lies in an equatorial position due to the steric demand of the trialkyl silyl ether. Having the carbamate in ***3*-40g** in the equatorial position diminishes the *syn*-selectivity.[138]

Scheme 3.18. Proposed mechanism for the stereoselective epoxidation of *cis*-β-N-protected amino ester *3*-40a.[138]

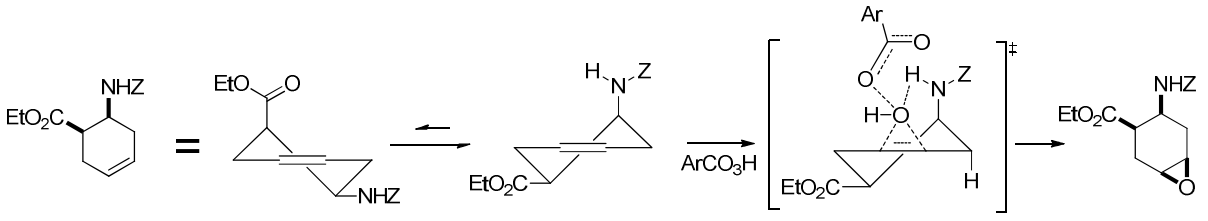

rac-3-40a NHZ-eq-*3*-40a NHZ-ax-*3*-40a ***3*-41a*** ***3*-41a**

However, if the R^1 substituent is hydrogen as in ***3*-40h-i**, the carbamate group is no longer forced into the axial position and the diastereoselectivity is greatly diminished as seen in

the work of Marco-Contelles laboratory; here the epoxidation reactions gave an inseparable mixture of both the *cis*- and *trans*-epoxides (Table 3.6).[140]

Table 3.6. Marco-Contelles' epoxidation of N-protected homoallylic amines.[138]

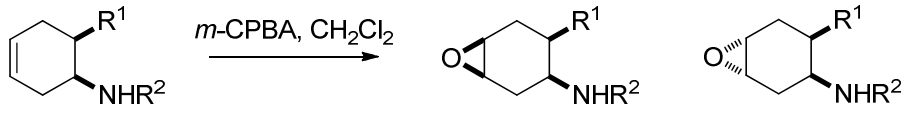

***3*-40h-i** ***3*-41h-i** ***3*-42h-i**

Entry	R^1	R^2	*Alkene*	*Major Epoxide*	*dr (syn:anti)*	*Total % Yield*
1	H	CO_2Bn	***3*-40h**	***3*-41h**	2.9:1	91
2	H	CO_2Et	***3*-40i**	***3*-41i**	4:1	55

Similarly related is in the work of the Donohoe researchers who observe poor *syn*-selectivity for the dihydroxylation of ***3*-43** when compared to the *syn*-selectivity for ***3*-44** (Scheme 3.19). The researchers claim that the reason for this poor selectivity can be the increased energy required to place the amide directing group in the axial position in ***3*-45***, where ***3*-46*** can direct *syn*-selectively from a lower energy equatorial position.[141]

Scheme 3.19. Donohoe's OsO_4 catalyzed dihydroxylations for allylic and homoallylic trichloroamides.[141,142]

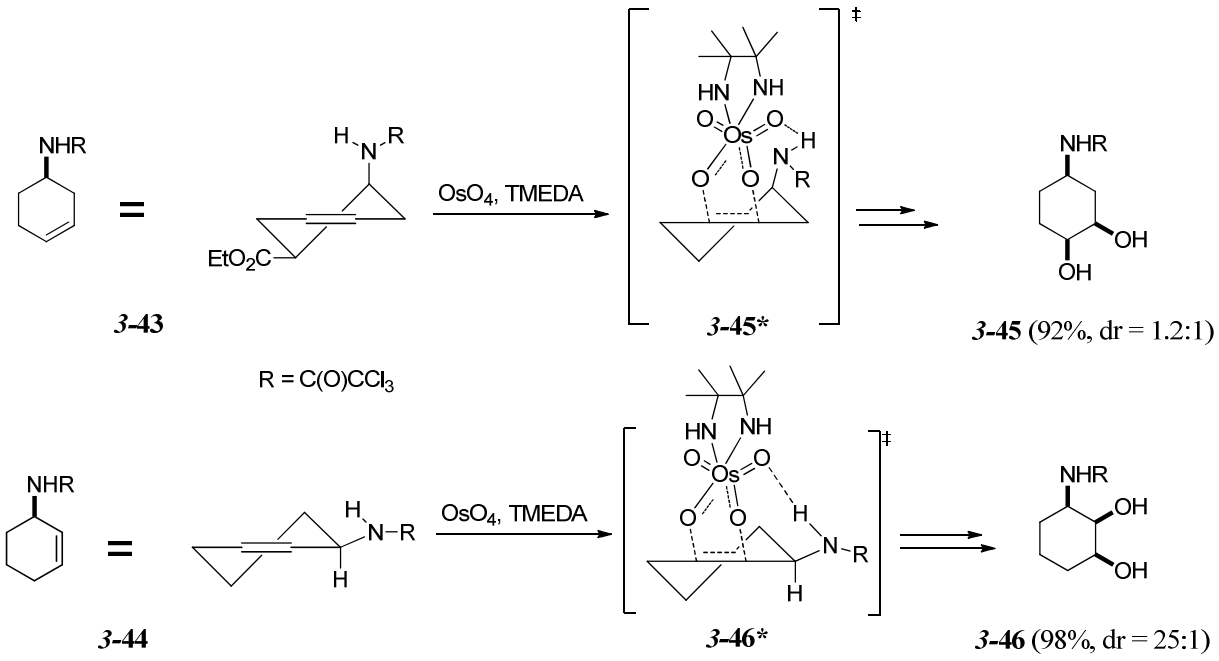

3.3.3 Synthesis of homoallylic amide *3*-42a and amide derivates in our laboratory.

In order to explore the possibility of an N-H assisted FP pathway for the opening of 3-amido substituted *syn*-cyclohexene oxides (***3*-41**) we needed to synthesize the requisite alkene. The Marco-Contelles group synthesized **40h** by a modification of the Curtius rearrangement of commercially available ***3*-47** in which DPPA is used to form the acyl azide (Scheme 3.20).[140,143] We combined aspects of this procedure and an Overman procedure[144-146] to produce ***3*-40h** in good (and comparable) yield.

Scheme 3.20. Curtius rearrangement of homoallylic carboxylic acid *3*-47 (Method B was performed by the author).

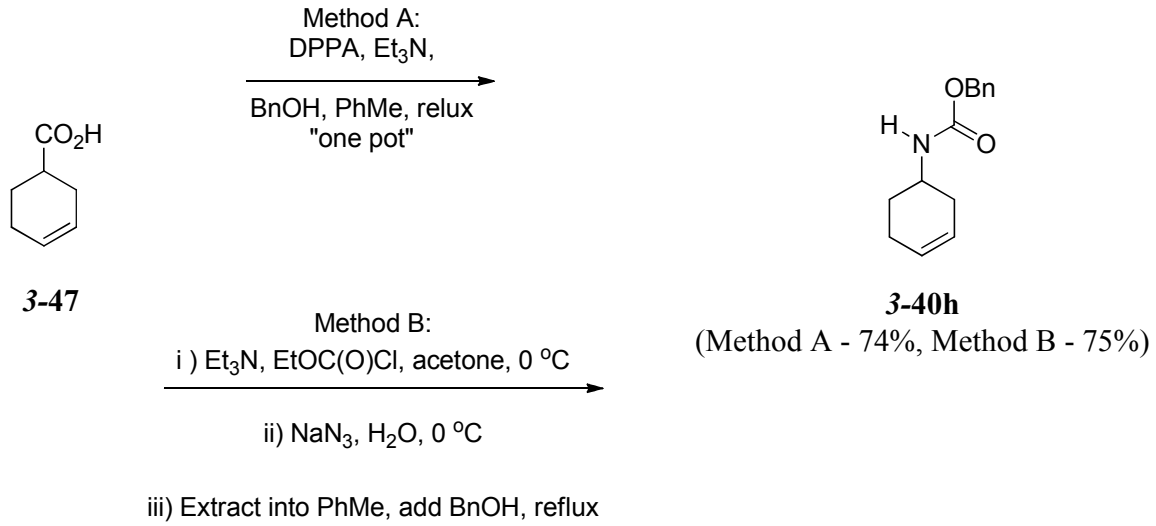

An exact repeat of the epoxidation of ***3*-40h** with *m*-CPBA as per the Marco-Contelles group,[140] gave an inseparable mixture of ***3*-41h** and ***3*-42h** with diastereoselectivity ratios of 73:27 (*cis:trans*, lit.[140] 74:26). We also attempted to use the Sharpless MTO epoxidation, but we were again frustrated by a poor diastereoselectivity ratio of 71:29 (*cis:trans*, Scheme 3.21).

Scheme 3.21. Our results from the oxidations of *3*-40h to give epoxide *3*-41h.

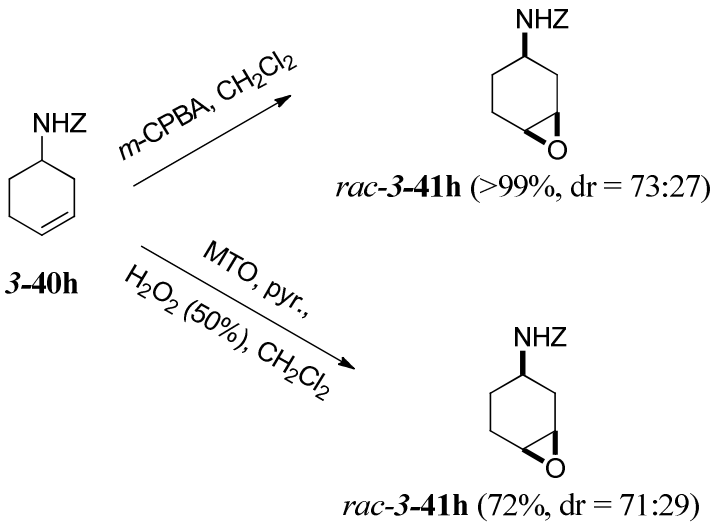

Prepared to resign to the fact that we were unable to synthesize ***3*-41** with high diastereoselectivity, we ran across a highly undervalued reference in *The Chinese Journal of Organic Chemistry*.[147] Here, the researchers were able to stereoselectively oxidize homoallylic amides ***3*-40j-m** using a relatively uncommon oxidant, monoperoxyphthalic acid (MPPA) ***3*-48**.[147]

Table 3.7. Huang's diastereoselective epoxidation of homoallylic amidocycloalkenes *3*-40.[147]

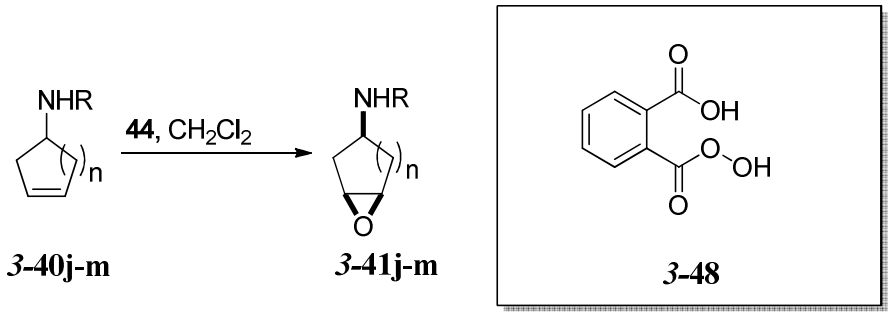

***3*-40j-m** ***3*-41j-m** ***3*-48**

Entry	*R*	*n*	*Alkene*	*Epoxide*	*dr (syn:anti)*	*% Yield*
1	$C(O)CH_3$	1	***3*-40j**	***3*-41j**	98:2	62
2	C(O)Ph	1	***3*-40k**	***3*-41k**	93:7	92
3	$C(O)CH_3$	2	***3*-40l**	***3*-41l**	97:3	68
4	C(O)Ph	2	***3*-40m**	***3*-41m**	93:7	65

Interestingly, when the epoxidation was performed on the homoallylic amide ***3*-40m** the *cis*-epoxide ***3*-41m** was formed, but in place of the *trans*-diastereomer ***3*-42m**, the transannular product ***3*-49m** (Scheme 22) was formed. This did not occur in the case of the oxidation of ***3*-40l**, suggesting that the increased nucleophilicity of the pendant benzamide (relative to the acetamide) allowed for FP controlled intramolecular cyclization (Scheme 3.21). In summary, the epoxidation of ***3*-40m** has a self-correcting mechanism, where the *trans*-intermediate (***3*-42m**) undergoes the transannular reaction to form ***3*-49m**, thus providing a method in which one can isolate diastereomerically pure ***3*-41m**.

Scheme 3.22. Proposed mechanism for the formation of transannular product *3*-49m.

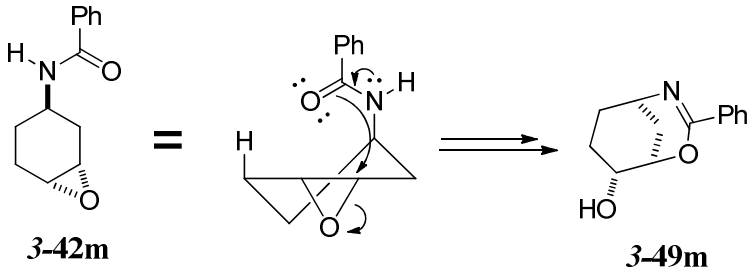

***3*-42m** ***3*-49m**

Encouraged by these results we set out to synthesize two homoallylic amidocycloalkenes (***3*-42f,g**) from the Curtius rearrangement of ***3*-43**. In order to synthesize ***3*-40n** (R^1 = $COCF_3$, R^2 = H, Scheme 3.23) it was necessary to redesign our previous Curtius conditions in order to trap the isocyanate intermediate with trifluoroacetate, rather than benzyl alcohol. Following a procedure from the Donohoe group,[141] we were able to furnish the trifluoroacetamide ***3*-40n** in comparable yield. Hydrolysis of the base labile trifluoroacetamide followed by acylation under Schotten-Baumann conditions[148,149] gave the benzamide ***3*-40m** in good yield.

Scheme 3.23. Our synthesis of homoallylic amides *3*-40m-n.

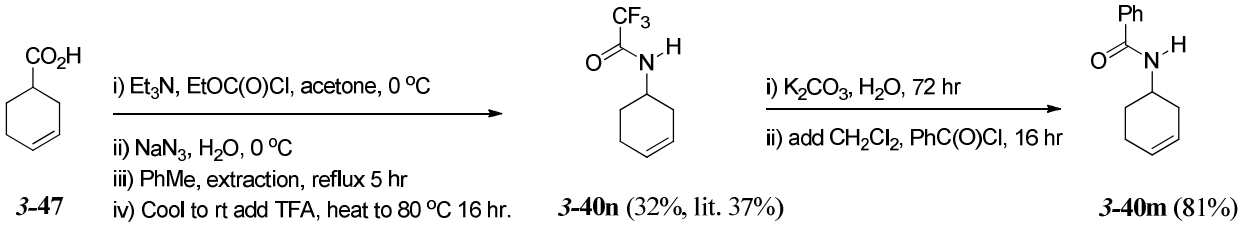

***3*-47** ***3*-40n** (32%, lit. 37%) ***3*-40m** (81%)

With the homoallylic amides in hand, we were poised to attempt epoxidation of these substrates. Our first studies involved oxidation of the benzamide ***3*-40m**, which to our gratification furnished the *syn*-epoxide ***3*-41m** exclusively after chromatographic isolation (Table 3.8).

Table 3.8. Our results for the epoxidation of homoallylic amides *3*-40m-n.

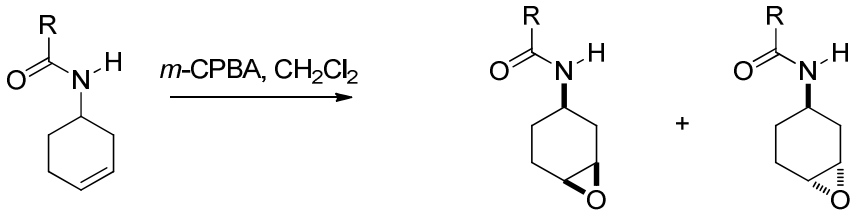

***3*-40m-n** ***3*-41m-n** ***3*-42m-n**

Entry	*R*	*Alkene*	*dr (41:42, cis:trans)*	*% Yield*
1	C(O)Ph	***3*-40m**	100:0	78
2	$C(O)CF_3$	***3*-40n**	95:5	82

We determined the relative configuration of ***3*-41m** unambiguously via X-ray crystallography (Figure 3.5). The structure does however show some disorder, but the data is adequate to confirm the *syn*-relationship between the amide and the epoxide.

Figure 3.5. Mercury representation of the x-ray crystal structure of *3*-41m.

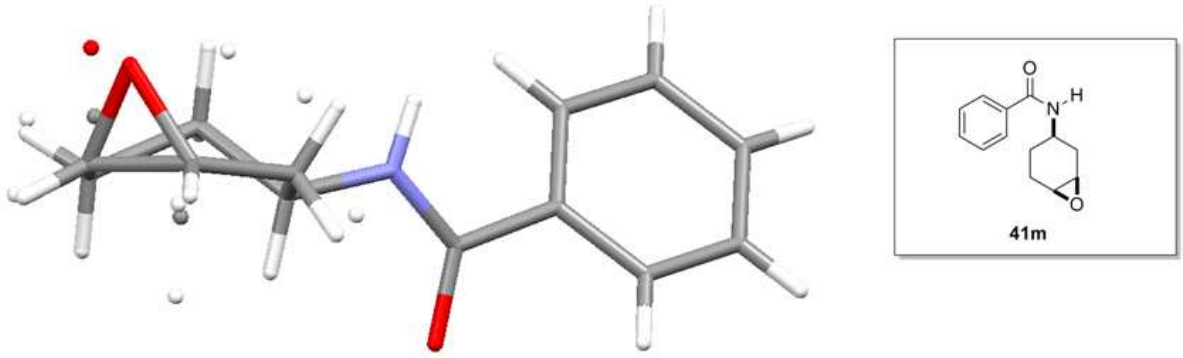

To our surprise, epoxidation of the trifluoroacetamide ***3*-40n** gave an inseparable 95:5 mixture of ***3*-41n** and ***3*-42n**, respectively (Table 3.8). This can be rationalized by the strong electron withdrawing character of the trifluoromethyl group, effectively diminishing the nucleophilicity of the amide oxygen. This diminished nucleophilicity does not allow for the self-correcting transannulation (cf. Scheme 3.22), thus allowing us to observe the *trans*-diastereomer ***3*-42n** in the both the ^{1}H- and ^{13}C-NMR.

It is interesting to note that the homoallylic benzyl carbamate ***3*-41h** gave marginal diastereoselectivity, while the analogous benzamide ***3*-41m** gave extremely high diastereoselectivty. The conformational energy ($-\Delta G_0$ or the "A value") has been defined as "the excess energy of a give confirmation over that conformation minimum energy of the same molecule."[150] The A value of a particular system is given by the equilibrium shown in Table

3.9.[106] The greater the A value, the less likely the substituent will adopt an axial position (recall that the axial position is necessary for homoallylic substrate direction).

Table 3.9. Conformational Energies for monosubsituted cyclohexanes.[151]

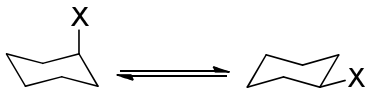

Entry	*X*	$-\Delta G_{0x}$ *(kcal mol^{-1})*
1	$COCH_3$	1.21
2	CO_2CH_3	1.2 – 1.3
3	$CO_2CH_2CH_3$	1.1 – 1.2
4	NHCOPh	1.6

Although we could not find a tabulated value for the conformational energy for a carbamate, we could postulate that the value would not be dramatically different from the benzamide substituent in ***3*-41m** based on the slight difference between an acetyl and carbomethoxy and carboethoxy substituents (Table 2.9 Entries 2 and 3). Therefore, with the assumption of similar conformational energies and the known similar N-H acidities of benzylcarbamate and benzamide we cannot account for the tremendous difference in diastereoselectivity between the two substrates.

3.4 N-H Directed and undirected FP controlled openings of 3-substituted cyclohexene oxides.

3.4.1 Opening of syn-3-substituted epoxides under N-H controlled FP.

As previously reviewed in **2.2.2**, Chini et al. has shown that the opening of *syn*-3-benzyloxy cyclohexene oxide (***2*-21**) under chelation controlled FP opening proceeds with high regioselectivity to furnish 3-hydroxy products ***2*-24**. If the reaction is run without a chelating metal, the reaction proceeds through standard FP to give the 4-hydroxy product ***2*-23**.[152] With epoxides ***3*-41m-n** in hand and cognizant that directed FP openings were possible with *syn*-3-substituted epoxides we were now prepared to attempt opening with anilines to further expand our N-H directed FP controlled openings. We began our experiments with ***3*-41m** since we could obtain it without any contamination from the *trans*-diastereomer ***3*-42m**, thus avoiding any confusion in the interpretation of our results. The possible products for the opening of ***3*-41m** are outlined in Scheme 3.24.

Scheme 3.24. FP and N-H assisted FP pathways for the opening of *3*-41m.

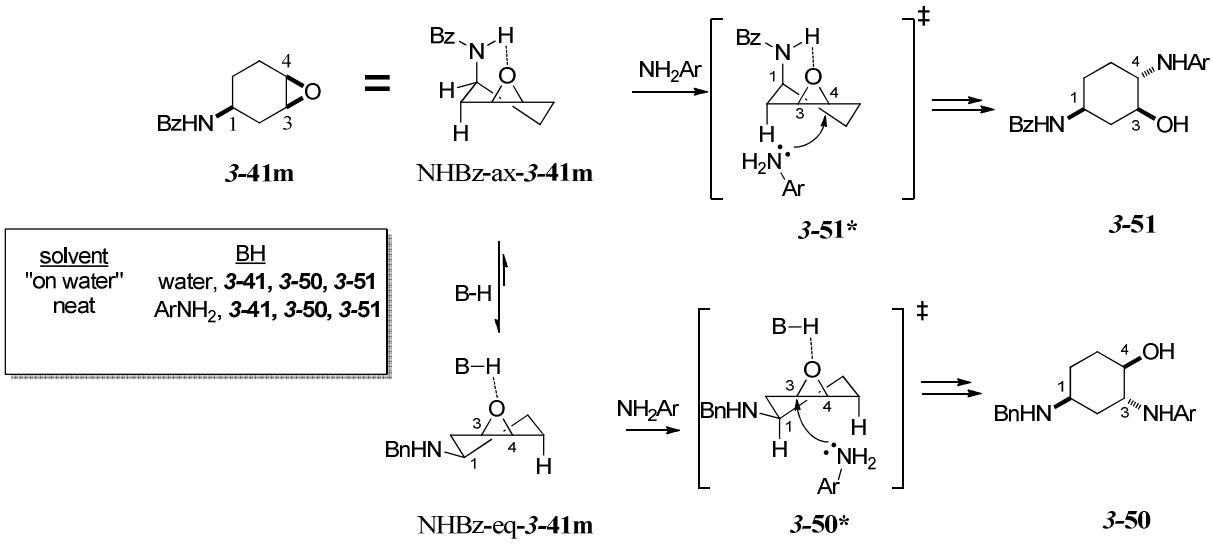

To our excitement when opening ***3*-41m** with *p*-anisidine (***2*-49d**) "on water", we determined that we had roughly a 1:1 mixture of unassisted FP opened product ***3*-50m** (4-hydroxy benzamide, see 3.4.2 for discussion on structural determination) and N-H assisted FP opened product ***3*-51m (**3-hydroxy benzamide, Table 3.10). However, when the nucleophile was switched to *m*-chloroaniline (***2*-49g**), the regioselectivity was relatively unchanged (Entry 2, Table 3.10).

Table 3.10. Our results for the opening of epoxide *3*-41m with aniline nucleophiles.

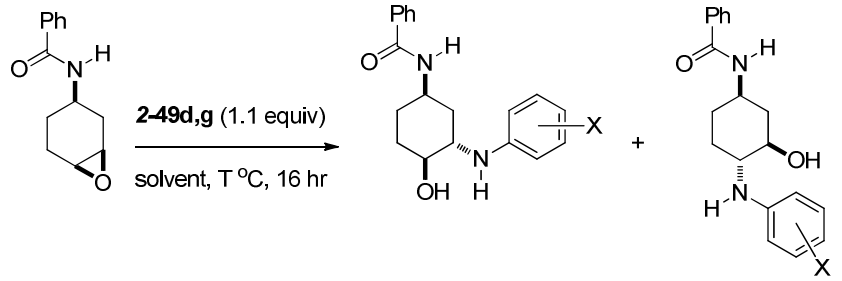

***3*-41m** ***3*-50d,g** ***3*-51d,g**

Entry	*Aniline*	*solvent*	*T °C*	*50:51*[a]	*% recovery*[b]
1	***2*-49d**	"on water"	95	45:55	92
2	***2*-49g**	"on water"	95	50:50	85
3	***2*-49d**	neat	150	24:76	>99%[c]
4	***2*-49g**	neat	150	24:76	80

[a] ratios determined by ^{1}H-NMR [b] % recovery indicates recovery inseparable regioisomers [c] % recovery of crude product mixture.

While changing from "on water" to solvent free reaction conditions improved regioselectivity for the N-H assisted FP opening, which is consistent with our findings when

opening the analogous 1,2:4,5-trans-diepoxide (***2*-29**). It is interesting to note that the regioselectivity is insensitive to the electronic nature of the aniline substituent (Table 3.10, Entries 3-4) when run in either solvent, highlighting the directing effect of the pendant amide.

3.4.2 ^{1}H-NMR structural determination from the opening of epoxide *3*-41m.

By examining the cyclohexane chair model of the 3-hydroxy benzamide (**51d**), one finds there is only one low energy, all-equatorial conformer (Figure 3.6).

Figure 3.6. ^{1}H-NMR analysis of the regioisomers *3*-50d and *3*-51d from the opening of *3*-41m with *p*-anisidine.

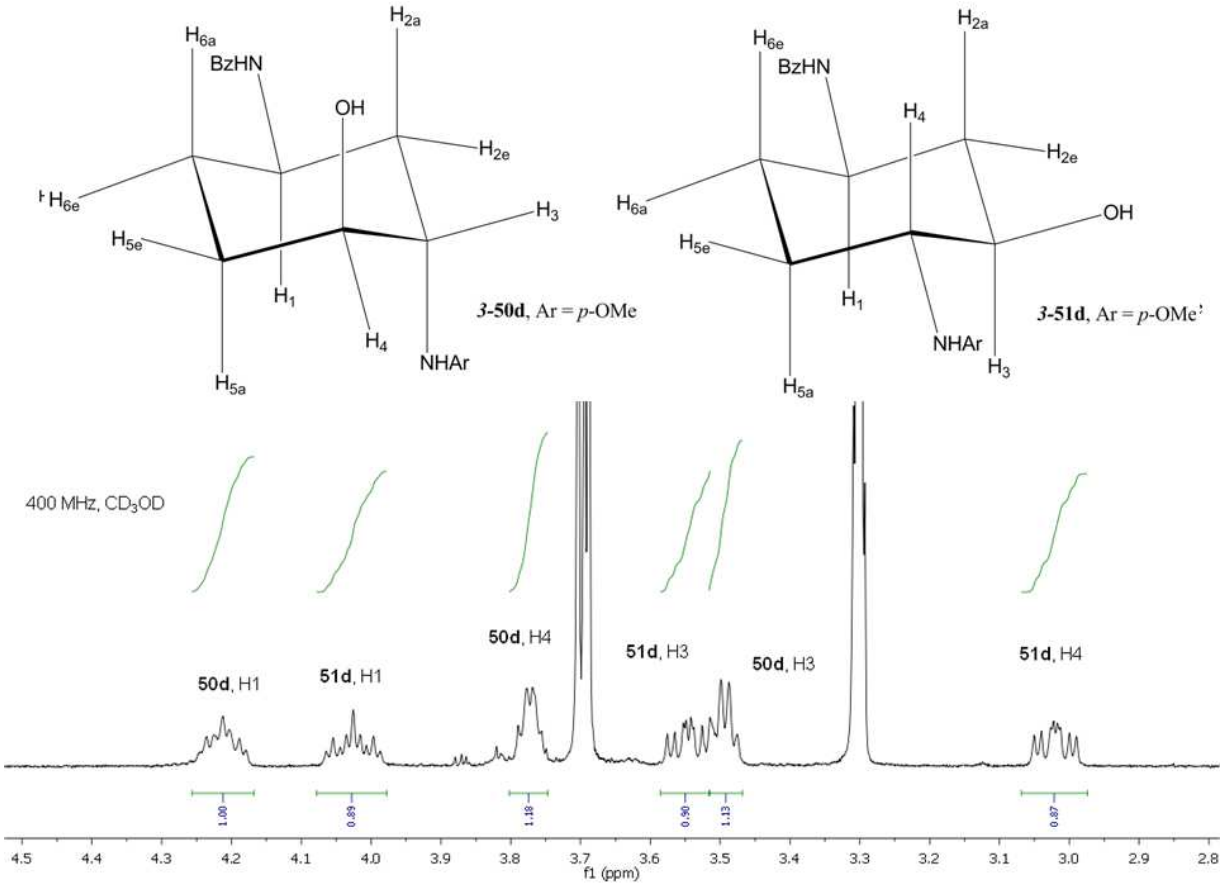

This structure will therefore not exhibit any evidence of dynamic behavior. Because of the locked all-equatorial conformation, H3 will always maintain an antiperiplanar (axial-axial or aa) relationship to H4. In this case one would predict a large coupling constant (9-12 Hz). In the analysis of ***3*-51d** a value of 9.4 Hz was observed for $^{3}J_{H3H4}$ (coupling constant appears to be attenuated by the presence of two electronegative atoms[107]). Additionally, the $^{3}J_{H4H5a}$, also a permanent antiperiplanar relationship due to the lack of dynamic behavior, was found to be 11.0 Hz. And finally, the *gauche* relationship between H4 and H5e gives a small coupling constant equal to 4.0 Hz. In the case of ***3*-50d** we can assume that our 4-hydroxy benzamides would favor having the benzamide group in an equatorial position, therefore placing both the anilino and hydroxyl substituents in the axial position, similar to the situation in ***3*-32c** (Figure 3.3) which was determined unambiguously by X-ray crystallography. Therefore, H3 in ***3*-50d** would have all gauche interactions with its three neighboring protons giving a quartet with a coupling constant found to be 4.5 Hz.

3.5 Conclusions

In the scope of our 2-substituted cyclohexene oxides, we have demonstrated a new synthetic route in which to arrive at the olefinic precursor ***3*-13**. Following O'Brien's procedure we were able to stereoselectively oxidize these compounds with high *syn*-selectivity. Subsequent opening of these epoxides (***3*-14**) did not show any evidence of N-H assisted FP opening that could override the inductive effect the amide has on the transition state. For the 3-substituted cyclohexene oxides we were able to show another route to homoallylic carbamates via the Curtius rearrangement to give ***3*-40** in good yields. Additionally, after finding the communication from Huang et al., we could reproduce their high diastereoselectivities in the

epoxidation of homoallylic amides. It is interesting to note that the while the amides did give high diastereoselectivity, the carbamate analogs did not. Finally we did demonstrate N-H directed FP opening for the epoxide ***3*-40m**, although our regioselectivities were not optimal. Future endeavors to improve regioselectivity may be to bias the amide in an axial position similar to the work by Rotella (Scheme 3.18). This would allow us to probe the efficacy of N-H activation by anilines and amide derivatives in epoxide openings.

Chapter 4 Experimental

4.1 General

^{1}H and ^{13}C NMR spectra were recorded on a JEOL Eclipse 500 (500 MHz) or Varian Inova 400 (400 MHz) spectrometer as indicated. Chemical shifts are reported in ppm using the known chemical shift of the indicated solvent as an internal reference. The following abbreviations are used to indicate coupling s (singlet), d (doublet), t (triplet), q (quartet), qt (quintet), and br. (broad). HRMS (TOF) was performed using a JEOL HX110 dual focusing mass spectrometer and (ESI) was performed using an Agilent 6220 Accurate Mass TOF LC/MS. TLC was performed using 200 μm silica gel 60-F plates from EMD Chemicals Inc. Column chromatography was performed using 60A, 40-63 μm silica gel from SorbTech or a Teledyne Isco Combiflash R_f system. Optical rotations were measured on a Jasco P-2000 polarimeter. Melting points were measured using a Buchi Melting Point B-540. Starting materials were purchased from commercial suppliers and used as received unless otherwise noted. Compounds **A5-A10** were donations from the laboratory of K. Barry Sharpless. Solvents (HPLC grade – including water) were used as received from Fisher Scientific.

4.2 Synthetic Procedures

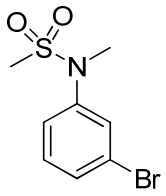

N-(3-bromophenyl)-*N*-methylmethanesulfonamide **(*1*-20)**.[46] To a 250 mL round bottom flask was added 3-bromoaniline (1.09 mL, 10 mmol) and methylene chloride (30 mL). The solution was then cooled to 0^{o}C via external ice bath. Anhydrous pyridine (2.4 mL, 30 mmol) was added followed by methanesulfonyl chloride (0.85 mL, 11 mmol). The solution was allowed to stir overnight while warming to room temperature. In the morning 1 N HCl (50 mL) was added. The mixture was poured into a separatory funnel and the aqueous layer was extracted with methylene chloride (3 x 15 mL). The combined organic extracts were dried over Na_2SO_4. After filtration the filtrate was concentrated to give 2.26 grams (90%) of a slightly yellow solid which was used without further purification. To a stirred suspension of NaH (60% dispersion in oil, 0.24g, 5.5 mmol) in anhydrous *N*,*N*-dimethylformamide (10 mL) under a nitrogen atmosphere was added a portion of the aforementioned crude sulfonamide (1.25 g, 5 mmol) followed by iodomethane (10 mmol, 0.6 mL). The mixture was allowed to stir under nitrogen for four hours. The reaction was quenched by the addition of 35 mL of water to the solution. The resulting biphasic solution was poured into a separatory funnel. The aqueous layer was extracted with ethyl acetate (3 x 30 mL). The organic extracts were combined and washed with brine and dried over Na_2SO_4. The solution was then filtered and concentrated to give a yellow residue. The residue was purified via flash chromatography to give 1.21 g (92%) of a white solid. The spectral data were found to be consistent with the literature values.[150,153] ^{1}H NMR (500 MHz,

$CDCl_3$) δ 7.54 – 7.13 (m, 4H), 3.31 (s, 3H), 2.85 (s, 3H). ^{13}C NMR (126 MHz, $CDCl_3$) δ 138.169, 131.09, 128.43, 123.35, 123.25, 39.75, 35.48.

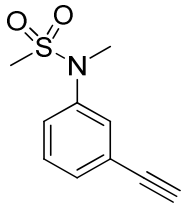

N-(3-ethynylphenyl)-*N*-methylmethanesulfonamide **(*1*-21, A1)**.[64] To an oven dried Schlenk flask containing a stir bar was added *trans*-dichlorobis(triphenylphosphine)palladium (II) (70 mg , 0.1 mmol), copper (I) iodide (19 mg, 0.1 mmol) and ***1*-20** (528 mg, 2 mmol). The flask was evacuated and backfilled with nitrogen three times. While under a positive stream of nitrogen freshly distilled DIPEA (10 mL), ethynyltrimethylsilane (0.57 mL, 4 mmol), and anhydrous THF (20 mL) were added to the flask. The flask was then capped and heated to 55^oC with stirring for 18 hours. After this period, mixture was cooled and filtered through a pad of celite to remove solids. The filtrate was evaporated and the resulting residue was purified via flash chromatography to give 497 mg (88%) of a brown solid which was used without further purification. A portion of the solid (141 mg, 0.5 mmol) was dissolved in THF (5 mL) and was cooled to 0^oC. A THF solution of TBAF (1.2 mL, 1M in THF, 1.2 mmol) was then added and the solution was allowed to warm to room temperature with stirring overnight. In the morning 15 mL of diethyl ether (Et_2O) was added followed by 10 mL of aqueous saturated ammonium chloride. The resulting biphasic solution was poured into a separatory funnel and the aqueous layer was extracted with Et_2O (3 x 5 mL). The organic extracts were combined and washed with brine and dried over Na_2SO_4. The solution was filtered and concentrated to give a yellow residue. The residue was purified via flash chromatography (35% EtOAc in hexanes) to give

100 mg (96%) of a slightly yellow solid. ^{1}H NMR (500 MHz, $CDCl_3$) δ 7.39 (m, 4H), 3.31 (s, 3H), 3.11 (s, 1H), 2.84 (s, 3H). ^{13}C NMR (126 MHz, $CDCl_3$) δ 141.61, 131.08, 129.48, 129.07, 127.23, 123.45, 82.59, 78.35, 38.05, 35.48. HRMS (FAB) calculated for $C_{10}H_{11}NO_2S$ (M+) 209.0511, found 209.0513 (+1.2 ppm, +0.2 mmu).

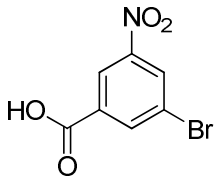

3-bromo-5-nitrobenzoic acid **(*1*-23)**.[66] 3-Nitrobenzoic acid (1.67g, 30 mmol) was added to a 250 mL round bottom flask equipped with a stir bar. Concentrated sulfuric acid (30 mL) was added and the mixture was heated to 80 ^{o}C. The suspension became homogenous when the temperature reached 60 ^{o}C. Freshly re-crystallized NBS (7.4g, 41.3 mmol) was added in nine equal portions over the course of 90 minutes (i.e. 822 mg every ten minutes). After addition of the ninth portion, the orange fuming solution was allowed to stir for an additional 30 minutes. The heating bath was removed and solution was allowed to cool to room temperature and then poured onto 60 grams of ice. The ice was allowed to melt and resulting suspension was filtered and the filter cake was dissolved in Et_2O and transferred to a separatory funnel. The organic layer was washed with water (2 x 20 mL). The organic layer was dried over $MgSO_4$. The solution was filtered and concentrated to give 6.94g (94%) of a white solid which was used without further purification. The spectral data were found to be consistent with the literature values.[154] ^{1}H NMR (500 MHz, $CDCl_3$) δ 8.88 (m, 1H), 8.62 (t, *J* = 2.0, 1H), 8.56 (t, *J* = 1.6, 1H). ^{13}C NMR (126 MHz, $CDCl_3$) δ 168.63, 148.96, 138.81, 132.29, 131.53, 123.87, 123.46.

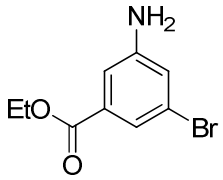

Ethyl 3-amino-5-bromobenzoate **(*1*-24)**. To a 50 mL round bottom flask equipped with a stir bar and reflux condenser was added ***1*-23** (2.46g, 10 mmol) and absolute ethanol (15 mL). To this stirred solution was added 1 mL concentrated sulfuric acid. The solution was heated to reflux for four hours. After this period, the solution was cooled to room temperature and ethanol was removed on a rotary evaporator. To the resulting slurry with stirring was carefully added saturated $NaHCO_3$ (20 mL) followed by EtOAc (10 mL). The resulting biphasic solution was poured into a separatory funnel. The upper organic layer was discarded. The remaining aqueous layer was extracted with EtOAc (3 x 15 mL). The combined organic layers were dried over Na_2SO_4. The solution was then filtered and concentrated to give 2.25 g (82%) of a white solid which was used without further purification. A portion of this material (2.96 g, 12.4 mmol) was added to a 2 neck round bottom flask equipped with a reflux condenser and N_2 inlet. Subsequently iron powder (2.07 g, 325 mesh, 37.2 mmol) and NH_4Cl (663 mg, 12.4 mmol) were added. The flask was evacuated and backfilled with nitrogen three times. Absolute ethanol (90 mL) and HPLC grade water (25 mL) were then added. The mixture was then heated at reflux with a heating mantle for 1.5 hours at which point TLC (60% EtOAc in hexanes) indicated complete conversion to the aniline. While still hot the contents were poured through a pad of celite. Most of the ethanol was then removed *in vacuo*. The resulting suspension was then transferred to a separatory funnel where 10 mL of a saturated $NaHCO_3$ was added followed by EtOAc (10 mL). The upper organic layer was collected followed by extraction of the aqueous layer with EtOAc (3 x 15 mL). The organic extracts were combined and dried over Na_2SO_4.

The solution was then filtered, concentrated, and dried *in vacuo* to give 2.82 g (93%) of light yellow oil which was used without further purification. A sample of the oil was analyzed by NMR and the spectral data were consistent with the literature values.[155] ^{1}H NMR (400 MHz, $CDCl_3$) δ 7.50 (t, *J* = 1.6, 1H), 7.24 – 7.23 (m, 1H), 6.99 – 6.94 (m, 1H), 4.33 (q, *J* = 7.1, 2H), 1.36 (t, *J* = 7.1, 3H). ^{13}C NMR (101 MHz, $CDCl_3$) δ 162.53, 144.65, 129.94, 125.64, 119.25, 118.57, 111.58, 58.29, 11.27.

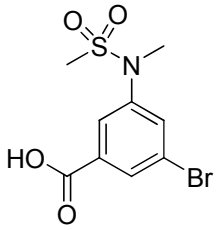

Ethyl 3-bromo-5-(*N*-methylmethylsulfonamido)benzoic acid **(*1*-25)**. The two step procedure to synthesize ***1*-20** was followed using ***1*-24** (2.82g, 11.5 mmol) to first give 3.63 g (98%) of ethyl 3-bromo-5-(methylsulfonamido)benzoate as white solid. A portion of this material (1.13g, 3.5 mmol) was methylated as per the synthesis of ***1*-20** to give 990 mg (84%) of a white solid (mp = 173.3 ^{o}C) which was used without further purification. The crude material (990 mg, 2.94 mmol), was dissolved in THF (4 mL) followed by the addition of methanol (4 mL) and HPLC grade water (4 mL). The solution was then cooled to 0 ^{o}C and then powdered NaOH (4.41 mmol, 176 mg) was added. The suspension was allowed to stir while warming to room temperature overnight. In the morning THF and methanol were removed on rotary evaporator. The resulting suspension was dissolved in water, transferred into a separatory funnel, and acidified by the addition of 10 mL of 1 N HCl solution. The aqueous layer was then extracted with EtOAc (3 x 8 mL). The combined organic extracts were dried over Na_2SO_4, filtered, concentrated, and dried *in vacuo* to give 770 mg (85%) of a white solid that was used without further purification. The

solid was analyzed by NMR and the spectral data were consistent with the literature values.[156] ^{1}H NMR (400 MHz, $CDCl_3$) δ 8.13 (t, *J* = 1.6, 1H), 7.98 (dd, *J* = 1.6, 2.0, 1H), 7.81 (t, *J* = 2.0, 1H), 3.35 (s, 3H), 2.88 (s, 3H). ^{13}C NMR (101 MHz, $CDCl_3$) δ 177.44, 145.99, 142.95, 134.33, 131.69, 125.12, 122.90, 37.81, 35.89. HRMS (FAB) calculated for $C_9H_{11}NO_4SBr$ (MH^+) 307.9572, found 307.9577 (-4.9 ppm, +-1.5 mmu).

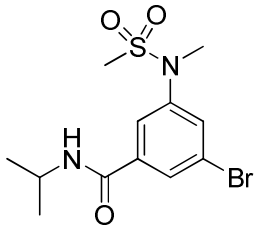

3-bromo-*N*-isopropyl-5-(*N*-methylmethylsulfonamido)benzamide **(*1*-26a)**. To a stirred solution containing ***1*-25** (510 mg, 1.65 mmol) in methylene chloride (15 mL) and DMF (1 mL) was added BOP (878 mg, 2.0 mmol), isopropylamine (0.17 mL, 2.0 mmol) and DIPEA (0.82 mL, 5.0 mmol). The solution was stirred at room temperature overnight. In the morning solution was concentrated and the resulting residue was purified via flash chromatography (60% EtOAc in hexanes) to give 530 mg (92%) of a white solid. ^{1}H NMR (400 MHz, $CDCl_3$) δ 7.72 (t, *J* = 1.5, 1H), 7.70 (m, 1H), 7.64 (t, *J* = 1.8, 1H), 5.98 (*NH*, d, *J* = 7.1, 1H), 4.31 – 4.17 (m, 1H), 3.31 (s, 3H), 2.86 (s, 3H), 1.25 (d, *J* = 6.6, 6H). ^{13}C NMR (101 MHz, $CDCl_3$) δ 164.16, 142.89, 137.57, 131.61, 128.35, 123.08, 122.69, 42.36, 37.88, 35.72, 22.65.

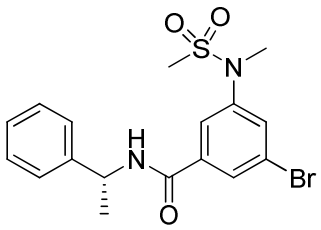

(*R*)-3-bromo-5-(*N*-methylmethylsulfonamido)-*N*-(1-phenylethyl)benzamide **(*1*-26b)**. The procedure for the synthesis of ***1*-26a** was followed using (770 mg, 2.5 mmol) of ***1*-25** and (*R*)-α-methylbenzyl amine (0.4 mL, 3 mmol). Purification by flash chromatography (60% EtOAc in hexanes) afforded 920 mg (90%) of a white solid. ^{1}H NMR (500 MHz, $CDCl_3$) δ 7.76 – 7.26 (m, 8H), 6.40 (*NH*, d, *J* = 7.6, 1H), 5.29 (apparent qt, *J* = 7.0, 1H), 3.31 (s, 3H), 2.86 (s, 3H), 1.61 (d, *J* = 6.9, 3H). ^{13}C NMR (126 MHz, $CDCl_3$) δ 164.18, 143.15, 142.61, 137.35, 132.01, 128.94, 128.45, 127.83, 126.38, 123.26, 122.86, 49.80, 37.98, 35.89, 21.64. HRMS (FAB) calculated for $C_{17}H_{20}N_2O_3SBr$ (MH^+) 411.0378, found 411.0379 (+0.2 ppm, +0.1 mmu).

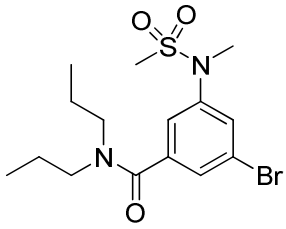

3-bromo-5-(*N*-methylmethylsulfonamido)-*N*,*N*-dipropylbenzamide **(*1*-26c)**. The procedure for the synthesis of ***1*-26a** was followed using (330 mg, 1.1 mmol) of ***1*-25** and dipropyl amine (0.2 mL, 1.32 mmol). Purification by flash chromatography (60% EtOAc in hexanes) afforded 410 mg (95%) of a white solid. ^{1}H NMR (500 MHz, $CDCl_3$) δ 7.53 (m, 1H), 7.41 (m, 1H), 7.31 (m, 1H), 3.42 (t, *J* = 7.0, 2H), 3.31 (s, 3H), 3.14 (t, *J* = 6.8, 2H), 2.87 (s, 3H), 1.72 – 1.62 (m, 2H), 1.59 – 1.49 (m, 2H), 0.96 (t, *J* = 6.9, 3H), 0.77 (t, *J* = 7.0, 3H). ^{13}C NMR (126 MHz, $CDCl_3$) δ 168.98, 142.77, 139.90, 128.98, 128.38, 122.93, 122.82, 77.36, 77.11, 76.85, 50.84, 46.69, 37.91,

35.97, 21.99, 20.75, 11.53, 11.09. HRMS (FAB) calculated for $C_{15}H_{24}N_2O_3SBr$ (MH^+) 391.0691, found 391.0669

(-5.6 ppm, -2.2 mmu).

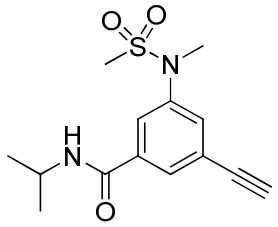

N-isopropyl-3-(*N*-methylmethylsulfonamido)-5-(ethynyl)benzamide **(*1*-27a, A2)**. The procedure for the synthesis of **A1** was followed using (511 mg, 1.46 mmol) of ***1*-26a**. The residue was purified by flash chromatography (60% EtOAc in hexanes) to give 278 mg (88%) of a slightly yellow solid. ^{1}H NMR (500 MHz, $CDCl_3$) δ 7.78 (m, 1H), 7.69 (t, *J* = 1.5, 1H), 7.61 (m, 1H), 5.99 (*NH*, d, *J* = 7.1, 1H), 4.26 (m, 1H), 3.33 (s, 1H), 3.15 (s, 3H), 2.86 (s, 3H), 1.26 (d, *J* = 6.6, 6H). ^{13}C NMR (126 MHz, $CDCl_3$) δ 164.77, 142.11, 136.59, 132.20, 128.74, 125.09, 123.76, 81.82, 79.29, 42.38, 37.99, 35.74, 22.80. HRMS (ESI-TOF) calculated for $C_{14}H_{19}N_2O_3S$ (MH^+) 295.1111, found 295.1120 (+3.1 ppm, +0.9 mmu).

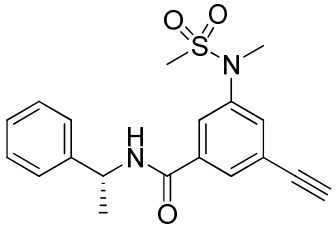

(*R*)-3-(*N*-methylmethylsulfonamido)-*N*-(1-phenylethyl)-5-(ethynyl)benzamide **((*R*)-*1*-27b, A3)**. The procedure for the synthesis of **A1** was followed using (910 mg, 2.2 mmol) of ***1*-26b**. The residue was purified by flash chromatography (60% EtOAc in hexanes) to give 570 mg (87%) of a slightly yellow solid. ^{1}H NMR (400 MHz, $CDCl_3$) δ 7.78 (t, *J* = 1.9, 1H), 7.70 (m, 1H), 7.64 –

7.56 (m, 1H), 7.39 – 7.24 (m, 5H), 6.44 (*NH*, d, *J* = 7.4, 1H), 5.28 (apparent qt, *J* = 7.0, 1H), 3.30 (s, 3H), 3.14 (s, 1H), 2.84 (s, 3H), 1.59 (d, *J* = 6.9, 3H). ^{13}C NMR (101 MHz, $CDCl_3$) δ 164.57, 142.61, 141.99, 136.05, 132.29, 128.78, 128.64, 127.60, 126.23, 125.07, 123.66, 81.63, 79.27, 49.59, 37.86, 35.60, 21.55. HRMS (FAB) calculated for $C_{19}H_{21}N_2O_3S$ (M+1) 357.1273, found 357.1266 (-2.0 ppm, -0.7 mmu). $[\alpha]_D^{25} =$ -57.8 (c = 1.1, CH_3OH)

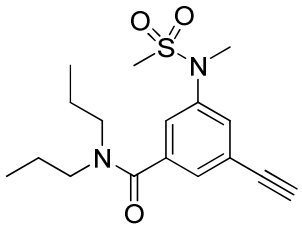

3-(*N*-methylmethylsulfonamido)-*N*,*N*-dipropyl-5-(ethynyl)benzamide **(*1*-27c, A4)**. The procedure for the synthesis of **A1** was followed using (391 mg, 1 mmol) of ***1*-26c**. The residue was purified via flash chromatography (60% EtOAc in hexanes) to give 219 mg (65%) of a yellow solid. ^{1}H NMR (500 MHz, $CDCl_3$) δ 7.47 (m, 1H), 7.36 (m, 1H), 7.35 (m, 1H), 3.40 (t, *J* = 7.3, 2H), 3.29 (s, 3H), 3.19 – 3.07 (m, 3H), 2.84 (s, 3H), 1.72 – 1.58 (m, 2H), 1.58 – 1.44 (m, 2H), 0.94 (t, *J* = 7.1, 3H), 0.74 (t, *J* = 6.9, 3H). ^{13}C NMR (126 MHz, $CDCl_3$) δ 169.60, 141.73, 138.78, 129.32, 128.88, 124.99, 123.78, 81.94, 79.18, 77.42, 77.16, 76.91, 50.83, 46.65, 37.89, 35.78, 21.97, 20.74, 11.51, 11.07. HRMS (ESI-TOF) calculated for $C_{17}H_{25}N_2O_3S$ (MH^+) 295.1111, found 295.1120 (+3.0 ppm, +1.0 mmu).

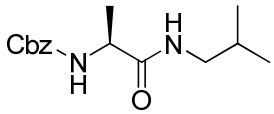

Z-Ala-NH*i*-Bu **((*S*)-*1*-29a)**. To a stirred solution of Z-Ala-OH (450 mg, 2.0 mmol) in CH_2Cl_2 (15 mL) was added DIPEA (1.2 mL, 7.0 mol) and isobutylamine (0.2mL, 2.2 mmol). Castro's

reagent (BOP, 978 mg, 2.2 mmol) was then added. The flask was capped and allowed to stir overnight at room temperature. In the morning, the solution was placed on a rotary evaporator to remove CH_2Cl_2 and excess isobutylamine. The residue was purified by flash chromatography (60% EtOAc in hexanes) to give a 540 mg (97%) of a white solid (mp = 115.1 ^oC). The solid was analyzed by NMR and the spectral data were consistent with the literature values.[51] ^1H NMR (500 MHz, $CDCl_3$) δ 7.45 – 7.17 (m, 7H), 6.23 (*NH*, s, 1H), 5.44 (*NH*, s, 1H), 5.15 – 5.05 (m, 2H), 4.29 – 4.14 (m, 1H), 3.15 – 2.98 (m, 2H), 1.85 – 1.65 (m, 1H), 1.47 – 1.30 (m, 3H), 0.96 – 0.80 (m, 6H). ^{13}C NMR (126 MHz, $CDCl_3$) δ 172.28, 156.14, 136.25, 128.64, 128.32, 128.13, 67.08, 50.70, 46.88, 28.53, 20.07, 18.73. HRMS (FAB) calculated for $C_{15}H_{23}N_2O_3$ (M+1) 279.1703, found 279.1710 (+2.5 ppm, +0.7 mmu).

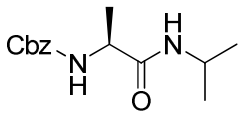

Z-Ala-NH*i*-Pr **((*S*)-*1*-29b)**. The procedure given for **(*S*)-*1*-29a** was followed using Z-Ala-OH (450 mg, 2.0 mmol) and isopropyl amine (0.2 mL, 2.2 mmol). Flash chromatography yielded 518 mg (99%) of a white solid (mp = 155.6 ^oC). The solid was analyzed by NMR and the spectral data were consistent with the literature values.[51] ^1H NMR (400 MHz, $CDCl_3$) δ 7.39 – 7.26 (m, 5H), 5.90 (*NH*, s, 1H), 5.39 (*NH*, s, 1H), 5.08 (s, 2H), 4.20 – 4.09 (m, 1H), 4.08 – 3.94 (m, 1H), 1.34 (d, *J* = 7.0, 3H), 1.10 (d, *J* = 6.5, 6H). ^{13}C NMR (101 MHz, $CDCl_3$) δ 171.16, 155.91, 136.15, 128.50, 128.17, 127.98, 66.94, 50.56, 41.47, 22.55, 22.52, 18.67. HRMS (FAB) calculated for $C_{14}H_{21}N_2O_3$ (M+1) 265.1547, found 265.1539 (-3.0 ppm, -0.8 mmu).

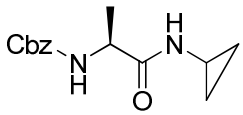

Z-Ala-NHCyP **((*S*)-*1*-29c)**. To a chilled solution of Z-Ala-OH (1.11 g, 5.0 mmol) in CH_2Cl_2 (25 mL) at 0 ^oC was added cyclopropylamine (0.4 mL, 5.5 mmol) with stirring. 1-Ethyl-3-(3-dimethylaminopropyl)carbodiimide hydrochloride (EDC, 1.05 g, 5.5 mmol), hydroxybenzotriazole (HOBt, 750 mg, 5.5 mmol), and DIPEA (1 mL, 5.5 mmol) were then added sequentially. The resulting solution was stirred overnight while warming to room temperature. In the morning, 15 mL of water was added to the solution and the contents were poured into a separatory funnel. The lower organic layer was collected and the aqueous layer was extracted with EtOAc (3 x 15 mL). The combined organic layers were dried over Na_2SO_4, filtered, and concentrated to give an oily residue. The residue was purified by flash chromatography (60% EtOAc in hexanes) to give a 1.19 g (91%) of a white solid (mp = 141.7 ^oC). The solid was analyzed by NMR and the spectral data were found to be consistent with the literature values.[51] ^1H NMR (400 MHz, $CDCl_3$) δ 7.42 – 7.25 (m, 5H), 6.33 (*NH*, s, 1H), 5.40 (*NH*, s, 1H), 5.05 (s, 2H), 4.19 – 4.02 (m, 1H), 2.76 – 2.59 (m, 1H), 1.31 (d, *J* = 7.0, 3H), 0.77 – 0.66 (m, 2H), 0.44 (br. s, 2H). ^{13}C NMR (101 MHz, CDCl3) δ 173.55, 155.96, 136.06, 128.51, 128.20, 127.98, 66.99, 50.31, 22.53, 6.44. HRMS (FAB) calculated for $C_{14}H_{19}N_2O_3$ (M+1) 263.1390, found 263.1389 (-0.4 ppm, -0.1 mmu).

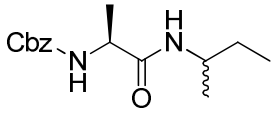

Z-Ala-NHs-Bu **((*S*)-*1*-29d)**. The procedure give **(*S*)-*1*-29c** was followed using Z-Ala-OH (670 mg, 3.0 mmol) and (±)-*sec*-butylamine (0.36 mL, 0.36 mmol). The residue was purified by flash chromatography (60% EtOAc in hexanes) to give a 695 mg (83%) of a white solid (mp = 148.6 ^{o}C). The solid was analyzed by NMR and the spectral data were found to be consistent with the literature the values.[51] ^{1}H NMR (400 MHz, $CDCl_3$) δ 7.35 – 7.27 (m, 5H), 5.79 (*NH*, s, 1H), 5.36 (*NH*, s, 1H), 5.09 (s, 2H), 4.23 – 4.13 (m, 1H), 3.91 – 3.80 (m, 1H), 1.46 – 1.37 (m, 2H), 1.35 (dd, *J* = 3.4, 7.0, 3H), 1.12 – 1.06 (m, 3H), 0.89 – 0.82 (m, 3H). ^{13}C NMR (101 MHz, CDCl3) δ 171.62, 136.42, 128.76, 128.43, 128.26, 67.17, 50.86, 46.93, 29.80, 29.76, 20.57, 20.54, 10.47. HRMS (FAB) calculated for $C_{15}H_{23}N_2O_3$ (M+1) 279.1703, found 279.1727 (+8.6 ppm, +2.4 mmu).

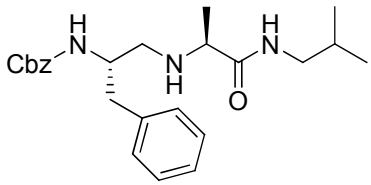

Benzyl (*S*)-1-((*S*)-1-(isobutylamino)-1-oxopropan-2-ylamino)-3-phenylpropan-2-ylcarbamate **((*S,S*)-*1*-32a)**.[68,157] To a Schlenk flask fitted with a balloon was added ***1*-29a** (480 mg, 5 mmol). Solid was dissolved in 10 mL of methanol followed by the addition of 10% Pd on carbon (60 mg per mmol Cbz protected substrate, 300 mg). The suspension was degassed and backfilled with nitrogen gas three times. The nitrogen atmosphere was evacuated and replaced with hydrogen. This suspension was stirred at room temperature for 18 hours. The contents of the Schlenk flask were then poured over a pad of celite in order to remove the catalyst. The filtrate was

concentrated and the crude amine was used without further purification. In a two necked 50 mL round bottom flask purged with nitrogen gas was added CH_2Cl_2 (10 mL) which was then cooled to -78 ^oC. Oxalyl choride (0.43 mL, 5 mmol) was then added slowly via syringe and this solution was allowed to stir at -78 ^oC for five minutes before a solution of anhydrous DMSO (0.75 mL, 10.4 mmol) in CH_2Cl_2 (5 mL) was added drop-wise via pipette. Upon cessation of visible bubbles, a solution of Z-Phe-ol (1.28 g, 4.5 mmol) in CH_2Cl_2 (8 mL) was added drop-wise via pipette. The resulting cloudy suspension was stirred at -78 ^oC for 20 minutes. DIPEA (3.0 mL, 7.6 mmol) was then added via syringe and the cooling bath was removed and the yellow solution was allowed to warm to room temperature. TLC indicated complete conversion of the alcohol. The solution of the crude aldehyde was concentrated and to this residue was added 4 mL of anhydrous 1,2-dichloroethane (DCE). The crude amine from the hydrogenolysis was taken up in 1 mL of DCE and added to the crude aldehyde solution. Magnesium sulfate (anhydrous, 50 mg) was added and the cloudy suspension was stirred for 5 minutes before the addition of sodium triacetoxyborohydride (1.53 g, 7.2 mmol). This mixture was stirred under a nitrogen atmosphere overnight. In the morning, 10 mL of aqueous saturated sodium bicarbonate was added. This suspension was stirred for 5 minutes and the contents were then poured into a separatory funnel where the lower organic layer was removed. The aqueous layer was then extracted with CH_2Cl_2 (3 x 15 mL). The combined organic extracts were dried over Na_2SO_4, filtered, and concentrated to give a yellow residue. This residue was purified by flash chromatography (60% EtOAc in hexanes) to give 1.31 g (64%) of a white solid. The solid was analyzed by NMR and the spectral data were found to be consistent with the literature values.[51] ^1H NMR (500 MHz, $CDCl_3$) δ 7.41 – 7.19 (m, 10H), 5.08 (s, 2H), 4.72 (*NH*, s, 1H), 4.01 (*NH*, s, 1H), 3.10 – 3.04 (m, 1H), 3.04 – 2.94 (m, 2H), 2.87 – 2.74 (m, 2H), 2.68 – 2.54 (m, 2H), 1.72 -

1.63 (m, 1H), 1.57 (s, 2H), 1.23 (d, *J* = 6.9, 3H), 0.83 (d, *J* = 6.4, 6H). ^{13}C NMR (126 MHz, $CDCl_3$) δ 174.66, 156.29, 137.27, 136.43, 129.27, 128.74, 128.66, 128.32, 128.17, 126.85, 66.89, 58.91, 52.81, 52.07, 46.23, 39.65, 28.61, 20.18, 20.14, 20.01. HRMS (ESI-TOF) calculated for $C_{24}H_{34}N_3O_3$ (MH^+) 412.2595, found 412.2620 (+6.1 ppm, +2.5 mmu).

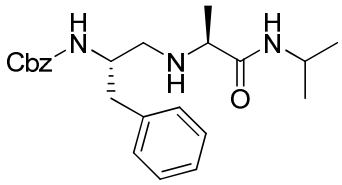

Benzyl (*S*)-1-((*S*)-1-(isopropylamino)-1-oxopropan-2-ylamino)-3-phenylpropan-2-ylcarbamate **((*S,S*)-*1*-32b)**. The procedure for the synthesis of **(*S,S*)-*1*-32a** was followed using Z-Phe-ol (571 mg, 2 mmol) and ***1*-29b** (529 mg, 2 mmol). The residue was purified by flash chromatography which afforded 263 mg (33%) of a white solid (mp = 129.3 °C). The solid was analyzed by NMR and the spectral data were found to be consistent with the literature values.[51] ^{1}H NMR (500 MHz, $CDCl_3$) δ 7.45 – 7.06 (m, 10H), 6.86 (*NH*, s, 1H), 5.07 (s, 2H), 4.85 (*NH*, br. d, *J* = 8.3, 1H), 4.08 – 3.88 (m, 2H), 3.02 (q, *J* = 6.8, 1H), 2.83 (dd, *J* = 13.4, 6.2 Hz, 1H), 2.76 (dd, *J* = 13.2, 7.4 Hz, 1H), 2.57 (d, *J* = 5.8, 2H), 1.20 (d, *J* = 6.9, 3H), 1.07 (d, *J* = 6.6, 3H), 1.00 (d, *J* = 6.5, 3H). ^{13}C NMR (126 MHz, $CDCl_3$) δ 173.69, 156.26, 137.35, 136.41, 129.21, 128.75, 128.66, 128.32, 128.21, 126.85, 66.91, 58.79, 52.82, 51.82, 40.64, 39.64, 22.74, 19.84. HRMS (FAB) calculated for $C_{23}H_{32}N_3O_3$ (MH^+) 398.2438, found 398.2416 (-5.5 ppm, -2.2 mmu).

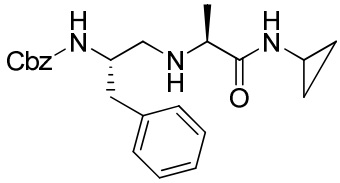

Benzyl (*S*)-1-((*S*)-1-(cyclopropylamino)-1-oxopropan-2-ylamino)-3-phenylpropan-2-ylcarbamate **((*S,S*)-*1*-32b)**. The procedure for the synthesis of **(*S,S*)-*1*-32a** was followed using Z-Phe-ol (571 mg, 2 mmol) and ***1*-29c** (525 mg, 2 mmol). The residue was purified by flash chromatography which afforded 520 mg (66%) of a white solid (mp = 124.2 ^{o}C). The solid was analyzed by NMR and the spectral data were found to be consistent with the literature values.[51] ^{1}H NMR (500 MHz, $CDCl_3$) δ 7.39 – 7.07 (m, 10H), 5.07 (s, 2H), 4.71 (*NH*, br. d, *J* = 8.3, 1H), 4.03 – 3.90 (*NH*, m, 1H), 3.04 (q, *J* = 6.3, 1H), 2.81 (dd, *J* = 13.7, 6.3 Hz, 1H), 2.75 (dd, *J* = 13.3, 7.2 Hz, 1H), 2.68 – 2.63 (m, 1H), 2.58 – 2.53 (m, *J* = 4.4, 2H), 1.20 (d, *J* = 6.9, 3H), 0.76 – 0.64 (m, 2H), 0.37 (br. s, 2H). ^{13}C NMR (126 MHz, $CDCl_3$) δ 176.18, 156.27, 137.25, 129.22, 128.76, 128.67, 128.66, 128.65, 128.33, 128.19, 126.89, 77.36, 77.10, 76.85, 66.92, 58.62, 51.93, 22.13, 19.71, 6.53, 6.37. HRMS (FAB) calculated for $C_{23}H_{30}N_3O_3$ (MH^+) 396.2282, found 396.2272 (-2.5 ppm, -1.0 mmu).

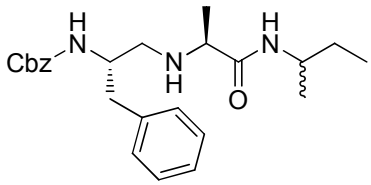

Benzyl (2*S*)-1-((2*S*)-1-(*sec*-butylamino)-1-oxopropan-2-ylamino)-3-phenylpropan-2-ylcarbamate **((*S,S*)-*1*-32d)**. The procedure for the synthesis of **(*S,S*)-*1*-32a** was followed using Z-Phe-ol (571 mg, 2 mmol) and ***1*-29d** (525 mg, 2 mmol). The residue was purified by flash chromatography which afforded 604 mg (73%) of a white solid (mp = 106.7 ^{o}C). The solid was analyzed by

NMR and the spectral data were consistent with the literature values.[51] ^{1}H NMR (400 MHz, $CDCl_3$) δ 7.40 – 7.05 (m, 10H), 6.79 (*NH*, s, 1H), 5.05 (s, 2H), 4.76 (*NH*, br. d, *J* = 8.6, 1H), 3.98 (*NH*, s, 1H), 3.82 – 3.72 (m, 1H), 3.01 (q, *J* = 6.7, 1H), 2.77 (qd, *J* = 6.8, 13.9, 2H), 2.56 (dd, *J* = 5.0, 8.0, 2H), 1.42 – 1.27 (m, 2H), 1.24 (dd, *J* = 6.9, 12.0, 1H), 1.19 (dd, *J* = 3.7, 6.9, 3H), 0.98 (dd, *J* = 6.6, 33.8, 3H), 0.78 (dt, *J* = 7.4, 23.3, 3H). ^{13}C NMR (101 MHz, $CDCl_3$) δ 173.76, 156.12, 137.18, 136.28, 129.10, 128.60, 128.51, 128.17, 128.04, 126.70, 66.80, 58.70, 51.84, 51.74, 45.82, 45.68, 29.62, 29.51, 20.34, 19.95, 19.82, 10.39, 10.29, 3.00. HRMS (ESI-TOF) calculated for $C_{24}H_{34}N_3O_3$ (MH^+) 412.2595, found 412.2620 (+6.1 ppm, +2.5 mmu).

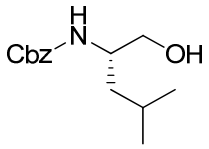

Synthesis of Z-Leu-ol. To a stirred solution of Leu-ol (0.65 mL, 5 mmol) in CH_2Cl_2 (5 mL) was added diisopropylethylamine (1.5 mL, 9 mmol). The solution was cooled to 0 ^{o}C via an external cooling bath. To this stirred solution was added benzyl chloroformate (0.85 mL, 6 mmol) and the solution was allowed to stir at 0 ^{o}C for 4 hours. Upon completion of reaction, water (5 mL) was added and the biphasic solution was poured into a separatory funnel where the lower organic layer was separated. The aqueous layer was extracted with EtOAc (2 x 10 mL) and the combined organic extracts were dried over Na_2SO_4. The solution was filtered and concentrated to give a colorless residue. This residue was purified by flash chromatography (35% EtOAc in hexanes) to give 1.19 g (95%) of white solid. The solid was analyzed by NMR and the spectral data were consistent with the literature values.[106]

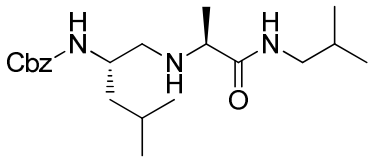

Benzyl (*S*)-1-((*S*)-1-(isobutylamino)-1-oxopropan-2-ylamino)-4-methylpentan-2-ylcarbamate **((*S,S*)-*1*-33a)**. The procedure for the synthesis of **(*S,S*)-*1*-32a** was followed using Z-Leu-ol (754 mg, 3 mmol) and ***1*-29a** (835 mg, 3 mmol). The residue was purified by flash chromatography which afforded 462 mg (42%) of a white solid. The spectral data were consistent with the literature values.[51] ^{1}H NMR (500 MHz, $CDCl_3$) δ 7.37 – 7.28 (m, 5H), 6.94 (d, *J* = 7.8 Hz, 1H), 5.10 (s, 2H), 4.87 (d, *J* = 8.7 Hz, 1H), 4.06 – 3.95 (m, 1H), 3.86 (d, *J* = 4.1 Hz, 1H), 3.36 (dd, *J* = 13.5, 6.8 Hz, 1H), 2.78 – 2.72 (m, 1H), 2.72 – 2.64 (m, 1H), 1.68 – 1.57 (m, 1H), 1.38 – 1.27 (m, 4H), 1.19 – 1.05 (m, 5H), 0.96 – 0.85 (m, 6H).^{13}C NMR (126 MHz, $CDCl_3$) δ 172.03, 157.00, 135.73, 128.67, 128.66, 128.64, 128.35, 128.19, 77.36, 77.10, 76.85, 67.26, 60.50, 58.47, 53.54, 49.46, 42.14, 41.37, 24.82, 23.03, 22.55, 22.50, 22.01, 21.03, 18.95, 14.27. HRMS (FAB) calculated for $C_{21}H_{36}N_3O_3$ (MH^+) 378.2751, found 378.2757 (+1.6 ppm, +0.6 mmu).

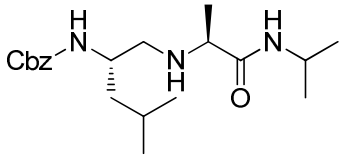

Benzyl (*S*)-1-((*S*)-1-(isopropylamino)-1-oxopropan-2-ylamino)-4-methylpentan-2-ylcarbamate **((*S,S*)-*1*-33b)**. The procedure for the synthesis of **(*S,S*)-*1*-32a** was followed using Z-Leu-ol (503 mg, 2 mmol) and ***1*-29a** (529mg, 2 mmol). The residue was purified by flash chromatography which afforded 338 mg (50%) of a white solid. The solid was analyzed by NMR and the spectral data were consistent with the literature values.[51] ^{1}H NMR (400 MHz, $CDCl_3$) δ 7.37 – 7.17 (m, 5H), 7.03 (s, 1H), 5.03 (s, 2H), 4.85 (d, *J* = 9.0, 1H), 4.02 – 3.89 (m, 1H), 3.73 (s, 1H), 3.07 –

2.94 (m, 1H), 2.74 (s, 1H), 2.61 – 2.49 (m, 2H), 1.65 – 1.51 (m, 1H), 1.22 (dd, *J* = 8.3, 14.4, 2H), 1.16 (d, *J* = 6.9, 3H), 1.03 (t, *J* = 8.4, 6H), 0.90 – 0.80 (m, 6H). ^{13}C NMR (101 MHz, $CDCl_3$) δ 173.75, 156.35, 136.40, 128.45, 128.10, 128.02, 66.66, 58.60, 53.36, 49.85, 42.52, 40.55, 24.79, 22.99, 22.62, 22.59, 22.06, 19.63, 2.93. HRMS (FAB) calculated for $C_{20}H_{34}N_3O_3$ (MH^+) 364.2595, found 364.2583 (-3.2 ppm, -1.2 mmu).

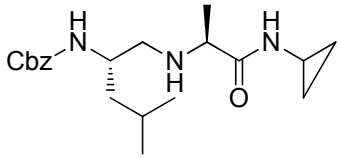

Benzyl (*S*)-1-((*S*)-1-(cyclopropylamino)-1-oxopropan-2-ylamino)-4-methylpentan-2-ylcarbamate **((*S,S*)-*1*-33c)**. The procedure for the synthesis of **(*S,S*)-*1*-32a** was followed using Z-Leu-ol (0.5 mmol, 125 mg) and ***1*-29c** (0.5 mmol, 131 mg). The residue was purified by flash chromatography which afforded 90 mg (54%) of a white solid. The solid was analyzed by NMR and the spectral data were found to be consistent with the literature values.[51] ^{1}H NMR (500 MHz, $CDCl_3$) δ 7.37 – 7.29 (m, 5H), 5.15 – 5.05 (m, 2H), 4.59 (d, *J* = 9.1 Hz, 1H), 3.86 – 3.69 (m, 1H), 3.09 (q, *J* = 6.9 Hz, 1H), 2.77 – 2.67 (m, 1H), 2.57 (dd, *J* = 12.1, 7.2 Hz, 1H), 2.51 (dd, *J* = 12.1, 4.5 Hz, 1H), 1.68 – 1.59 (m, 1H), 1.33 – 1.15 (m, 6H), 0.97 – 0.87 (m, 5H), 0.81 – 0.66 (m, 2H), 0.47 (s, 2H). ^{13}C NMR (126 MHz, $CDCl_3$) δ 180.58, 176.05, 175.40, 156.63, 136.54, 128.59, 128.23, 128.12, 66.84, 58.38, 57.60, 53.16, 49.79, 42.42, 24.87, 23.10, 22.30, 22.12, 21.50, 19.24, 14.24, 6.42, 6.28. HRMS (FAB) calculated for $C_{20}H_{32}N_3O_3$ (MH^+) 362.2438, found 362.2427 (-3.0 ppm, -1.1 mmu).

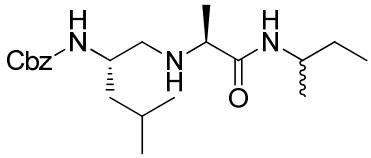

Benzyl (*S*)-1-((*S*)-1-(*sec*-butylamino)-1-oxopropan-2-ylamino)-4-methylpentan-2-ylcarbamate **((*S,S*)-*1*-33d)**. The procedure for the synthesis of **(*S,S*)-*1*-32a** was followed using Z-Leu-ol (503 mg, 2 mmol) and ***1*-29d** (557 mg, 2 mmol). The residue was purified by flash chromatography which afforded 392 mg (52%) of a white solid. The solid was analyzed by NMR and the spectral data were found to be consistent with the literature values.[51] ^{1}H NMR (400 MHz, $CDCl_3$) δ 7.30 – 7.22 (m, 5H), 7.02 (d, *J* = 8.6, 1H), 5.09 – 4.99 (m, 2H), 3.78 (s, 2H), 3.04 (q, *J* = 6.8, 1H), 2.56 – 2.43 (m, 2H), 2.30 (s, 1H), 1.58 (dt, *J* = 6.3, 12.2, 1H), 1.37 (dd, *J* = 6.9, 13.0, 2H), 1.31 – 1.21 (m, 2H), 1.17 (dd, *J* = 3.1, 6.9, 3H), 1.02 (d, *J* = 6.5, 3H), 0.90 – 0.77 (m, 9H). ^{13}C NMR (101 MHz, $CDCl_3$) δ 174.07, 156.40, 136.42, 128.44, 128.08, 128.00, 76.75, 66.63, 58.80, 58.68, 53.54, 53.42, 49.87, 45.87, 45.72, 42.59, 42.52, 29.58, 29.52, 24.75, 23.03, 22.99, 22.02, 20.42, 20.36, 19.88, 19.74, 10.44, 10.30. HRMS (FAB) calculated for $C_{21}H_{36}N_3O_3$ (MH^+) 378.2751, found 378.2765 (+3.7 ppm, +1.4 mmu).

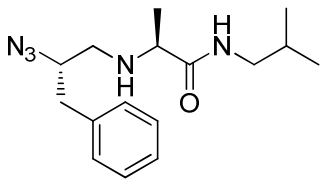

(*S*)-2-((*S*)-2-azido-3-phenylpropylamino)-*N*-isobutylpropanamide **((*S,S*)-*1*-34a , Z1)**.[69]

Compound **(*S,S*)-*1*-32a** (1.31g, 3.18 mmol) was subjected to hydrogenolysis conditions previously described for the synthesis of (**(*S,S*)-*1*-32a**). The crude amine was transferred to a 100 mL round bottom flask followed by the addition of 12 mL of a 3 μM copper (II) sulfate

pentahydrate solution. In a separate 25 mL round bottom flask equipped with a stir bar was added sodium azide (1.24 g, 19.1 mmol) and water (3.4 mL). An equal volume of CH_2Cl_2 was added. The biphasic solution was cooled to 0 ^oC via external ice bath. To this stirred solution was added trifluoromethanesulfonic anhydride (Tf_2O, 1.58 mL, 9.6 mmol) drop-wise via syringe. This mixture was allowed to stir for 2 hours at 0 ^oC. During the first 0.75 hr, the mixture was cloudy giving way to slightly yellow biphasic solution. After two hours 3 mL of an aqueous saturated solution of sodium bicarbonate was added at 0 ^oC and the contents of the flask were then poured into a separatory funnel. The lower colorless organic layer was removed and the aqueous layer was extracted with CH_2Cl (2 x 4.25 mL each). The combined organic layers were poured back into the separatory funnel and washed with 3 mL of saturated sodium bicarbonate. The organic layer was drained into a pear shaped flask and was immediately added to the stirred aqueous amine solution via pipette. To the resulting biphasic mixture was added methanol (36 mL) and DIPEA (1.66 mL, 9.54 mmol). The resulting homogenous solution was allowed to stir overnight. In the morning, as much CH_2Cl_2 and methanol were removed on the rotorary evaporator as possible while maintaining a bath temperature below 40 ^oC. The contents of the flask were poured into a separatory funnel and extracted with CH_2Cl_2 (3 x 15 mL each). The organic extracts were combined and dried over Na_2SO_4, filtered, and concentrated to give a green residue. This residue was purified by flash chromatography (100% EtOAc) to give 570 mg (60%) of a yellow oil. ^1H NMR (500 MHz, $CDCl_3$) δ 7.35 – 7.19 (m, 5H), 7.16 (s, 1H), 3.72 – 3.62 (m, 1H), 3.12 – 3.03 (m, 2H), 3.02 – 2.95 (m, 1H), 2.90 (dd, *J* = 13.8, 7.3 Hz, 1H), 2.85 – 2.77 (m, 1H), 2.66 – 2.56 (m, 2H), 1.73 – 1.62 (m, 1H), 1.31 – 1.26 (m, 3H), 0.84 (d, *J* = 2.5 Hz, 3H), 0.83 (d, *J* = 2.5 Hz, 3H). ^{13}C NMR (126 MHz, $CDCl_3$) δ 174.49, 136.83, 129.22, 128.87, 127.15, 64.36, 58.69, 51.75, 46.27, 39.02, 28.60, 20.14, 20.11, 19.96. $[\alpha]_D^{25} =$ -32.3 (c = 1.3,

CH_3OH). HRMS (ESI-TOF) calculated for $C_{16}H_{26}N_5O$ (MH^+) 304.2132, found 304.2133 (+0.3 ppm, +0.1 mmu).

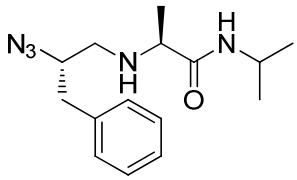

(*S*)-2-((*S*)-2-azido-3-phenylpropylamino)-*N*-isopropylpropanamide **((*S,S*)-*1*-34b, Z2)**. The procedure for the synthesis of **Z1** was followed using **(*S,S*)-*1*-32b** (262 mg, 0.66 mmol). Purification by flash chromatography (100% EtOAc) afforded 168 mg (88%) of a yellow oil. ^{1}H NMR (500 MHz, $CDCl_3$) δ 7.35 – 7.15 (m, 5H), 6.88 (s, 1H), 4.05 – 3.92 (m, 1H), 3.65 (qd, *J* = 3.7, 7.2, 1H), 3.06 (q, *J* = 6.9, 1H), 2.85 (ddd, *J* = 7.1, 13.8, 56.9, 2H), 2.59 (ddd, *J* = 6.0, 12.4, 16.1, 2H), 1.27 (d, *J* = 6.9, 3H), 1.10 (d, *J* = 6.6, 3H), 1.01 (d, *J* = 6.6, 3H). ^{13}C NMR (126 MHz, $CDCl_3$) δ 173.51, 136.91, 129.18, 128.87, 127.14, 64.28, 58.53, 51.52, 40.66, 38.90, 22.79, 22.69, 19.76. $[\alpha]_D^{25}$ = -25.4 (c = 0.87, CH_3OH). HRMS (ESI-TOF) calculated for $C_{12}H_{24}N_5O$ (MH^+) 290.1975, found 290.1976 (+0.3 ppm, +0.1 mmu).

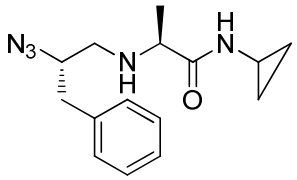

(*S*)-2-((*S*)-2-azido-3-phenylpropylamino)-*N*-cyclopropylpropanamide **((*S,S*)-*1*-34c, Z3)**. The procedure for the synthesis of **Z1** was followed using **(*S,S*)-*1*-32c** (518 mg, 1.31 mmol). Purifcation by flash chromatography (100% EtOAc) afforded 254 mg (67%) of a yellow oil. ^{1}H NMR (400 MHz, $CDCl_3$) δ 7.36 – 7.15 (m, 5H), 7.12 (s, 1H), 3.61 (ddd, *J* = 3.7, 7.2, 15.3, 1H), 3.05 (q, *J* = 6.9, 1H), 2.86 (dd, *J* = 7.4, 13.8, 1H), 2.77 (dd, *J* = 6.8, 13.8, 1H), 2.65 (ddd, *J* = 3.8,

7.4, 11.0, 1H), 2.60 (dd, *J* = 8.4, 12.4, 1H), 2.52 (dd, *J* = 3.7, 12.4, 1H), 1.25 (d, *J* = 6.9, 3H), 0.75 – 0.66 (m, 2H), 0.39 – 0.32 (m, 2H). ^{13}C NMR (101 MHz, $CDCl_3$) δ 175.97, 136.73, 129.04, 128.73, 127.03, 64.02, 58.21, 51.37, 38.73, 22.03, 19.46, 6.38, 6.28. $[\alpha]_D^{25}$ = -32.3 (c = 0.93, CH_3OH). HRMS (ESI-TOF) calculated for $C_{15}H_{21}N_5O$ (M^+) 287.1741, found 287.1761 (+7.0ppm, +2.0 mmu).

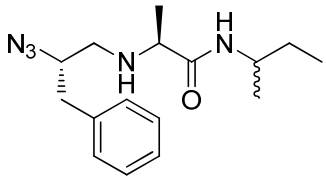

(2*S*)-2-((*S*)-2-azido-3-phenylpropylamino)-*N*-*sec*-butylpropanamide **((*S,S*)-*1*-34d, Z4)**. The procedure for the synthesis of **Z1** was followed using **(*S,S*)-*1*-32d** (446 mg, 1.47 mmol). Purification by flash chromatography (100% EtOAc) afforded 333 mg (75%) of a yellow oil. ^{1}H NMR (400 MHz, $CDCl_3$) δ 7.39 – 7.12 (m, 6H), 6.87 (s, 1H), 3.89 – 3.76 (m, 1H), 3.71 – 3.62 (m, 1H), 2.92 (dd, *J* = 13.7, 7.1 Hz, 1H), 2.79 (dd, *J* = 13.7, 7.1 Hz, 1H), 2.68 – 2.53 (m, 1H), 1.51 – 1.31 (m, 3H), 1.29 (dd, *J* = 6.9, 3.0 Hz, 3H), 1.08 (d, *J* = 6.6 Hz, 1H), 0.97 (d, *J* = 6.6 Hz, 1H), 0.86 (t, *J* = 7.5 Hz, 2H), 0.77 (t, *J* = 7.5 Hz, 1H). ^{13}C NMR (101 MHz, CDCl3) δ 173.72, 136.74, 136.68, 129.13, 129.05, 128.72, 126.99, 64.22, 64.13, 58.53, 58.45, 51.49, 51.37, 45.84, 45.72, 38.86, 38.77, 29.61, 29.47, 20.33, 20.29, 19.85, 19.74, 10.29, 10.23. $[\alpha]_D^{25}$ = -1.1 (c = 1.0, CH_3OH). HRMS (ESI-TOF) calculated for $C_{16}H_{26}N_5O$ (MH^+) 304.2132, found 304.2148 (+5.3 ppm, +1.6 mmu).

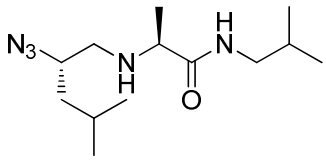

(*S*)-2-((*S*)-2-azido-4-methylpentylamino)-*N*-isobutylpropanamide **((*S,S*)-*1*-35a, Z5)**. The procedure for the synthesis of **Z1** was followed using **(*S,S*)-*1*-33a** (493 mg, 1.83 mmol). Purification by flash chromatography (100% EtOAc) afforded 400 mg (81%) of a yellow oil. ^{1}H NMR (500 MHz, $CDCl_3$) δ 7.29 (s, 1H), 3.48 – 3.40 (m, 1H), 3.14 (q, *J* = 7.2 Hz, 1H), 3.12 – 3.02 (m, 2H), 2.65 (dd, *J* = 12.3, 8.4 Hz, 1H), 2.59 (dd, *J* = 12.3, 3.7 Hz, 1H), 1.82 – 1.71 (m, 2H), 1.54 – 1.44 (m, 1H), 1.31 (d, *J* = 6.9 Hz, 3H), 0.92 (apparent dd, *J* = 13.5, 6.7 Hz, 12H). ^{13}C NMR (126 MHz, $CDCl_3$) δ 174.75, 61.20, 58.69, 52.67, 46.36, 41.28, 28.63, 25.06, 22.96, 22.13, 20.15, 20.13, 19.93. HRMS (FAB) calculated for $C_{13}H_{28}N_5O$ (MH^+) 270.2294, found 270.2301(+2.7 ppm, +0.7 mmu). $[\alpha]_D^{25}$ = -11.9 (c = 1.3, CH_3OH).

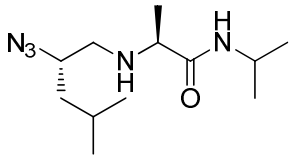

(*S*)-2-((*S*)-2-azido-4-methylpentylamino)-*N*-isopropylpropanamide **((*S,S*)-*1*-35a, Z6)**. The procedure for the synthesis of **Z1** was followed using **(*S,S*)-*1*-33b** (3.64 mg, 1.00 mmol). Purification by flash chromatography (100% EtOAc) afforded 163 mg (66%) of a yellow oil. ^{1}H NMR (400 MHz, $CDCl_3$) δ 6.99 (d, *J* = 7.1, 1H), 4.09 – 3.93 (m, 1H), 3.46 – 3.35 (m, 1H), 3.08 (q, *J* = 6.9, 1H), 2.63 (dd, *J* = 8.1, 12.4, 1H), 2.55 (dd, *J* = 3.8, 12.4, 1H), 1.79 – 1.57 (m, 3H), 1.55 – 1.43 (m, 1H), 1.27 (d, *J* = 6.9, 3H), 1.12 (dd, *J* = 2.3, 6.5, 6H), 0.92 (d, *J* = 6.6, 6H). ^{13}C NMR (101 MHz, $CDCl_3$) δ 170.61, 58.02, 55.53, 49.45, 38.08, 37.67, 22.02, 19.82, 19.73, 19.71,

19.11, 16.69. $[\alpha]_D^{25}$ = -9.4 (c = 0.87, CH_3OH). HRMS (ESI-TOF) calculated for $C_{12}H_{25}N_5O$ (M^+) 255.2054, found 255.2038 (-6.3 ppm, -1.6 mmu).

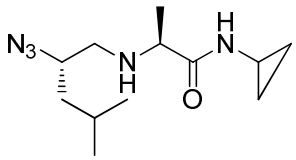

(*S*)-2-((*S*)-2-azido-4-methylpentylamino)-*N*-cyclopropylpropanamide **((*S,S*)-*1*-35c, Z7)**. The procedure for the synthesis of **Z1** was followed using **(*S,S*)-*1*-33c** (481 mg, 1.33 mmol). Purification by flash chromatography (100% EtOAc) afforded 218 mg (65%) of a yellow oil. ^{1}H NMR (500 MHz, $CDCl_3$) δ 7.20 (s, 1H), 3.38 (s, 1H), 3.09 (d, *J* = 6.9, 1H), 2.72 (d, *J* = 3.8, 1H), 2.64 – 2.58 (m, 1H), 2.64 – 2.58 (m, 1H), 1.71 (s, 1H), 1.51 – 1.39 (m, 2H), 1.31 – 1.20 (m, 5H), 0.76 (d, *J* = 7.2, 2H), 0.46 (s, 2H). ^{13}C NMR (126 MHz, $CDCl_3$) δ 176.09, 61.04, 58.50, 52.55, 41.13, 25.09, 22.95, 22.21, 22.14, 19.64, 6.47, 6.45. HRMS (FAB) calculated for $C_{12}H_{24}N_5O$ (MH^+) 254.1981, found 254.1978 (-1.1 ppm, -0.3 mmu). $[\alpha]_D^{25}$ = -11.9 (c = 1.0, CH_3OH).

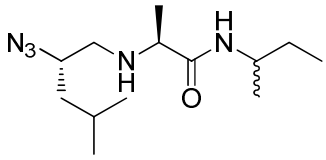

(*S*)-2-((*S*)-2-azido-4-methylpentylamino)-*N*-*sec*-butylpropanamide **((*S,S*)-*1*-35d, Z8)**. The procedure for the synthesis of **Z1** was followed using **(*S,S*)-*1*-33d** (393 mg, 1.04 mmol). Purification by flash chromatography (100% EtOAc) afforded 194 mg (70%) of a yellow oil. ^{1}H NMR (400 MHz, $CDCl_3$) δ 6.97 (d, *J* = 7.1, 1H), 3.93 – 3.78 (m, 1H), 3.45 – 3.36 (m, 1H), 3.16 – 3.05 (m, 1H), 2.67 – 2.53 (m, 2H), 1.78 – 1.67 (m, 1H), 1.58 – 1.36 (m, 3H), 1.33 – 1.20 (m, 4H), 1.09 (dd, *J* = 2.2, 6.6, 3H), 0.92 (d, *J* = 6.6, 6H), 0.87 (td, *J* = 1.8, 7.4, 3H). ^{13}C NMR (101 MHz, $CDCl_3$) δ 173.84, 60.96, 58.53, 52.42, 45.92, 41.13, 29.55, 24.95, 22.76, 22.03, 20.39,

19.88, 10.37. HRMS (FAB) calculated for $C_{13}H_{28}N_5O$ (MH^+) 270.2294, found 270.2291(-1.1 ppm, -0.3 mmu). $[\alpha]_D^{25}$ = -7.1 (c = 0.93, CH_3OH).

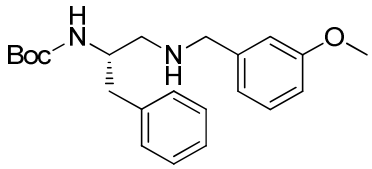

(*S*)-*tert*-butyl 1-(3-methoxybenzylamino)-3-phenylpropan-2-ylcarbamate (**(*S*)-*1*-37a**).[68,157] In a two necked 50 mL round bottom flask purged with nitrogen gas was added CH_2Cl_2 (8 mL). With stirring under a nitrogen atmosphere the solvent was cooled to -78 ^oC. Oxalyl choride (0.19 mL, 2.2 mmol) was added slowly via syringe. The solution was allowed to stir at -78 ^oC for five minutes before a solution of anhydrous DMSO (0.33 mL, 4.6 mmol) in CH_2Cl_2 (3.5 mL) was added drop-wise via pipette. Upon cessation of visible bubbles, a solution of Boc-Phe-ol (502 mg, 2 mmol) in CH_2Cl_2 (3.5 mL) was added drop-wise via pipette. The cloudy suspension was stirred at -78 ^oC for 20 minutes. DIPEA (1.26 mL, 7.6 mmol) was added via syringe. Cooling bath was removed and the yellow solution was allowed to warm to room temperature. TLC indicated complete conversion of the alcohol. The solution of the crude aldehyde was concentrated and to the residue was added 4 mL of anhydrous 1,2-dichloroethane (DCE), 3-methoxybenzylamine (0.51 mL, 4 mmol), and magnesium sulfate (50 mg). The cloudy suspension was stirred for 5 minutes before the addition of sodium triacetoxyborohydride (678 mg, 3.2 mmol). The mixture was stirred under a nitrogen atmosphere overnight. In the morning, 10 mL of aqueous saturated sodium bicarbonate was added. The suspension was stirred for 5 minutes. The contents were poured into a separatory funnel and lower organic layer was removed. The aqueous layer was extracted with CH_2Cl_2 (2 x 15mL) and the combined organic extracts were dried over Na_2SO_4, filtered, and concentrated to give a yellow residue. This

residue was purified by flash chromatography (100% EtOAc) to give 596 mg (80%) of a pale yellow oil. ^{1}H NMR (500 MHz, $CDCl_3$) δ 7.31 – 7.11 (m, 6H), 6.86 (d, *J* = 7.4, 2H), 6.81 – 6.77 (m, 1H), 3.78 – 3.66 (m, 2H), 2.92 – 2.70 (m, 2H), 2.65 (dd, *J* = 12.3, 4.9 Hz, 1H), 2.65 (dd, *J* = 12.3, 4.9 Hz, 1H), 1.40 (s, 9H). ^{13}C NMR (126 MHz, $CDCl_3$) δ 159.82, 155.69, 142.06, 138.18, 129.47, 129.46, 128.48, 126.43, 120.49, 113.53, 112.54, 60.38, 55.27, 53.75, 51.43, 28.46, 23.59, 21.12, 20.25, 14.21. HRMS (FAB) calculated for $C_{22}H_{31}N_2O_3$ (MH^+) 371.2335, found 371.2345(+2.8 ppm, +1.0 mmu).

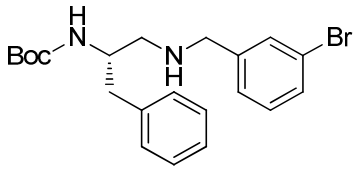

(*S*)-*tert*-butyl 1-(3-bromobenzylamino)-3-phenylpropan-2-ylcarbamate **((*S*)-*1*-37b)**. The procedure for the synthesis of **(*S*)-*1*-37a** was followed using Boc-Phe-ol (502 mg, 2 mmol) and 3-bromobenzylamine hydrochloride (890 mg, 4 mmol). Purification by flash chromatography (35% EtOAc in hexanes) afforded 492 mg (59%) of a yellow oil. ^{1}H NMR (500 MHz, $CDCl_3$) δ 7.45 (s, 1H), 7.36 (dt, *J* = 7.6, 1.6 Hz, 1H), 7.31 – 7.25 (m, 2H), 7.24 – 7.13 (m, 5H), 3.74 (d, *J* = 13.5 Hz, 1H), 3.67 (d, *J* = 13.5 Hz, 1H), 2.85 (dd, *J* = 13.2, 7.5 Hz, 1H), 2.75 (dd, *J* = 13.4, 7.3 Hz, 1H), 2.64 (dd, *J* = 12.3, 4.8 Hz, 1H), 2.57 (dd, *J* = 12.3, 6.6 Hz, 1H), 1.41 (s, 9H). ^{13}C NMR (126 MHz, $CDCl_3$) δ 155.75, 142.81, 138.04, 131.19, 130.16, 130.03, 129.43, 128.64, 128.54, 126.79, 126.60, 126.50, 122.61, 79.50, 60.46, 53.19, 51.50, 51.32, 28.48, 21.23, 14.24. HRMS (FAB) calculated for $C_{21}H_{28}N_2O_2Br$ (MH^+) 419.1334, found 419.1320 (-3.4 ppm, -1.4 mmu).

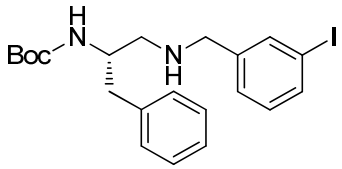

(*S*)-*tert*-butyl 1-(3-iodobenzylamino)-3-phenylpropan-2-ylcarbamate **((*S*)-*1*-37c)**. The procedure for the synthesis of **(*S*)-*1*-37a** was followed using Boc-Phe-ol (502mg, 2 mmol) and 3-iodobenzylamine (technical grade, 0.28 mL, 2.1 mmol). Purification by flash chromatography (35% EtOAc in hexanes) afforded 304 mg (34%) of a yellow oil. ^{1}H NMR (500 MHz, $CDCl_3$) δ 7.65 (s, 1H), 7.57 (d, *J* = 7.9, 1H), 7.29 (dt, *J* = 8.2, 9.2, 2H), 7.25 – 7.18 (m, 2H), 7.16 (d, *J* = 7.1, 2H), 7.03 (t, *J* = 7.7, 1H), 4.68 (s, 1H), 3.94 (s, 1H), 3.72 (d, *J* = 13.5 Hz, 1H), 3.64 (d, *J* = 13.4 Hz, 1H), 2.90 – 2.80 (m, 1H), 2.75 (dd, *J* = 13.4, 7.3 Hz, 1H), 2.64 (dd, *J* = 12.3, 4.8 Hz, 1H), 2.57 (dd, *J* = 12.3, 6.6 Hz, 1H), 1.41 (s, 9H). ^{13}C NMR (126 MHz, $CDCl_3$) δ 155.75, 142.79, 138.03, 137.16, 136.16, 130.22, 129.42, 129.38, 128.66, 128.55, 127.46, 126.64, 126.51, 53.08, 51.52, 51.29, 39.21, 28.48, 21.82, 15.16. HRMS (ESI-TOF) calculated for $C_{21}H_{28}N_2O_2I$ (MH^+) 467.1190, found 467.1177 (-2.8 ppm, -1.3 mmu).

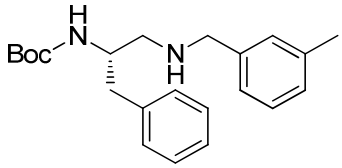

(*S*)-*tert*-butyl 1-(3-methylbenzylamino)-3-phenylpropan-2-ylcarbamate **((*S*)-*1*-37d).** The procedure for the synthesis of **(*S*)-*1*-37a** was followed using Boc-Phe-ol (50 mg, 2 mmol) and 3-methylbenzylamine (0.48 mL, 4 mmol). Purification by flash chromatography (35% EtOAc in hexanes) afforded 458 mg (65%) of a pale yellow oil. ^{1}H NMR (500 MHz, $CDCl_3$) δ 7.30 – 7.24 (m, 2H), 7.23 – 7.14 (m, 4H), 7.08 (dd, *J* = 8.5, 16.0, 3H), 4.80 (s, 1H), 3.95 (s, 1H), 3.75 (d, *J* = 13.1 Hz, 1H), 3.67 (d, *J* = 13.1 Hz, 1H), 2.94 – 2.82 (m, 1H), 2.76 (dd, *J* = 13.2, 7.3 Hz,

1H), 2.66 (dd, *J* = 12.3, 4.8 Hz, 1H), 2.60 (dd, *J* = 12.3, 6.6 Hz, 1H), 1.44 (s, 9H). ^{13}C NMR (126 MHz, $CDCl_3$) δ 155.77, 140.20, 138.22, 138.09, 129.48, 129.00, 128.48, 128.40, 127.84, 126.42, 125.29, 79.25, 60.48, 53.79, 51.40, 39.19, 28.48, 21.49, 21.13, 20.30, 14.30. HRMS (ESI-TOF) calculated for $C_{22}H_{31}N_2O_2$ (MH^+) 355.2380, found 355.2366 (-3.9 ppm, -1.4 mmu).

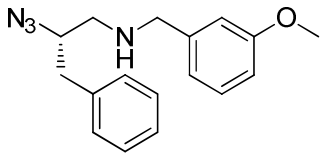

(*S*)-2-azido-*N*-(3-methoxybenzyl)-3-phenylpropan-1-amine **((*S*)-*1*-38a, Z9)**.[69] In a 100 mL round bottom flask equipped with a stir bar was added **(*S*)-*1*-37a** (593 mg, 1.6 mmol) and CH_2Cl_2 (50 mL). The solution was cooled to 0 ^oC via an external cooling bath and trifluoroacetic acid (7.5 mL) was added. The solution was allowed to stir at 0 ^oC for 3 hours at which time TLC (100% EtOAc) indicated complete reaction. CH_2Cl_2 and TFA were removed on the rotary evaporator and the crude amine trifluoroacetate was used without further purification. The diazotransfer reaction was performed in the usual way to give a green residue. This residue was purified by flash chromatography (35% EtOAc in hexanes) to give 204 mg (43%) of a yellow oil. ^{1}H NMR (400 MHz, $CDCl_3$) δ 7.32 – 7.12 (m, 6H), 6.85 (dd, *J* = 2.8, 4.4, 2H), 6.81 – 6.75 (m, 1H), 3.81 – 3.67 (m, 6H), 2.88 – 2.76 (m, 2H), 2.73 (dd, *J* = 3.9, 12.5, 1H), 2.63 (dd, *J* = 8.2, 12.5, 1H). ^{13}C NMR (101 MHz, $CDCl_3$) δ 156.80, 138.44, 134.36, 126.48, 126.27, 125.62, 123.82, 117.36, 110.52, 109.68, 60.91, 52.21, 50.65, 49.19, 35.92. HRMS (FAB) calculated for $C_{17}H_{21}N_4O$ (MH^+) 297.1715, found 297.1699 (-5.5 ppm, -1.6 mmu). $[\alpha]_D^{25} =$ -47.6 (c = 0.53, CH_3OH).

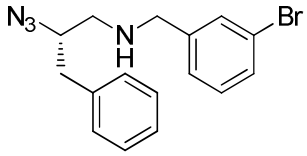

(*S*)-2-azido-*N*-(3-bromobenzyl)-3-phenylpropan-1-amine **((*S*)-*1*-38b, Z10)**.[69] To a stirred solution of 4 M HCl in dioxane (16 mL) at 0°C, was added a solution of **(*S*)-*1*-37b** (453 mg, 1.08 mmol) in anhydrous dioxane (3 mL) drop-wise via pipette. The solution was allowed to stir at 0 °C for 10 minutes. After 10 minutes, the cooling bath was removed and the solution was allowed to stir while warming to room temperature for 1.5 hours. During this warming period the hydrochloride salt began precipitating out of solution. Methanol (1-2 mL) was added in order to achieve solvency. The solvents were removed *in vacuo* to give 398 mg (94%) of a white solid. The diazotransfer was performed in the usual way to give a green residue. This residue was purified by flash chromatography (35% EtOAc in hexanes) to give 246 mg (71%) of a yellow oil. ^{1}H NMR (500 MHz, $CDCl_3$) δ 7.50 – 7.45 (m, 1H), 7.42 – 7.37 (m, 1H), 7.36 – 7.30 (m, 2H), 7.29 – 7.15 (m, 5H), 3.84 – 3.68 (m, 3H), 2.93 – 2.80 (m, 2H), 2.74 (dd, *J* = 12.4, 3.9 Hz, 1H), 2.64 (dd, *J* = 12.4, 8.1 Hz, 1H). ^{13}C NMR (126 MHz, $CDCl_3$) δ 142.44, 137.40, 131.21, 130.32, 130.15, 129.37, 128.76, 126.98, 126.76, 122.71, 63.98, 53.20, 52.17, 38.94. HRMS (FAB) calculated for $C_{16}H_{18}N_4Br$ (MH^+) 345.0715, found 345.0727 (+3.5 ppm, +1.2 mmu). $[\alpha]_D^{25} =$ -46.5 (c = 0.33, CH_3OH).

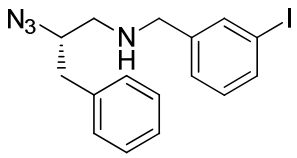

(*S*)-2-azido-*N*-(3-iodobenzyl)-3-phenylpropan-1-amine **((*S*)-*1*-38c, Z11)**. The procedure for the synthesis of **Z10** was followed using (317mg, 0.68 mmol) of **(*S*)-*1*-37c**. The residue was

purified by flash chromatography to give 147 mg (56%) of a yellow oil. ^{1}H NMR (400 MHz, $CDCl_3$) δ 7.65 (t, *J* = 1.5, 1H), 7.58 – 7.54 (m, 1H), 7.34 – 7.14 (m, 6H), 7.03 (t, *J* = 7.7, 1H), 3.76 – 3.64 (m, 3H), 2.90 – 2.76 (m, 2H), 2.70 (dd, *J* = 3.9, 12.4, 1H), 2.61 (dd, *J* = 8.0, 12.4, 1H). ^{13}C NMR (101 MHz, $CDCl_3$) δ 142.41, 137.26, 137.01, 136.11, 130.15, 129.21, 128.65, 128.60, 127.24, 126.88, 126.81, 77.31, 76.99, 76.67, 63.87, 53.00, 52.06, 38.80. $[\alpha]_D^{25}$ = -48.1 (c = 0.33, CH_3OH). HRMS (ESI-TOF) calculated for $C_{16}H_{18}N_4I$ (MH^+) 393.0571, found 393.0557 (-3.6 ppm, -1.4 mmu).

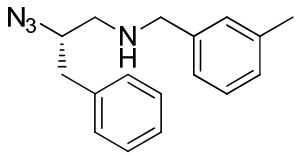

(*S*)-2-azido-*N*-(3-methylbenzyl)-3-phenylpropan-1-amine **((*S*)-*1*-37d, Z12)**. The procedure for the synthesis of **Z10** was followed using (458 mg, 1.29 mmol) of **(*S*)-*1*-38d**. The residue was purified by flash chromatography to give 313 mg (87%) of a yellow oil. ^{1}H NMR (400 MHz, $CDCl_3$) δ 7.34 – 7.01 (m, 9H), 3.79 – 3.65 (m, 3H), 2.88 – 2.76 (m, 2H), 2.73 (dd, *J* = 3.7, 12.5, 1H), 2.61 (dd, *J* = 8.7, 12.5, 1H), 2.32 (s, 3H). ^{13}C NMR (101 MHz, $CDCl_3$) δ 138.68, 138.29, 137.01, 129.21, 128.93, 128.63, 128.48, 128.13, 126.88, 125.19, 63.39, 53.29, 51.77, 38.98, 21.33. $[\alpha]_D^{25}$ = -47.04 (c = 1.1, CH_3OH). HRMS (ESI-TOF) calculated for $C_{17}H_{21}N_2$ (MH^+) 281.1766, found 281.1755 (-3.9 ppm, -1.1 mmu).

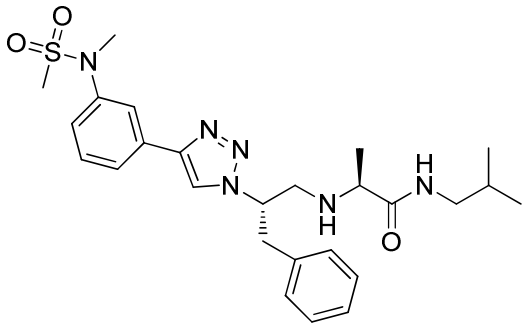

(*S*)-*N*-isobutyl-2-((*S*)-2-(4-(3-(*N*-methylmethylsulfonamido)phenyl)-1H-1,2,3-triazol-1-yl)-3-phenylpropylamino)propanamide **(A1Z1)**. To a 1 dram vial was added **A1** (11.0mg, 0.052 mmol). In a separate vial was added **Z1** (17.7mg, 0.058 mmol). The azide was dissolved in 0.5 mL dry THF and then transferred to the vial containing the alkyne. After a mixing, a freshly prepared sodium ascorbate solution (25 uL of a 1 M aqueous solution) was added. *t*-Butanol and HPLC grade water (25 uL of each) were then added. Nitrogen was then bubbled through solution for 10 minutes. Finally, an aqueous solution of copper (II) sulfate pentahydrate (5 uL of a 0.5 M solution) was added. A temporary darkening of the solution occurred followed by a transformation to a transparent yellow solution. The solution was stirred under nitrogen and monitored by TLC (5% methanol in ethyl acetate). The reaction was judged to be complete in two hours. Water (1 mL) and Et_2O (2 mL) were added and the contents were poured into a separatory funnel. The aqueous layer was extracted with Et_2O (3 x 2 mL). The combined organic extracts were dried over Na_2SO_4, filtered, concentrated, and purified via column chromatography (5% methanol in EtOAc) to give 15.5 mg (59%) of a white solid. ^{1}H NMR (500 MHz, $CDCl_3$) δ 7.81 (t, *J* = 1.8, 1H), 7.69 – 7.60 (m, 1H), 7.57 (s, 1H), 7.44 – 7.30 (m, 2H), 7.24 – 7.17 (m, 3H), 7.06 – 6.96 (m, 2H), 6.85 (s, 1H), 4.72 (s, 1H), 3.41 – 2.92 (m, 10H), 2.85 (s, 3H), 1.70 – 1.58 (m, 1H), 1.19 (d, *J* = 6.9, 2H), 0.88 – 0.71 (m, 6H). ^{13}C NMR (126 MHz, $CDCl_3$) δ 174.28, 146.49, 142.16, 136.12, 131.85, 129.93, 128.99, 128.91, 127.42, 126.03,

124.58, 123.22, 120.18, 64.51, 58.64, 51.72, 46.28, 39.99, 38.19, 35.44, 28.59, 20.15, 20.12, 19.86. HRMS (FAB) calculated for $C_{26}H_{37}N_6O_3S$ (MH^+) 513.2648, found 513.2650 (+0.4 ppm, +0.2 mmu).

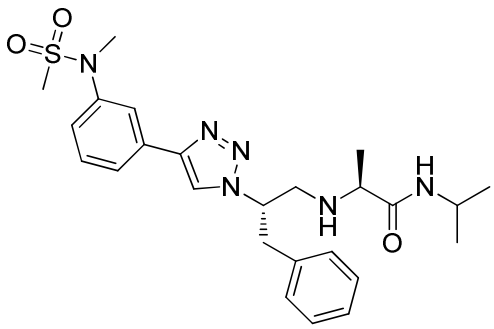

(*S*)-*N*-isopropyl-2-((*S*)-2-(4-(3-(*N*-methylmethylsulfonamido)phenyl)-1H-1,2,3-triazol-1-yl)-3-phenylpropylamino)propanamide **(A1Z2)**. The procedure for the synthesis of **A1Z1** was followed using **A1** (21.2 mg, 0.1 mmol) and **Z2** (34.6mg, 0.12 mmol). The crude triazole was purified by flash chromatography (5% methanol in EtOAc) to give 36 mg (73%) of a foamy white solid. ^{1}H NMR (500 MHz, $CDCl_3$) δ 7.82 (t, *J* = 1.8, 1H), 7.68 – 7.63 (m, 1H), 7.62 (s, 1H), 7.45 – 7.38 (m, 1H), 7.36 – 7.33 (m, 1H), 7.28 – 7.17 (m, 4H), 7.07 – 7.01 (m, 2H), 6.59 (d, *J* = 8.3, 1H), 4.80 – 4.69 (m, 1H), 4.01 – 3.88 (m, 1H), 3.36 (s, 3H), 3.34 – 3.23 (m, 2H), 3.02 (q, *J* = 6.9, 1H), 2.97 (dd, *J* = 4.0, 12.9, 1H), 2.85 (s, 3H), 1.17 (d, *J* = 6.9, 3H), 1.05 (d, *J* = 6.6, 3H), 0.98 (d, *J* = 6.6, 3H). ^{13}C NMR (126 MHz, $CDCl_3$) δ 173.33, 146.55, 142.17, 136.19, 131.89, 129.93, 129.01, 128.89, 127.42, 126.03, 124.60, 123.22, 120.03, 64.43, 58.50, 51.53, 40.79, 39.96, 38.19, 35.46, 22.73, 19.67. HRMS (FAB) calculated for $C_{25}H_{33}N_6O_3S$ (MH^+) 497.2335, found 497.2300 (-7.0 ppm, -3.5 mmu).

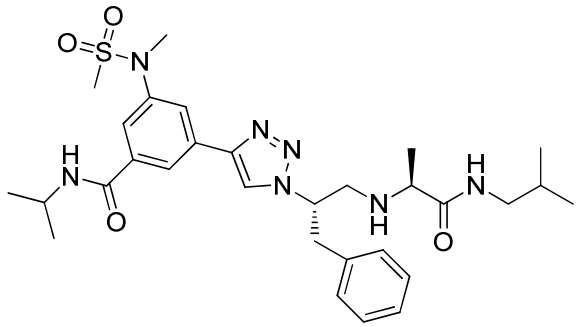

N-isopropyl-3-(*N*-methylmethylsulfonamido)-5-(1-((*S*)-1-((*S*)-1-oxo-1-(isobutylamino)propan-2-ylamino)-3-phenylpropan-2-yl)-1H-1,2,3-triazol-4-yl)benzamide **(A2Z1)**. The procedure for the synthesis of **A1Z1** was followed using **A2** (29.4 mg, 0.1 mmol) and **Z1** (30.3 mg, 0.1 mmol). The crude triazole was purified by flash chromatography (5% methanol in EtOAc) to give 43 mg (72%) of a foamy white solid. ^{1}H NMR (500 MHz, $CDCl_3$) δ 8.03 (s, 1H), 7.87 (s, 1H), 7.72 (s, 1H), 7.69 (s, 1H), 7.27 – 7.15 (m, 3H), 7.01 (d, *J* = 6.6, 2H), 6.88 (s, 1H), 6.23 (d, *J* = 7.9, 1H), 4.75 (s, 1H), 4.26 (dd, *J* = 6.7, 14.1, 1H), 3.38 – 2.94 (m, 10H), 2.88 (s, 3H), 1.26 (d, *J* = 6.6, 6H), 1.19 (d, *J* = 6.9, 3H), 0.81 (d, *J* = 6.7, 6H). ^{13}C NMR (126 MHz, $CDCl_3$) δ 174.29, 165.12, 145.74, 142.46, 136.79, 136.71, 136.01, 132.05, 129.01, 128.85, 127.46, 126.12, 124.03, 122.36, 120.71, 64.65, 58.68, 51.74, 46.31, 42.37, 39.93, 38.15, 35.57, 28.60, 22.80, 20.16. HRMS (FAB) calculated for $C_{30}H_{44}N_7O_4S$ (MH^+) 598.3176, found 598.3175 (-0.1 ppm, 0.0 mmu).

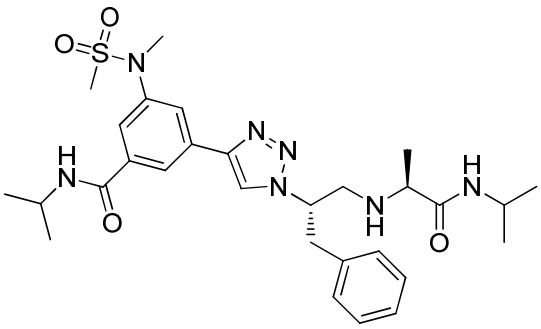

N-isopropyl-3-(1-((*S*)-1-((*S*)-1-(isopropylamino)-1-oxopropan-2-ylamino)-3-phenylpropan-2-yl)-1H-1,2,3-triazol-4-yl)-5-(*N*-methylmethylsulfonamido)benzamide **(A2Z2)**. The procedure for the synthesis of **A1Z1** was followed using **A2** (29.4 mg, 0.1 mmol) and **Z2** (28.9 mg, 0.1 mmol). The crude triazole was purified by flash chromatography (5% methanol in EtOAc) to give 41.1 mg (71%) of a foamy white solid. ^{1}H NMR (500 MHz, $CDCl_3$) δ 8.05 (s, 1H), 7.89 (s, 1H), 7.74 (s, 1H), 7.73 (s, 1H), 7.22 (dd, *J* = 7.2, 13.2, 3H), 7.04 (d, *J* = 6.8, 2H), 6.62 (d, *J* = 8.3, 1H), 6.27 (d, *J* = 7.7, 1H), 4.82 – 4.72 (m, 1H), 4.34 – 4.20 (m, 1H), 4.02 – 3.91 (m, 1H), 3.36 (s, 3H), 3.33 – 3.15 (m, 3H), 3.05 (q, *J* = 6.9, 1H), 2.98 (dd, *J* = 3.9, 12.9, 1H), 2.89 (s, 3H), 1.27 (d, *J* = 6.6, 6H), 1.18 (d, *J* = 6.9, 3H), 1.07 (d, *J* = 6.6, 3H), 1.00 (d, *J* = 6.6, 3H). ^{13}C NMR (126 MHz, $CDCl_3$) δ 173.39, 165.14, 145.79, 142.42, 136.69, 136.06, 132.03, 129.03, 128.86, 127.47, 126.13, 124.08, 122.41, 120.56, 64.58, 58.57, 51.56, 42.37, 40.80, 39.92, 38.17, 35.55, 22.80, 22.75, 19.70. HRMS (FAB) calculated for $C_{29}H_{42}N_7O_4S$ (MH^+) 584.3019, found 584.3005 (-2.4 ppm, -1.4 mmu).

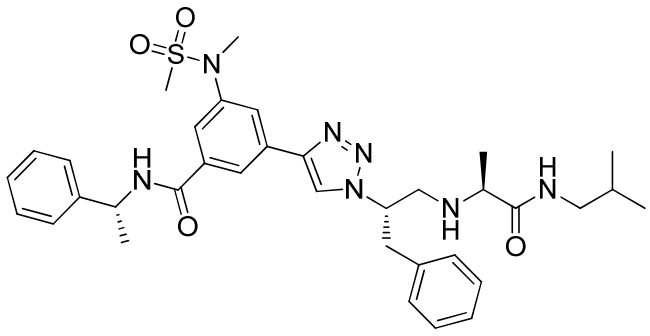

3-(1-((*S*)-1-((*S*)-1-(isobutylamino)-1-oxopropan-2-ylamino)-3-phenylpropan-2-yl)-1H-1,2,3-triazol-4-yl)-5-(*N*-methylmethylsulfonamido)-*N*-((*R*)-1-phenylethyl)benzamide **(A3Z1)**. The procedure for the synthesis of **A1Z1** was followed using **A3** (42.8 mg, 0.12 mmol) and **Z1** (32.1

mg, 0.11 mmol). The crude triazole was purified by flash chromatography (5% methanol in EtOAc) to give 65 mg (86%) of a foamy white solid. ^{1}H NMR (500 MHz, $CDCl_3$) δ 7.94 (s, 1H), 7.81 (s, 1H), 7.68 (s, 1H), 7.64 (s, 1H), 7.40 (d, *J* = 7.3 Hz, 2H), 7.33 (t, *J* = 7.6 Hz, 2H), 7.27 – 7.21 (m, 1H), 7.24 – 7.14 (m, 2H), 7.08 – 6.94 (m, 3H), 5.28 (apparent qt, *J* = 6.9 Hz, 1H), 4.80 – 4.68 (m, 1H), 3.28 (s, 3H), 3.22 – 3.08 (m, 3H), 3.04 – 2.90 (m, 2H), 2.85 (s, 3H), 1.60 (d, *J* = 6.9 Hz, 3H), 1.18 (d, *J* = 6.9 Hz, 3H), 0.80 (d, *J* = 6.7 Hz, 6H). ^{13}C NMR (126 MHz, $CDCl_3$) δ 174.50, 165.17, 145.52, 143.22, 142.31, 136.24, 136.11, 131.99, 128.97, 128.95, 128.86, 128.83, 127.60, 127.39, 126.52, 126.50, 126.34, 124.17, 122.47, 120.80, 64.63, 58.67, 51.69, 49.80, 46.32, 39.88, 38.15, 35.63, 28.60, 21.79, 20.19, 20.15, 19.77. HRMS (FAB) calculated for $C_{35}H_{46}N_7O_4S$ (MH^+) 660.3332, found 660.3332 (0.0 ppm, 0.0 mmu).

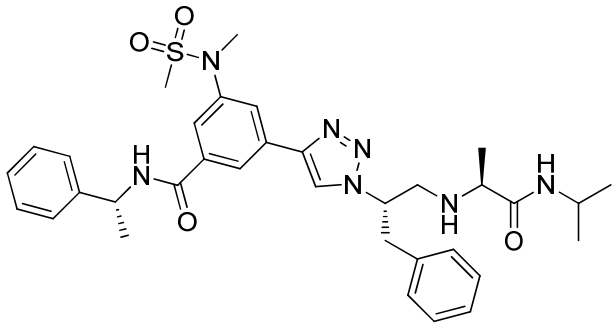

3-(1-((*S*)-1-((*S*)-1-(isopropylamino)-1-oxopropan-2-ylamino)-3-phenylpropan-2-yl)-1H-1,2,3-triazol-4-yl)-5-(*N*-methylmethylsulfonamido)-*N*-((*R*)-1-phenylethyl)benzamide **(A3Z2)**. The procedure for the synthesis of **A1Z1** was followed using **A3** (37.4 mg, 0.105 mmol) and **Z2** (28.9 mg, 0.1 mmol). The crude triazole was purified by flash chromatography (5% methanol in EtOAc) to give 30 mg (46%) of a foamy white solid. ^{1}H NMR (500 MHz, $CDCl_3$) δ 8.07 (s, 1H), 7.89 (s, 1H), 7.75 (s, 1H), 7.69 (s, 1H), 7.42 – 7.18 (m, 8H), 7.04 (d, *J* = 6.7, 2H), 6.63 (dd,

J = 8.0, 24.4, 1H), 5.32 (p, 1H), 4.82 – 4.70 (m, 1H), 4.03 – 3.91 (m, *J* = 6.6, 14.8, 1H), 3.35 (s, 3H), 3.22 – 3.06 (m, 3H), 2.98 (dd, *J* = 3.9, 13.0, 1H), 2.87 (s, 3H), 1.63 (d, *J* = 6.9, 3H), 1.18 (d, *J* = 6.9, 3H), 1.07 (d, *J* = 6.6, 3H), 1.00 (d, *J* = 6.6, 3H). ^{13}C NMR (126 MHz, $CDCl_3$) δ 165.13, 142.91, 142.52, 136.25, 136.03, 129.04, 128.90, 128.85, 127.70, 127.49, 126.44, 124.08, 122.34, 120.57, 64.61, 58.54, 49.79, 40.79, 38.12, 35.48, 22.76, 21.77, 19.73. HRMS (FAB) calculated for $C_{34}H_{44}N_7O_4S$ (MH^+) 646.3176, found 646.3177 (+0.2 ppm, +0.1 mmu).

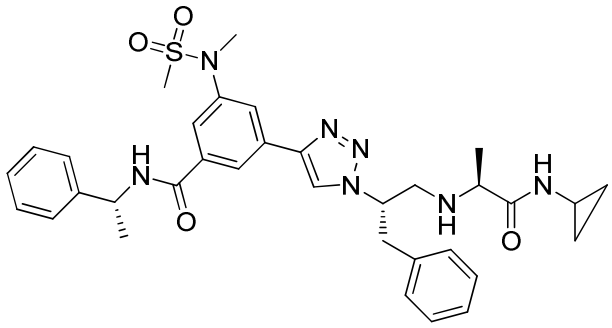

3-(1-((*S*)-1-((*S*)-1-(cyclopropylamino)-1-oxopropan-2-ylamino)-3-phenylpropan-2-yl)-1H-1,2,3-triazol-4-yl)-5-(*N*-methylmethylsulfonamido)-*N*-((*R*)-1-phenylethyl)benzamide **(A3Z3)**. The procedure for the synthesis of **A1Z1** was followed using **A3** (42.8 mg, 0.12 mmol) and **Z3** (32.1 mg, 0.112 mmol). The crude triazole was purified by flash chromatography (5% methanol in EtOAc) to give 46 mg (65%) of a foamy white solid. ^{1}H NMR (500 MHz, $CDCl_3$) δ ^{1}H NMR (500 MHz, $CDCl_3$) δ 7.94 (s, 1H), 7.81 (s, 1H), 7.68 (s, 1H), 7.64 (s, 1H), 7.41 (d, *J* = 7.7, 2H), 7.34 (t, *J* = 7.6, 2H), 7.30 – 7.15 (m, 4H), 7.02 (d, *J* = 6.9, 2H), 6.99 (d, *J* = 7.5, 1H), 6.94 (s, 1H), 5.29 (t, *J* = 7.1, 1H), 4.72 (s, 1H), 3.28 (d, *J* = 13.5, 4H), 3.24 – 3.06 (m, 3H), 2.95 (dd, *J* = 3.4, 13.0, 1H), 2.87 (s, 3H), 2.65 – 2.57 (m, *J* = 3.7, 1H), 1.62 (d, *J* = 6.9, 3H), 1.17 (d, *J* = 6.9, 3H), 0.66 (d, *J* = 7.2, 2H), 0.33 (t, *J* = 3.9, 2H). ^{13}C NMR (126 MHz, $CDCl_3$) δ 175.98, 165.16,

145.54, 143.21, 142.32, 136.21, 136.11, 131.97, 128.99, 128.95, 128.84, 128.83, 127.62, 127.43, 126.53, 126.37, 124.21, 122.43, 120.70, 77.40, 77.15, 76.90, 64.42, 58.38, 51.54, 49.83, 39.76, 38.15, 35.65, 22.25, 21.79, 19.43, 6.51, 6.42. HRMS (FAB) calculated for $C_{34}H_{42}N_7O_4S$ (MH^+) 644.3019, found 644.3064 (+7.0 ppm, +4.5 mmu).

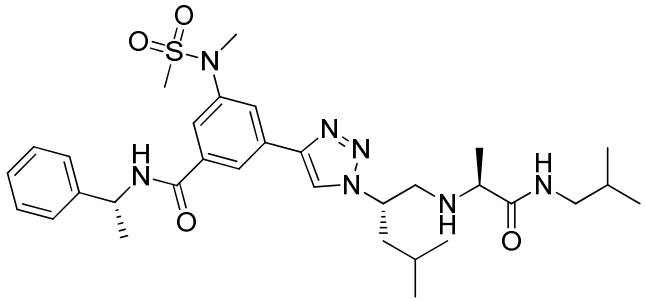

3-(1-((*S*)-1-((*S*)-1-(isobutylamino)-1-oxopropan-2-ylamino)-4-methylpentan-2-yl)-1H-1,2,3-triazol-4-yl)-5-(*N*-methylmethylsulfonamido)-*N*-((*R*)-1-phenylethyl)benzamide **(A3Z5)**. The procedure for the synthesis of **A1Z1** was followed using **A3** (40.1 mg, 0.11 mmol) and **Z5** (28.3 mg, 0.11 mmol). The crude triazole was purified by flash chromatography (5% methanol in EtOAc) to give 45 mg (68%) of a foamy white solid. ^{1}H NMR (500 MHz, $CDCl_3$) δ 7.32 – 7.12 (m, 9H), 6.89 (s, 2H), 3.85 – 3.73 (m, 2H), 3.67 – 3.59 (m, 2H), 3.08 – 3.02 (m, 2H), 2.87 (dd, *J* = 7.2, 13.8, 2H), 2.76 (dd, *J* = 7.0, 13.8, 2H), 2.61 – 2.51 (m, 4H), 1.50 – 1.27 (m, 4H), 1.24 (dd, *J* = 3.6, 6.9, 6H), 1.04 (d, *J* = 6.6, 3H), 0.94 (d, *J* = 6.6, 3H), 0.83 (t, *J* = 7.4, 3H), 0.74 (t, *J* = 7.4, 2H). ^{13}C NMR (126 MHz, $CDCl_3$) δ 174.48, 165.11, 146.02, 142.97, 142.48, 136.26, 132.15, 128.88, 127.68, 126.47, 124.17, 122.44, 119.55, 77.37, 77.12, 76.86, 61.26, 58.78, 53.07, 49.80, 46.34, 41.92, 38.16, 35.53, 28.64, 24.68, 22.93, 21.77, 21.73, 20.19, 20.16, 19.84. HRMS (FAB) calculated for $C_{32}H_{48}N_7O_4S$ (MH^+) 626.3489, found 626.3458 (-4.8 ppm, -3.0 mmu).

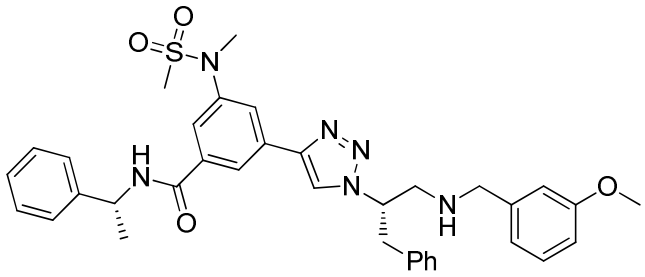

3-(1-((*S*)-1-(3-methoxybenzylamino)-3-phenylpropan-2-yl)-1H-1,2,3-triazol-4-yl)-5-(*N*-methylmethylsulfonamido)-*N*-((*R*)-1-phenylethyl)benzamide **(A3Z9)**. The procedure for the synthesis of **A1Z1** was followed using **A3** (38.5 mg, 0.11 mmol) and **Z9** (38.8 mg, 0.11 mmol). The crude triazole was purified by flash chromatography (60% EtOAc in hexanes) to give 46 mg (71%) of a foamy white solid. ^{1}H NMR (500 MHz, $CDCl_3$) δ 8.04 (s, 1H), 7.86 – 7.84 (m, 1H), 7.73 (t, *J* = 1.7, 1H), 7.58 (s, 1H), 7.43 – 7.32 (m, 4H), 7.28 (d, *J* = 7.2, 1H), 7.24 – 7.15 (m, 4H), 7.03 – 6.97 (m, 2H), 6.83 – 6.75 (m, 3H), 6.69 (d, *J* = 7.6, 1H), 5.32 (apparent qt, *J* = 7.0, 1H), 4.78 (s, 1H), 3.79 – 3.66 (m, 5H), 3.33 (s, 3H), 3.31 – 3.18 (m, 3H), 3.11 (dd, *J* = 4.2, 13.0, 1H), 2.85 (s, 3H). ^{13}C NMR (126 MHz, $CDCl_3$) δ 165.16, 159.84, 145.32, 142.99, 142.44, 136.53, 136.18, 132.30, 129.61, 128.93, 128.88, 128.87, 128.87, 128.85, 127.65, 127.20, 126.46, 126.34, 124.07, 122.36, 121.00, 120.47, 113.75, 112.70, 64.20, 55.27, 55.26, 53.64, 52.15, 49.75, 39.61, 38.13, 35.45, 21.80. HRMS (FAB) calculated for $C_{36}H_{41}N_6O_4S$ (MH^+) 653.2910, found 653.2953 (+6.6 ppm, +4.3 mmu). $[\alpha]_D^{25}$ = -63.1 (c = 0.28, EtOH).

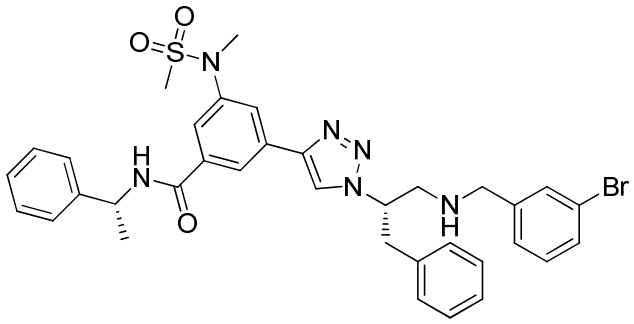

3-(1-((*S*)-1-(3-bromobenzylamino)-3-phenylpropan-2-yl)-1H-1,2,3-triazol-4-yl)-5-(*N*-methylmethylsulfonamido)-*N*-((*R*)-1-phenylethyl)benzamide **(A3Z10)**. The procedure for the synthesis of **A1Z1** was followed using **A3** (37.4 mg, 0.1 mmol) and **Z10** (34.7 mg, 0.1 mmol). The crude triazole was purified by flash chromatography (60% EtOAc in hexanes) to give 51 mg (73%) of a foamy white solid. ^{1}H NMR (500 MHz, $CDCl_3$) δ 8.05 (t, *J* = 1.5, 1H), 7.86 (dd, *J* = 2.1, 1.5 Hz, 1H), 7.74 (t, *J* = 2.0, 1H), 7.61 (s, 1H), 7.44 – 7.32 (m, 6H), 7.28 (dd, *J* = 4.3, 11.5, 1H), 7.25 – 7.18 (m, 3H), 7.17 – 7.12 (m, 2H), 7.05 – 6.98 (m, 2H), 6.65 (d, *J* = 7.7, 1H), 5.32 (dt, *J* = 6.6, 13.3, 1H), 4.81 – 4.72 (m, 1H), 3.71 (q, *J* = 13.7, 2H), 3.34 (s, 3H), 3.29 – 3.18 (m, 3H), 3.09 (dd, *J* = 4.2, 13.0, 1H), 2.86 (s, 3H). ^{13}C NMR (126 MHz, $CDCl_3$) δ 165.14, 145.40, 142.96, 142.44, 142.22, 136.45, 136.20, 132.26, 131.16, 130.38, 130.16, 128.92, 128.90, 128.89, 128.88, 128.87, 128.87, 127.67, 127.26, 126.74, 126.45, 126.44, 126.36, 124.05, 122.68, 122.37, 120.96, 64.23, 53.05, 52.11, 49.75, 39.58, 38.14, 35.45, 21.80. HRMS (FAB) calculated for $C_{35}H_{38}N_6O_3$ (MH^+) 701.1909, found 701.1917 (+1.1 ppm, +0.8 mmu). $[\alpha]_D^{25} =$ -63.9 (c = 0.35, EtOH).

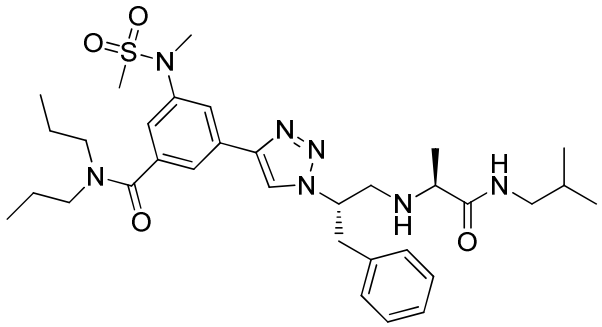

3-(1-((*S*)-1-((*S*)-1-(isobutylamino)-1-oxopropan-2-ylamino)-3-phenylpropan-2-yl)-1H-1,2,3-triazol-4-yl)-5-(*N*-methylmethylsulfonamido)-*N*,*N*-dipropylbenzamide **(A4Z1)**. The procedure for the synthesis of **A1Z1** was followed using **A4** (17.5 mg, 0.05 mmol) and **Z1** (15.2 mg, 0.05 mmol). The crude triazole was purified by flash chromatography (5% methanol in EtOAc) to give 17.9 mg (56%) of an orange solid. ^{1}H NMR (500 MHz, $CDCl_3$) δ 7.87 (t, *J* = 1.6, 1H), 7.65 (t, *J* = 1.5, 1H), 7.60 (s, 1H), 7.34 (dd, *J* = 1.4, 2.1, 1H), 7.25 – 7.19 (m, 2H), 7.04 – 6.99 (m, 2H), 6.85 (s, 1H), 6.79 – 6.74 (m, 0H), 4.73 (s, 1H), 3.45 (t, *J* = 7.3, 2H), 3.39 – 3.33 (m, 4H), 3.32 – 3.14 (m, 4H), 3.09 (q, *J* = 6.8, 1H), 3.05 – 2.96 (m, 2H), 2.88 (s, *J* = 1.3, 3H), 1.73 – 1.63 (m, *J* = 6.7, 13.4, 3H), 1.62 – 1.50 (m, 3H), 1.21 (d, *J* = 7.0, 3H), 0.98 (t, *J* = 7.2, 3H), 0.83 (d, *J* = 6.7, 6H), 0.77 (t, *J* = 7.0, 3H). ^{13}C NMR (101 MHz, $CDCl_3$) δ 174.19, 170.05, 145.70, 142.00, 138.87, 135.93, 132.08, 128.82, 128.79, 128.73, 127.26, 127.21, 123.94, 123.15, 123.06, 122.59, 120.48, 64.42, 58.49, 51.57, 50.80, 46.62, 46.16, 39.78, 37.93, 35.48, 28.45, 21.88, 20.66, 20.03, 20.00, 19.70, 11.44, 10.98. HRMS (FAB) calculated for $C_{33}H_{50}N_7O_4S$ (MH^+) 640.3645, found 640.3701 (+8.8 ppm, +5.6 mmu).

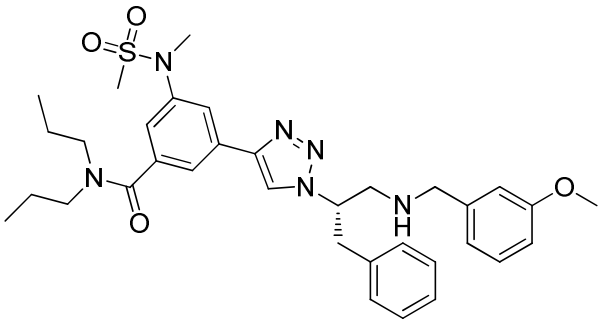

(*S*)-3-(1-(1-(3-methoxybenzylamino)-3-phenylpropan-2-yl)-1H-1,2,3-triazol-4-yl)-5-(*N*-methylmethylsulfonamido)-*N*,*N*-dipropylbenzamide **(A4Z9)**. The procedure for the synthesis of **A1Z1** was followed using **A4** (16.8 mg, 0.05mmol) and **Z9** (14.8 mg, 0.5 mmol). The crude triazole was purified by flash chromatography (60% EtOAc in hexanes) to give 24 mg (77%) of a foamy white solid. ^{1}H NMR (500 MHz, $CDCl_3$) δ 7.88 – 7.82 (m, 1H), 7.61 (t, *J* = 1.4, 1H), 7.55 (s, 1H), 7.36 – 7.30 (m, 1H), 7.24 – 7.13 (m, 4H), 7.02 – 6.97 (m, 2H), 6.79 (dd, *J* = 7.8, 15.9, 3H), 4.80 – 4.72 (m, 1H), 3.78 – 3.67 (m, 5H), 3.44 (t, *J* = 7.4, 2H), 3.35 (s, 3H), 3.32 – 3.17 (m, 5H), 3.11 (dd, *J* = 4.4, 13.0, 1H), 2.87 (s, 3H), 1.75 – 1.47 (m, 4H), 0.98 (t, *J* = 7.2, 3H), 0.75 (t, *J* = 7.2, 3H). ^{13}C NMR (126 MHz, $CDCl_3$) δ 170.24, 159.86, 145.52, 142.07, 141.46, 138.98, 136.60, 132.47, 129.60, 128.95, 128.83, 127.17, 124.28, 123.00, 122.78, 120.84, 120.42, 113.72, 112.65, 77.39, 77.14, 76.88, 64.26, 55.27, 53.68, 52.15, 50.92, 46.72, 39.67, 38.09, 35.56, 22.02, 20.80, 11.59, 11.12. HRMS (FAB) calculated for $C_{34}H_{45}N_6O_4S$ (MH^+) 633.3223, found 633.3181 (-6.6 ppm, -4.2 mmu).

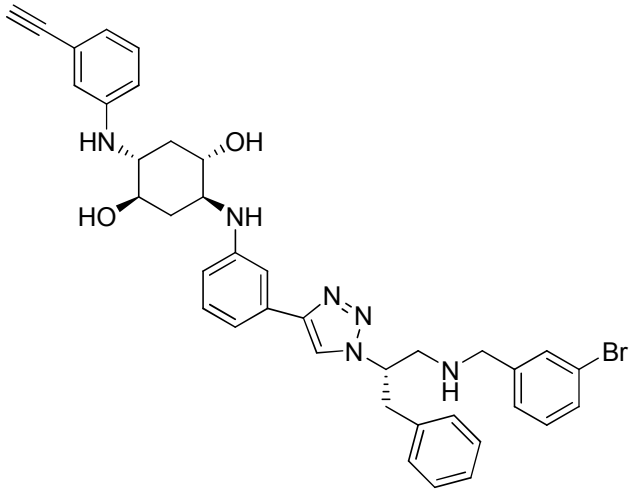

(1*S*,2*S*,4*R*,5*R*)-2-((3-(1-((*S*)-1-((3-bromobenzyl)amino)-3-phenylpropan-2-yl)-1H-1,2,3-triazol-4-yl)phenyl)amino)-5-((3-ethynylphenyl)amino)cyclohexane-1,4-diol *and* (1*S*,2*S*,4*R*,5*R*)-5-((3-(1-((*S*)-1-((3-bromobenzyl)amino)-3-phenylpropan-2-yl)-1H-1,2,3-triazol-4-yl)phenyl)amino)-2-((3-ethynylphenyl)amino)cyclohexane-1,4-diol **(A10aZ10)**. In a 1 dram vial containing **A10a** (16.8 mg, 48.5 μmol) and a stir bar was added 87 μL of THF. In a separate vial containing **Z10** (13.5 mg, 39.1 μmol) was dissolved in 1 mL of THF and 413 μL of this solution (16 μmol) was withdrawn and added to the vial containing **A10a**. To this solution was added 50 μL of *t*-butanol followed by 50 μL of HPLC grade water. With stirring was added 80.8 μL of an aqueous 0.1 M solution of sodium ascorbate (8 μmol). Nitrogen gas was carefully bubbled through for 10 minutes. Finally, 8.08 mL of an aqueous 0.1 M solution of copper (II) sulfate pentahydrate (0.8 μmol) was added and the vial was capped and allowed to stir for 24 hours. TLC indicated consumption of azide and formation of the monotriazole. The mixture was separated via gradient column chromatography. The excess **A10a** was isolated and recycled using 50% EtOAc in hexanes. The triazole was isolated by washing the column with 100% EtOAc giving 6.7 mg (61%) of lightly brown foamy solid. ^{1}H NMR (500 MHz, $(CD_3)_2CO$) δ 8.14 (d, J = 2.3, 1H),

7.51 (s, 1H), 7.38 (d, *J* = 7.8, 1H), 7.28 (d, *J* = 7.8, 1H), 7.25 – 6.99 (m, 11H), 6.80 (s, 1H), 6.72 (d, *J* = 8.2 Hz, 1H), 6.69 (d, *J* = 7.5 Hz, 1H), 6.63 (d, *J* = 8.1 Hz, 1H), 4.07 (s, 1H), 3.78 (q, *J* = 14.1, 4H), 3.49 (s, 1H), 3.45 – 3.34 (m, 3H), 3.29 (dd, *J* = 9.2, 14.0, 1H), 3.20 (dd, *J* = 12.9, 7.9 Hz, 1H), 3.14 (dd, *J* = 12.7, 5.0 Hz, 1H), 2.46 – 2.33 (m, 2H), 1.55 (s, 1H), 1.52 – 1.41 (m, 2H), 0.86 (d, *J* = 7.3, 1H). ^{13}C NMR (126 MHz, $(CD_3)_2CO$) δ 149.03, 148.77, 147.13, 143.76, 137.80, 132.27, 130.95, 130.19, 129.73, 129.35, 129.12, 129.06, 129.05, 129.04, 128.40, 126.99, 126.59, 122.81, 121.98, 120.15, 120.12, 119.91, 115.70, 113.97, 113.91, 112.63, 109.80, 84.42, 76.88, 71.02, 63.27, 56.23, 52.48, 52.30, 38.98. HRMS (ESI) calculated for $C_{38}H_{39}N_6O_2Br$ (MH^+) 691.2396, found 691.2397 (+0.92 ppm, +0.1 mmu). $[\alpha]_D^{25} = 35.6$ (c = 0.36, THF).

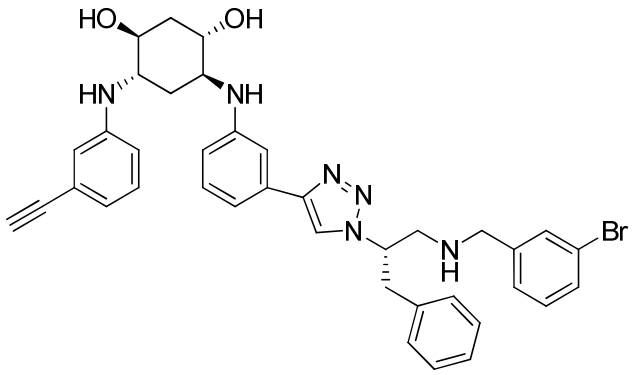

(1*S*,3*S*,4*S*,6*S*)-4-((3-(1-((*S*)-1-((3-bromobenzyl)amino)-3-phenylpropan-2-yl)-1H-1,2,3-triazol-4-yl)phenyl)amino)-6-((3-ethynylphenyl)amino)cyclohexane-1,3-diol *and* (1*S*,3*S*,4*S*,6*S*)-6-((3-(1-((*S*)-1-((3-bromobenzyl)amino)-3-phenylpropan-2-yl)-1H-1,2,3-triazol-4-yl)phenyl)amino)-4-((3-ethynylphenyl)amino)cyclohexane-1,3-diol **(A10bZ10)**. In a 1 dram vial containing **A10b** (7.8 mg, 27.4 μmol) and a stir bar was added 302 μL of THF. In a separate vial containing **Z10** (15.9 mg, 46.1 μmol) was dissolved in 1 mL of THF and 198 μL of this solution (9.13 μmol) was withdrawn and added to the vial containing **A10b**. To this solution was added 50 μL of *t*-butanol followed by 50 μL of HPLC grade water. With stirring was added 45.7 μL of an

aqueous 0.1 M solution of sodium ascorbate (4.54 μmol). Nitrogen gas was carefully bubbled through for 10 minutes. Finally 4.57 mL of an aqueous 0.1 M solution of copper (II) sulfate pentahydrate (0.454 μmol) was added and the vial was capped and allowed to stir for 24 hours. TLC indicated consumption of azide and formation of the monotriazole. The mixture was separated via gradient column chromatography. The excess **A10b** was isolated and recycled using 80% EtOAc in hexanes. The triazole was isolated by washing the column with 100% EtOAc giving 2.7 mg (52%) of white solid. ^{1}H NMR (500 MHz, $(CD_3)_2CO$) δ 8.05 (s, 1H), 7.50 (s, 1H), 7.38 (d, *J* = 7.8, 1H), 7.28 (d, *J* = 7.7, 1H), 7.24 – 6.97 (m, 10H), 6.85 (s, 1H), 6.75 (d, *J* = 8.0, 1H), 6.66 (t, *J* = 7.2, 2H), 4.03 – 3.91 (m, 3H), 3.83 – 3.72 (m, 2H), 3.71 – 3.59 (m, 2H), 3.46 (s, 1H), 3.37 (dd, *J* = 5.4, 14.0, 1H), 3.29 (dd, *J* = 13.9, 9.3 Hz, 1H), 3.22 – 3.11 (m, 2H), 1.98 – 1.95 (m, 2H). ^{13}C NMR (126 MHz, $(CD_3)_2CO$) δ 147.16, 137.78, 132.21, 130.97, 130.19, 129.75, 129.31, 129.04, 128.39, 127.01, 126.58, 122.76, 121.98, 120.03, 119.82, 115.82, 113.83, 112.43, 109.88, 84.47, 76.87, 68.54, 63.24, 54.00, 52.51, 52.32, 38.98, 36.03, 31.81, 30.80, 22.50. HRMS (ESI) calculated for $C_{38}H_{39}N_6O_2Br$ (MH^+) 691.2396, found 691.2414 (+3.38 ppm, +1.8 mmu). $[\alpha]_D^{25} = 19.4$ (c = 0.34, THF).

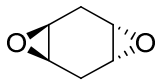

<u>*trans*-1,2,4,5-diepoxycyclohexane</u> (***2*-29**). A modification of Sharpless'[100] procedure was used. To a 50 mL round bottom flask equipped with a stir bar was added 1,4-cyclohexadiene (1.6 g, 20 mmol) followed by methyltrioxorhenium (50 mg, 0.2 mmol). Dichloromethane (10 mL) was added and stirring was initiated. Pyridine (400 μL, 4.8 mmol) was added and the colorless solution turned light yellow. Flask was immersed in a water bath and equipped with an addition funnel. The funnel was charged with a 50% H_2O_2 solution (5.0 mL, 80 mmol). The peroxide

was added dropwise over the course of 10 minutes (a bright yellow color developed) and the biphasic solution was allowed to stir until disappearance of the yellow color (ca. 48 hours). The contents were poured into a separatory funnel and the lower organic layer was collected. The upper peroxide containing aqueous layer was drained into a large beaker containing 200 mL of water. The aqueous solution was treated with saturated sodium thiosulfate prior to disposal. The organic layer was washed with a saturated sodium thiosulfate (10 mL) solution, dried over Na_2SO_4, filtered, and concentrated. The crude white solid was taken up in diethyl ether and washed through a short silica gel column deactivated with triethylamine. The filtrate was concentrated to give 1.88 g (84%) of white needles (mp = 109.9 ^oC). ^1H NMR (500 MHz, $CDCl_3$) δ 3.05 (dt, J = 2.8, 1.4, 2H), 2.30 (dt, J = 2.7, 1.4, 2H). The spectrum is consistent with a lower resolution spectrum found in the literature.[100]

Representative procedure for reaction of *2*-29 with amines/anilines "on water":

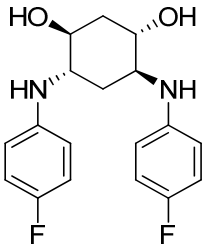

4,6-bis((4-fluorophenyl)amino)cyclohexane-1,3-diol **(*rac*-*2*-51f)**. This procedure was employed for all "on water" reactions, however stoichiometric amounts vary depending on amine/aniline used. To a 1 dram scintillation vial equipped with a magnetic stir bar was added ***2*-49f** (222 mg, 2.0 mmol), ***2*-29** (56 mg, 0.5 mmol), and HPLC grade water (1 mL). The suspension was stirred vigorously and heated to 95 ^oC for 16 hours. Upon cooling, a solid formed and 1 mL of EtOAc was added. TLC analysis (50% EtOAc in hexanes) of the organic layer indicated formation of the less polar 1,4-diol (R_f = 0.6, minor product) and the more polar 1,3-diol (R_f = 0.3, major

product). The contents of the vial were poured into a separatory funnel. The vial was chased with 4 mL of EtOAc and the organic layer was collected. The aqueous layer was extracted with EtOAc (2 x 5 mL) each followed by drying over $MgSO_4$. A small aliquot (ca. 1.5 mL) was added to a vial followed by removal and drying of the solvent *in vacuo* for ^{1}H-NMR analysis to determine the ratio of 1,3- to 1,4-diol regioselectivity. Upon ^{1}H-NMR analysis the analyte was recombined with the crude solution and was evaporated onto celite and purified via flash chromatography (50% EtOAc in hexanes) to give 103 mg (62%) of the 1,3-diol as a yellow solid (***2*-51f**). ^{1}H NMR (400 MHz, CD_3OD) δ 6.85 – 6.78 (m, 4H), 6.70 – 6.63 (m, 4H), 3.89 (q, J = 5.7, 2H), 3.46 (q, J = 5.8, 2H), 1.97 – 1.90 (m, 4H). ^{13}C NMR (101 MHz, CD_3OD) δ 156.92 (d, $^1J_{CF}$ = 233.1 Hz), 145.83 (d, $^4J_{CF}$ = 1.8 Hz), 116.19 (d, $^2J_{CF}$ = 22.3 Hz), 115.43 (d, $^3J_{CF}$ = 7.3 Hz), 69.91, 55.60, 36.80, 31.19. HRMS (ESI-TOF) calculated for $C_{18}H_{21}F_2N_2O_2$ (MH^+) 336.1597, found 336.1606 (2.7 ppm, 0.9 mmu).

Representative procedure for reaction of (*2*-29) with amines/anilines under neat conditions:

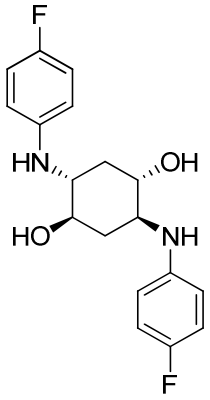

2,5-bis((4-fluorophenyl)amino)cyclohexane-1,4-diol **(*2*-52f)**. This procedure was employed for all neat reactions. A detailed procedure for the preparation of ***2*-52f** is given however; stoichiometric amounts vary depending on amine/aniline used. To a 1 dram scintillation vial

equipped with a magnetic stir bar was added ***2*-49f** (222 mg, 2.0 mmol) followed by ***2*-29** (56 mg, 0.5 mmol). The vial was capped and with stirring mixture was heated to 150 ^{o}C using a silicone oil bath for 16 hours. Upon cooling, 1 mL of hot EtOH (or THF when necessary) was added and TLC analysis (50% EtOAc in hexanes) of the organic layer indicated formation of the less polar 1,4-diol (R_f = 0.6, major) and the more polar 1,3-diol (R_f = 0.3, trace). The contents of the vial were poured into a 100 mL round bottom flask. The vial was chased with 14 mL of EtOH and was collected into the flask. A small aliquot (ca. 1.5 mL) was added to a vial followed by removal and drying of the solvent *in vacuo* for ^{1}HNMR analysis to determine the ratio of 1,3- to 1,4-diol regioselectivity. Upon ^{1}HNMR analysis the analyte was recombined with the crude solution and was evaporated onto celite and purified via flash chromatography to give 124 mg (74%) of the 1,4-diol as a yellow solid (***2*-52f**). ^{1}H NMR (400 MHz, CD_3OD) δ 6.89 – 6.81 (m, 4H), 6.72 – 6.65 (m, 4H), 3.55 (ddd, *J* = 11.1, 9.2, 4.3, 2H), 3.19 (ddd, *J* = 11.5, 9.3, 4.0, 2H), 2.34 (dt, *J* = 13.0, 4.2, 2H), 1.31 (dt, *J* = 12.9, 11.3, 2H). 157.11 (d, $^{1}J_{CF}$ = 233.3 Hz), 146.16, 116.25 (d, $^{2}J_{CF}$ = 22.3 Hz), 115.87 (d, $^{3}J_{CF}$ = 7.3 Hz), 72.70, 58.79, 38.05. HRMS (ESI-TOF) calculated for $C_{18}H_{21}F_2N_2O_2$ (MH^+) 336.1597, found 336.1616 (5.7 ppm, 1.9 mmu)

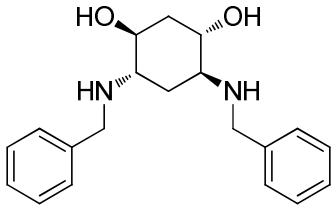

<u>4,6-bis(benzylamino)cyclohexane-1,3-diol</u> **(***rac*-***2*-51b)**. Two procedures were used to afford this compound. A) The "on water" procedure was followed using benzylamine ***2*-49b** (214 mg, 2.0 mmol) and ***2*-29** (112mg, 1.0 mmol). Evaporation onto celite followed by flash chromatography yielded 296 mg (91%) of an off white solid. ^{1}H NMR (400 MHz, CD_3OD) δ 7.35 – 7.21 (m,

10H), 3.76 (m, 6H), 2.80 (q, *J* = 5.7, 2H), 1.84 (dt, *J* = 21.8, 5.6, 4H). ^{13}C NMR (101 MHz, CD_3OD) δ 141.25, 129.65, 129.64, 128.28, 70.42, 58.30, 52.11, 37.14, 29.01. HRMS (ESI-TOF) calculated for $C_{20}H_{27}N_2O_2$ (MH^+) 327.2067, found. 327.2081 (+4.3 ppm, +1.4 mmu).

B) The neat procedure was followed using benzylamine ***2*-49b** (2.0 mmol, 214 mg) and ***2*-29** (1.0 mmol, 112 mg). Evaporation onto celite followed by flash chromatography yielded 309 mg (95%) of an off white solid. ^{1}H NMR indicated the product was pure *rac*-***2*-51b**.

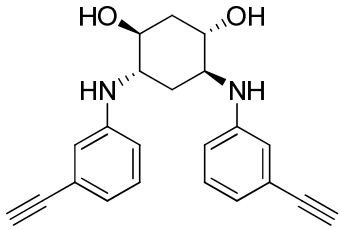

4,6-bis(3-ethynylphenylamino)cyclohexane-1,3-diol **(*rac*-*2*-51a, A10b)**. The "on water" procedure was followed using 3-ethynylaniline ***2*-49a** (468 mg, 4.0 mmol) and ***2*-29** (56 mg, 0.5 mmol). Evaporation onto celite followed by flash chromatography yielded 154 mg (44%) of an off white solid. ^{1}H NMR (500 MHz, CD_3OD) δ 7.06 – 6.99 (m, 2H), 6.84 – 6.80 (m, 2H), 6.74 – 6.65 (m, 4H), 3.89 (q, *J* = 5.7, 2H), 3.53 (q, *J* = 5.8, 2H), 3.29 (s, 2H), 1.93 (td, *J* = 5.6, 2.3, 4H). ^{13}C NMR (126 MHz, CD_3OD) δ 148.12, 128.75, 122.84, 120.14, 116.08, 113.62, 84.11, 75.79, 68.63, 53.47, 35.47, 30.13. HRMS (ESI-TOF) calculated for $C_{22}H_{23}N_2O_2$ (MH^+) 347.1754, found 347.1770 (+4.6 ppm, +1.6 mmu).

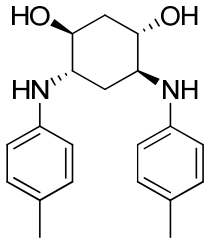

4,6-bis(p-tolylamino)cyclohexane-1,3-diol **(***rac*-***2*****-51c)**. The "on water" procedure was followed using *p*-toluidine **2c** (208 mg, 1.94 mmol) and ***2*****-29** (109 mg, 0.97 mmol). Evaporation onto celite followed by flash chromatography yielded 304 mg (96%) of an off white solid. ^{1}H NMR (400 MHz, CD_3OD) δ 6.89 (d, *J* = 8.0, 4H), 6.63 – 6.60 (m, 4H), 3.90 (q, *J* = 5.7, 2H), 3.48 (q, *J* = 5.8, 2H), 2.18 (s, 3H), 1.94 (dt, *J* = 11.4, 5.6, 4H). ^{13}C NMR (101 MHz, CD_3OD) δ 145.52, 129.05, 125.87, 113.87, 113.58, 68.57, 53.98, 35.36, 29.83, 19.06. HRMS (ESI-TOF) calculated for $C_{20}H_{27}N_2O_2$ (MH^+) 327.2067, found 327.2083 (+4.9 ppm, +1.6 mmu.)

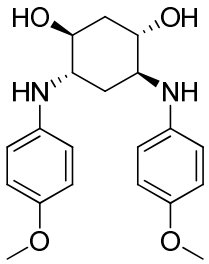

4,6-bis(4-methoxyphenylamino)cyclohexane-1,3-diol **(***rac*-***2*****-51d)**. The "on water" procedure was followed using *p*-anisidine ***2*****-49d** (123 mg, 1.0 mmol) and ***2*****-29** (56 mg, 0.5 mmol). Evaporation onto celite followed by flash chromatography yielded 161 mg (90%) of a pink solid. ^{1}H NMR (400 MHz, CD_3OD) δ 6.74 – 6.64 (m, 8H), 3.89 (q, *J* = 5.7, 2H), 3.70 (s, 3H), 3.42 (q, *J* = 5.7, 2H), 1.93 (dt, *J* = 18.4, 5.6, 4H). ^{13}C NMR (101 MHz, CD_3OD) δ 153.84, 143.37, 116.79, 115.89, 70.16, 56.36, 56.31, 36.95, 31.26. HRMS (ESI-TOF) calculated for $C_{20}H_{27}N_2O_4$ (MH^+) 359.1965, found 356.1977 (+3.3 ppm, +1.2 mmu).

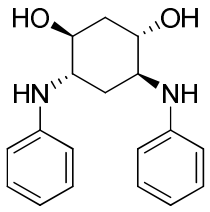

4,6-bis(phenylamino)cyclohexane-1,3-diol **(***rac*-***2*****-51e)**. The "on water" procedure was followed using aniline ***2*****-49e** (93 mg, 1.0 mmol) and ***2*****-29** (56 mg, 0.5 mmol). Evaporation onto celite followed by flash chromatography yielded 122 mg (82%) of an off white solid. ^{1}H NMR (500 MHz, CD_3OD) δ 7.08 – 7.04 (m, 4H), 6.71 – 6.69 (m, 4H), 6.59 (tt, *J* = 7.4, 1.1, 2H), 3.92 (q, *J* = 5.7, 2H), 3.54 (q, *J* = 5.7, 2H), 1.96 (dd, *J* = 12.2, 5.8, 4H). ^{13}C NMR (101 MHz, CD_3OD) δ 130.16, 118.11, 114.67, 70.15, 55.14, 31.68, 26.59. HRMS (ESI-TOF) calculated for $C_{18}H_{23}N_2O_2$ (MH^+) 299.1754, found. 299.1767 (+4.3 ppm, +1.3 mmu).

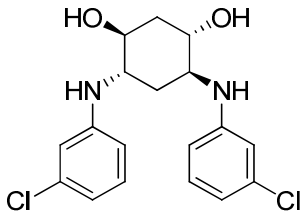

4,6-bis(3-chlorophenylamino)cyclohexane-1,3-diol **(***rac*-***2*****-51g)**. The "on water" procedure was followed using *m*-chloroaniline **2g** (508 mg, 4.0 mmol) and **1** (56 mg, 0.5 mmol). Evaporation onto celite followed by flash chromatography yielded 32 mg (18%) of an off white solid. ^{1}H NMR (500 MHz, CD_3OD) δ 7.01 (t, *J* = 8.1, 2H), 6.72 (t, *J* = 2.1, 2H), 6.64 – 6.56 (m, 2H), 6.53 (ddd, *J* = 7.8, 1.8, 0.7, 2H), 3.90 (q, *J* = 5.7, 2H), 3.52 (q, *J* = 5.8, 2H), 1.94 (td, *J* = 5.6, 3.1, 4H). ^{13}C NMR (101 MHz, CD_3OD) δ 149.24, 134.17, 129.42, 115.46, 111.90, 110.70, 68.15, 53.01, 35.14, 29.59. HRMS (ESI-TOF) calculated for $C_{18}H_{21}Cl_2N_2O_2$ (MH^+) 367.0975, found 367.0987 (+3.3 ppm, +1.2 mmu).

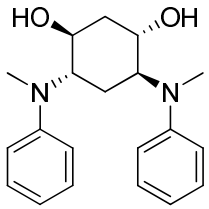

4,6-bis(methyl(phenyl)amino)cyclohexane-1,3-diol **(***rac*-***2***-**51h)**. The "on water" procedure was followed using *N*-methylaniline ***2***-**49h** (134 mg, 1.25 mmol) and ***2***-**29** (56 mg, 0.5 mmol). Evaporation onto celite followed by flash chromatography yielded 158 mg (97%) of a brown powder. ^{1}H NMR (500 MHz, CD_3OD) δ 7.22 – 7.13 (m, 4H), 6.95 (d, *J* = 7.9 Hz, 4Hz), 6.80 (t, *J* = 7.3 Hz, 2Hz), 4.06 (q, *J* = 5.8 Hz, 2Hz), 3.65 (q, *J* = 5.8 Hz, 2H), 2.71 (s, 6), 1.95 (t, *J* = 5.6 Hz, 2Hz), 1.88 (t, *J* = 5.6 Hz, 2H). ^{13}C NMR (126 MHz, CD_3OD) δ 153.42, 130.13, 121.38, 120.15, 67.82, 62.05, 37.16, 37.08, 25.72. HRMS (ESI-TOF) calculated for $C_{20}H_{27}N_2O_2$ (MH^+) 327.2067, found. 327.2086 (+5.8 ppm, +1.9 mmu)

4,6-bis(methyl(phenyl)amino)cyclohexane-1,3-diol **(***rac*-***2***-**51h)**. The neat procedure was followed using ***2***-**49h** (1.96 mmol, 213 μL) and ***2***-**29** (0.49 mmol, 109 mg). Evaporation onto celite followed by flash chromatography yielded 145 mg (91%) of a brown powder. ^{1}H NMR indicated the product was pure *rac*-***2***-**51h**.

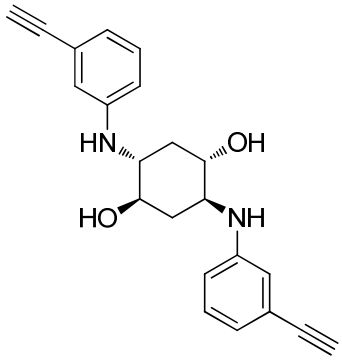

2,5-bis(3-ethynylphenylamino)cyclohexane-1,4-diol **(*2*-52a)**. The neat procedure was followed using 3-ethynylaniline ***2*-49a** (468 mg, 4.0 mmol) and ***2*-29** (56 mg, 0.5 mmol). Evaporation onto celite followed by flash chromatography yielded 49 mg (28%) of a brown powder. ^{1}H NMR (500 MHz, CD_3OD) δ 7.06 (t, *J* = 7.9, 2H), 6.80 – 6.78 (m, 2H), 6.73 – 6.69 (m, 4H), 3.58 (ddd, *J* = 11.0, 9.2, 4.2, 2H), 3.34 (s, 2H), 3.30 – 3.23 (m, 2H), 2.34 (dt, *J* = 13.0, 4.2, 2H), 1.34 (dt, *J* = 12.9, 11.3, 2H). ^{13}C NMR (126 MHz, CD_3OD) δ 148.60, 128.88, 122.74, 120.32, 116.12, 113.84, 84.12, 75.88, 71.39, 56.42, 41.97, 36.44. HRMS (ESI-TOF) calculated for $C_{22}H_{23}N_2O_2$ (MH^+) 347.1754, found 347.1775 (+6.0 ppm, +2.1 mmu).

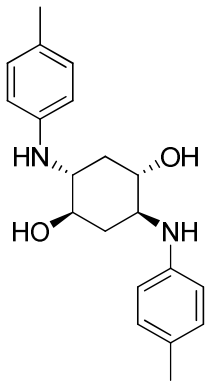

2,5-bis(p-tolylamino)cyclohexane-1,4-diol **(*2*-52c)**. The neat procedure was followed using *p*-toluidine ***2*-49c** (114 mg, 1.0 mmol) and ***2*-29** (112 mg, 1 mmol). Evaporation onto celite followed by flash chromatography yielded 137 mg (42%) of a brown powder. ^{1}H NMR (500

MHz, CD_3OD) δ 6.93 (d, *J* = 8.1, 4H), 6.66 – 6.57 (m, 4H), 3.54 (ddd, *J* = 10.9, 8.9, 3.8, 2H), 3.20 (ddd, *J* = 11.5, 9.3, 4.0, 2H), 2.35 (dt, *J* = 13.0, 4.1, 2H), 2.19 (s, 6H), 1.29 – 1.27 (m, 2H). ^{13}C NMR (101 MHz, d_6-DMSO) δ 146.40, 146.37, 129.23, 123.73, 123.69, 112.64, 70.44, 56.40, 37.42, 20.08. HRMS (ESI-TOF) calculated for $C_{20}H_{27}N_2O_2$ (MH^+) 327.2067, found. 327.2074 (+2.1 ppm, +0.7 mmu).

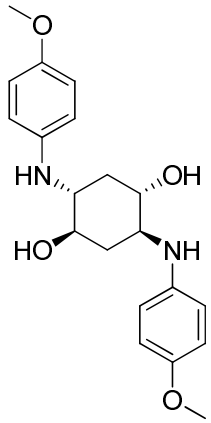

2,5-bis(4-methoxyphenylamino)cyclohexane-1,4-diol **(*2*-52d)**. The neat procedure was followed using *p*-anisidine ***2*-49d** (247 mg, 2.0 mmol) and ***2*-29** (112 mg, 1.0 mmol). Evaporation onto celite followed by flash chromatography yielded 92 mg (51%) of a brown powder. ^1H NMR (400 MHz, CD_3OD) δ 6.76 – 6.66 (m, 8H), 3.69 (s, 6H), 3.50 (ddd, *J* = 11.1, 9.3, 4.3, 2H), 3.10 (ddd, *J* = 11.4, 9.2, 4.0, 2H), 2.32 (dt, *J* = 13.0, 4.2, 2H), 1.32 – 1.22 (m, 2H). ^{13}C NMR (101 MHz, d_6-DMSO) δ 150.59, 142.89, 114.53, 113.81, 70.59, 57.17, 55.34, 37.56. (ESI-TOF) calculated for $C_{20}H_{27}N_2O_4$ (MH^+) 359.1965, found. 359.1965 (0 ppm, 0 mmu).

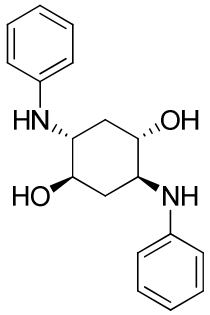

2,5-bis(phenylamino)cyclohexane-1,4-diol **(*2*-52e)**. The neat procedure was followed using aniline ***2*-49e** (187 mg, 2.0 mmol) and ***2*-29** (56 mg, 0.5 mmol). Evaporation onto celite followed by flash chromatography yielded 66 mg (45%) of a brown powder. ^{1}H NMR (500 MHz, CD_3OD) δ 7.11 – 7.07 (m, 4H), 6.70 – 6.67 (m, 4H), 6.61 – 6.58 (m, 2H), 3.57 (ddd, *J* = 11.0, 9.2, 4.2 Hz, 2H), 3.28 – 3.24 (m, 2H), 2.36 (dt, *J* = 13.1, 4.1 Hz, 2H), 1.31 (dt, *J* = 13.0, 11.2 Hz, 2H). ^{13}C NMR (126 MHz, CD_3OD) δ 148.44, 128.73, 116.85, 113.40, 71.30, 56.67, 36.68, 32.94. HRMS (ESI-TOF) calculated for $C_{18}H_{23}N_2O_2$ (MH^+) 299.1754, found. 299.1773 (+6.4 ppm, +1.9 mmu)**.**

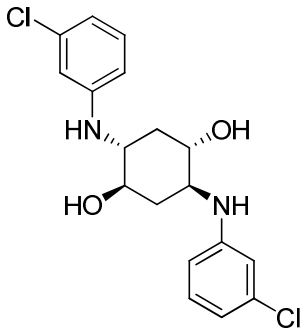

2,5-bis(3-chlorophenylamino)cyclohexane-1,4-diol **(*2*-52g)**. The "on water" procedure was followed using 3-chloroaniline ***2*-49g** (471 mg, 4.0 mmol) and ***2*-29** (56 mg, 0.5 mmol). Evaporation onto celite followed by flash chromatography yielded 103 mg (44%) of an off white solid. ^{1}H NMR (400 MHz, CD_3OD) δ 7.04 (t, *J* = 8.0, 2H), 6.68 (t, *J* = 2.1, 2H), 6.59 (dd, *J* =

8.6, 1.9, 2H), 6.55 (dd, *J* = 8.2, 1.6, 2H), 3.58 (ddd, *J* = 11.0, 9.2, 4.3, 2H), 3.29 – 3.21 (m, 2H), 2.32 (dt, *J* = 13.1, 4.2, 2H), 1.35 (dt, *J* = 13.0, 11.3, 2H). ^{13}C NMR (101 MHz, CD_3OD) δ 149.87, 134.23, 129.87, 115.74, 112.33, 111.36, 70.96, 56.08, 36.56. . HRMS (ESI-TOF) calculated for $C_{18}H_{21}Cl_2N_2O_2$ (MH^+) 367.0975, found 367.0984 (+2.5 ppm, +0.9 mmu).

2,5-bis(3-chlorophenylamino)cyclohexane-1,4-diol **(*2*-52g)**. The neat procedure was followed using 3-chloroaniline ***2*-49g** (510 mg, 4.0 mmol) and ***2*-29** (56 mg, 0.5 mmol). Evaporation onto celite followed by flash chromatography yielded 156 mg (84%) of an off white powder. ^{1}H-NMR indicated the product was pure ***2*-52g**.

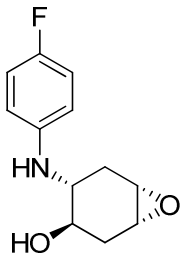

4-(4-fluorophenylamino)-7-oxabicyclo[4.1.0]heptan-3-ol **(*rac*-*2*-50f)**. Based on a procedure by Scheunemann,[93] a Schlenck flask was equipped with a stir bar and charged with ***2*-29** (448 mg, 4.0 mmol), *i*-PrOH (5 mL), and p-fluoroaniline ***2*-49f** (96 μL, 1.0 mmol). The flask was backfilled and purged with N_2 and then heated to 80 ^{o}C for 16 hours. In the morning the solution was allowed to cool and TLC (50% EtOAc in hexanes) analysis indicated formation of the less polar 1,4-diol (R_f = 0.6) which was the desired epoxyaminoalcohol product *rac*-***2*-50f** (Rf = 0.5), and the more polar 1,3-diol (R_f = 0.3). Evaporation of the *i*-PrOH solvent followed by purification of the residue by column chromatography afforded 152 mg (68%) of a colorless oil. ^{1}H NMR (500 MHz, CD_3OD) δ 6.88 – 6.81 (m, 2H), 6.67 – 6.61 (m, 2H), 3.68 (td, *J* = 6.9, 4.9, 1H), 3.23 (dt, *J* = 19.0, 3.8, 2H), 2.51 (ddd, *J* = 15.6, 6.2, 3.8, 1H), 2.39 (dd, *J* = 15.5, 4.8, 1H),

1.91 (ddd, *J* = 15.5, 6.6, 3.3, 1H), 1.83 (dd, *J* = 15.6, 6.8, 1H). ^{13}C NMR (126 MHz, CD_3OD) δ 157.28 (d, $^1J_{CF}$ = 233.5 Hz), 146.01, 116.47 (d, $^3J_{CF}$ = 22.5 Hz), 115.86 (d, $^2J_{CF}$ = 7.4 Hz), 116.56, 116.38, 115.89, 115.83, 67.24, 54.94, 53.26, 53.19, 32.27, 29.26. HRMS (ESI-TOF) calculated for $C_{12}H_{15}FNO_2$ (MH^+) 224.1081, found 224.1082 (+0.4 ppm, +0.1 mmu).

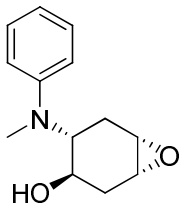

4-(methyl(phenyl)amino)-7-oxabicyclo[4.1.0]heptan-3-ol **(*rac*-*2*-50h)**. The same procedure was used for the synthesis of *rac*-***2*-50f** using ***2*-29** (448 mg, 4.0 mmol), *i*-PrOH (5 mL), and *N*-methylaniline ***2*-49f** (108 μL, 1.0 mmol) save for the reaction time, which was extended to 48 hours. Evaporation of the *i*-PrOH solvent followed by purification of the residue yielded 92 mg (42%) of a yellow oil. ^{1}H NMR (400 MHz, CD_3OD) δ 7.16 (dd, *J* = 8.9, 7.2 Hz, 2H), 6.85 (d, *J* = 8.0 Hz, 2H), 6.65 (t, *J* = 7.3 Hz, 1H), 3.85 (td, *J* = 10.2, 5.0 Hz, 1H), 3.68 (td, *J* = 10.7, 7.1 Hz, 1H), 3.29 – 3.22 (m, 1H), 3.15 (t, *J* = 4.4 Hz, 1H), 2.74 (s, 3H), 2.58 (ddd, *J* = 14.4, 5.1, 2.4 Hz, 1H), 2.19 (ddd, *J* = 15.7, 7.1, 5.0 Hz, 1H), 1.99 (dd, *J* = 15.7, 11.0 Hz, 1H), 1.84 (ddd, *J* = 14.4, 10.1, 1.6 Hz, 1H). ^{13}C NMR (101 MHz, CD_3OD) δ 152.47, 130.08, 118.15, 115.02, 66.23, 61.55, 55.41, 53.03, 35.38, 31.25, 26.95. HRMS (ESI-TOF) calculated for $C_{13}H_{18}NO_2$ (MH^+) 220.1332, found 220.1338 (+2.7 ppm, +0.6 mmu).

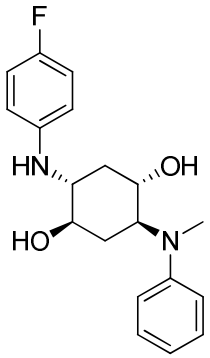

2-(4-fluorophenylamino)-5-(methyl(phenyl)amino)cyclohexane-1,4-diol **(*rac*-*2*-52fh)**. The neat procedure was followed using ***2*-49h** (252 μL, 2.23 mmol) and *rac*-***2*-50f** (260 mg, 1.16 mmol). Evaporation onto celite followed by flash chromatography yielded 360 mg (94%) of a yellow oil. ^{1}H NMR (500 MHz, CD_3OD) δ 7.21 – 7.13 (m, 3H), 7.13 – 7.05 (m, 1H), 6.92 – 6.80 (m, 6H), 6.73 – 6.55 (m, 6H), 3.87 (td, *J* = 10.4, 4.4, 1H), 3.65 – 3.58 (m, 1H), 3.53 (ddd, *J* = 11.0, 9.6, 4.5, 1H), 3.15 (ddd, *J* = 12.0, 9.6, 4.0, 1H), 2.78 (d, *J* = 35.0, 6H), 2.37 (dt, *J* = 12.8, 4.2, 1H), 1.94 (dt, *J* = 12.7, 4.1, 1H), 1.63 (dd, *J* = 23.8, 12.5, 1H), 1.27 (dd, *J* = 24.2, 11.6, 1H). ^{13}C NMR (126 MHz, CD_3OD) δ 155.82 (d, $^{1}J_{CF}$ = 233.5 Hz), 151.16, 144.94 (d, $^{4}J_{CF}$ = 1.9 Hz), 128.62, 117.10, 114.94 (d, $^{2}J_{CF}$ = 22.3 Hz), 114.58 (d, $^{3}J_{CF}$ = 7.3 Hz), 114.20, 72.11, 67.72, 62.63, 57.51, 37.13, 32.69, 30.01. HRMS (ESI-TOF) calculated for $C_{19}H_{24}FN_2O_2$ (MH^+) 331.1816, found 331.1825 (+2.7 ppm, +0.9 mmu).

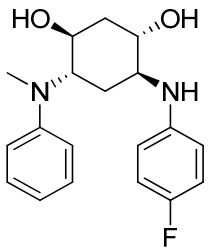

4-(4-fluorophenylamino)-6-(methyl(phenyl)amino)cyclohexane-1,3-diol **(*rac*-*2*-51fh)**. The neat procedure was followed using ***2*-49f** (46 μL, 0.48 mmol) and *rac*-***2*-50h** (53 mg, 0.24 mmol).

Evaporation onto celite followed by flash chromatography yielded 74 mg (93%) of a yellow oil. ^{1}H NMR (400 MHz, CD_3OD) δ 7.09 (dt, *J* = 7.3, 5.0, 2H), 6.90 – 6.78 (m, 4H), 6.71 – 6.65 (m, 2H), 6.61 (t, *J* = 7.3, 1H), 4.15 (dt, *J* = 10.9, 4.7, 1H), 3.98 (s, 1H), 3.95 – 3.81 (m, 1H), 3.56 (s, 1H), 2.82 (s, 3H), 2.09 (ddd, *J* = 16.5, 8.9, 4.0, 2H), 1.88 (ddd, *J* = 13.8, 11.1, 2.8, 1H), 1.73 (d, *J* = 13.5, 1H). ^{13}C NMR 157.15 (d, $^{1}J_{CF}$ = 233.2 Hz), 152.58, 145.60 (d, $^{4}J_{CF}$ = 1.9 Hz), 130.16, 129.94, 118.06, 116.44, 116.43 (d, $^{2}J_{CF}$ = 22.3 Hz), 116.22, 115.54 (d, $^{3}J_{CF}$ = 7.3 Hz), 115.33, 114.65, 69.79, 66.78, 60.78, 55.69, 37.26, 31.62, 27.05, 21.24. HRMS (ESI-TOF) calculated for $C_{19}H_{24}FN_2O_2$ (MH^+) 331.1816, found 331.1823 (+2.1 ppm, +0.7 mmu).

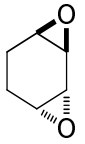

<u>*trans*-1,2;3,4-diepoxycyclohexane</u> **(*rac*-*2*-54)**.[111] To a solution of of 1,3-cyclohexadiene (800 mg, 10 mmol) in CH_2Cl_2 (250 mL) was added *m*-CPBA (50%, 7.7 g, 22 mmol) at 0 ^{o}C in 5 portions. The suspension was allowed to warm to room temperature overnight. In the morning 10 mL of a 3 M NaOH solution was added. The contents were then poured into a separatory funnel and was extracted with CH_2Cl_2 (3 x 30 mL). The combined organics were dried over Na_2SO_4 and evaporated to a give colorless oil. The oil was purified by silica gel flash chromatography (35% EtOAc in hexanes) and visualized by PMA stain. 504 mg (45%) of colorless oil was obtained. The oil was analyzed by NMR and the spectral data were found to be consistent with the literature values.[111] ^{1}H NMR (400 MHz, $CDCl_3$) δ 3.34 (dd, *J* = 3.5, 1.6 Hz, 2H), 3.18 – 3.14 (m, 2H), 1.90 (s, 4H). ^{13}C NMR (101 MHz, $CDCl_3$) δ 53.24, 50.20, 19.12.

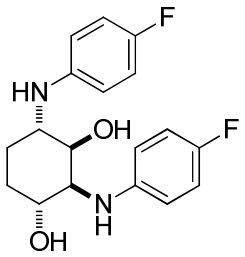

2,4-bis((4-fluorophenyl)amino)cyclohexane-1,3-diol **(*rac*-*2*-58f)**. To a 1 dram scintillation vial equipped with a magnetic stir bar was added ***2*-49f** (198 uL, 2.05 mmol), *rac*-***2*-54** (56 mg, 0.5 mmol), and HPLC grade water (1 mL). The suspension was stirred vigorously and heated to 95 ^{o}C for 16 hours. Upon cooling, a solid formed and 1 mL of EtOAc was added. TLC analysis (75% EtOAc in hexanes) of the organic layer indicated formation of the less polar 1,3-diol (R_f = 0.6) and the more polar 1,2-diol (R_f = 0.3). The contents of the vial were poured into a separatory funnel. The vial was chased with 4 mL of EtOAc and the organic layer was collected. The aqueous layer was extracted with EtOAc (2 x 5 mL) followed by drying over $MgSO_4$. A small aliquot (ca. 1.5 mL) was added to a vial followed by removal and drying of the solvent *in vacuo* for ^{1}H-NMR analysis to determine the ratio of 1,3- to 1,2-diol regioselectivity. Upon ^{1}H-NMR analysis the analyte was recombined with the crude solution and was evaporated onto celite and purified via flash chromatography (75% EtOAc in hexanes) to give 82 mg (50%) of the 1,3-diol as a brown solid. ^{1}H NMR (400 MHz, CD_3OD) δ 6.89 – 6.82 (m, 2H), 6.81 – 6.73 (m, 2H), 6.73 – 6.67 (m, 2H), 6.66 – 6.59 (m, 2H), 4.07 – 4.01 (m, 1H), 3.83 (td, *J* = 8.7, 4.2 Hz, 1H), 3.57 – 3.47 (m, 2H), 2.09 – 1.99 (m, 1H), 1.94 – 1.84 (m, 1H), 1.77 – 1.61 (m, 2H). ^{13}C NMR (101 MHz, CD_3OD) δ 157.03 (d, $^{1}J_{CF}$ = 233.2 Hz), 156.99 (d, $^{1}J_{CF}$ = 233.1 Hz), 146.21 (d, $^{4}J_{CF}$ = 1.9 Hz), 145.85 (d, $^{4}J_{CF}$ = 1.9 Hz), 116.32 (d, $^{2}J_{CF}$ = 14.6 Hz), 116.09 (d, $^{2}J_{CF}$ = 14.6 Hz), 115.72 (d, $^{3}J_{CF}$ = 7.3 Hz), 115.39 (d, $^{3}J_{CF}$ = 7.3 Hz), 70.05, 69.60, 60.12, 55.34, 28.98, 24.96.

HRMS (ESI-TOF) calculated for $C_{18}H_{20}F_2N_2O_2$ (M^+) 334.1487, found 334.175 (-3.6 ppm, -1.2 mmu).

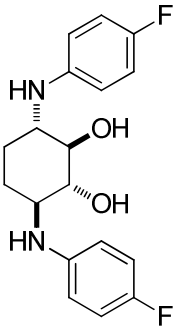

3,6-bis((4-fluorophenyl)amino)cyclohexane-1,2-diol **(*rac*-*2*-57f)**. During the chromatographic separation described above 50mg (30%) of the 1,2-diol was collected as a brown solid. ^{1}H NMR (400 MHz, CD_3OD) δ 6.87 – 6.80 (m, 4H), 6.72 – 6.64 (m, 4H), 3.40 – 3.32 (m, 2H), 3.20 – 3.10 (m, 2H), 2.12 – 1.99 (m, 2H), 1.24 – 1.16 (m, 2H). ^{13}C NMR (101 MHz, CD_3OD) δ 157.12 (d, $^1J_{CF}$ = 233.3 Hz), 146.27 (d, $^4J_{CF}$ = 1.8 Hz), 116.21 (d, $^3J_{CF}$ = 22.4 Hz), 115.94 (d, $^2J_{CF}$ = 7.4 Hz), 78.53, 58.96, 28.97. HRMS (ESI-TOF) calculated for $C_{18}H_{20}F_2N_2O_2$ (M^+) 334.1487, found 334.1499 (+3.6 ppm, +1.2 mmu).

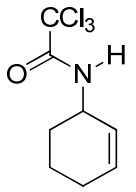

2,2,2-trichloro-*N*-(cyclohex-2-en-1-yl)acetamide **(*rac*-*3*-13h)**.[123] To an oven dried air-free Schlenk flask under N_2 was added dry CH_2Cl_2 (25 mL), 2-cyclohexen-1-ol (*rac*-***3*-1**, 0.5 mL, 5.0 mmol), and DBU (1.1 mL, 7.5 mmol). The solution was cooled to -20 ^{o}C followed by addition of Cl_3CCN (0.9 mL, 9.0 mmol) via syringe. The solution was allowed to stir for 1 hour at -20 ^{o}C. The reaction was then quenched at -20 ^{o}C by addition of 10 mL of a saturated NH_4Cl

solution. The cooling bath was removed and solution was allowed to warm to room temperature over a period of 15 minutes. The contents were then poured into a separatory funnel and extracted with CH_2Cl_2 (2 x 20 mL), dried over Na_2SO_4, and concentrated. The residue was passed through a column containing anhydrous Na_2SO_4 and a thin layer of anhydrous K_2CO_3 eluting with a 35% EtOAc in hexanes solution. The washings were concentrated and the crude imidate was taken up in 50 mL of xylenes. To this solution was added approximately 300 mg of anhydrous K_2CO_3. The suspension was heated to reflux with vigorous stirring under N_2 for 16 hours. The black solution was cooled and filtered thru a pad of celite. The filtrate was evaporated and purified via silica gel flash chromatography (10% EtOAc in hexanes) to give 1.04 g (86%) of a white solid. The solid was analyzed by NMR and the spectral data were found to be consistent with the literature values.[122] ^{1}H NMR (400 MHz, $CDCl_3$) δ 6.57 (s, 1H), 6.00 – 5.94 (m, 1H), 5.67 – 5.61 (m, 1H), 4.45 (s, 1H), 2.10 – 2.03 (m, 2H), 2.02 – 1.93 (m, 1H), 1.73 – 1.61 (m, 3H).

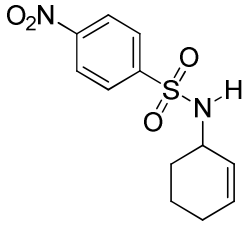

N-(cyclohex-2-en-1-yl)-4-nitrobenzenesulfonamide **(*rac*-*3*-13d)**. To an air-free Schlenk flask under N_2 was added 3-bromocyclohexene (805 mg, 5.0 mmol) in THF (10 mL). To this was added a solution of sodium azide (975 mg, 15.0 mmol) in water (2 mL). The flask was sealed and heated to 50 ^{o}C for 16 hours. After cooling, 15 mL of Et_2O was added and the contents of the flask were poured into a separatory funnel. The aqueous layer was extracted with Et_2O (2 x 15 mL), dried over $MgSO_4$, and filtered into a dry 2 neck round bottom flask equipped with a N_2

inlet and stir bar. $LiAlH_4$ (950 mg, 15 mmol) was added carefully and the suspension was heated to 35 ^oC for 48 hours (adding dry Et_2O as needed). After cooling a typical Fieser workup was preformed (950 uL water, 950 uL 15% aqueous KOH, 3 mL 0.29 mL water) and the white solids were filtered. The filtrate was treated with triethylamine (2.1 mL, 15 mmol) and cooled to 0 ^oC. With stirring was added *p*-nitrobenzenesulfonyl chloride (1.33 g, 6 mmol) and the solution was allowed to warm to room temperature overnight. In the morning, the solution was concentrated and the residue was purified via silica gel flash chromatography to give 800 mg (57%) of a solid. The solid was analyzed by NMR and the spectral data were found to be consistent with the literature values.[122] ^1H NMR (400 MHz, $CDCl_3$) δ 8.44 – 8.33 (m, 2H), 8.18 – 8.04 (m, 2H), 5.85 – 5.78 (m, 1H), 5.39 – 5.31 (m, 1H), 4.76 (d, *J* = 8.7 Hz, 1H), 3.96 – 3.86 (m, 1H), 2.05 – 1.92 (m, 2H), 2.05 – 1.92 (m, 2H), 1.85 – 1.74 (m, 1H), 1.66 – 1.48 (m, 3H).

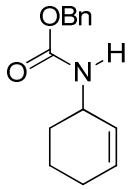

benzyl cyclohex-2-en-1-yl carbamate **(***rac*-***3*****-13f)**. The procedure to synthesize ***3*****-31d** was followed using benzylchloroformate (1 mL, 7 mmol) to trap the amine. The residue was purified via silica gel flash chromatography to give 647 mg (56%) of a solid. The solid was analyzed by NMR and the spectral data were found to be consistent with the literature values.[122] ^1H-NMR (400 MHz, $CDCl_3$) δ 7.36 (m, 5H), 5.86 – 5.00 (m, 1H), 5.39 – 5.31 (m, 1H), 5.64 – 5.58 (m, 1H), 5.10 (s, 2H), 4.75 (d, *J* = 7.9 Hz, 1H), 4.23 (s, 1H), 2.02 – 1.96 (m, 1H), 1.94 – 1.86 (m, 1H), 1.67 – 1.60 (m, 2H), 1.56 – 1.50 (m, 1H).

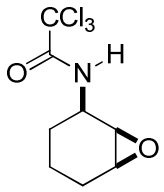

cis-*N*-(7-oxabicyclo[4.1.0]heptan-2-yl)-2,2,2-trichloroacetamide **(*rac*-*3*-14h)**.[122] To a solution of ***rac*-*3*-13h** (121 mg, 0.5 mmol) in CH_2Cl_2 (10 mL) under a blanket of N_2 was added *m*-CPBA (50%, 345 mg, 1.0 mmol) and $NaHCO_3$ (84 mg, 1.0 mmol). The suspension was stirred at room temperature for 16 hours. In the morning, the contents were poured in a flask containing 10 mL of Na_2SO_3 and 10 mL of $NaHCO_3$. The biphasic solution was stirred vigorously for 10 minutes before pouring into a separatory funnel where the aqueous layer was extracted with CH_2Cl_2 (2 x 15 mL) and dried over Na_2SO_4. The filtrate was concentrated to give a pale yellow solid (132 mg, quantitative). The crude solid was analyzed by ^{1}H-NMR found to be consistent with a 95:5 cis:trans diastereomeric ratio which is also seen in the work of O'Brien.[122]

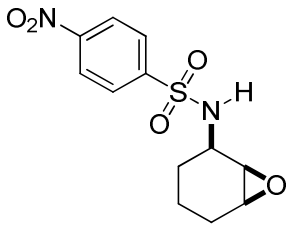

cis-*N*-(7-oxabicyclo[4.1.0]heptan-2-yl)-4-nitrobenzenesulfonamide **(*rac*-*3*-14d)**.

The epoxidation was carried out using the procedure described for ***rac*-*3*-14dh** using ***rac*-*3*-13d** (565 mg, 2.0 mmol), *m*-CPBA (50%, 1.38 mg, 4.0 mmol), and $NaHCO_3$ (336 mg, 4.0 mmol). The suspension was stirred at room temperature for 16 hours. In the morning, the contents were poured in a flask containing 20 mL of Na_2SO_3 and 20 mL of $NaHCO_3$. The biphasic solution was stirred vigorously for 10 minutes before pouring into a separatory funnel were the aqueous

layer was extracted with CH_2Cl_2 (2 x 30 mL) and dried over Na_2SO_4. The filtrate was concentrated to give 567 mg of a pale yellow solid (95%). The crude solid was analyzed by ^{1}H-NMR found to be consistent with a 95:5 cis:trans diastereomeric ratio which is also seen in the work of O'Brien.[122]

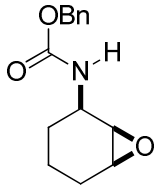

cis-benzyl-7-oxabicyclo[4.1.0]heptan-2-ylcarbamate **(*rac*-*3*-14f)**. The epoxidation was carried out using the procedure described for ***rac*-*3*-14dh** using ***rac*-*3*-13f** (565 mg, 2.0 mmol), *m*-CPBA (50%, 1.38 mg, 4.0 mmol), and $NaHCO_3$ (336 mg, 4.0 mmol). The suspension was stirred at room temperature for 16 hours. In the morning, the contents were poured in a flask containing 20 mL of Na_2SO_3 and 20 mL of $NaHCO_3$. The biphasic solution was stirred vigorously for 10 minutes before pouring into a separatory funnel were the aqueous layer was extracted with CH_2Cl_2 (2 x 30 mL) and dried over Na_2SO_4. The filtrate was concentrated to give a pale yellow solid (245 mg, quantitative). The crude solid was analyzed by ^{1}H-NMR found to be consistent with a 90:10 cis:trans diastereomeric ratio which is also seen in the work of O'Brien.[122]

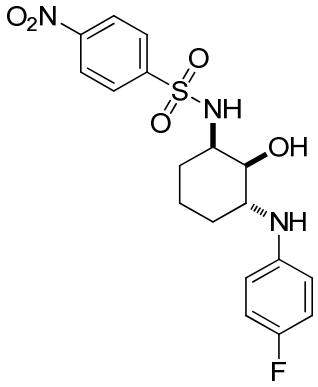

N-3-((4-fluorophenyl)amino)-2-hydroxycyclohexyl)-4-nitrobenzenesulfonamide **(*rac*-*3*-32c)**. To a 1 dram scintillation vial equipped with a magnetic stir bar was added *p*-fluoroaniline (***2*-49f**, 21 uL, 0.21 mmol), *rac*-***3*-14d** (60 mg, 0.2 mmol), and HPLC grade water (0.5 mL). The suspension was stirred vigorously and heated to 95 ^{o}C for 16 hours. Upon cooling, a solid formed and 1 mL of EtOAc was added. TLC analysis (50% EtOAc in hexanes) of the organic layer indicated formation of a single product. The vial was chased with 4 mL of EtOAc and the organic layer was collected. The aqueous layer was extracted with EtOAc (2 x 5 mL) followed by drying over $MgSO_4$. The solution was filtered and evaporated onto celite and purified via flash chromatography (50% EtOAc in hexanes) to give 45 mg (55%) of a brown solid (mp = 173.4 ^{o}C). ^{1}H NMR (400 MHz, CD_3OD) δ 8.13 (d, *J* = 8.4 Hz, 2H), 7.96 (d, *J* = 8.4 Hz, 2H), 6.76 (t, *J* = 8.5 Hz, 2H), 6.49 (dd, *J* = 8.7, 4.4 Hz, 2H), 3.52 (dt, *J* = 5.9, 3.2 Hz, 1H), 3.39 – 3.26 (m, 4H), 1.96 – 1.84 (m, 1H), 1.95 – 1.83 (m, 1H), 1.80 – 1.31 (m, 6H), 1.80 – 1.27 (m, 6H). ^{13}C NMR (101 MHz, CD_3OD) δ 156.85 (d, $^{1}J_{CF}$ = 233.5 Hz), 151.03, 148.76, 145.18, 129.23, 125.12, 116.25 (d, $^{2}J_{CF}$ = 22.3 Hz), 114.96 (d, $^{3}J_{CF}$ = 7.2 Hz), 69.83, 55.16, 53.97, 28.84, 26.28, 20.60. HRMS (ESI-TOF) calculated for $C_{18}H_{20}FN_3O_5S$ (M+) 409.1102, found 409.1117 (+3.7 ppm, +1.5 mmu).

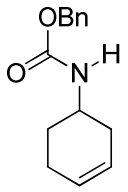

benzyl cyclohex-3-en-1-ylcarbamate **(*rac*-*3*-40h)**. The following preparation is a modified procedure by Overman et al.[144] In a 2 necked 100 mL round bottom flask under N_2 was added 3-cyclohexene-1-carboxylic acid (*rac*-***3*-47**, 1.0 g, 7.93 mmol) and 2 mL of water followed by 4 mL acetone. The solution was cooled to 0 ^oC followed by the addition of a solution of triethylamine (1.3 mL, 9.22 mmol) in acetone (16 mL). This was followed by addition of a solution of ethyl chloroformate (0.97 mL) in acetone (4 mL). The mixture was allowed to stir at 0 ^oC for 30 minutes. A chilled solution of sodium azide (780 mg, 12 mmol) in water (3 mL) was added via pipette and the mixture was allowed to stir for an additional 30 minutes. Toluene (10 mL) was then added followed by 15 mL of water. Contents were poured into a separatory funnel and extracted with toluene (3 x 10 mL). The combined organic extracts were dried over $MgSO_4$. Following filtration, benzyl alcohol (1.24 mL, 12 mmol) was added to the filtrate. This solution was placed on a rotary evaporator. Approximately 10 mL of toluene was removed while keeping bath temperature below 40 ^oC (azeotropic removal of water). After evaporation, the flask was equipped with a stir bar and reflux condenser and heated to 120 ^oC for 5 hours. After cooling, the solution was concentrated and the residue was purified via silica gel flash chromatography (30% EtOAc in hexanes) to give a yellow oil that solidified upon standing. Recovered 1.38 g (75%). The solid was analyzed by NMR and the spectral data were found to be consistent with the literature values.[140] ^1H NMR (400 MHz, $CDCl_3$) δ 7.43 – 7.29 (m, 5H), 5.68 (d, J = 10.0 Hz, 1H), 5.59 (d, J = 10.0 Hz, 1H), 5.10 (s, 2H), 4.80 (s, 1H), 3.87 (s, 1H), 2.40 (d, J = 17.1 Hz, 1H),

2.13 (m, 2H), 1.94 – 1.85 (m, 2H), 1.63 – 1.51 (m, 1H). ^{13}C NMR (101 MHz, $CDCl_3$) δ 155.84, 136.72, 128.66, 128.30, 128.24, 127.13, 124.41, 66.68, 46.26, 32.05, 28.34, 23.53.

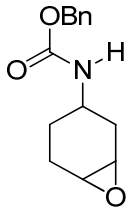

benzyl 7-oxabicyclo[4.1.0]heptan-3-ylcarbamate **(*rac*-*3*-41h)**.[140] The epoxidation procedure used to synthesize ***3*-32c** was followed using *rac*-***3*-40h** (463 mg, 2.0 mmol), *m*-CPBA (50%, 1.38 g, 4.0 mmol) and $NaHCO_3$ (336 g, 4.0 mmol) in CH_2Cl_2 (40 mL) to give 495 mg (quantitative) of an inseparable mixture of stereoisomers. The crude solid was analyzed by ^{1}H-NMR, consistent with a 3:1 cis:trans diastereomeric ratio which is also seen in the work of Marco-Contelles group.[140]

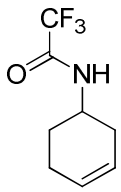

N-(cyclohex-3-en-1-yl)-2,2,2-trifluoroacetamide **(*rac*-*3*-40n)**.[141,142] In a 2 necked 100 mL round bottom flask under N_2 was added 3-cyclohexene-1-carboxylic acid (*rac*-***3*-47**, 1.0g, 7.93 mmol) and 2 mL of water followed by 4 mL acetone. The solution was cooled to 0 ^{o}C followed by the addition of a solution of triethylamine (1.3 mL, 9.22 mmol) in acetone (16 mL). This was followed by addition of a solution of ethyl chloroformate (0.97 mL) in acetone (4 mL). Mixture was allowed to stir at 0 ^{o}C for 30 minutes. A chilled solution of sodium azide (780 mg, 12 mmol) in water (3 mL) was added via pipette and the mixture was allowed to stir for an additional 30 minutes. Toluene (10 mL) was then added followed by 15 mL of water. The

contents of the flask were poured into a separatory funnel and extracted with toluene (3 x 10 mL). Dried combined organic layers over $MgSO_4$ and filtered into a 250 mL round bottom flask. The flask was equipped with a stir bar and reflux condenser and heated to 120 ^oC for 16 hours. After cooling, 1.5 mL (11.9 mmol) of TFA was added followed by heating to 80 ^oC overnight. In the morning the solution was concentrated and the residue was purified via silica gel flash chromatography (10% EtOAc in hexanes) to give a white solid. The purified oil was analyzed by NMR and the spectral data were consistent with the literature values.[141,158] Recovered 490 mg (32%).

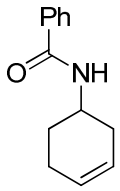

N-(cyclohex-3-en-1-yl)benzamide **(*rac*-*3*-40m)**. In a 50 mL round bottom flask equipped with a stir bar was added K_2CO_3 (415 mg, 3.0 mmol) and 5 mL of water. To this solution was added ***rac*-*3*-40n** (193 mg, 1.0 mmol). The suspension was allowed to stir for 72 hours. During this period the suspension became a homogenous solution to which 5 mL of CH_2Cl_2 and benzoyl chloride (140 uL, 1.2 mmol) was added. The biphasic solution was allowed to stir for 16 hours. In the morning the contents were poured into a separatory funnel and extracted with CH_2Cl_2 (2 x 15 mL) and dried over Na_2SO_4. The solution was filtered and concentrated to give a colorless residue. The residue was purified via silica gel flash chromatography (15% EtOAc in hexanes) to give 163 mg (81%) of a white solid. The purified solid was analyzed by NMR and the spectral data were consistent with the literature values.[156] ^1H NMR (500 MHz, $CDCl_3$) δ 7.28 – 7.22 (m, 3H), 6.84 – 6.81 (m, 2H), 6.80 (br. s, 1H), 5.23 (q, J = 3.1, 1H), 4.10 (br. s, 1H), 3.81 (ddd, J = 12.1, 3.5, 2.7, 1H), 2.07 – 1.91 (m, 2H), 1.86 – 1.72 (m, 2H), 1.71 – 1.59 (m, 2H).

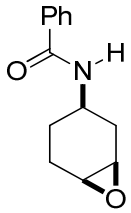

N-7-oxabicyclo[4.1.0]heptan-3-yl)benzamide **(*rac*-*3*-41m)**.[147] To a solution of *rac*-***3*-40m** (5151 mg, 2.56 mmol) in CH_2Cl_2 (50 mL) under a blanket of N_2 was added *m*-CPBA (50%, 1.77 mg, 5.12 mmol). The suspension was stirred at room temperature for 16 hours. In the morning, the contents were poured in a flask containing 20 mL of Na_2SO_3 and 20 mL of $NaHCO_3$. The biphasic solution was stirred vigorously for 10 minutes before pouring into a separatory funnel. The aqueous layer was extracted with CH_2Cl_2 (2 x 30 mL) and dried over Na_2SO_4. The solution was then filtered and concentrated to give a residue. The residue was purified via silica gel flash chromatography (50% EtOAc in hexanes) to give 426 mg of a white solid (77%). The solid was analyzed by ^1H and ^{13}C NMR indicating perfect diastereoselectivity consistent with the findings of Huang.[147] ^1H NMR (500 MHz, $CDCl_3$) δ 7.79 – 7.75 (m, 2H), 7.51 – 7.46 (m, 1H), 7.45 – 7.40 (m, 2H), 6.87 (d, *J* = 7.3 Hz, 1H), 4.33 – 4.26 (m, 1H), 3.27 (br. s, 2H), 2.26 (ddd, *J* = 15.5, 5.5, 2.3 Hz, 1H), 2.16 – 1.99 (m, 3H), 1.76 – 1.67 (m, 1H), 1.57 – 1.49 (m, 1H).

References:

(1) Hebert, L. E.; Scherr, P. A.; Bienias, J. L.; Bennett, D. A.; Evans, D. A. *Arch. Neurol.* **2003**, *60*, 1119-1122.

(2) *Alzheimer's and Dementia* **2009**, *5*, 234-270.

(3) Glenner, G. G.; Wong, C. W. *Biochem. biophys. res. comm.* **1984**, *120*, 885-890.

(4) Lee, V. M.; Balin, B. J.; Otvos, L., Jr.; Trojanowski, J. Q. *Science* **1991**, *251*, 675-678.

(5) Naslund, J.; Haroutunian, V.; Mohs, R.; Davis, K. L.; Davies, P.; Greengard, P.; Buxbaum, J. D. *JAMA* **2000**, *283*, 1571-1577.

(6) Vassar, R. *Adv. Drug Deliv. Rev.* **2002**, *54*, 1589-1602.

(7) Younkin, S. G. *J. phys., Paris* **1998**, *92*, 289-292.

(8) Cole, S. L.; Vassar, R. *Neurobiol. Dis.* **2006**, *22*, 209-222.

(9) Scheuner, D.; Eckman, C.; Jensen, M.; Song, X.; Citron, M.; Suzuki, N.; Bird, T. D.; Hardy, J.; Hutton, M.; Kukull, W.; Larson, E.; Levy-Lahad, E.; Viitanen, M.; Peskind, E.; Poorkaj, P.; Schellenberg, G.; Tanzi, R.; Wasco, W.; Lannfelt, L.; Selkoe, D.; Younkin, S. *Nat. Med.* **1996**, *2*, 864-870.

(10) Haass, C.; Selkoe, D. J. *Cell* **1993**, *75*, 1039-1042.

(11) Selkoe, D. J. *J. Biol. Chem.* **1996**, *271*, 18295-18298.

(12) Schechter, I.; Berger, A. *Biochem. biophys. res. comm.***1967**, *27*, 157-162.

(13) Mullan, M.; Crawford, F.; Axelman, K.; Houlden, H.; Lilius, L.; Winblad, B.; Lannfelt, L. *Nat. Genet.* **1992**, *1*, 345-347.

(14) Hussain, I.; Powell, D.; Howlett, D. R.; Tew, D. G.; Week, T. D.; Chapman, C.; Gloger, I. S.; Murphy, K. E.; Southan, C. D.; Ryan, D. M.; Smith, T. S.; Simmons, D. L.; Walsh, F. S.; Dingwall, C.; Christie, G. *Mol. Cell. Neurosci.* **1999**, *14*, 419-427.

(15) Lin, X.; Koelsch, G.; Wu, S.; Downs, D.; Dashti, A.; Tang, J. *Proc. Natl. Acad. Sci. U.S.A.* **2000**, *97*, 1456-1460.

(16) Sinha, S.; Anderson, J. P.; Barbour, R.; Basi, G. S.; Caccavello, R.; Davis, D.; Doan, M.; Dovey, H. F.; Frigon, N.; Hong, J.; Jacobson-Croak, K.; Jewett, N.; Keim, P.; Knops, J.; Lieberburg, I.; Power, M.; Tan, H.; Tatsuno, G.; Tung, J.; Schenk, D.; Seubert, P.; Suomensaari, S. M.; Wang, S. W.; Walker, D.; Zhao, J.; McConlogue, L.; John, V. *Nature* **1999**, *402*, 537-540.

(17) Vassar, R.; Bennett, B. D.; Babu-Khan, S.; Kahn, S.; Mendiaz, E. A.; Denis, P.; Teplow, D. B.; Ross, S.; Amarante, P.; Loeloff, R.; Luo, Y.; Fisher, S.; Fuller, L.; Edenson, S.; Lile, J.; Jarosinski, M. A.; Biere, A. L.; Curran, E.; Burgess, T.; Louis, J. C.; Collins, F.; Treanor, J.; Rogers, G.; Citron, M. *Science* **1999**, *286*, 735-741.

(18) Yan, R.; Bienkowski, M. J.; Shuck, M. E.; Miao, H.; Tory, M. C.; Pauley, A. M.; Brashier, J. R.; Stratman, N. C.; Mathews, W. R.; Buhl, A. E.; Carter, D. B.; Tomasselli, A. G.; Parodi, L. A.; Heinrikson, R. L.; Gurney, M. E. *Nature* **1999**, *402*, 533-537.

(19) Cai, H.; Wang, Y.; McCarthy, D.; Wen, H.; Borchelt, D. R.; Price, D. L.; Wong, P. C. *Nat. Neurosci.* **2001**, *4*, 233-234.

(20) Luo, Y.; Bolon, B.; Kahn, S.; Bennett, B. D.; Babu-Khan, S.; Denis, P.; Fan, W.; Kha, H.; Zhang, J. H.; Gong, Y. H.; Martin, L.; Louis, J. C.; Yan, Q.; Richards, W. G.; Citron, M.; Vassar, R. *Nat. Neurosci.* **2001**, *4*, 231-232.

(21) Roberds, S. L.; Anderson, J.; Basi, G.; Bienkowski, M. J.; Branstetter, D. G.; Chen, K. S.; Freedman, S. B.; Frigon, N. L.; Games, D.; Hu, K.; Johnson-Wood, K.; Kappenman, K. E.; Kawabe, T. T.; Kola, I.; Kuehn, R.; Lee, M.; Liu, W.; Motter, R.; Nichols, N. F.; Power, M.; Robertson, D. W.; Schenk, D.; Schoor, M.; Shopp, G. M.; Shuck, M. E.; Sinha, S.; Svensson, K. A.; Tatsuno, G.; Tintrup, H.; Wijsman, J.; Wright, S.; McConlogue, L. *Hum. Mol. Genet.* **2001**, *10*, 1317-1324.

(22) Sauder, J. M.; Arthur, J. W.; Dunbrack, R. L., Jr. *J. Mol. Biol.* **2000**, *300*, 241-248.

(23) Hong, L.; Koelsch, G.; Lin, X. L.; Wu, S. L.; Terzyan, S.; Ghosh, A. K.; Zhang, X. C.; Tang, J. *Science* **2000**, *290*, 150-153.

(24) Bursavich, M. G.; Rich, D. H. *J. Med. Chem.* **2002**, *45*, 541-558.

(25) Cooper, J. B. *Curr. Drug Targets* **2002**, *3*, 155-173.

(26) Suguna, K.; Bott, R. R.; Padlan, E. A.; Subramanian, E.; Sheriff, S.; Cohen, G. H.; Davies, D. R. *J. Mol. Biol.* **1987**, *196*, 877-900.

(27) Pauling, L. *Chem. Eng. News* **1946**, 1375-1377.

(28) Brik, A.; Wong, C. H. *Org. Biomol. Chem.* **2003**, *1*, 5-14.

(29) Hong, L.; Koelsch, G.; Lin, X.; Wu, S.; Terzyan, S.; Ghosh, A. K.; Zhang, X. C.; Tang, J. *Science* **2000**, *290*, 150-153.

(30) Tung, J. S.; Davis, D. L.; Anderson, J. P.; Walker, D. E.; Mamo, S.; Jewett, N.; Hom, R. K.; Sinha, S.; Thorsett, E. D.; John, V. *J. Med. Chem.* **2002**, *45*, 259-262.

(31) Hom, R. K.; Fang, L. Y.; Mamo, S.; Tung, J. S.; Guinn, A. C.; Walker, D. E.; Davis, D. L.; Gailunas, A. F.; Thorsett, E. D.; Sinha, S.; Knops, J. E.; Jewett, N. E.; Anderson, J. P.; John, V. *J. Med. Chem.* **2003**, *46*, 1799-1802.

(32) Sakurai, M.; Higashida, S.; Sugano, M.; Nishi, T.; Saito, F.; Ohata, Y.; Handa, H.; Komai, T.; Yagi, R.; Nishigaki, T.; Yabe, Y. *Chem. Pharm. Bull.* **1993**, *41*, 1378-1386.

(33) Capraro, H. G.; Bold, G.; Fassler, A.; Cozens, R.; Klimkait, T.; Lazdins, J.; Mestan, J.; Poncioni, B.; Rosel, J. L.; Stover, D.; Lang, M. *Arch. Pharm. (Weinheim)* **1996**, *329*, 273-278.

(34) Lazdins, J. K.; Bold, G.; Capraro, H. G.; Cozens, R.; Fassler, A.; Flesch, G.; Klimkait, T.; Lang, M.; Mestan, J.; Poncioni, B.; Rosel, J.; Stover, D.; Tintelnot-Blomley, M.; Walker, M. R.; Woods-Cook, K. *Schweiz. Med. Wochenschr.* **1996**, *126*, 1849-1851.

(35) Ghosh, A. K.; Shin, D.; Downs, B.; Koelsch, G.; Lin, X.; Ermolieff, J.; Tang, J. *J. Am. Chem. Soc.* **2000**, *122*, 3522-3523.

(36) Turner, R. T., 3rd; Koelsch, G.; Hong, L.; Castanheira, P.; Ermolieff, J.; Ghosh, A. K.; Tang, J. *Biochemistry* **2001**, *40*, 10001-10006.

(37) Hong, L.; Turner, R. T., 3rd; Koelsch, G.; Shin, D.; Ghosh, A. K.; Tang, J. *Biochemistry* **2002**, *41*, 10963-10967.

(38) Lamar, J.; Hu, J.; Bueno, A. B.; Yang, H. C.; Guo, D.; Copp, J. D.; McGee, J.; Gitter, B.; Timm, D.; May, P.; McCarthy, J.; Chen, S. H. *Bioorg. Med. Chem. Lett.* **2004**, *14*, 239-243.

(39) Lipinski, C. A.; Lombardo, F.; Dominy, B. W.; Feeney, P. J. *Adv. Drug Deliv. Rev.* **2001**, *46*, 3-26.

(40) Abdel-Rahman, H. M.; Al-karamany, G. S.; El-Koussi, N. A.; Youssef, A. F.; Kiso, Y. *Curr. Med. Chem.* **2002**, *9*, 1905-1922.

(41) Randolph, J. T.; DeGoey, D. A. *Curr. Top. Med. Chem.* **2004**, *4*, 1079-1095.

(42) Tamamura, H.; Koh, Y.; Ueda, S.; Sasaki, Y.; Yamasaki, T.; Aoki, M.; Maeda, K.; Watai, Y.; Arikuni, H.; Otaka, A.; Mitsuya, H.; Fujii, N. *J. Med. Chem.* **2003**, *46*, 1764-1768.

(43) Maillard, M. C.; Hom, R. K.; Benson, T. E.; Moon, J. B.; Mamo, S.; Bienkowski, M.; Tomasselli, A. G.; Woods, D. D.; Prince, D. B.; Paddock, D. J.; Emmons, T. L.; Tucker, J. A.; Dappen, M. S.; Brogley, L.; Thorsett, E. D.; Jewett, N.; Sinha, S.; John, V. *J. Med. Chem.* **2007**, *50*, 776-781.

(44) Tamamura, H.; Kato, T.; Otaka, A.; Fujii, N. *Org. Biomol. Chem.* **2003**, *1*, 2468-2 473.

(45) Dovey, H. F.; John, V.; Anderson, J. P.; Chen, L. Z.; Andrieu, P. D.; Fang, L. Y.; Freedman, S. B.; Folmer, B.; Goldbach, E.; Holsztynska, E. J.; Hu, K. L.; Johnson-Wood, K. L.; Kennedy, S. L.; Kholedenko, D.; Knops, J. E.; Latimer, L. H.; Lee, M.; Liao, Z.; Lieberburg, I. M.; Motter, R. N.; Mutter, L. C.; Nietz, J.; Quinn, K. P.; Sacchi, K. L.; Seubert, P. A.; Shopp, G. M.; Thorsett, E. D.; Tung, J. S.; Wu, J.; Yang, S.; Yin, C. T.; Schenk, D. B.; May, P. C.; Altstiel, L. D.; Bender, M. H.; Boggs, L. N.; Britton, T. C.; Clemens, J. C.; Czilli, D. L.; Dieckman-McGinty, D. K.; Droste, J. J.; Fuson, K. S.; Gitter, B. D.; Hyslop, P. A.; Johnstone, E. M.; Li, W. Y.; Little, S. P.; Mabry, T. E.; Miller, F. D.; Ni, B.; Nissen, J. S.; Porter, W. J.; Potts, B. D.; Reel, J. K.; Stephenson, D.; Su, Y.; Shipley, L. A.; Whitesitt, C. A.; Yin, T.; Audia, J. E. *J. Neurochem.* **2001**, *76*, 173-181.

(46) Stachel, S. J.; Coburn, C. A.; Steele, T. G.; Jones, K. G.; Loutzenhiser, E. F.; Gregro, A. R.; Rajapakse, H. A.; Lai, M. T.; Crouthamel, M. C.; Xu, M.;

Tugusheva, K.; Lineberger, J. E.; Pietrak, B. L.; Espeseth, A. S.; Shi, X. P.; Chen-Dodson, E.; Holloway, M. K.; Munshi, S.; Simon, A. J.; Kuo, L.; Vacca, J. P. *J. Med. Chem.* **2004**, *47*, 6447-6450.

(47) Brady, S. F.; Singh, S.; Crouthamel, M.-C.; Holloway, M. K.; Coburn, C. A.; Garsky, V. M.; Bogusky, M.; Pennington, M. W.; Vacca, J. P.; Hazuda, D.; Lai, M.-T. *Bioorg. Med. Chem. Lett.* **2004**, *14*, 601-604.

(48) Szelke, M.; Leckie, B.; Hallett, A.; Jones, D. M.; Sueiras, J.; Atrash, B.; Lever, A. F. *Nature* **1982**, *299*, 555-557.

(49) Coburn, C. A.; Stachel, S. J.; Jones, K. G.; Steele, T. G.; Rush, D. M.; DiMuzio, J.; Pietrak, B. L.; Lai, M. T.; Huang, Q.; Lineberger, J.; Jin, L. X.; Munshi, S.; Holloway, M. K.; Espeseth, A.; Simon, A.; Hazuda, D.; Graham, S. L.; Vacca, J. P. *Bioorg. Med. Chem. Lett.* **2006**, *16*, 3635-3638.

(50) Stachel, S. J.; Coburn, C. A.; Steele, T. G.; Jones, K. G.; Loutzenhiser, E. F.; Gregro, A. R.; Rajapakse, H. A.; Lai, M. T.; Crouthamel, M. C.; Xu, M.; Tugusheva, K.; Lineberger, J. E.; Pietrak, B. L.; Espeseth, A. S.; Shi, X. P.; Chen-Dodson, E.; Holloway, M. K.; Munshi, S.; Simon, A. J.; Kuo, L.; Vacca, J. P. *J. Med. Chem.* **2004**, *47*, 6447-6450.

(51) Stachel, S. J.; Coburn, C. A.; Sankaranarayanan, S.; Price, E. A.; Pietrak, B. L.; Huang, Q.; Lineberger, J.; Espeseth, A. S.; Jin, L. X.; Ellis, J.; Holloway, M. K.; Munshi, S.; Allison, T.; Hazuda, D.; Simon, A. J.; Graham, S. L.; Vacca, J. P. *J. Med. Chem.* **2006**, *49*, 6147-6150.

(52) Hu, X.; Nguyen, K. T.; Jiang, V. C.; Lofland, D.; Moser, H. E.; Pei, D. *J. Med. Chem.* **2004**, *47*, 4941-4949.

(53) Nguyen, K. T.; Hu, X.; Pei, D. *Bioorg. Chem.* **2004**, *32*, 178-191.

(54) Tsantrizos, Y. S.; Bolger, G.; Bonneau, P.; Cameron, D. R.; Goudreau, N.; Kukolj, G.; LaPlante, S. R.; Llinas-Brunet, M.; Nar, H.; Lamarre, D. *Angew. Chem. Int. Ed. Engl.* **2003**, *42*, 1356-1360.

(55) Bourne, Y.; Kolb, H. C.; Radic, Z.; Sharpless, K. B.; Taylor, P.; Marchot, P. *Proc. Natl. Acad. Sci. U.S.A.* **2004**, *101*, 1449-1454.

(56) Brik, A.; Alexandratos, J.; Lin, Y. C.; Elder, J. H.; Olson, A. J.; Wlodawer, A.; Goodsell, D. S.; Wong, C. H. *ChemBioChem* **2005**, *6*, 1167-1169.

(57) Rajapakse, H. A.; Nantermet, P. G.; Selnick, H. G.; Munshi, S.; McGaughey, G. B.; Lindsley, S. R.; Young, M. B.; Lai, M.-T.; Espeseth, A. S.; Shi, X.-P.; Colussi, D.; Pietrak, B.; Crouthamel, M.-C.; Tugusheva, K.; Huang, Q.; Xu, M.; Simon, A. J.; Kuo, L.; Hazuda, D. J.; Graham, S.; Vacca, J. P. *J. Med. Chem.* **2006**, *49*, 7270-7273.

(58) Brik, A.; Wu, C. Y.; Wong, C. H. *Org. Biomol. Chem*. **2006**, *4*, 1446-1457.

(59) Congreve, M.; Aharony, D.; Albert, J.; Callaghan, O.; Campbell, J.; Carr, R. A.; Chessari, G.; Cowan, S.; Edwards, P. D.; Frederickson, M.; McMenamin, R.; Murray, C. W.; Patel, S.; Wallis, N. *J. Med. Chem.* **2007**, *50*, 1124-1132.

(60) Lewis, W. G.; Green, L. G.; Grynszpan, F.; Radic, Z.; Carlier, P. R.; Taylor, P.; Finn, M. G.; Sharpless, K. B. *Angew. Chem. Int. Ed. Engl.* **2002**, *41*, 1053-1057.

(61) Manetsch, R.; Krasinski, A.; Radic, Z.; Raushel, J.; Taylor, P.; Sharpless, K. B.; Kolb, H. C. *J. Am. Chem. Soc.* **2004**, *126*, 12809-12818.

(62) Whiting, M.; Muldoon, J.; Lin, Y. C.; Silverman, S. M.; Lindstrom, W.; Olson, A. J.; Kolb, H. C.; Finn, M. G.; Sharpless, K. B.; Elder, J. H.; Fokin, V. V. *Angew. Chem. Int. Ed. Engl.* **2006**, *45*, 1435-1439.

(63) Ghosh, A. K.; Kumaragurubaran, N.; Hong, L.; Kulkarni, S. S.; Xu, X.; Chang, W.; Weerasena, V.; Turner, R.; Koelsch, G.; Bilcer, G.; Tang, J. *J. Med. Chem.* **2007**, *50*, 2399-2407.

(64) Jian, H.; Tour, J. M. *J. Org. Chem.* **2003**, *68*, 5091-5103.

(65) Tour, J. M.; Rawlett, A. M.; Kozaki, M.; Yao, Y.; Jagessar, R. C.; Dirk, S. M.; Price, D. W.; Reed, M. A.; Zhou, C. W.; Chen, J.; Wang, W.; Campbell, I. *Chem. Eur. J.* **2001**, *7*, 5118-5134.

(66) Miroshnikova, O. V.; Hudson, T. H.; Gerena, L.; Kyle, D. E.; Lin, A. J. *J. Med. Chem.* **2007**, *50*, 889-896.

(67) Wissner, A.; Overbeek, E.; Reich, M. F.; Floyd, M. B.; Johnson, B. D.; Mamuya, N.; Rosfjord, E. C.; Discafani, C.; Davis, R.; Shi, X.; Rabindran, S. K.; Gruber, B. C.; Ye, F.; Hallett, W. A.; Nilakantan, R.; Shen, R.; Wang, Y. F.; Greenberger, L. M.; Tsou, H. R. *J. Med. Chem.* **2003**, *46*, 49-63.

(68) Kozikowski, A. P.; Shum, P. W.; Basu, A.; Lazo, J. S. *J. Med. Chem.* **1991**, *34*, 2420-2430.

(69) Nyffeler, P. T.; Liang, C. H.; Koeller, K. M.; Wong, C. H. *J. Am. Chem. Soc.* **2002**, *124*, 10773-10778.

(70) Hillisch, A.; Lorenz, M.; Diekmann, S. *Curr. Opin. Struct. Biol.* **2001**, *11*, 201-207.

(71) Atkins, P. W. *Physical chemistry*; 6th ed.; Freeman: New York, 1998.

(72) Brik, A.; Lin, Y. C.; Elder, J.; Wong, C. H. *Chem. Biol.* **2002**, *9*, 891-896.

(73) Brik, A.; Wu, C. Y.; Wong, C. H. *Org. Biomol. Chem.* **2006**, *4*, 1446-1457.

(74) Kolb, H. C.; Finn, M. G.; Sharpless, K. B. *Angew. Chem. Int. Ed. Engl.* **2001**, *40*, 2004-2021.

(75) Lee, L. V.; Mitchell, M. L.; Huang, S. J.; Fokin, V. V.; Sharpless, K. B.; Wong, C. H. *J. Am. Chem. Soc.* **2003**, *125*, 9588-9589.

(76) Brik, A.; Muldoon, J.; Lin, Y. C.; Elder, J. H.; Goodsell, D. S.; Olson, A. J.; Fokin, V. V.; Sharpless, K. B.; Wong, C. H. *Chembiochem* **2003**, *4*, 1246-1248.

(77) Rajapakse, H. A.; Nantermet, P. G.; Selnick, H. G.; Munshi, S.; McGaughey, G. B.; Lindsley, S. R.; Young, M. B.; Lai, M. T.; Espeseth, A. S.; Shi, X. P.; Colussi, D.; Pietrak, B.; Crouthamel, M. C.; Tugusheva, K.; Huang, Q.; Xu, M.; Simon, A.

J.; Kuo, L.; Hazuda, D. J.; Graham, S.; Vacca, J. P. *J. Med. Chem.* **2006**, *49*, 7270-7273.

(78) Bruice, P. Y. *Organic Chemistry*; 4th ed.; Pearson/Prentice Hall: Upper Saddle River, NJ, 2004; pp 446-454.

(79) Deslongchamps, P. *Stereoelectronic effects in organic chemistry*; 1st ed.; Pergamon Press: Oxford [Oxfordshire] ; New York, 1983.

(80) Valls, J.; Toromanoff, E. *Bull. Soc. Chim. Fr.* **1961**, 758.

(81) Fürst, A.; Plattner, P. A. *Helv. Chim. Acta* **1949**, *32*, 275-283.

(82) Fürst, A.; Plattner, P. A. *12th Int. Congr. Pure Appl. Chem. New York* **1951**, 409.

(83) Bagal, S. K.; Davies, S. G.; Lee, J. A.; Roberts, P. M.; Russell, A. J.; Scott, P. M.; Thomson, J. E. *Org. Lett.*, *12*, 136-139.

(84) Bordwell, F. G.; Algrim, D. J. *J. Am. Chem. Soc.* **1988**, *110*, 2964-2968.

(85) Davies, S. G.; Polywka, M. E. C.; Thomas, S. E. *J. Chem. Soc. Perkin Trans. I* **1986**, 1277-1282.

(86) Goodman, L.; Winstein, S.; Boschan, R. *J. Am. Chem. Soc.* **1958**, *80*, 4312-4317.

(87) Martinez, L. E.; Leighton, J. L.; Carsten, D. H.; Jacobsen, E. N. *J. Am. Chem. Soc.* **1995**, *117*, 5897-5898.

(88) Breslow, R. *Acc. Chem. Res.* **1991**, *24*, 159-164.

(89) Serrano, P.; Llebaria, A.; Vazquez, J.; de Pablo, J.; Anglada, J. M.; Delgado, A. *Chem. Eur. J.* **2005**, *11*, 4465-4472.

(90) Serrano, P.; Llebaria, A.; Delgado, A. *J. Org. Chem.* **2002**, *67*, 7165-7167.

(91) Narayan, S.; Muldoon, J.; Finn, M. G.; Fokin, V. V.; Kolb, H. C.; Sharpless, K. B. *Angew. Chem. Int. Ed. Engl.* **2005**, *44*, 3275-3279.

(92) Craig, T. W.; Harvey, G. R.; Berchtold, G. A. *J. Org. Chem.* **1967**, *32*, 3743-3749.

(93) Scheunemann, M.; Sorger, D.; Kouznetsova, E.; Sabri, O.; Schliebs, R.; Wenzel, B.; Steinbach, J. *Tetrahedron Lett.* **2007**, *48*, 5497-5501.

(94) Barz, M.; Glas, H.; Thiel, W. R. *Synthesis (Stuttg)* **1998**, 1269-1273.

(95) Gruber-Khadjawi, M.; Hönig, H.; Illaszewicz, C. *Tetrahedron Asymmetry* **1996**, *7*, 807-814.

(96) Kavadias, G.; Droghini, R. *Can. J. Chem.* **1978**, *56*, 2743-2749.

(97) Hansen, K. B.; Leighton, J. L.; Jacobsen, E. N. *J. Am. Chem. Soc.* **1996**, *118*, 10924-10925.

(98) Ironmonger, A.; Stockley, P.; Nelson, A. *Org. Biomol. Chem.* **2005**, *3*, 2350-2353.

(99) Herrmann, W. A.; Fischer, R. W.; Rauch, M. U.; Scherer, W. *J. Mol. Catal.* **1994**, *86*, 243-266.

(100) Rudolph, J.; Reddy, K. L.; Chiang, J. P.; Sharpless, K. B. *J. Am. Chem. Soc.* **1997**, *119*, 6189-6190.

(101) Skoog, D. A.; West, D. M.; Holler, F. J. *Analytical chemistry : an introduction*; 6th ed.; Saunders College Pub.: Philadelphia, 1994.

(102) Clique, B.; Ironmonger, A.; Whittaker, B.; Colley, J.; Titchmarsh, J.; Stockley, P.; Nelson, A. *Org. Biomol. Chem.* **2005**, *3*, 2776-2785.

(103) Klijn, J. E.; Engberts, J. B. *Nature* **2005**, *435*, 746-747.

(104) Rideout, D. C.; Breslow, R. *J. Am. Chem. Soc.* **1980**, *102*, 7816-7817.

(105) Jung, Y.; Marcus, R. A. *J. Am. Chem. Soc.* **2007**, *129*, 5492-5502.

(106) Kumar, G. D. K.; Baskaran, S. *J. Org. Chem.* **2005**, *70*, 4520-4523.

(107) Friebolin, H. *Basic One- and Two-dimensional NMR Spectroscopy*; 4th ed.; WILEY-VCH: Weinheim 2005; pp 93-35.

(108) Carey, F. A.; Sundberg, R. J.; 5th ed ed.; Springer: New York, NY, 2007; p 339.

(109) Bordwell, F. G.; Drucker, G. E.; Fried, H. E. *J. Org. Chem.* **1981**, *46*, 632-635.

(110) Kavadias, G.; Droghini, R. *Can. J. Chem.* **1979**, *57*, 1870-1876.

(111) Aldegunde, M. J.; Castedo, L.; Granja, J. R. *Chem. Eur. J.* **2009**, *15*, 4785-4787.

(112) Kozlov, N. S.; Prishchepenko, V. M.; Zhavnerko, K. A. *Dokl. Akad. Nauk BSSR* **1990**, *34*, 334-337.

(113) Kozlov, N. S.; Zhavnerko, K. A.; Yakubovich, L. S.; Prishchepenko, V. M. *Vestsi Akad. Navuk BSSR, Ser. Khim. Navuk* **1982**, *1*, 56-58.

(114) Hartman, B. C.; Rickborn, B. *J. Org. Chem.* **1972**, *37*, 4246-4249.

(115) Kozlov, N. S.; Zhavnerko, K. A.; Yakubovich, L. S.; Prishchepenko, V. M. *Vestsi Akad. Navuk BSSR, Ser. Khim. Navuk* **1975**, *5*, 84-89.

(116) Hoveyda, A. H.; Evans, D. A.; Fu, G. C. *Chem. Rev.* **1993**, *93*, 1307-1370.

(117) Henbest, H. B.; Wilson, R. A. L. *J. Chem. Soc.* **1957**, 1958-1965.

(118) Bartlett, P. D. *Rec. Chem . Prog.* **1950**, *11*, 47.

(119) Chamberlain, P.; Roberts, M. L.; Whitham, G. H. *J. Chem. Soc. (B)* **1970**, 1374-1381.

(120) Lukacs, G.; Fukushima, D. K. *J. Org. Chem.* **1969**, *34*, 2707-2710.

(121) Baeckvall, J. E.; Oshima, K.; Palermo, R. E.; Sharpless, K. B. *J. Org. Chem.* **1979**, *44*, 1953-1957.

(122) O'Brien, P.; Childs, A. C.; Ensor, G. J.; Hill, C. L.; Kirby, J. P.; Dearden, M. J.; Oxenford, S. J.; Rosser, C. M. *Org. Lett.* **2003**, *5*, 4955-4957.

(123) Nishikawa, T.; Asai, M.; Ohyabu, N.; Isobe, M. *J. Org. Chem.* **1998**, *63*, 188-192.

(124) Overman, L. E. *J. Am. Chem. Soc.* **1976**, *98*, 2901-2910.

(125) Overman, L. E. *Tetrahedron Lett.* **1975**, 1149-1152.

(126) Johannsen, M.; Jorgensen, K. A. *Chem. Rev.* **1998**, *98*, 1689-1708.

(127) Brouillette, W. J.; Saeed, A.; Abuelyaman, A.; Hutchison, T. L.; Wolkowicz, P. E.; McMillin, J. B. *J. Org. Chem.* **1994**, *59*, 4297-4303.

(128) Quick, J.; Khandelwal, Y.; Meltzer, P. C.; Weinberg, J. S. *J. Org. Chem.* **1983**, *48*, 5199-5203.

(129) Asensio, G.; Mello, R.; Boix-Bernardini, C.; Gonzalez-Nunez, M. E.; Castellano, G. *J. Org. Chem.* **1995**, *60*, 3692-3699.

(130) Edwards, A. S.; Wybrow, R. A. J.; Johnstone, C.; Adams, H.; Harrity, J. P. A. *Chem. Commun.* **2002**, 1542-1543.

(131) Aciro, C.; Claridge, T. D. W.; Davies, S. G.; Roberts, P. M.; Russell, A. J.; Thomson, J. E. *Org. Biomol. Chem.* **2008**, *6*, 3751-3761.

(132) Parker, R. E.; Isaacs, N. S. *Chem. Rev.* **1959**, *59*, 737-799.

(133) Sharpless, K. B.; Verhoeven, T. R. *Aldrichimica Acta* **1979**, *12*, 63-74.

(134) Sharpless, K. B.; Michaelson, R. C. *J. Am. Chem. Soc.* **1973**, *95*, 6136-6137.

(135) Mousseron-Canet, M.; Guilleux, J. C. *Bull. Soc. Chim. Fr.* **1966**, *12*, 3853-3858.

(136) Kiss, L.; Forró, E.; Fülöp, F. *Tetrahedron Lett.* **2006**, *47*, 2855-2858.

(137) Kiss, L.; Forró, E.; Martinek, T. A.; Bernáth, G.; De Kimpe, N.; Fülöp, F. *Tetrahedron* **2008**, *64*, 5036-5043.

(138) Rotella, D. P. *Tetrahedron Lett.* **1989**, *30*, 1913-1916.

(139) Witiak, D. T.; Rotella, D. P.; Wei, Y.; Filppi, J. A.; Gallucci, J. C. *J. Med. Chem.* **1989**, *32*, 214-217.

(140) Gómez-Sánchez, E.; Marco-Contelles, J. *Tetrahedron* **2005**, *61*, 1207-1219.

(141) Donohoe, T. J.; Mitchell, L.; Waring, M. J.; Helliwell, M.; Bell, A.; Newcombe, N. J. *Org. Biomol. Chem.* **2003**, *1*, 2173-2186.

(142) Donohoe, T. J.; Blades, K.; Moore, P. R.; Waring, M. J.; Winter, J. J. G.; Helliwell, M.; Newcombe, N. J.; Stemp, G. *J. Org. Chem.* **2002**, *67*, 7946-7956.

(143) Shioiri, T.; Ninomiya, K.; Yamada, S. *J. Am. Chem. Soc.* **1972**, *94*, 6203-6205.

(144) Jessup, P. J.; Petty, C. B.; Roos, J.; Overman, L. E. *Organic Synth.* **1988**, *50-9*, 95-101.

(145) Overman, L. E.; Taylor, G. F.; Jessup, P. J. *Tetrahedron Lett.* **1976**, 3089-3092.

(146) Overman, L. E.; Taylor, G. F.; Petty, C. B.; Jessup, P. J. *J. Org. Chem.* **1978**, *43*, 2164-2167.

(147) Huang, L.; Zhou, Y.; Ye, D. *Chin. J. Org. Chem.* **2006**, *26*, 379-382.

(148) Baumann, E. *Ber. Dtsch. Chem. Ges.* **1886**, *19*, 3218-3222.

(149) Schotten, C. *Ber. Dtsch. Chem. Ges.* **1884**, *17*, 2544-2547.

(150) Gabos, B.; Munck, A. R. M.; Ripa, L.; Astrazeneca AB: 2009, p 72pp.

(151) Hirsch, J. A. In *Advances in Stereochemistry* John Wiley & Sons, Inc.: 1967; Vol. 3, p 199.

(152) Chini, M.; Crotti, P.; Flippin, L. A.; Macchia, F. *J. Org. Chem.* **1991**, *56*, 7043-7048.

(153) Ward, S. E.; Thewlis, K. M.; Glaxo Group Limited: 2006, p 46 pp.

(154) Rajesh, K.; Somasundaram, M.; Saiganesh, R.; Balasubramanian, K. K. *J. Org. Chem.* **2007**, *72*, 5867-5869.

(155) Bit, R. A.; Giblin, G. M. P.; Hall, A.; Hurst, D. N.; Kilford, I. R.; Miller, N. D.; Scoccitti, T.; Glaxo Group Limited: 2004, p 96 pp.

(156) Barrow, J. C.; McGaughey, G. B.; Nantermet, P. G.; Rajapakse, H. A.; Selnick, H. G.; Stauffer, S. R.; Coburn, C. A.; Merck & Co.: 2005, p 212 pp.

(157) Abdel-Magid, A. F.; Carson, K. G.; Harris, B. D.; Maryanoff, C. A.; Shah, R. D. *J. Org. Chem.* **1996**, *61*, 3849-3862.

(158) Pfister, J. R.; Wymann, W. E. *Synthesis* **1983**, 38-40.